

TITLE:

Scale effect propeller calculations - twin screw wake field

CANDIDATE NAME:

Justas Kavaliauskas

DATE:

29.05.2015

COURSE CODE:

IP501909

COURSE TITLE:

M. Sc. Ship Design

RESTRICTION:

STUDY PROGRAM:

Ship Design

PAGES/APPENDIX:

143/74

LIBRARY NO.:

SUPERVISOR(S):

Karl Henning Halse, Gunnar Hugo Nyland

ABSTRACT:

This Master Thesis is all about scale effects which appears in results after performing model and full scale simulations of a twin screw vessel hull, which is anchor handler (STX-413). In this project main purpose is to perform towing tank tests where main considerations are done on results which contain resistance force coefficients and nominal wake fraction on a propeller plane. These are compared to each other in a range of Froude numbers. Simulations for model and full scale ship are done by software called STAR CCM+. Computations has been performed on a case where hull does not have ability to sink and trim. In general all set up for computations was given by Marintek as an example.

Because there is no experimental data to validate computational results, in thesis are done several different calculations to compare with: two different turbulence models are tried, calculations made with several different time steps to determine which is best for each case (model and full scale), and few simulations containing different domain size in number of cells. Main results shows that pressure force coefficients are lower in full scale up to 17% and wake fraction distribution follows the same: in full scale averaged values in propeller plane in certain Froude numbers are up to 28% lower than in model scale computations. Conclusions gives an indication that it needs to have further investigation regarding these scale effects on this particular vessel which is under investigation.

This thesis is submitted for evaluation at Ålesund University College.

Postal address:

 Høgskolen i Ålesund
 N-6025 Ålesund
 Norway

Visit adress

 Larsgårdsvegen 2
Internett
www.hials.no
Telephone

70 16 12 00

E-mail
postmottak@hials.no
Fax

70 16 13 00

Bank

 7694 05 00636
Enterprise no.
 NO 971 572 140

MASTER THESIS 2015

FOR

STUD.TECHN. Justas Kavaliauskas

Scale effects of the wake field behind of the twin screw vessel

Background.

The scale effect on the wake field of ship models is shown to be an important cause of prediction inaccuracies of wake field behind of the full scale ship. These errors could cause an unexpected propeller vibrations, which leads to failure of mechanical parts or discomfort of passengers. In addition to that, inaccuracies may cause a wrong design of the propulsion system, which could be not efficient enough or even not powerful for desired service speed. Beside this, having a good prediction model vessels stern shapes could be designed to achieve better overall resistance and achieve more evenly distributed wake on a propeller plane.

Objectives.

Purpose of this Master Thesis is to make a prediction model for model tests, where wake field behind of ship hull is analyzed. Thesis will contain simulations of full and model scale ship hulls, to determine wake fields. For the simulations CFD tool will be used (STAR CCM+), the results should be analyzed and according to them differences defined, due to scale effects made on simulation for model and full scale ship hulls. After this prediction model should be established of wake fraction for full scale vessel due to scale effects

The Thesis should be done by following steps:

A. Literature study

- Ship resistance/propulsion
- Wake field
- Scale effects
- CFD
 - Navier–Stokes equations
 - Viscous/turbulent flows
 - RANS
 - RSM
 - Turbulence model (k - ϵ ; ω - ϵ ; Spalart–Allmaras model)

B. Define computational model

- Mesh type & size
- Boundary layer treatment
- Turbulence model
- Initial conditions

C. Analysis set up for case study

- Froude number
- Drought
- Free sinkage/trim

D. Results comparison/post processing

- Full & model scale
 - Nominal wake field
 - Resistance
 - Sinkage/trim

The scope of work may prove to be larger than initially anticipated. Subject to approval from the advisor, topics from the list above may be deleted or reduced in extent.

The thesis should be written as a research report with summary, conclusion, literature references, table of contents, etc. During preparation of the text, the candidate should make efforts to create a well arranged and well written report. To ease the evaluation of the thesis, it is important to cross-reference text, tables and figures. For evaluation of the work a thorough discussion of results is needed. Discussion of research method, validation and generalization of results is also appreciated.

In addition to the thesis, a research paper for publication shall be prepared.

Three weeks after start of the thesis work, a pre-study have to be delivered. The pre-study have to include:

- Research method to be used
- Literature and sources to be studied
- A list of work tasks to be performed
- An A3 sheet illustrating the work to be handed in.

A templates and instructions for thesis documents and A3-poster are available on the Fronter website under MSc-thesis. Please follow the instructions closely, and ask your supervisor or program coordinator if needed.

The thesis shall be submitted in electronic version according to new procedures from 2014. Instructions are found on the college web site. In addition one paper copy of the full thesis with a CD including all relevant documents and files shall be submitted to your supervisor.

Supervision at AAUC: Karl H. Halse,
Contact at: Aalesund University College



Karl H. Halse
Supervisor

Delivery: 15.01.2015

Signature candidate: _____



PREFACE

Author of this thesis is student in Alesund University College who is studying Master studies in Ship Design. With strong interests in CFD analysis gained throughout applied computational fluid dynamics lecture course given in second semester by D. Ponkratov, author of this project decided to choose existing topic which demands CFD analyse tools. Topic has been given by Halse Karl Henning who is also one of project supervisors together with Nyland Gunnar Hugo.

This Master Thesis is a part of Propscale project which have purpose to investigate the scale effects on ship and propulsor characteristics, placing emphasis on podded and ducted propulsors (though single screw vessels are also an important part of the project scope). With the ultimate goal of improved performance predictions from numerical and model scale experimental results, and to provide a set of practical methods and tools for CFD analysis of ship resistance and propulsion, primarily for the benefit of the industrial partners.

Problems which are under investigation in Propscale project are solved numerically with CFD tool called STAR CCM+ by CD-Adapco. This is driven by the preferences of the project partners, and was further strengthened by having CD-Adapco participate in the project. Due to that Alesund University College is also a project partner, for this Master thesis same CFD software tools are used to investigate scale effects of wake field behind twin screw offshore type vessel.

ABSTRACT

This Master Thesis is all about scale effects which appears in results after performing model and full scale simulations of a twin screw vessel hull, which is anchor handler (STX-413). In this project main purpose is to perform towing tank tests where main considerations are done on results which contain resistance force coefficients and nominal wake fraction on a propeller plane. These are compared to each other in a range of Froude numbers. Simulations for model and full scale ship are done by software called STAR CCM+. Computations has been performed on a case where hull does not have ability to sink and trim. In general all set up for computations was given by Marintek as an example.

Because there is no experimental data to validate computational results, in thesis are done several different calculations to compare with: two different turbulence models are tried, calculations made with several different time steps to determine which is best for each case (model and full scale), and few simulations containing different domain size in number of cells. Main results shows that pressure force coefficients are lower in full scale up to 17% and wake fraction distribution follows the same: in full scale averaged values in propeller plane in certain Froude numbers are up to 28% lower than in model scale computations. Conclusions gives an indication that it needs to have further investigation regarding these scale effects on this particular vessel which is under investigation.

Table of contents

LIST OF FIGURES	8
LIST OF TABLES	ERROR! BOOKMARK NOT DEFINED.
TERMINOLOGY	10
SYMBOLS	ERROR! BOOKMARK NOT DEFINED.
ABBREVIATIONS	ERROR! BOOKMARK NOT DEFINED.
1 INTRODUCTION	11
1.1 PROJECT BACKGROUND	11
1.2 PROBLEM FORMULATION	12
1.3 OBJECTIVES	13
2 BACKGROUND AND THEORETICAL BASIS.....	14
2.1 TOWING TANK TESTS	14
2.2 SHIP RESISTANCE COMPONENTS	16
2.3 WAKE	20
2.3.1 <i>Wake components</i>	20
2.3.2 <i>Wake distribution</i>	20
2.4 SCALE EFFECTS	22
2.4.1 <i>General scale effects</i>	22
2.4.2 <i>Wake scale effects</i>	22
2.5 CFD.....	23
2.5.1 <i>What is CFD</i>	23
2.5.2 <i>Main phases in CFD analysis process</i>	25
3 CFD ANALYSIS METHODOLOGY	27
3.1 DISCRETIZATION METHOD	27
3.2 VISCOUS TURBULENT FLOW SOLVER (RANS).....	28
3.3 CFD TOOL	33
4 CASE STUDY.....	34
4.1 SHIP MODEL FOR ANALYSIS.....	34
4.2 SET UP FOR SIMULATION	35
4.2.1 <i>Boundary conditions</i>	35
4.2.2 <i>Meshing</i>	36
4.2.3 <i>Physics</i>	36
4.2.4 <i>Interface capturing scheme</i>	36
5 RESULTS.....	38
5.1 MESH.....	38
5.2 TURBULENCE MODEL.....	40

5.3	TIME STEP & CFL NUMBER.....	41
5.3.1	<i>Model scale</i>	41
5.3.2	<i>Full scale</i>	43
5.4	FORCE COEFFICIENTS	46
5.4.1	<i>Ct, Cf and Cp in model scale</i>	47
5.4.2	<i>Ct, Cf and Cp in full scale</i>	48
5.4.3	<i>Cp comparison in model and full scale</i>	50
5.5	SURFACE ELEVATION	51
5.6	NOMINAL WAKE	53
5.6.1	<i>Nominal wake fraction on a propeller plane</i>	54
5.6.2	<i>Averaged wake on propeller plane</i>	55
6	DISCUSSION	59
6.1	APPLIED SETTINGS	59
6.1.1	<i>Mesh</i>	59
6.1.2	<i>Turbulence model</i>	60
6.1.3	<i>Time step</i>	61
6.2	SCALE EFFECTS OF FORCE COEFFICIENTS	62
6.3	SCALE EFFECTS OF NOMINAL WAKE FIELDS	63
7	CONCLUSIONS	64
8	FURTHER WORK	66
	REFERENCES	68
	APPENDIX	70

LIST OF FIGURES

Figure 2-1 Waves and wake [1]	16
Figure 2-2 frictional and pressure forces [1]	17
Figure 2-3 Measurement of total viscous resistance [1]	18
Figure 2-4 Basic resistance components [1]	18
Figure 2-5 Detailed resistance components [1]	19
Figure 2-6 Wake distribution: twin-screw vessel. [1]	21
Figure 2-7 Influence of after body shape on wake distribution. [1]	21
Figure 2-8 Model and full-scale boundary layers. [1]	23
Figure 4-1 Ship geometry STX413	34
Figure 5-1 Positions of volume controls. a) Scaled model & domain, b) Scaled model & domain (2)	39
Figure 5-2 Residuals. a) Directly scaled mesh, b) Scaled model & domain	40
Figure 5-3 CFL number on free surface in model scale. a) time step=0.025s, b) time step=0.05s	41
Figure 5-4 Residuals in model scale. a) time step=0.025s, b) time step=0.05s	42
Figure 5-5 Cp force coefficient plot throughout full simulation. a) time step=0.05s, b) time step=0.15s, c) time step=0.15&0.05s	44
Figure 5-6 Cp force coefficient plot in last 100 seconds. a) time step=0.05s, b) time step=0.15s, c) time step=0.15&0.05s	44
Figure 5-7 Residuals of full scale simulations. a) time step=0.05s, b) time step=0.15s, c) time step=0.15&0.05s	45
Figure 5-8 Ct and Cf plot (model scale)	47
Figure 5-9 Cf & Cp for last 20 seconds of simulation (full scale, Fr=0,2628)	48
Figure 5-10 Ct & Cf plot (full scale)	50
Figure 5-11 Cp plots. Blue – model and orange – full scale	51
Figure 5-12 Generated surface elevation in full scale	51
Figure 5-13 Model scale FS elevation	52
Figure 5-14 Full scale FS elevation	52
Figure 5-15 Model scale	53
Figure 5-16 Full scale	53
Figure 5-17 Nominal wake fraction. Model scale	54
Figure 5-18 Nominal wake fraction. Full scale	54
Figure 5-19 Wake distribution on model scale	55
Figure 5-20 wake distribution in full scale	55
Figure 5-21 Fr=0,2628	57
Figure 5-22 Mean wake in model and full scale simulations	58

Figure 6-1 Cp force coefficients. a) Directly scaled mesh, b) Scaled geometry & domain.....	60
Figure 7-1 Averaged nominal wake fraction on a propeller plane.....	65
Figure 0-1 $Fr=0,2628$	109

LIST OF TABLES

Table 4-1 Ship main particulars in model and full scale.....	35
Table 4-2 Propeller parameters in model and full scale.....	35
Table 5-1 Amount of cells in model and full scale	38
Table 5-2 Force coefficients.....	41
Table 5-3 Force coefficients calculated on different time step	43
Table 5-4 Summary of three simulations of different time step	43
Table 5-5 Set of different Fr numbers for simulations.....	46
Table 5-6 Force coefficients in model scale simulations	47
Table 5-7 Force coefficients in full scale simulations.....	49
Table 5-8 Cp in model and full scale simulations	50
Table 5-9 Comparison between surface min & max elevation points	52
Table 5-10 Averaged wake fraction distribution ($Fr=0,2628$)	56
Table 5-11 Mean nominal wake fraction values in model and full scale.....	58
Table 6-1 Force coefficients according to turbulence model.....	60
Table 7-1 Summary of domain size	64
Table 7-2 Summary of time step used.....	64
Table 7-3 Summary of force coefficient results	65

TERMINOLOGY

Symbols

$\vec{F} = (F_x, F_y, F_z)$	Body forces [N]
$\vec{U} = (u, v, w)$	Fluid velocities in x, y and z directions [m/s]
$\bar{u}, \bar{v}, \bar{w}$	Mean values of velocities in directions of x, y, z [m/s]
μ_t	Turbulent viscosity [N*s/m ²]
Δt	Time step [sec]
Δx	Cell size [m]
∇	Displacement [m ³]
CB	Block coefficient
C_F	Skin friction/shear force coefficient
C_P	Pressure force coefficient
C_T	Total force coefficient
D	Propeller diameter [m]
Fr	Froude number
g	gravity [m/s ²]
L	length of body [m]
L_m	length of ship model [m]
P	pressure [Pa]
Re	Reynolds number
Sw	Wetted surface area [m ²]
T	Draft [m]
u', v', w'	Fluctuations of velocities in directions of x, y, z [m/s]
V	velocity [m/s]
w_t	wake fraction
λ	scale factor
ρ	Density [kg/m ³]
τ	tangential shear force [N]
Bwl	Maximum beam in waterline [m]
Lpp	Length between perpendiculars [m]
μ	Dynamic viscosity [N*s/m ²]
ϑ	Kinematic viscosity [m ² /s]

Abbreviations

CFD	Computational Fluid Dynamics
CFL	Courant Friedrichs Lewy condition
FS	Free Surface
HRIC	High Resolution Interface Capturing
ITTC	International Towing Tank Conference
RANS	Reynolds Averaged Navier-Stokes

1 INTRODUCTION

Today, the offshore maritime community is witnessing continuous decrease of oil prices all over the globe, which leads to less profitable offshore operations. As a result ship building industry faced a huge impact in terms of numbers of new orders. Designers nowadays have to be as efficient as possible in order to create best possible design solution at affordable price range for customers. One way to achieve this kind of goal would be investigations of fluid dynamics, which could be an alternative to experimental testing or at least decrease of these tests. CFD analysis of various problems could save lot of time compared to experiments, and in present days - time=money. A bigger implementation of CFD in marine industry also caused a window for developing more efficient and less polluting various systems, such as propulsors.

This Master Thesis contains with an investigation to the scale effects on a wake field behind twin screw vessel, in particular anchor handler STX-413. To analyse problem related to scale effects computational fluid dynamics software was used. The most important point in this project is to perform towing tank resistance tests in model and full scale ship. These resistance tests are performed in number of various Froude values, due to get a good understanding how scaling effect vessel parameters such as: resistance force coefficients (C_f , C_p and C_t), surface elevation and velocity on the propeller plane in order to get wake fraction.

1.1 *Project background*

Master Thesis done by candidate in Alesund University College is a part of Propscale project developed by Marintek in Trondheim. Propscale project's primary objective for the present is knowledge-building, to acquire theoretical knowledge and develop practical methods for the accurate prediction of full-scale performance of the vessels equipped with innovative propulsion systems. Mission target can be achieved by means of:

- Development and application of the state-of-the-art numerical methods offered by Computational Fluid Dynamics (CFD) to the analysis of novel propulsor concepts and hull-propulsor interaction.
- Systematic verification and validation of the numerical methods with the primary focus on the problem of scale effect and full scale performance prediction.
- Bringing the methods of CFD for ship propulsion to the level of practical design and production tool.

- Elaboration of recommendations and guidelines regarding full scale performance prognosis for vessels equipped with innovative propulsion systems.
- Increasing the level of cooperation between the industrial, academic and research sectors.

CFD analysis tool have to be used in order to deal with this Master project investigation, and software which is obtained as main results performing program is STAR CCM+ by CD-Adapco company. Alesund University College provide a license key for candidate to perform CFD analysis in so called “CFD machine” on virtual desktop solution. Limitations for performance were set to be 8 processors with approx. 10 GB of RAM memory.

Computations is performed by the method called RANS. This is most common methodology to solve various fuscous flow problems. Method is based on few main assumptions: fluid is incompressible and viscosity not varying from point to point. Also in this method components of flow velocity and pressure are represented as superposition of their mean values and imposed turbulent fluctuations. Then Reynolds Averaged Navier-Stokes (RANS) equations can be solved by implementing turbulence model, where in this project $k-\omega$ turbulence model was used.

1.2 Problem formulation

To design propulsion system designer needs to take into account things like, what kind of resistance ship have, how big is hull efficiency, machinery systems, type of propulsor, etc. As it was already mentioned this project deals with scale effects of the wake field on a propeller plane. Presents of that effect is also import as all other things which have to be weighted before taking decision what system for propulsion should be used.

Scaling model to full scale it is crucial to know for designer, what will be real values. This can lead to more advance design solutions, when architects will have a good prediction model and understanding how values in a wake field would be changed when full size product will be under operations. By performing towing tank resistance tests in both model and full scale, with help of CFD tools, designer can investigate nominal wake on a propeller plane effected by scaling. This could help for naval architect to:

- Design better stern shapes in order to get more evenly distributed wake along the propeller, this would lead to for example less vibrations or even better overall propulsion system efficiency.
- Achieve same propeller characteristics with less performance from power plant.

- Decrease of exhaust emissions.

1.3 Objectives

Purpose of this Master Thesis is to analyse presents of scale effects on nominal wake field behind twin screw vessel. Thesis contains simulations of full and model scale ship hulls, to determine wake fields. This is done in case where vessel is in fixed position without sinkage and trim. Results in the project have been analysed and their differences been defined, which appeared due to scale effects made on simulations for model and full scale ship hulls.

Thesis contain with:

E. Literature study

- Ship resistance/propulsion
- Wake field
- Scale effects
- CFD
 - Navier–Stokes equations
 - Viscous/turbulent flows
 - RANS

F. Definition of computational model

- Mesh type & size
- Boundaries
- Turbulence model
- Initial conditions
- Free surface modelling

G. Analysis set up for case study

- Froude numbers
- Drought

H. Results comparison/post processing

- Full & model scale
 - Nominal wake field
 - Resistance
 - Surface elevation

2 BACKGROUND AND THEORETICAL BASIS

This section gives a brief description about theoretical background, which will be applied in Master Thesis Project. The subchapters gives an overview what kind of background information is generally used to do towing tank simulation in full and model scale due to finding the scale effects behind of the vessel, precisely on the propeller plane.

The chapter contains only background foundation for how towing tank tests are performed, what are resistance components, which will be looked further for validation of the simulation results. Also general information about wake scale effects and CFD are given.

2.1 Towing tank tests

Towing tanks and experimental set-up

Despite the ever increasing importance of numerical methods for ship hydrodynamics, model tests in towing tanks are still seen as an essential part in the design of a ship to predict (or validate) hull resistance and the power requirements in calm.

The prediction methodology of a ship's resistance came from William Froude, who presented his approach in 1874 to the predecessor of the RINA in England. "His hypothesis was that the ship resistance is divisible into frictional and wave making resistance, with the wave making resistance following his 'law of comparison' (Froude similarity). This ingenious concept allowed Froude to show, for the first time, how the resistance of a full-scale ship may be determined by testing scale models. His success motivated building the first model basin in 1879 in Torquay, England. Soon further model basins followed in Europe and the USA". [3]

Tests are usually carried out in towing tanks, where the water is still and the model is towed by a special equipment (carriage). The carriage in a towing tank keeps its speed with high precision. The model is kept on course by special wires at the ship ends. Usually, models are free to trim and sink. After the initial acceleration, sometime has to pass before a stationary state is reached. Then the remaining measuring time is determined by the remaining towing tank distance and the deceleration time of the carriage. Due to that, towing tanks usually are sufficiently long, that can be several hundred meters, and this allows sufficient measuring time.

The model size is determined by a number of boundary conditions:

- The model should be as large as possible to minimize viscosity scale effects, especially concerning laminar/turbulent flow and flow separation.

- The model should be small enough to avoid strength problems (both internal strength of the model and loads on the test carriage).
- The model should be small enough such that the corresponding test speed can be achieved by the carriage.
- The model should be small enough to avoid noticeable effects of restricted water in the test basin. [3]

Those boundary conditions leads to a bandwidth of acceptable model sizes. Typically models for resistance and propulsion tests have a size $4\text{m} \leq L_m \leq 10\text{ m}$. Model scales range between $15 \leq \lambda \leq 45$, where L_m – model length, λ – scale.

Tests are performed keeping similarity of Froude number, i.e. number of model and full scale are the same. The scale effect of not keeping similarity of Reynolds number is compensated with the empirical corrections. Usually Reynolds number for model and full scale varies by two orders of magnitude.

“Models operate at considerably lower Reynolds numbers. (Typically for models $R_n \approx 10^7$ and for full-scale ships $R_n \approx 10^9$.), where:

$$Rn = \frac{vL}{\vartheta}; \quad (2.1)$$

v – velocity [m/s];

ϑ – kinematic viscosity [m²/s];

L – length of body [m].

This means that in the model the transition from laminar to turbulent flow occurs relatively further aft. As a consequence, the resistance would be more difficult to scale. Therefore, the model is equipped with artificial turbulence stimulators (sand strip, studs, or trip wire) in the fore body. One assumes that the transition from laminar to turbulent flow occurs at a length corresponding to $R_n = 0.5 \cdot 10^6$ from the stem. In practice, often the turbulence stimulators are located somewhat further aft. Then the reduced resistance due to the longer laminar flow compensates (at least partially) the additional resistance of the turbulence stimulators.” [3]

2.2 Ship resistance components

It is necessary to have an idea about components of ship resistance and their behaviour, in order to use them when it comes to scaling resistance from model to full size. Wrong estimations of hull resistance, could be a cause of under/over powered propulsive system.

“Observation of a ship moving through water indicates two features of the flow, Figure 2.2-1, namely that there is a wave pattern moving with the hull and there is a region of turbulent flow building up along the length of the hull and extending as a wake behind the hull. Both of these features of the flow absorb energy from the hull and, hence, constitute a resistance force on the hull. This resistance force is transmitted to the hull as a distribution of pressure and shear forces over the hull; the shear stress arises because of the viscous property of the water. This leads to the first possible physical breakdown of resistance which considers the *forces acting* [1]:

- **Frictional resistance**

The fore and aft components of the tangential shear forces τ acting on each element of the hull surface, Figure 2-1, can be summed over the hull to produce the total shear resistance or *frictional resistance*.

- **Pressure resistance**

The fore and aft components of the pressure force P acting on each element of hull surface, Figure 2-2, can be summed over the hull to produce a *total pressure resistance*.

The frictional drag arises purely because of the viscosity, but the pressure drags due in part to viscous effects and to hull wave making. An alternative physical breakdown of resistance considers *energy dissipation*.

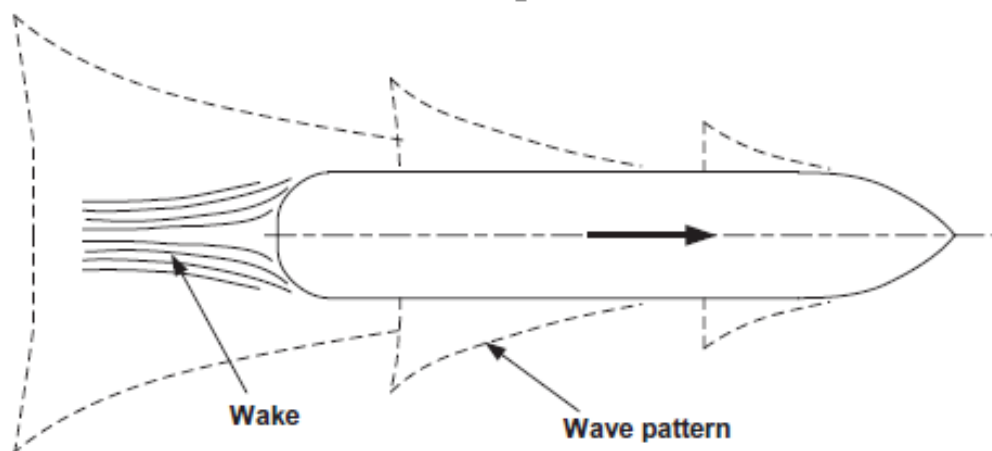


Figure 2-1 Waves and wake [1]

- **Total viscous resistance**

Bernoulli's theorem (eq. 2.2.) states that and, in the absence of viscous forces, H is constant throughout the flow. By means of a Pitot tube, local total head can be measured.

$$H = \frac{P}{\rho g} + \frac{v^2}{2g} + h; \quad (2.1)$$

Where P – pressure, v – velocity, g – gravity, h – height, H – total height.

Since losses in total head are due to viscous forces, it is possible to measure the *total viscous resistance* by measuring the total head loss in the wake behind the hull, Figure 2-3.

This resistance will include the skin frictional resistance and part of the pressure resistance force, since the total head losses in the flow along the hull due to viscous forces result in a pressure loss over the after body which gives rise to a resistance due to pressure forces.

- **Total wave resistance**

The wave pattern created by the hull can be measured and analysed into its component waves. The energy required to sustain each wave component can be estimated and, hence, the *total wave resistance* component obtained. Thus, by physical measurement it is possible to identify the following methods of breaking down the total resistance of a hull:

- Pressure resistance + frictional resistance
- Viscous resistance + remainder
- Wave resistance + remainder

These three can be combined to give a final resistance breakdown as:

Total resistance = Frictional resistance + Viscous pressure resistance + Wave resistance

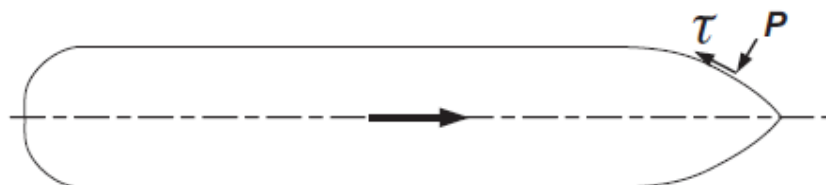


Figure 2-2 frictional and pressure forces [1]

Where, τ - tangential shear force, P – pressure force.



Figure 2-3 Measurement of total viscous resistance [1]

It should also be noted that each of the resistance components obeys a different set of scaling laws and the problem of scaling is made more complex because of interaction between these components.

According to [1], these basic hydrodynamic components of ship hull resistance can be summarized as shown in Figure 2-4. When considering the forces acting, the total resistance is made up of the sum of the tangential shear and normal pressure forces acting on the wetted surface of the vessel, as shown in Figure 2-2 and at the top of Figure 2-4.

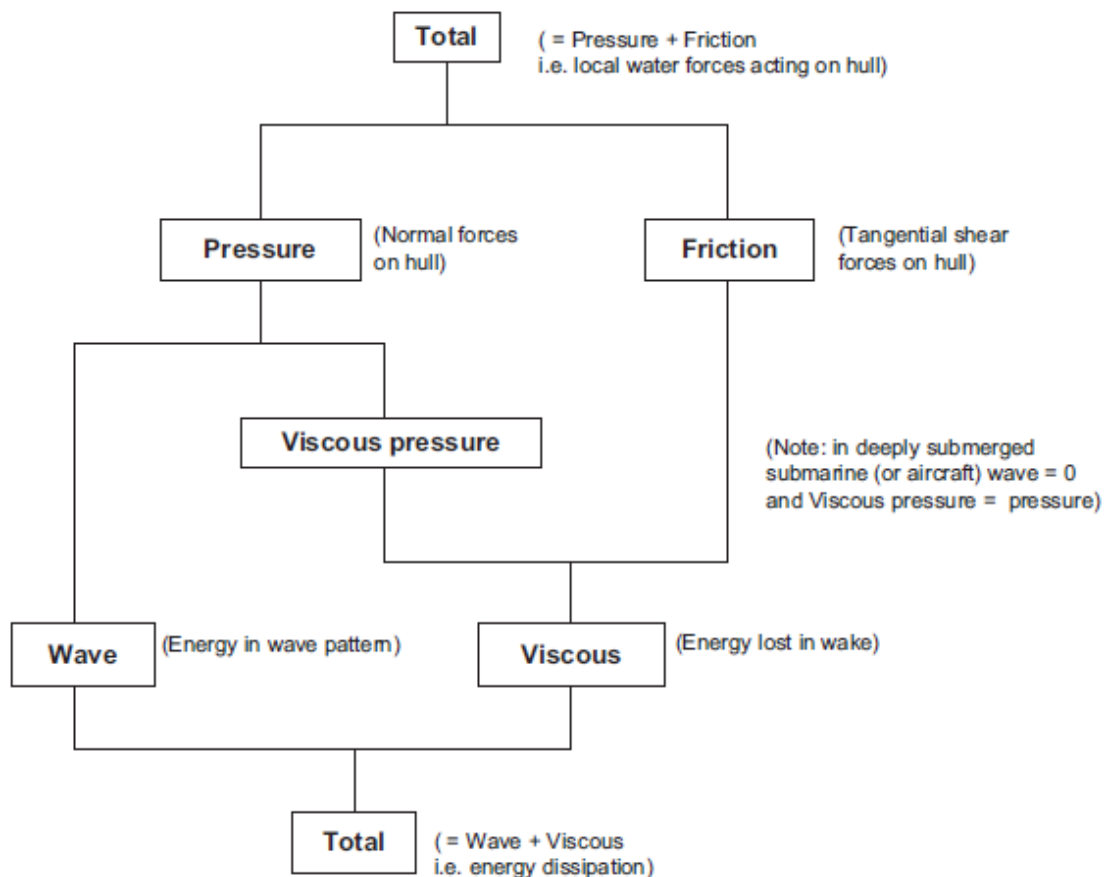


Figure 2-4 Basic resistance components [1]

Figure 2-5 shows a more detailed breakdown of the basic resistance components together with other contributing components, including wave breaking and spray, transom and induced drag. The total skin friction in Figure 2-5 has two subdivisions: two-dimensional flat plate friction and three-dimensional effects.

“Wave breaking and spray can be important in high-speed craft and, in the case of the catamaran, significant wave breaking may occur between the hulls at particular speeds. Wave breaking and spray should form part of the total wave making resistance, but, in practice, this energy will normally be lost in the wake; the dotted line in Figure 2-5 illustrates this effect.

The transom stern, used on most high-speed vessels, is included as a pressure drag component. It is likely that the large low-pressure area directly behind the transom, which causes the transom to be at atmospheric pressure rather than stagnation pressure, causes waves and wave breaking and spray which are not fully transmitted to the far field. Again, this energy is likely to be lost in the wake, as illustrated by the dotted line in Figure 2-5.

Induced drag will be generated in the case of yachts, resulting from the lift produced by keels and rudders. Catamarans can also create induced drag because of the asymmetric nature of the flow between and over their hulls and the resulting production of lift or side force on the individual hulls.” [Ship resistance and prop]

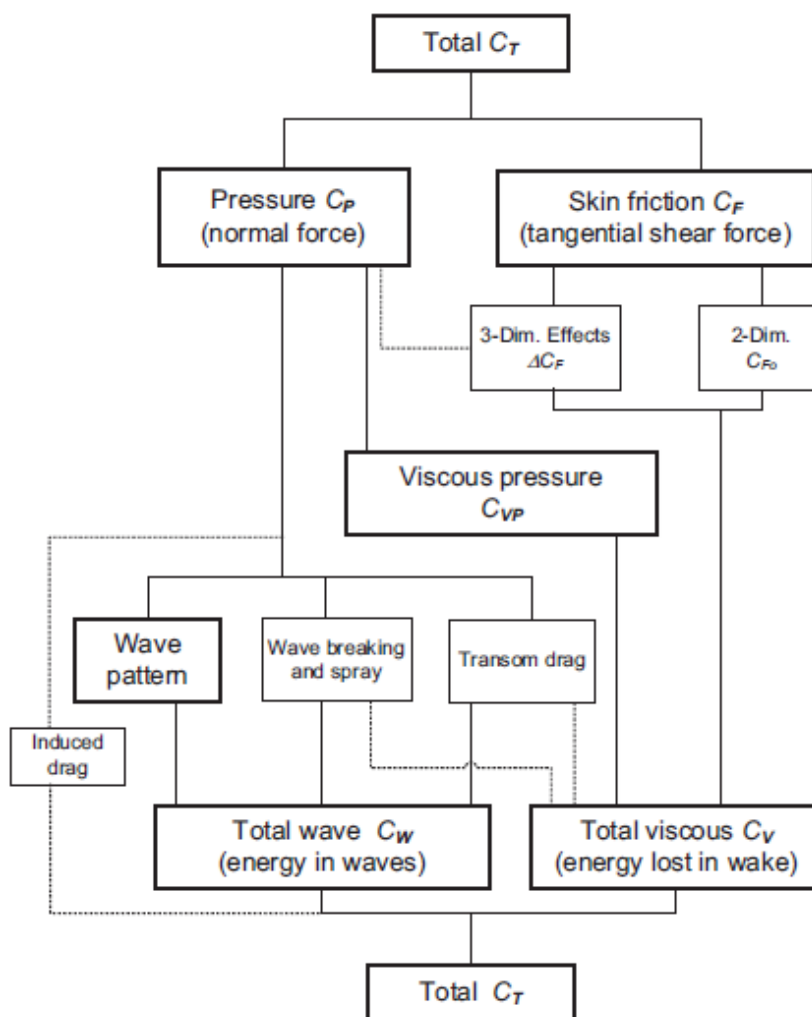


Figure 2-5 Detailed resistance components [1]

2.3 Wake

Flow around propeller is effected by the presence of a hull (stern shapes, appendixes, etc.), development of wake appears where potential and viscous flow nature is contributing on the boundary layer. The propeller inflow is generally slower than the vessel speed due to the created wake.

“The wake behind the ship without propeller is called the nominal wake. The propeller action accelerates the flow field by typically 5–20%. The wake behind the ship with operating propeller is called the effective wake. The wake distribution is either measured by laser-Doppler velocimetry or computed by CFD”. [3]

2.3.1 Wake components

The wake itself comes from three main sources:

- **Potential wake**

In an ideal fluid without viscosity and free surface, the flow velocity at the stern resembles the flow velocity at the bow, featuring lower velocities with a stagnation point.

- **Frictional wake**

Potential flow causes retardation of the flow inside ships boundary layer and this flow layer thickness increases towards the stern. Frictional wake comes due to the hull surface skin friction effects. This wake component is around 80-90% of total wake. Vessels which are single screw mainly operates in viscous wake so this is important effect, but twin screws operates outside frictional wake, so therefore this components is less important.

- **Wave wake**

This component originates from waves generated by ship, which have orbital motions so crests above the propeller increases the wake fraction, a wave trough decreases it. Wave wake component in single screw vessels normally is small, but in twin screw ships this component might be significant due to location of the propeller, which closer to free surface.

2.3.2 Wake distribution

General Distribution. The presents of the hull shape at the aft end and boundary layer development effects, the wake distribution is non-uniform in the general vicinity of the

propeller. An example of the wake distribution (contours of constant wake fraction w_T) for a twin-screw vessel is given in figure 2-6. Twin-screw ship's typical wake distribution showing the effects of the boundary layer and local changes around the shafting and bossings. The average wake fraction for twin-screw vessels is normally less than for single-screw vessels.

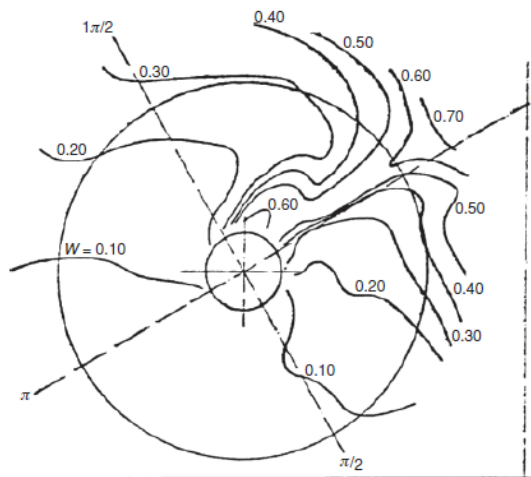


Figure 2-6 Wake distribution: twin-screw vessel. [1]

Different hull stern shapes usually lead to different wake distributions, which are shown in figure 2-7. “It can be seen that as the stern becomes more ‘bulbous’, moving from left to right across the diagram, the contours of constant wake become more ‘circular’ and concentric. This approach may be adopted to provide each radial element of the propeller blade with a relatively uniform circumferential inflow velocity, reducing the levels of blade load fluctuations”. [1]

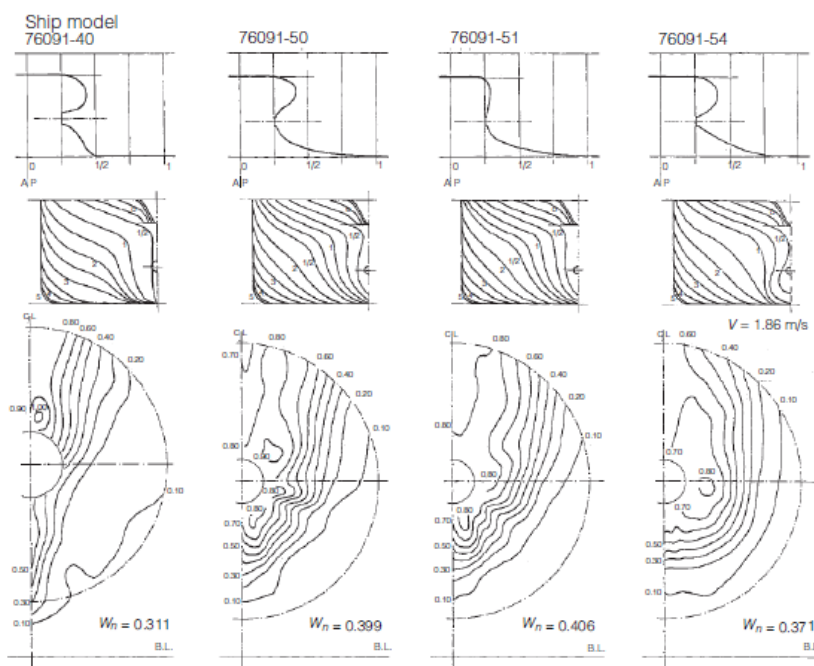


Figure 2-7 Influence of after body shape on wake distribution. [1]

2.4 Scale effects

In the past naval architects were only relied on model tests when it comes to analyze and predict ship hydrodynamics. With the progress in CFD and a series of dedicated validation workshops and research projects, designers are able to analyze more complicated cases and compare results in model and full scale. CFD becoming more and more important in cases where it is crucial to simulate in both scales (full & model) objects and validate them with empirical data, which have been obtain from model tests.

2.4.1 General scale effects

According to the published paper [14] there are three main scale effects:

- “[...] Boundary layer. The boundary layer is relatively thinner in full-scale flows than in model test conditions. The wake fraction is therefore larger in model tests than in full scale. Propulsion improving devices operate (at least partially) in the boundary layer, which results in different behaviour of such devices between model scale and full scale.
- Flow separation and vortex formation. Flow separation is generally delayed in full scale and vortices encounter higher damping. Thus ship wakes in the propeller plane are significantly changed. Vortices from bilge or struts are much weaker and vanish sometimes altogether in full-scale simulations, e.g. Visonneau et al. (2006).
- Wave breaking. The decomposition of a ship resistance into wave resistance, frictional resistance and viscous pressure resistance is artificial. In reality, wave making and viscous flows interact. Changes in the viscous flow field lead to changes in the wave pattern. Especially in the aft body, this interaction can be significant. Mizine et al. (2009) give an example, where the modification of the pressure field results in a local suction of the free-surface leading to local wave breaking, which dramatically increases the resistance.

Visonneau et al. (2006) come to the conclusion that a “[...] complete analysis of the scale effects on free-surface and of the structure of the viscous stern flow reveals that these scale effects are not negligible and depend strongly on the stern geometries.” [14]

2.4.2 Wake scale effects

The model boundary layer when scaled (see figure 2-8) is thicker than the ship boundary layer. Hence, the wake fraction w_t tends to be smaller for the ship, although extra ship roughness

compensates to a certain extent. Detailed full-scale measurements of wake are relatively sparse. Work, such as by Lubke, is helping to shed some light on scale effects, as are the increasing abilities of CFD analyses to predict aft end flows at higher Reynolds numbers. Lubke describes an investigation into the estimation of wake at model and full scale. At model scale the agreement between computational fluid dynamics (CFD) and experiment was good. The comparisons of CFD with experiment at full scale indicated that further validation was required. [1]

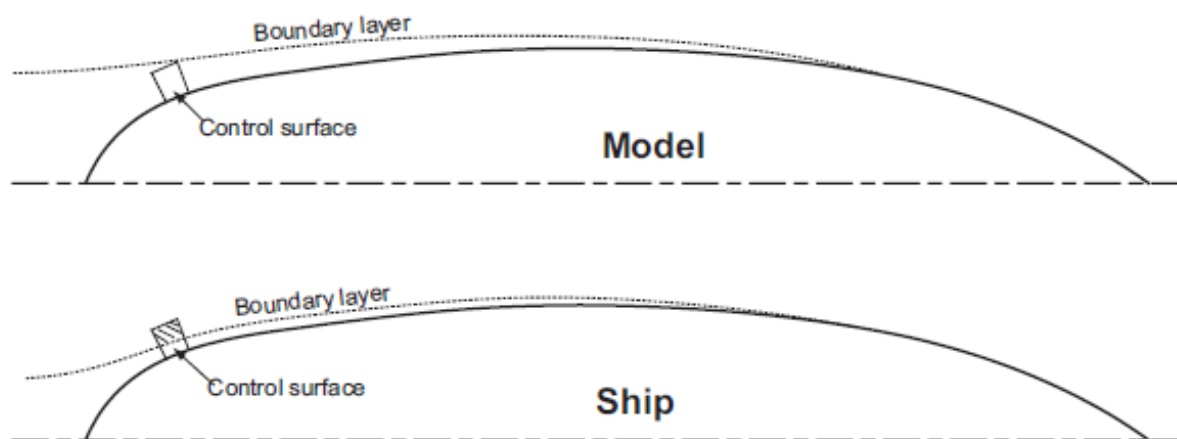


Figure 2-8 Model and full-scale boundary layers. [1]

2.5 CFD

CFD is known as Computational Fluid Dynamics, within this topic is given brief overview what is CFD, where these computational analysis can be applied. Also the activities, where user is involved during whole simulation process and furthermore what kind of CFD analysis tool is used in this Master Project.

2.5.1 What is CFD

“Computational Fluid Dynamics, or CFD, is the computational technology for the analysis of systems involving fluid flow, heat transfer and associated phenomena by means of Computer – based simulation. This technology employs numerical methods and algorithms to solve the equations that describe fluid flows and heat transfer.

Computers are used to prepare the data, build computational domain and mesh, perform numerical solution of the equations, and to analyse the solution results. The equations that describe the dynamics of fluid represent fundamental laws of physics stating conservation of mass, momentum and energy.” [4].

In other words according to [2], to obtain an approximate solution numerically in a simulation, it needs to use a discretization method which approximates the differential equations by a system of algebraic equations, which can then be solved on a computer. The approximations are applied to small domains in space and/or time so the numerical solution provides results at discrete locations in space and time. Much as the accuracy of experimental data depends on the quality of the tools used, the accuracy of numerical solutions is dependent on the quality of discretization used.

Thus, CFD is intended to model realistic media and various bodies interacting with it by virtual (non-physical) means, and to predict their behaviour under different conditions.” [4]

Currently CFD are widely applicable in a wide range of cluster in several different areas. According [4] the application areas could be:

- Aerodynamics of aircraft and space vehicles (prediction of lift and drag, and air flow analysis);
- Ship and propulsor hydrodynamics (prediction of resistance, propulsor characteristics, cavitation, manoeuvring forces);
- Marine engineering (estimation of wind, wave and current loads on offshore structures);
- Power plant technological processes (combustion processes in engine and gas turbines, functions of cooling systems);
- Turbomachinery (analysis of flow in rotating blade-row passages and diffusers, cavitation);
- Chemical process engineering (studies on chemical reactions, mixing, separation, polymer moulding);
- Architecture and building construction (calculation of wind loads on buildings, design of heating, ventilation, water supply and sewage systems); Environmental engineering (analysis of distribution of pollutants and effluents);
- Hydrology and oceanography (studies on flows in rivers, estuaries, oceans);
- Meteorology (weather prediction and long term climate forecasting);
- Biomedical engineering (modelling of blood flows through arteries and veins).

In the maritime cluster, CFD analysis for viscous flows are used since 1980-s, where in 1990s there have been a huge progress within an introduction of greater computing power and the development of advanced computational technique. “However, compared to the structural

stress analysis tools, CFD methods are still significantly less mature. This is due to much more complex nature and behaviour of fluid flows which have impact on both the development of CFD methods and their practical application.

After the main equations describing the fluid motion have been obtained and proved, it has been found that their exact analytical solutions are possible only for a limited number of conditions, many of which have little value for practice. These analytical solutions are very important as test examples for the verification of numerical models, but they can hardly be used directly when one needs to study, for example, the flow around a wing, a ship hull, a propeller or an oil platform. The main problem is that the equations we have to solve are non-linear, partial differential or integral-differential, and mathematics simply does not have analytical solutions for such equations, in general case. Therefore, the exact solution of the equations governing fluid flow should be replaced by an approximate one, which is achieved by the discretization of the equations on some kind of computational mesh and their reduction to the linear systems that can be solved by means of corresponding mathematical methods. While it is possible theoretically, in practice such discretization often results in so fine meshes that even most powerful computer systems cannot handle them, or that the computation time required is unacceptable.” [4]

2.5.2 Main phases in CFD analysis process

According to [4], there are three main stages during CFD analysis:

- Pre-processing;
- Solving;
- Post-processing.

These three elements consists in all commercial CFD codes.

Pre-processing. At this point of CFD analysis, user have availability to input the data and create set up for problem, which have to be simulated. User who is setting up the simulation usually is involved with these pre-processing activities:

- Preparation of geometry;
- Definition and sub-division of computation domain;
- Choice of the mesh model and mesh generation;
- Definition of fluid properties;

- Selection and setup of the adequate solution models;
- Specification of appropriate boundary conditions.

Those activities are briefly described in [4].

Solving. There are four distinct streams of numerical solution techniques:

- Finite difference methods;
- Finite element methods;
- Spectral methods and
- Finite volume methods.

It is have to be mentioned that different views are expressed in CFD literature concerning the finite volume methods, which represent the main and most thoroughly validated tool for the solution of fluid motion equations. According to [4] opinion, the principle of discretization employed in finite volume methods and their “conservativeness by construction” is most important thing in finite volume method. “These features are sufficient to assign finite volume methods to a separate stream.

In short, all numerical methods that are used for solving the governing flow equations shall perform the following steps:

- Approximation of the unknown variables by means of simple functions;
- Discretization of governing flow equations by substitution of these approximations and subsequent reduction to a system of algebraic equations;
- Solution of the algebraic equations.” [4]

The main differences between 4 different solution techniques are associated with the ways in which the flow variables are approximated and the discretization is done.

Post-processing “in CFD serves the purposes of facilitation of solution setup, execution control and interpretation of simulation results. With constantly improving graphics capabilities of modern PCs and workstations, visualization tools in CFD play more and more important role and become more elaborate and, at the same time, user friendly. It is fair to say that post-processing begins already at the pre-processing stage when one visualizes domain geometry and displays generated surface and volume meshes.” [4]

Very crucial thing what can give work done on post-processing in pre-processing stage, is that user is able to avoid critical mistakes in early stage, which will lead in saved time and increased

accuracy. Avoidance of mistakes can be simply achieved by investigating model surfaces or mesh quality. While computer is computing solution, user for instance is able to monitor residuals or desired integral flow characteristics, such as forces, surface averaged and volume averaged fluxes, etc. By monitoring these convergence of the iterative processes is under control.

After the solution is obtained, post-processing tools allow to visualize numbers of desirable values, distribution tables, three dimensional surface scenes, vector diagrams, streamline, etc. The most advanced post-processing tools gives possibility to create animations of dynamic computation results, which can be both the post-execution and runtime. In addition to graphics, all codes produce alphanumeric output and provide data converters to save results in formats that can further be used by external programs. [4]

3 CFD ANALYSIS METHODOLOGY

To analyse any existing problem, which requires CFD simulation, engineers need to have basic knowledge about what they are doing, i.e. what kind of mathematical model should be describing simulation domain, and basic physics behind that. First and most important thing in simulation should be decision, how the simulation domain should be discretized. When it is clear what discretization model will be used, next step is to choose solver, accord which the computation is done.

For case, which is under question in this master thesis the RANS viscous turbulent flow solver is chosen, because it is most popular when it comes to calculate viscous turbulent flow in marine CFD analysis. RANS code have most of commercial use CFD analysis tools, this solver method provides solution of Navier-Stokes equation in good precision and reasonable time consumption. In order to solve turbulent flows, this solver comes with turbulence models, which are key components to solve momentum equations, there are empirical or semi-empirical turbulence models. In this project $k-\epsilon$ and $k-\omega$ turbulent models are under investigation.

3.1 Discretization method

The finite volume method for discretization of domain is spread in most of commercial CFD codes, the Star CCM+ is no exception, which is actually used for simulations in this project. The finite volume method first was introduced in 1971 by McDonald and 1972 by MacCormack

& Paullay. The method works with the cell volumes for solution with time depended Euler equations, which describes ideal fluid.

“The method employs discretization of the integral form of the conservation equations directly in physical space. Therefore, the resulting equations express the exact conservation of relevant fluid characteristics for each finite cell volume (also referred to as “control volume”).” [4]

This method is suitable for complex geometries, because it is valid for arbitrary shape of cells, and is working with all types of mesh, which includes: structured, unstructured or hybrid.

More information about discretization methods, especially finite volume method can be found in [2].

3.2 Viscous turbulent flow solver (RANS)

The RANS, i.e. Reynolds Averaging of Navier Stokes equations, approach is based on time averaging of general transport equations (eq. 3.1 – 3.4) and representation of total flow characteristics (velocity and pressure) as a sum of averaged and fluctuating values.

Continuity equation:

$$\nabla(\vec{U}) = 0 \quad (3.1)$$

Momentum (Navier-Stokes) equations:

$$\rho \frac{Du}{Dt} = -\frac{\partial p}{\partial x} + \frac{\partial}{\partial x} \left(2\mu \frac{\partial u}{\partial x} \right) + \frac{\partial}{\partial y} \left[\mu \left(\frac{\partial v}{\partial x} + \frac{\partial u}{\partial y} \right) \right] + \frac{\partial}{\partial z} \left[\mu \left(\frac{\partial u}{\partial z} + \frac{\partial w}{\partial x} \right) \right] + \rho F_x; \quad (3.2)$$

$$\rho \frac{Dv}{Dt} = -\frac{\partial p}{\partial y} + \frac{\partial}{\partial x} \left[\mu \left(\frac{\partial u}{\partial y} + \frac{\partial v}{\partial x} \right) \right] + \frac{\partial}{\partial y} \left(2\mu \frac{\partial v}{\partial y} \right) + \frac{\partial}{\partial z} \left[\mu \left(\frac{\partial v}{\partial z} + \frac{\partial w}{\partial y} \right) \right] + \rho F_y; \quad (3.3)$$

$$\rho \frac{Dw}{Dt} = -\frac{\partial p}{\partial z} + \frac{\partial}{\partial x} \left[\mu \left(\frac{\partial u}{\partial z} + \frac{\partial w}{\partial x} \right) \right] + \frac{\partial}{\partial y} \left[\mu \left(\frac{\partial v}{\partial z} + \frac{\partial w}{\partial y} \right) \right] + \frac{\partial}{\partial z} \left(2\mu \frac{\partial w}{\partial z} \right) + \rho F_z \quad (3.4)$$

Where:

$$\frac{D}{Dt} = \frac{\partial}{\partial t} + u \frac{\partial}{\partial x} + v \frac{\partial}{\partial y} + w \frac{\partial}{\partial z} \quad (3.5)$$

ρ – water density;

$\vec{U} = (u, v, w)$ – fluid velocities in x, y and z directions;

p – pressure;

μ – dynamic viscosity;

$\vec{F} = (F_x, F_y, F_z)$ body force.

For finite volume method the most convenient formulation are Navier Stokes (eq 3.2-3.4) also known as momentum equations.

In their general form, the transport equations governing fluid flow as shown above are coupled, non-linear partial differential equations. “Such equations do not allow for an analytical solution, in general case, and it is difficult to prove by the existing mathematical methods that a unique solution to these equations exists for particular boundary conditions. However, a number of simplified flow models can be derived from the general formulation to approximate the solution in those cases where some of the contributions are irrelevant or unimportant and, therefore, can be neglected. Such simplifications always introduce a certain error, but still remain adequate for a range of flows of practical interest. While, in most cases, even the simplified equations can only be solved numerically (no analytical solution exists), the computational efforts appear reduced which makes the simplification justified.” [4]

One of the simplified flow models would be *incompressible fluid*, which means that incompressible flow has constant density from point to point and does not change with time. Also another assumption in this model is that if the fluid is isothermal then viscosity μ is also constant. For the majority of marine problems solved by CFD simulation is done by adopting incompressible flow method. Keeping in mind these assumption in this model continuity equation becomes:

$$\nabla(\vec{U}) = \frac{\partial u}{\partial x} + \frac{\partial v}{\partial y} + \frac{\partial w}{\partial z} = 0 \quad (3.6)$$

Also model allows following transformations for momentum equations:

$$\begin{aligned} \rho \frac{Du}{Dt} &= -\frac{\partial p}{\partial x} + \frac{\partial}{\partial x} \left(2\mu \frac{\partial u}{\partial x} \right) + \frac{\partial}{\partial y} \left[\mu \left(\frac{\partial v}{\partial x} + \frac{\partial u}{\partial y} \right) \right] + \frac{\partial}{\partial z} \left[\mu \left(\frac{\partial u}{\partial z} + \frac{\partial w}{\partial x} \right) \right] + \rho F_x \\ &= -\frac{\partial p}{\partial x} + \mu \left[\left(\frac{\partial^2 u}{\partial x^2} + \frac{\partial^2 u}{\partial y^2} + \frac{\partial^2 u}{\partial z^2} \right) + \frac{\partial}{\partial x} \left(\frac{\partial u}{\partial x} + \frac{\partial v}{\partial y} + \frac{\partial w}{\partial z} \right) \right] + \rho F_x \end{aligned} \quad (3.7)$$

Because of the continuity equation (3.5), it is able to simplify even more:

$$\rho \frac{Du}{Dt} = -\frac{\partial p}{\partial x} + \mu \left(\frac{\partial^2 u}{\partial x^2} + \frac{\partial^2 u}{\partial y^2} + \frac{\partial^2 u}{\partial z^2} \right) + \rho F_x \quad (3.8)$$

The conservation of y and z momentum equations are derived same way:

$$\rho \frac{Dv}{Dt} = -\frac{\partial p}{\partial y} + \mu \left(\frac{\partial^2 v}{\partial x^2} + \frac{\partial^2 v}{\partial y^2} + \frac{\partial^2 v}{\partial z^2} \right) + \rho F_y \quad (3.9)$$

$$\rho \frac{Dw}{Dt} = -\frac{\partial p}{\partial z} + \mu \left(\frac{\partial^2 w}{\partial x^2} + \frac{\partial^2 w}{\partial y^2} + \frac{\partial^2 w}{\partial z^2} \right) + \rho F_z \quad (3.10)$$

Equations 3.8 – 3.10 are much simpler to solve numerically compared to the general equations (eq. 3.2-3.4). Non-linearity of those equations have immediate physical consequences in a system. Systems governed with non-linear momentum equations are tend to be unstable. “As far as fluids are concerned, these instabilities arise and grow due to the presence in the flow of eddies (vortices) of various scales which, above a certain value of Reynolds number, become engaged in a complicated series of events such as distortion and mutual interaction resulting in a random state of motion with velocity and pressure fields changing continuously in time within large flow domains. This mechanism has the name turbulence, and the unsteady flows whose properties are random functions of time are termed turbulent flows”. [4]

In order to avoid instabilities the components of flow velocity and pressure are represented as superposition of their mean values and imposed turbulent fluctuations:

$$u = \bar{u} + u' \quad (3.11)$$

$$v = \bar{v} + v' \quad (3.12)$$

$$w = \bar{w} + w' \quad (3.13)$$

Where \bar{u} , \bar{v} , \bar{w} are mean values and u' , v' , w' are fluctuations. Then transport equations becomes:

$$\frac{\partial \bar{u}}{\partial x} + \frac{\partial \bar{v}}{\partial y} + \frac{\partial \bar{w}}{\partial z} = 0 \quad (3.14)$$

$$\begin{aligned} & \rho \left(\frac{\partial \bar{u}}{\partial t} + \bar{u} \frac{\partial \bar{u}}{\partial x} + \bar{v} \frac{\partial \bar{u}}{\partial y} + \bar{w} \frac{\partial \bar{u}}{\partial z} \right) = \\ & = -\frac{\partial p}{\partial x} + \frac{\partial}{\partial x} \left(\mu \frac{\partial \bar{u}}{\partial x} - \rho \overline{u'u'} \right) + \frac{\partial}{\partial y} \left(\mu \frac{\partial \bar{u}}{\partial y} - \rho \overline{u'v'} \right) + \frac{\partial}{\partial z} \left(\mu \frac{\partial \bar{u}}{\partial z} - \rho \overline{u'w'} \right) + \rho F_x \end{aligned} \quad (3.15)$$

$$\begin{aligned} & \rho \left(\frac{\partial \bar{v}}{\partial t} + \bar{u} \frac{\partial \bar{v}}{\partial x} + \bar{v} \frac{\partial \bar{v}}{\partial y} + \bar{w} \frac{\partial \bar{v}}{\partial z} \right) = \\ & = -\frac{\partial p}{\partial y} + \frac{\partial}{\partial x} \left(\mu \frac{\partial \bar{v}}{\partial x} - \rho \overline{v'u'} \right) + \frac{\partial}{\partial y} \left(\mu \frac{\partial \bar{v}}{\partial y} - \rho \overline{v'v'} \right) + \frac{\partial}{\partial z} \left(\mu \frac{\partial \bar{v}}{\partial z} - \rho \overline{v'w'} \right) + \rho F_y \end{aligned} \quad (3.16)$$

$$\begin{aligned} & \rho \left(\frac{\partial \bar{w}}{\partial t} + \bar{u} \frac{\partial \bar{w}}{\partial x} + \bar{v} \frac{\partial \bar{w}}{\partial y} + \bar{w} \frac{\partial \bar{w}}{\partial z} \right) = \\ & = -\frac{\partial p}{\partial z} + \frac{\partial}{\partial x} \left(\mu \frac{\partial \bar{w}}{\partial x} - \rho \overline{w'u'} \right) + \frac{\partial}{\partial y} \left(\mu \frac{\partial \bar{w}}{\partial y} - \rho \overline{w'v'} \right) + \frac{\partial}{\partial z} \left(\mu \frac{\partial \bar{w}}{\partial z} - \rho \overline{w'w'} \right) + \rho F_z \end{aligned} \quad (3.17)$$

Equations 3.15 – 3.17 are so called Reynolds-Averaged Navier-Stokes equations (RANS), and those equations is set to be solved in RANS method. RANS equations contain additional unknowns, which are cause of turbulent stresses. These stresses are often termed Reynolds stresses and they form, by analogy with viscous laminar stresses, a symmetric matrix (3.18) which contains six additional unknowns.

$$\begin{bmatrix} -\rho \overline{u'u'} & -\rho \overline{u'v'} & -\rho \overline{u'w'} \\ -\rho \overline{v'u'} & -\rho \overline{v'v'} & -\rho \overline{v'w'} \\ -\rho \overline{w'u'} & -\rho \overline{w'v'} & -\rho \overline{w'w'} \end{bmatrix} \quad (3.18)$$

These six additional unknowns requires either six additional transport equations either empirical or semi-empirical turbulence model. Most common turbulence models are:

- Spalart Allmaras – one equation model;
- RSM – Reynolds stress equation model;
- k-ε – two equations model;
- k-ω – two equation model.

In this Master Project only last two turbulence models are used in simulations.

k-ε turbulence model.

The most common variations in the k-ε model lineup is standard RNG and realizable k-ε models. “All three models are similar, with the two transport equations which are written for the turbulent kinetic energy k [m²/s²] and its dissipation rate ε [m²/s³]. The essentially common features are related to the definition of turbulent production, turbulence generation due to body forces and inclusion of the effects of compressibility and mass transfer.”[4]

Here is only focus given for standard k-ε model, where turbulent viscosity (eq. 3.19) is computed as follows:

$$\mu_t = \rho C_\mu \frac{k^2}{\varepsilon} \quad (3.19)$$

Where kinetic energy and dissipation rate:

$$\frac{\partial}{\partial t}(k) + \frac{\partial}{\partial x_j}(u_j k) = \frac{\partial}{\partial x_i} \left[\left(\nu + \frac{\nu_t}{\sigma_k} \right) \frac{\partial k}{\partial x_i} \right] + \tau_{ij} \frac{\partial \bar{u}_i}{\partial x_j} - \varepsilon; \quad (3.20)$$

$$\frac{\partial}{\partial t}(\varepsilon) + \frac{\partial}{\partial x_j}(u_j \varepsilon) = \frac{\partial}{\partial x_i} \left[\left(\nu + \frac{\nu_t}{\sigma_\varepsilon} \right) \frac{\partial \varepsilon}{\partial x_i} \right] + C_{1\varepsilon} \tau_{ij} \frac{\partial u_i \varepsilon}{\partial x_j k} - C_{2\varepsilon} \frac{\varepsilon^2}{k}; \quad (3.21)$$

$$C_{1\varepsilon} = 1.44;$$

$$C_{2\varepsilon} = 1.92;$$

$$C_\mu = 0.09;$$

$$\sigma_k = 1.0;$$

$$\sigma_\varepsilon = 1.3.$$

“Since the k-ε models are based on the assumption of isotropic turbulence, one cannot expect them to resolve accurately the flow properties in the regions of high turbulence anisotropy. One practical example is given by the flow in the vicinity of vertical structures. The isotropic turbulence models are known to over-predict the levels of turbulent viscosity in the vortex core which results in excessively diffusive and dissipative tip vortex. If such a vortex bounds a slipstream region (e.g., propeller tip vortex), the slipstream boundary appears more blurred and smeared than it is measured in the experiment.” [4]

k-ω turbulence model.

The k-ω turbulence models is the same as k-ε, when it comes for number of equation. Those two transport equations solves kinetic energy k and its specific dissipation rate ω. The specific dissipation rate, which is used instead of ε, is understood as the dissipation rate per unit turbulent kinetic energy and which is, thus, proportional to ε/k. It has the dimension [1/s]. In this standard k-ω model turbulent viscosity is computed as follows:

$$\mu_t = \rho \alpha^* \frac{k}{\varepsilon} \quad (3.22)$$

Where turbulence kinetic energy and its specific dissipation rate are obtained from the following transport equations:

$$\frac{\partial}{\partial t}(\rho k) + \frac{\partial}{\partial x_j}(\rho u_j k) = \frac{\partial}{\partial x_i} \left[\Gamma_k \frac{\partial k}{\partial x_i} \right] - Y_k + S_k + G_k; \quad (3.23)$$

$$\frac{\partial}{\partial t}(\rho \omega) + \frac{\partial}{\partial x_j}(\rho u_j \omega) = \frac{\partial}{\partial x_i} \left[\Gamma_\omega \frac{\partial \omega}{\partial x_i} \right] - Y_\omega + S_\omega + G_\omega; \quad (3.24)$$

$$\alpha^* = \alpha_\infty^* \frac{\alpha_0^* + Re_t/R_k}{1 + Re_t/R_k}; \quad (3.25)$$

$$Re_t = \frac{\rho k}{\mu \omega}; R_k = 6; \alpha_0^* = \beta_t/3; \beta_t = 0.072; \alpha_\infty^* = 1;$$

G_k and G_ω represents the generation of turbulence kinetic energy and its dissipation rate due to mean velocity gradients;

Γ_k and Γ_ω represent the effective diffusivity of k and ω respectively;

Y_k and Y_ω represent the dissipation of k and ω due to turbulence;

S_k and S_ω are user-defined source terms.

The k - ω models are more suitable to the simulations of flows involving re-circulation and separation. The standard k - ω model is known to predict reliable results for the free shear turbulent flows (jets, wakes, mixing layers). However, it reveals sensitivity to initial and boundary conditions in the free stream region, especially for internal flows. [4]

3.3 CFD tool

There are many CFD simulation tools such as Open FOAM, Flash, Gadget CFX, FLOW3D and many more, but during the master thesis all analysis regarding to CFD simulations will be done by using CD-ADAPCO product. Alesund University College has a licensed version of 10.02.010 version, which is in virtual desktop solution by University's system.

“STAR-CCM+ is unrivalled in its ability to tackle problems involving multi-physics and complex geometries. STAR-CCM+ has an established reputation for producing high-quality results in a single code with minimum user effort.

Designed to fit easily within your existing engineering process, STAR-CCM+ helps you to entirely automate your simulation workflow and perform iterative design studies with minimal user interaction.

The net result of this is that engineers get to spend more time actually analysing engineering data and less time preparing and setting up simulations.

The STAR-CD solver provides one of the most effective numerical methodologies available in an industrial CFD code with the high level of accuracy needed for complex unstructured meshes. This is delivered with the speed, efficiency and robustness demanded by engineering design and development cycles. STAR-CD uses state-of-the-art, proprietary numerical schemes to achieve the highest levels of accuracy in both steady and transient simulations, making this solver one of the least sensitive to mesh type and quality, including distorted tetrahedral meshes. Remarkably, this has been achieved without sacrificing efficiency or robustness. So, whatever the choice of mesh or engineering application, the STAR solver will provide the best solution in the shortest time. A particular feature of STAR-CD is its fast CPU performance for transient flows. As the first to introduce moving mesh into a CFD code, we have always been technology leaders in this area. The meshes can not only move and deform, but they can also slide along non-matching interfaces; furthermore, selected cells or cell regions can be deleted or added, detached and again attached to the core model". [15]

4 CASE STUDY

4.1 *Ship model for analysis*

The model geometry, which is under CFD simulation came from Marintek and it is anchor handler STX413 (fig. 4-1). This twin screw vessel with design water line 7m above base line in full scale and designed velocity is 14,5 knots. Model does not consist with structures, which are above main deck. Those are not necessary attributes for this project simulation, because here, hull resistance and nominal wake fraction investigations are done.

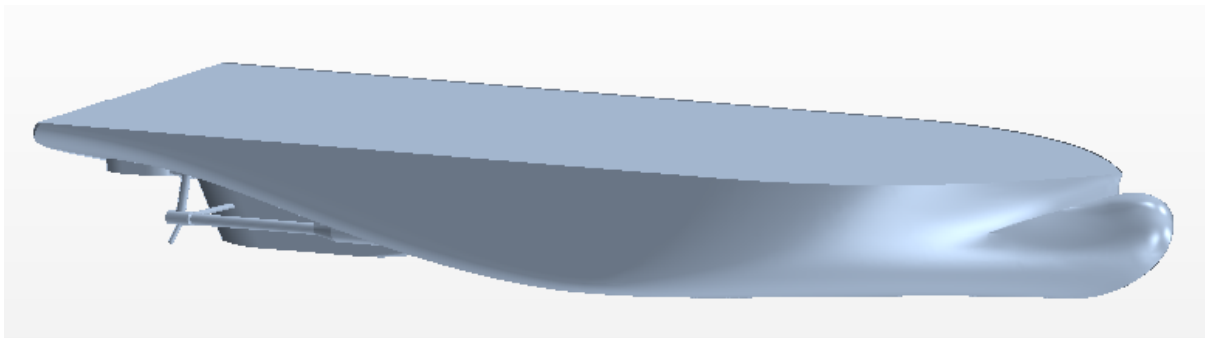


Figure 4-1 Ship geometry STX413

In a table below main particulars of vessel in full scale and model scale are given. The model scale is 1:23, which should represent model in experimental tests.

Table 4-1 Ship main particulars in model and full scale

Parameter		Full scale	Model scale [1:23]
Length between perpendiculars	LPP (m)	82,1	3,570
Maximum beam of waterline	BWL (m)	22	0,957
Draft	T (m)	7	0,304
Displacement volume	∇ (m ³)	9192,8	0,756
Wetted surface area w/o ESD	SW (m ²)	2550	4,820
Block coefficient (CB)	$\nabla/(LPP*BWL*T)$	0,7065	0,707

Note that in table 4-1 values are for the whole vessel, but in order to reduce computational time in simulation only half of the vessel in domain is used, because ship is symmetrical, so values such as BWL, ∇ and wetted surface area have to be reduced twice. This should be done in CFD software, where it demands those parameters.

When it comes for wake measurements behind of the vessel is essential to know where propeller disc is located. In a table 4-2 propeller parameters are shown. It have to be noted that propeller location coordinates are given according main coordinate system, which starting point is on the stern perpendicular and the ship base line. In the table value y, i.e. transverse propeller location is for starboard propeller, because that side of the vessel is used in computational domain.

Table 4-2 Propeller parameters in model and full scale

Parameter		Full scale	Model scale [1:23]
Diameter	D (m)	4,6	0,2
Center, long. location	x (m)	1,8	0,07826
Center, vert. location	z (m)	2,2	0,09565
Center, transverse location	y (m)	-6,4	-0,27826
Direction for rotation (view from stern)	-	Anticlockwise	Anticlockwise

4.2 Set up for simulation

4.2.1 Boundary conditions

In project there are chosen only 4 different boundary conditions for simulation:

- Velocity inlet – this boundary is applied for domain inlet, top, side and bottom;
- Pressure outlet – applied for computational domain outlet;
- Wall – this condition describes ship hull and all appendixes on it;

- Symmetry plane – this is applied in ship centre line, because ship is symmetrical and computed result is expected to be symmetrical.

4.2.2 Meshing

All meshing operations are performed as Parts-Based Meshing, instead of Region-Based Meshing. The Parts-Based Meshing introduced in the recent versions of STAR-CCM+ has the advantage that it allows for a higher automation of the simulations setup when altering the input geometry. Unlike Region-Based Meshing, all meshing settings are contained in the Geometry group (Geometry->Operations->Automated mesh), which means that they are attributed to the geometry parts, but not to the region boundaries. If one changes the geometry following the necessary name conventions, the mesh can easily be rebuilt by simply repeating the same automated mesh operation. If region settings are modified or deleted, one does not lose any mesh settings, and they can again be easily reproduced, by re-executing the same automated mesh operation.

In general mesh properties have been made to keep $y^+ > 30$. As it is noted in [9] the y^+ (see eq. 4.1) should be in a range of from 30 to 300, this is necessary for accuracy of the results when there is used wall functions.

$$y^+ = \frac{uy}{\vartheta} \quad (4.1)$$

Where, u – velocity, y – nearest distance, ϑ – kinematic viscosity.

4.2.3 Physics

Physics which were used for computation in project is described in chapter 3.2. For analysis of free surface elevation, in STAR CCM+ also had to be selected multiphase model in order to capture interaction between water and air. Here VOF (volume of fluid) waves is used, i.e. VOF waves are used to simulate surface gravity waves on a light fluid and heavy fluid interface. Here light fluid represents air and heavy – water.

4.2.4 Interface capturing scheme

In simulations is used the pure High Resolution Interface Capturing (HRIC) scheme, which was enforced by setting up very high Courant number (CFL) limits $CFL_l=200$ and $CFL_u=250$, which stands for lower and upper Courant number respectively. The interface capturing scheme in STAR-CCM+ is the blended HRIC, which works in such a way that:

- When $CFL < CFL_l$ – pure HRIC scheme is used;
- When $CFL_l < CFL < CFL_u$ – a blend of HRIC and UD (Upwind Difference) schemes is used;
- When $CFL > CFL_u$ – pure UD scheme is used.

For simulations having supposedly steady state solution, as towing resistance case, the results should not depend on time step. It is achieved by setting up intentionally high CFL limits so that only the pure HRIC scheme is used. Larger values of time step can be used to increase solution speed.

However, according to Marintek experience, it shows that with the pure HRIC scheme, the vessel resistance is usually under-predicted, when using shear stress transport (SST) k-w turbulence model and coarse near-wall treatment ($Y^+ > 30$). It is also found that in the simulations with free vessel sinkage and trim, the solution with the pure HRIC scheme may become unstable. So that normally the blended scheme is used with default setting of $CFL_l = 0.5$, $CFL_u = 1.0$, while effort is made to place most of the free surface domain in the range of pure HRIC scheme ($CFL < CFL_l$). It is achieved by an appropriate combination of time step and cell size on the free surface. CFL equation is:

$$CFL = \frac{u\Delta t}{\Delta x} \quad (4.2)$$

Where:

Δt – time step;

Δx – size of cell;

u – velocity.

More about HRIC schemes can be found in [16]

Another important comment which is given by Vladimir Krasilnikov, is related to the assumption of "supposedly steady solution". If the flow pattern over the hull and free surface is separation free, the above assumption holds fairly well. However, STX413 hull reveal separation and vortex generation domains. Large separation vortices are generated on the central skeg, and smaller separation zones occur on the brackets. These separation phenomena are associated with *unsteady* (!) vortex shedding. So, even though our solution for averaged resistance value and free surface may be independent on time step (and should in principal converge to "steady state"), the solution for the hull flow will depend on time step (and hence

Courant number), due to vortex shedding frequency. It will also cause poorer convergence of residuals, and the resulting resistance convergence plot will reveal minor oscillations, indicating its dependence on vortex shedding. It is therefore important to investigate into the influence of time step on solution results. Time step should in general be decreased from a very coarse value of $dt=0.05$ [s], in order to provide reasonably low Courant numbers, 0.0 to 2.0 being the desired range. Note that it almost never can be met in the whole domain. One would always have local "jumps" in Courant number over sharp edges, separation lines and in the areas of free surface break-up.

5 RESULTS

5.1 Mesh

Mesh generated in model scale have 4.67 million cells (table 5-1), and this is only one mesh, which was used throughout model scale simulation. In full scale there have been done several variations of domain mesh. That came from various ways from scaling existing model to full scale.

Table 5-1 Amount of cells in model and full scale

Scale	Number of cells in millions		
<i>Model scale</i>	4.67		
<i>Full scale</i>	Mesh scaled directly	Scaled model & domain	Scaled model & domain (2)
	4.67	5.39	4.65

First way to scale from model to full is direct scaling of the mesh, i.e. existing mesh is scaled according to user's defined value (in this case 23). Other two mesh generated methods are same. First whole domain with volume controls and model is scaled to the desired size, after that base size of the cell is scaled. According base size mesh is automatically generated in STAR CCM+ software. But during simulation there have been seen that in mesh where is 5.39 million cells, some of the volume controls are not in the right positions fig. 5-1, this would cause inadequate results. In order to avoid this, same procedure was repeated, but there local coordinate systems were not relocated, that lead to the right positions of volume controls and significantly reduced cell numbers.



Figure 5-1 Positions of volume controls. a) Scaled model & domain, b) Scaled model & domain (2)

As it shown in figure above, volume controls (Box-Stern & Box-Bow) in b) are offset from their actual location, where it shown in a). Due to this offset, simulations with that offset weren't proceed anymore. In mesh where it is scaled directly are 20 000 more cells than in third full scale mesh (see table 5-1), figure 5-2) shows that both meshes have similar residuals, but b) mesh configuration has slightly lower residuals, and because it has less volume cells, the decision have been made to proceed with this meshing in full scale.

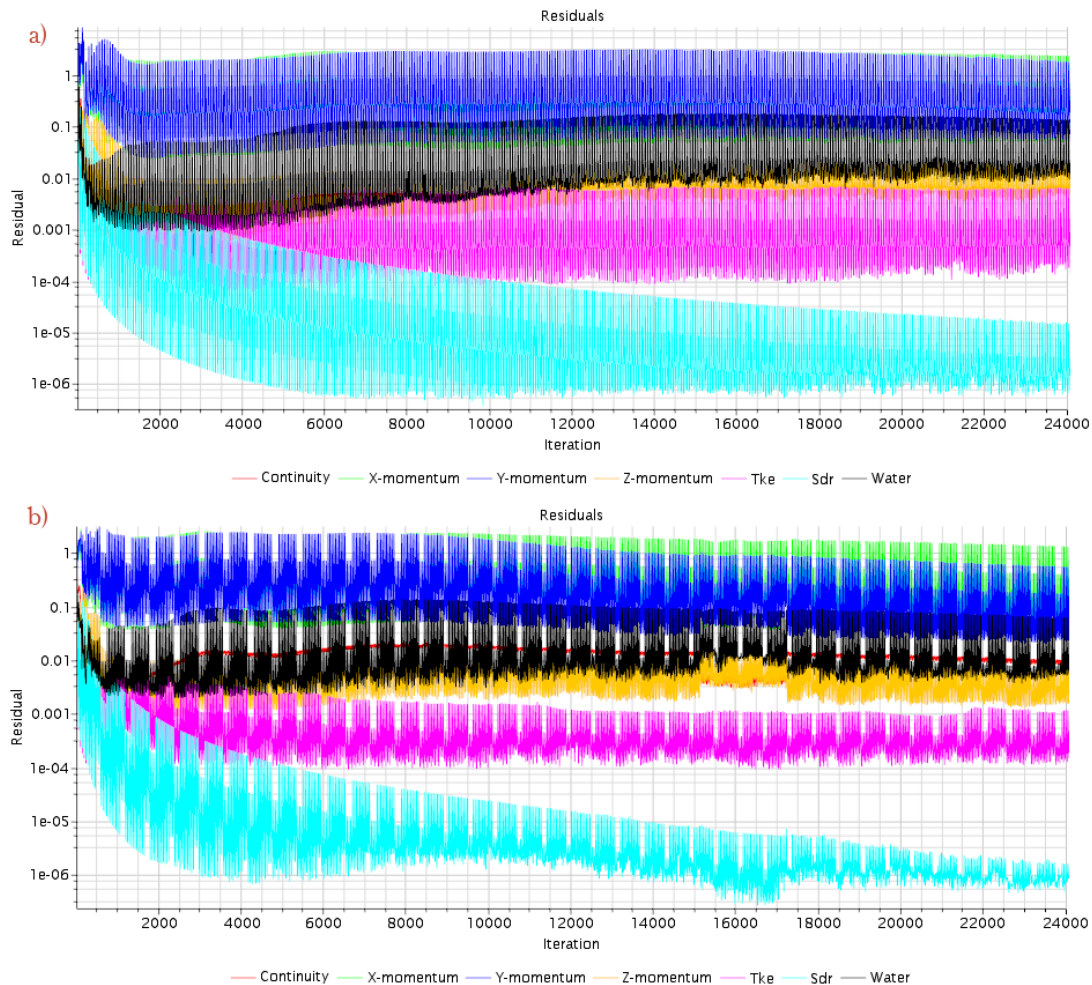


Figure 5-2 Residuals. a) Directly scaled mesh, b) Scaled model & domain

5.2 Turbulence model

As it was mentioned earlier, in this project two turbulence models have been considered $k-\epsilon$ and $k-\omega$. Decision for which should be used is done on simulation in model scale $Fr=0.2628$, due to small simulation time. Model is simulated for approx. 82 seconds. Aspect which is evaluated is force coefficients: C_t , C_p and C_f . Table 5-2 shows simulated results of force coefficients. There isn't any difference between shear force coefficients, but pressure is slightly less in the $k-\epsilon$ turbulence model simulation, due to that also total force coefficient is also less than in $k-\omega$ model.

Note that those simulated values are based on full wetted hull surface area, which means it have to be multiplied by 2, because actual simulation is done on half hull. So in the differences will grow twice. Because simulations with under predicted resistance is not desirable, in further simulations $k-\omega$ turbulence model will be used. Best practice of Marintek in wake prediction shows that is better to use $k-\omega$ model for these kind of simulations.

Table 5-2 Force coefficients

Turbulence model	Ct	Cp	Cf
	10^{-3}		
k-ϵ	3.45	1.64	1.81
k-ω	3.52	1.71	1.81

5.3 Time step & CFL number

5.3.1 Model scale

In the chapter 4.2.4 is noted that this simulation should depend on time step and courant number (CFL), due to flow separation and vortex shedding in the stern of the vessel. In model scale simulations were tried with two strategies. One with time step=0.025s and other 0.05s.

In figure 5-3 courant number on free surface is given in model scale simulations on $Fr=0.2628$. It is clearly noticeable that with twice increased time step there are twice as big CFL number, due to (4.1) equation.

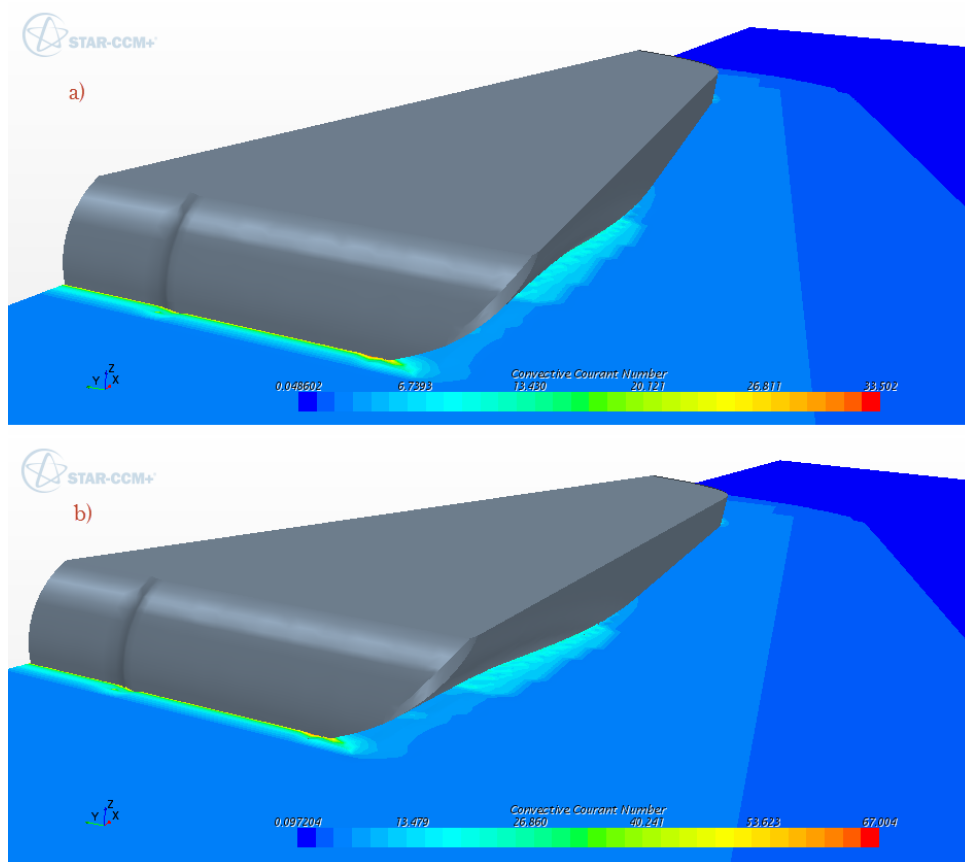


Figure 5-3 CFL number on free surface in model scale. a) time step=0.025s, b) time step=0.05s

Figure 5-4 shows residuals on different strategies with time step in model scale simulations. Computational time on simulation with time step=0.05s lasts twice as less as with time step=0.025s, residuals are slightly lower, but the plot shows that it is not stable, there are many fluctuations throughout simulation. However there are fluctuations in simulation with time step=0.025s, but those are much more predictable and steadily decreasing during simulation. In the end of simulation, in this case around more than 16000 iterations (see appendix A), residuals are a bit lower than in the same simulated time with time step=0.05s and number of iterations approx. 9000. Table 5-3 gives both calculated values of force coefficients on those two simulations. Results are close, but because of fluctuating values in simulation with 0.05s time step, coefficients could vary a bit, but not significant. Note that values in table 5-3 have to be multiply by 2 in order to compare real values. Simulation for other Froude numbers in model scale will be done by using time step=0.025s.

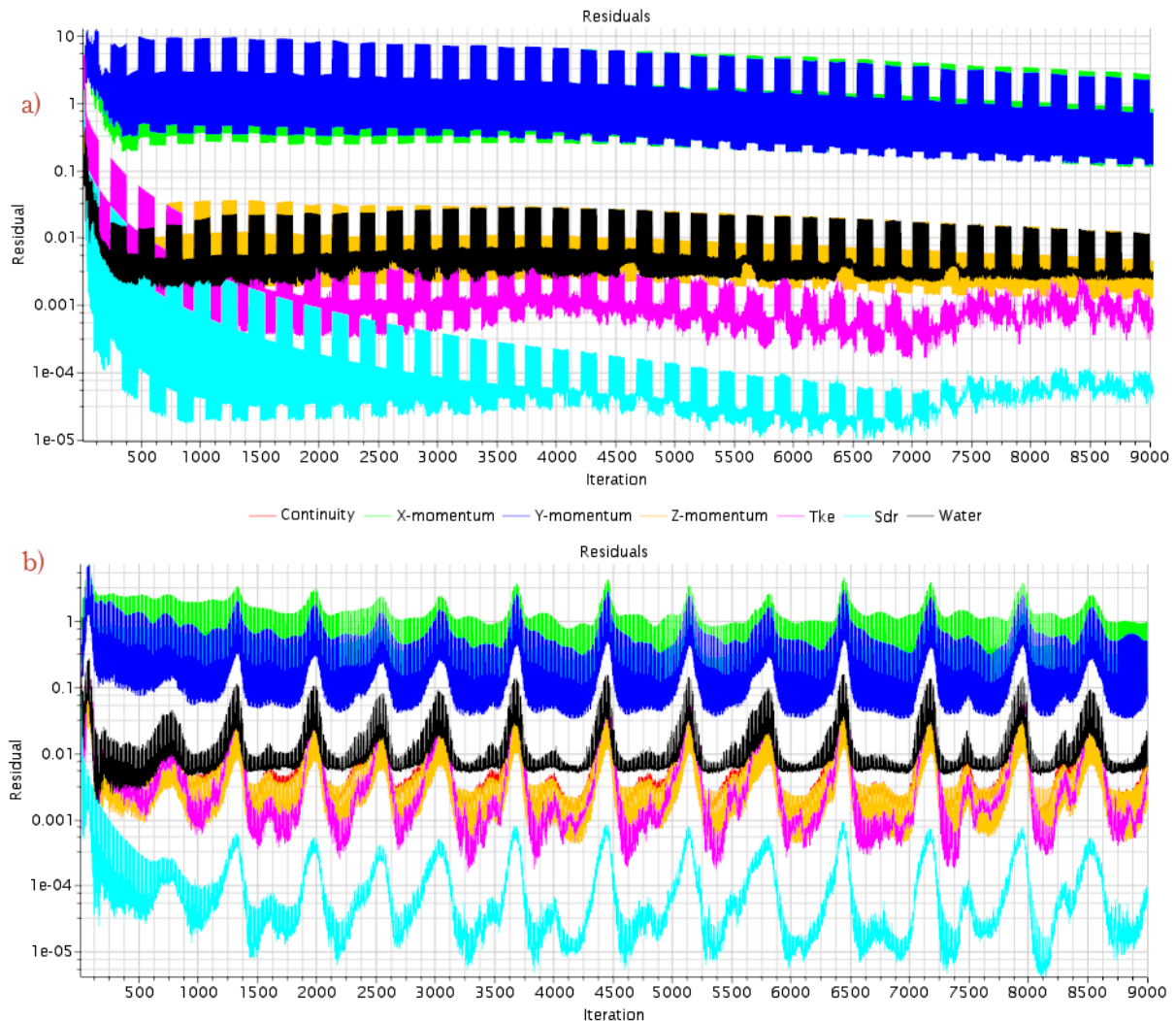


Figure 5-4 Residuals in model scale. a) time step=0.025s, b) time step=0.05s

Table 5-3 Force coefficients calculated on different time step

Time step	Ct	Cp	Cf
[seconds]	10^{-3}		
0.05	3.59	1.77	1.82
0.025	3.52	1.71	1.81

5.3.2 Full scale

Decision on full scale simulations are based on three different strategies by setting different time step. First it is tried to simulate with time step=0.05s, later – 0.15s and last – a combination of those two time steps. The third option is done in such a way: first time step is set to be 0.15s and computed for first 150s of physical time in simulation, later the time step is reduced to 0.05s and simulation goes on until it computes for 500s.

Summary of these three simulations with different time step is given in a table 5-4. When it comes to computational time, simulation with time step=0.15s is the fastest, where 0.05s is the slowest, but in fastest calculations it is noticeable that force coefficient values are bit higher than in other two. Combination of time steps 0.05s and 0.15s reduces time consumption by approx. 30% comparing with simulation with time step=0.05s, and force coefficient values are basically same.

Table 5-4 Summary of three simulations of different time step

Time step	0,05	0,15	0,15&0.05
Cp	0,003017	0,003095	0,003019
Cf	0,001916	0,001940	0,001917
Ct	0,004936	0,005036	0,004936
Simulation time [hours]	156	50	104
No of iterations	57 500	17 260	40 000

During full scale simulations it has been noticed that Cp values doesn't get complete convergence. It varies even after 500 simulated seconds, hence the values for force coefficients are mean values from last 20 seconds. In figures 5-5 and 5-6 Cp plots are shown, calculations based on time step=0.05s has biggest fluctuations and strange increase of them from 250 seconds. Nether less these fluctuations are proportional and mean value does not change significantly. With combined time step fig. 5-5 and 5-6 c) Cp values are varying the most, but

amplitude of those variations are significantly smaller than in other two simulations. This might be due to smaller residual values.

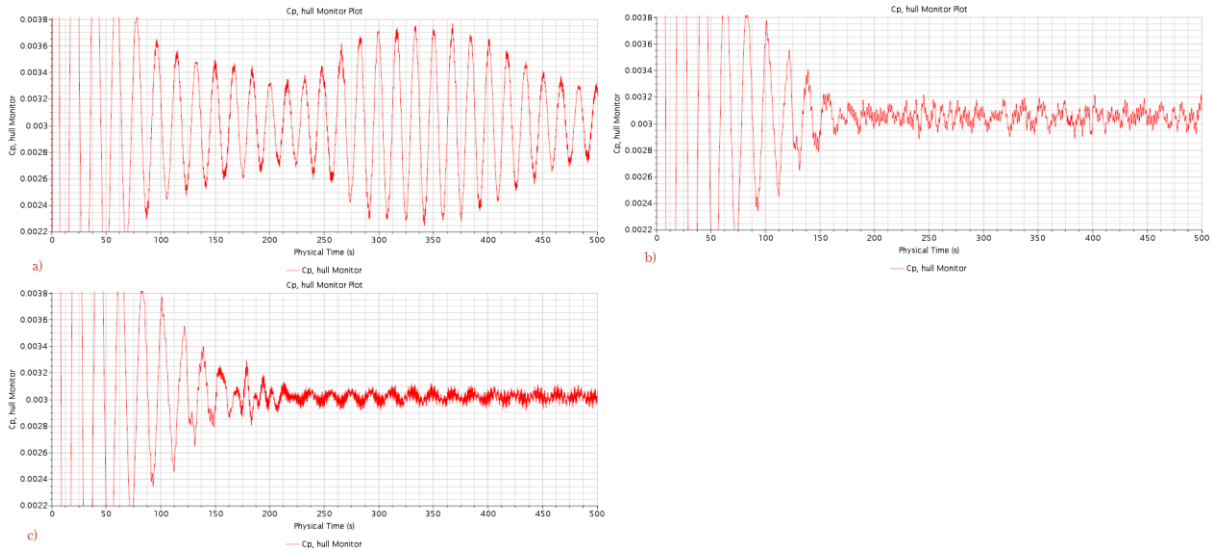


Figure 5-5 Cp force coefficient plot throughout full simulation. a) time step=0.05s, b) time step=0.15s, c) time step=0.15&0.05s

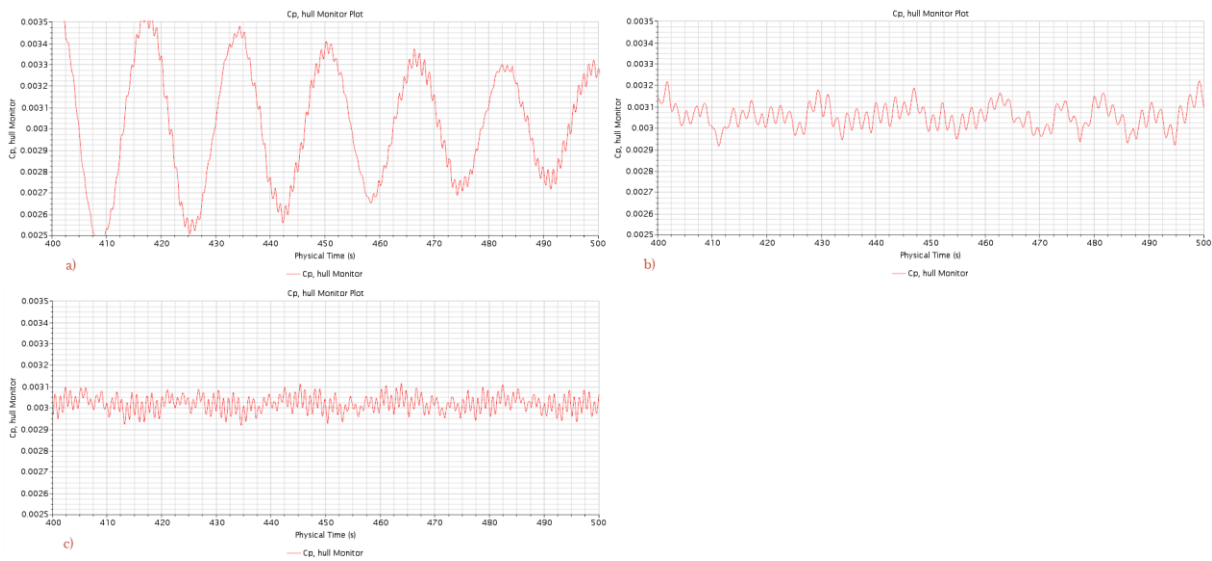


Figure 5-6 Cp force coefficient plot in last 100 seconds. a) time step=0.05s, b) time step=0.15s, c) time step=0.15&0.05s

Figure 5-7 shows the residuals for those three simulations in different strategy of time step. It is clearly visible that in the end of simulation, i.e. when it is simulated for 500 seconds, the computation with combined time step have the lowest residuals of all three calculations. In this residual plot on iteration=5000 time step has been changed, that was done after 12 hours of computational time with 0.15s time step. Since then residuals started to decrease steadily and after approx. 17500 iteration, values dropped even more, where later in the end residuals were not changing a lot, but with small tendency for decreasing.

Because of smaller residual values, Cp fluctuations and time consumption, simulations for full scale vessel will be done by using combined time step computations. For full scale CFL number wasn't under consideration, because these values became significantly smaller than in model scale, due to 23 times bigger cell size (see equation 4.1).

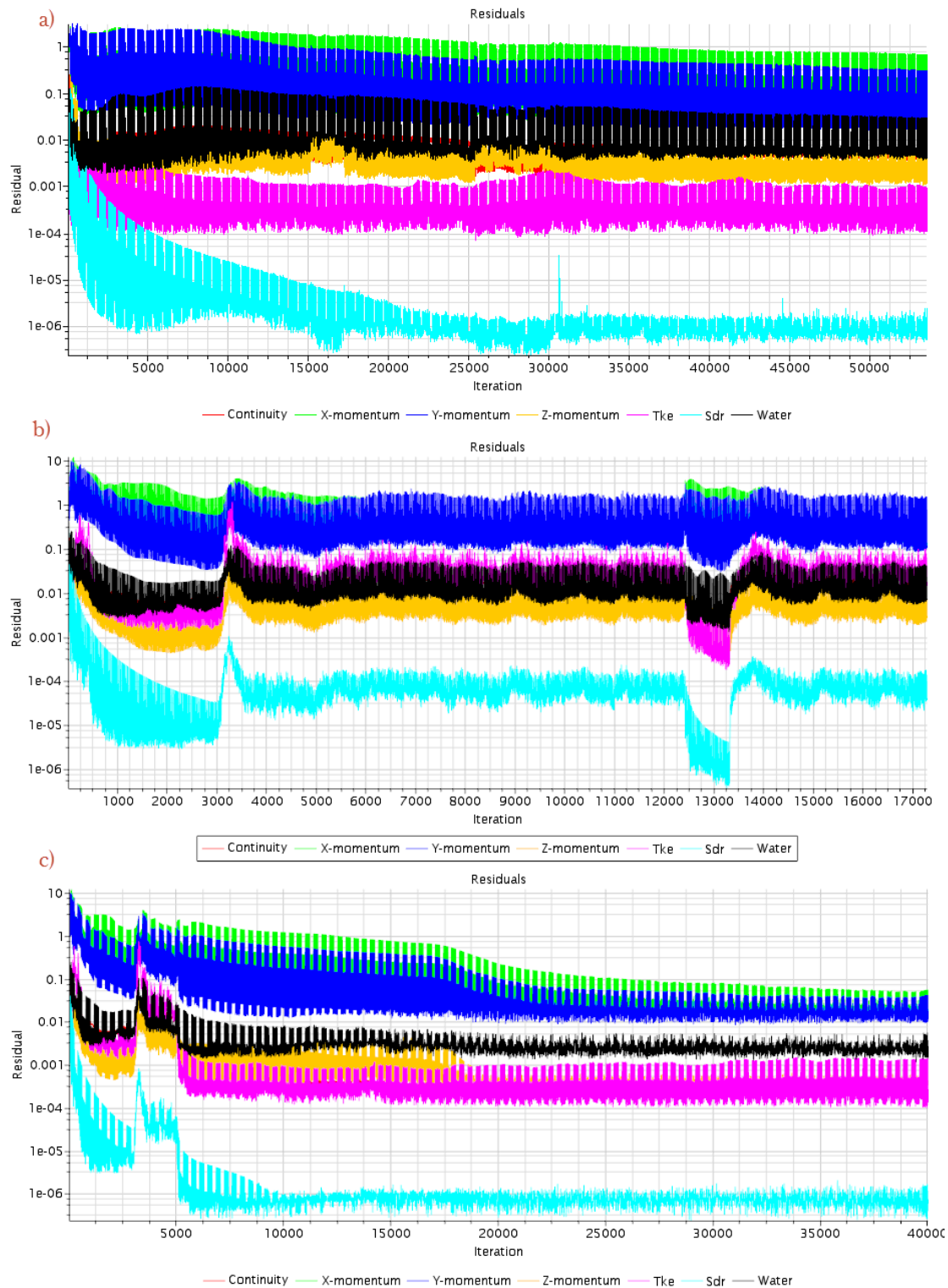


Figure 5-7 Residuals of full scale simulations. a) time step=0.05s, b) time step=0.15s, c) time step=0.15&0.05s

5.4 Force coefficients

In previous chapter there was mentioned hull resistance components, in this section results are provided on calculated force coefficients, i.e. Ct, Cf, and Cp. Those values were the basis for monitoring convergence of the computation. For low Rn numbers, during model scale simulations, convergence was achieved significant faster than in full scale calculations.

Convergence was noticeable when software has been simulated approx. 80 or less seconds, but both in full scale and model scale computations, real convergence hasn't been reached. Values have been oscillating even with low residual values, especially pressure force coefficient, which is key component for evaluating results between model and full scale simulations. Expectations for values of Cp is supposed to be approx. same.

Results from model scale simulations on force coefficients are not entirely right, because of the user mistake by imputing reference values of the wetted surface. These values were assumed to be for full ship hull, where computation domain consists with only half of the vessel. Nether the less computed Cp coefficients can be multiply by 2, because of the equation (5.1), in order to get real values.

$$\text{Force coefficient} = \frac{F}{\frac{1}{2} \rho v^2 A} \quad (5.1)$$

Where: F – force, g – gravity, v – velocity, A – area.

In table below (5-5) is a set of simulations in different Froude numbers are given. According to the simulation type (model or full scale) different speeds are set up for vessel. This range of several speeds should give a reasonable prediction of force coefficients.

Table 5-5 Set of different Fr numbers for simulations

Fr=V/(g*LPP) ^{0,5}	Full scale			Model scale	
	v	v	Re=(v*LPP)/v	v	Re=(V*LPP)/v
-	[knots]	[m/s]	-	[m/s]	-
0,145006	8	4,1152	3,05E+08	0,858079	2,77E+06
0,181257	10	5,144	3,82E+08	1,072598	3,46E+06
0,217508	12	6,1728	4,58E+08	1,287118	4,15E+06
0,235634	13	6,6872	4,96E+08	1,394378	4,50E+06
0,262823	14,5	7,4588	5,53E+08	1,555267	5,02E+06
0,271886	15	7,716	5,72E+08	1,608897	5,19E+06
0,308137	17	8,7448	6,49E+08	1,823417	5,88E+06
				v=	1,11E-6 m ² /s
				Lpp=	82,1 & 3,57 m
				g=	9,81 m/s ²

5.4.1 Ct, Cf and Cp in model scale

In a table 5-6 are computed values for force coefficients and actual values which were corrected by multiplying them by 2. From total force resistance coefficient it is visible in figure 5-8, that vessel performs best, i.e. has least amount of resistance at Froude number 0,2628, which corresponds to 1,555 m/s of actual model speed. Beyond that ship resistance increases drastically because of the higher Ct values. This part of total force coefficient curve seems to be linearly increasing. In Ct and Cf plot distance between each two curves point at same Fr number is pressure coefficient value. Keeping in mind that, pressure coefficient is the parameter which effects increase of Ct according to fig. 5-8.

Table 5-6 Force coefficients in model scale simulations (Fr=0,2628)

Fr number	Computed values			Corrected values		
	Ct	Cf	Cp	Ct	Cf	Cp
	10^{-3}			10^{-3}		
0,1450	3,697	2,041	1,656	7,395	4,083	3,312
0,1813	3,669	1,948	1,721	7,337	3,895	3,442
0,2175	3,534	1,881	1,653	7,069	3,763	3,306
0,2356	3,496	1,825	1,671	6,992	3,650	3,342
0,2628	3,544	1,811	1,733	7,088	3,622	3,466
0,2719	3,657	1,798	1,859	7,315	3,597	3,718
0,3081	4,525	1,857	2,668	9,050	3,714	5,336

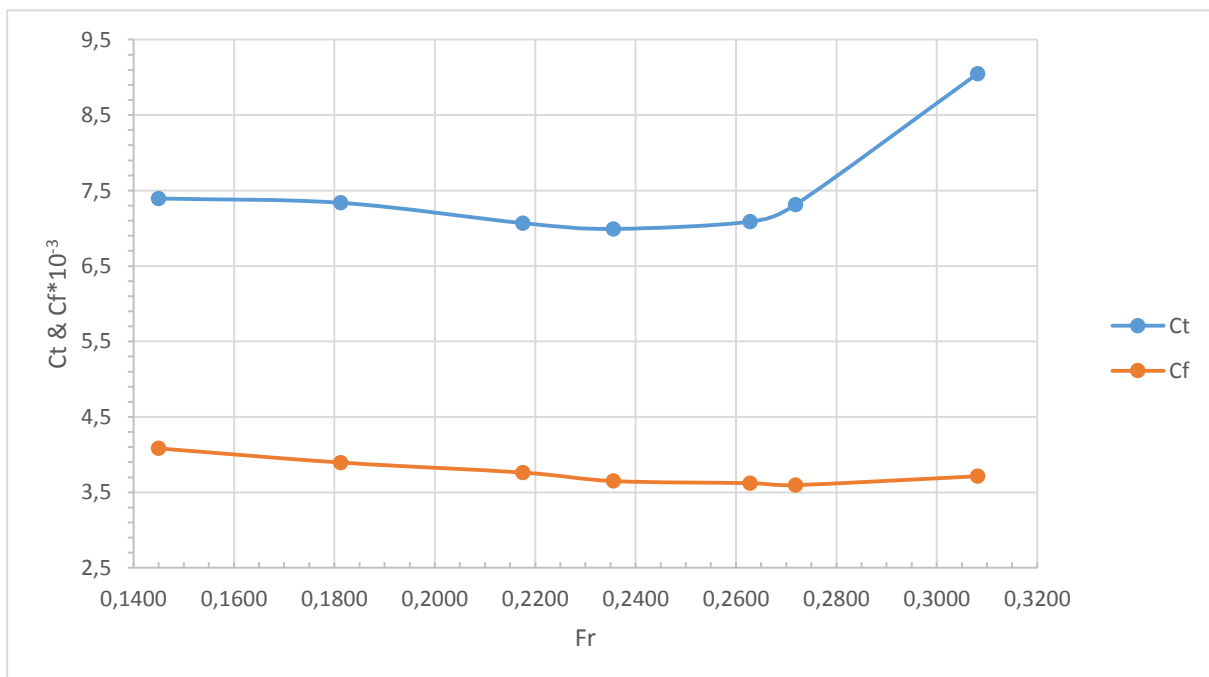


Figure 5-8 Ct and Cf plot (model scale Fr=0,2628)

5.4.2 Ct, Cf and Cp in full scale

Time consumed for computation in full scale calculations was much bigger than in model scale, due to convergence of Cp values, which actually didn't converged completely. Cp results given in table 5-7 is based on mean values, which are taken from last simulated 20 seconds, i.e. 480-500s. To get results from STAR CCM+ were exported files to excel file format, which contain with information what exact value of Cp been in a particular time step.

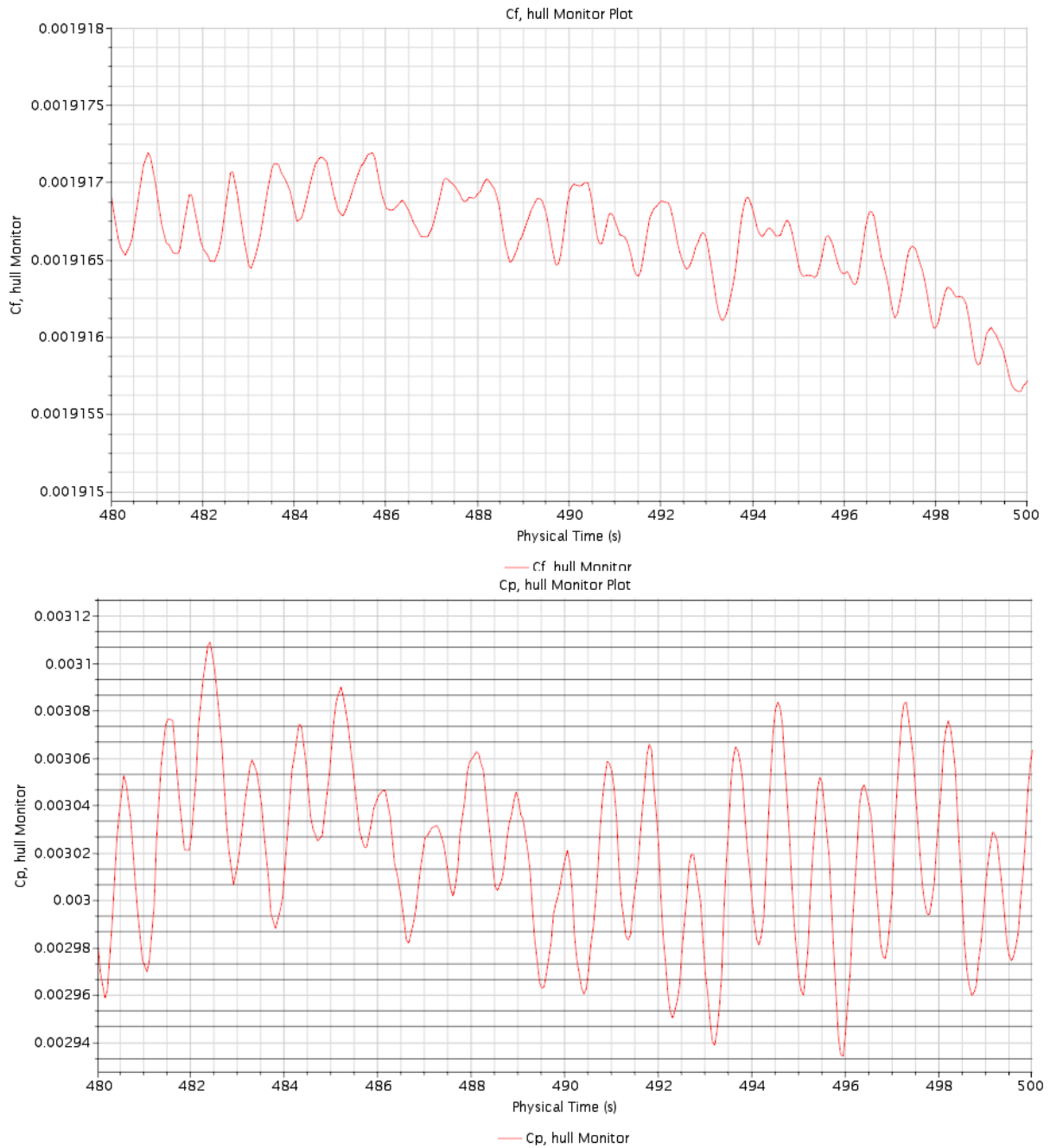


Figure 5-9 Cf & Cp for last 20 seconds of simulation (full scale, Fr=0,2628)

Averages of pressure coefficients is calculated in an excel spreadsheet and given in a 5-7 table. Examples of a C_p and C_f graphs, where last 20 seconds are simulated are given in figure 5-9. C_f values are fluctuating significantly less than C_p , usually 6th number after comma or even 7th are oscillating. Nether the less, to get accurate force coefficients, mean values are calculated as well for C_f values in the same manner as the C_p . There wasn't point to do same procedure for total force coefficient, because mean values based on last 20 seconds of simulation are completely same as sum of C_f and C_p averaged results.

In a table 5-7 simulated force coefficients are given, also calculated C_f values. Calculated C_f values are for better evaluation of computed results. Shear force coefficient can be calculated as ITTC (1957) adopted equation:

$$C_t = \frac{0,075}{(\log_{10} Re - 2)^2} \quad (5.2)$$

Shear force coefficients which are calculated, differs from simulated from approx. 14 to 18%. Seems like results based on calculations have a bit lower values – about 0,3. Since simulations which contains results with under predicted resistance are not desirable, it is at least positive sign that C_f values are a bit higher.

Table 5-7 Force coefficients in full scale simulations

Fr number	Computed values			Calculated	Difference between Computed & calculated
	Ct	Cf	Cp	Cf	
	10 ⁻³			10 ⁻³	%
0,1450	4,845	2,093	2,752	1,784	14,78
0,1813	5,089	2,037	3,052	1,731	15,00
0,2175	4,753	1,974	2,779	1,691	14,36
0,2356	4,709	1,948	2,761	1,673	14,12
0,2628	4,937	1,917	3,020	1,650	13,95
0,2719	5,151	1,907	3,244	1,642	13,88
0,3081	6,969	1,975	4,994	1,616	18,16

Figure 5-10 gives an overview how total and shear force coefficients are distributed among different Fr numbers. Same as in the model scale, ship total resistance coefficient is linearly increasing above service speed, which is 14,5 knots. Curvature of C_t and C_f presented in figure 5-10 looks very similar to those which are given in figure 5-8 – force coefficients of model scale, but values in this plot are a bit lower.

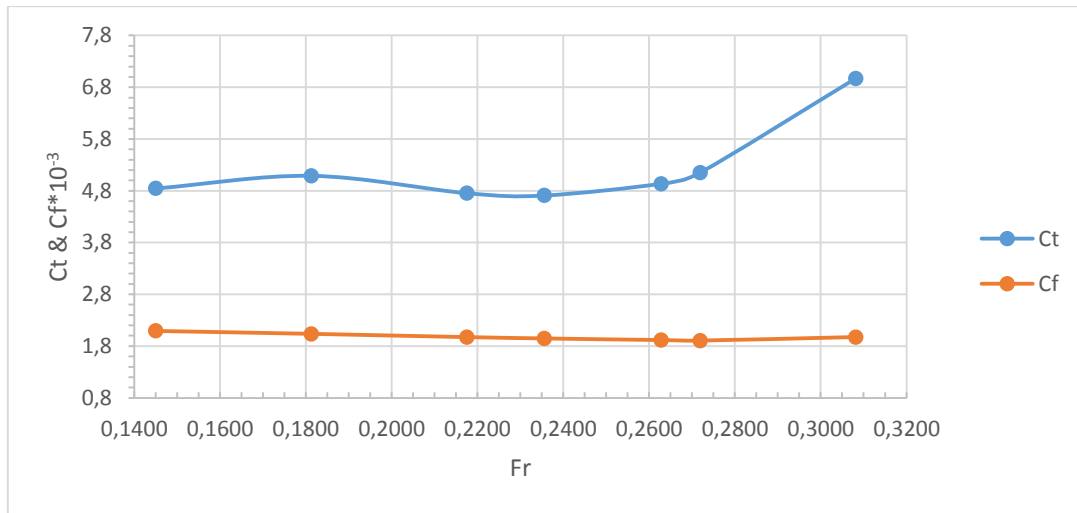


Figure 5-10 Ct & Cf plot (full scale)

5.4.3 Cp comparison in model and full scale

As it was mentioned and shown in figure 5-10 values are bit lower than in model scale, but this is more or less expected results of decreased numbers in Cf and Ct. Expectations are for Cp coefficients in model and full scale that results have to be the same or at least very close. Simulations showed that reality is a bit different, because full scale pressure coefficient is lower than model scale by approx. 6.4-17.4% (see table 5-8).

Actual different is not so big, only 10⁻⁴ number is varying between two cases, but still percentages gives better indication what kind of consequences could be on real pressure resistance of the vessel. Curvatures of Cp coefficient plots in figure 5-11 follow each other in the same manner, which indicates that simulations in model and full scale were done with same settings, but with different speed parameters and domain size. It is good indications that in simulations were not any user made mistakes and calculations are performed with ability to evaluate results.

Table 5-8 Cp in model and full scale simulations

Fr number	Cp in scale of:		Difference [%]
	Model 10 ⁻³	Full 10 ⁻³	
0,1450	3,312	2,752	16,91
0,1813	3,442	3,052	11,33
0,2175	3,306	2,779	15,94
0,2356	3,342	2,761	17,37
0,2628	3,466	3,02	12,87
0,2719	3,718	3,244	12,75
0,3081	5,336	4,994	6,41

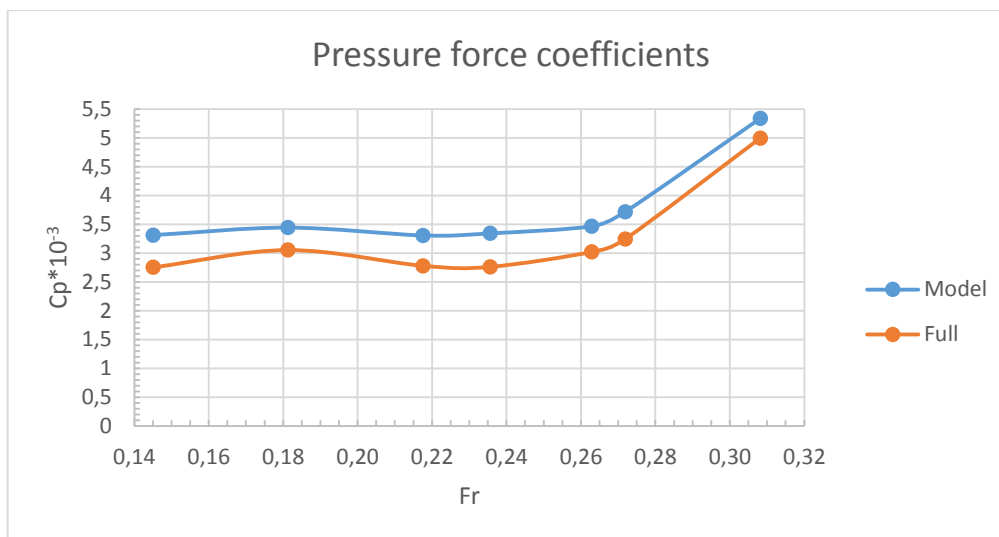


Figure 5-11 Cp plots. Blue – model and orange – full scale

5.5 Surface elevation

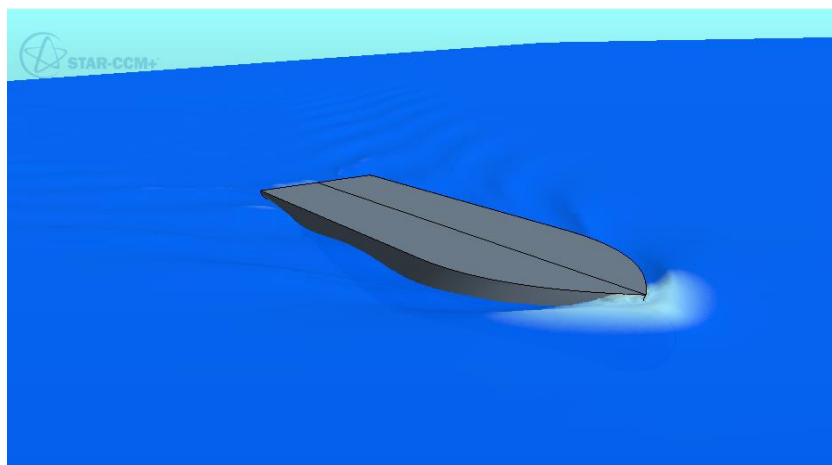


Figure 5-12 Generated surface elevation in full scale

This section contains results on how free surface is generated (fig 5-12) due to moving vessel in various speeds (given in a table 5-5). Free surface (FS) is set to be at the same level as design water line, which is 7m above the base line in full scale simulation and 0,304m in model scale. From figures 5-13 and 5-14, results shows that surface elevation pattern looks very similar. Results shown there are based on local coordinate systems, which have origins of (0.0, 0.0, 7.0) and (0.0, 0.0, 0.304) in full and model scale respectively. Similarity can be seen by looking at maximum and minimum points on a figures below.

It seems that if max or min values in model scale simulation would be multiply by 23, which is actual scale factor, as a result it would be almost the same as in full scale computations, table 5-9 gives a comparison between these values. Results shows that scaled values based on model scale simulation have difference between actual simulations under **1%**.

Table 5-9 Comparison between surface min & max elevation points

Values	Model		Full scale	Difference between scaled and simulated
	Simulated	Scaled to full scale	Simulated	
	[m]	[m]	[m]	[%]
Max	0,1038	2,3872	2,3885	0,056
Min	-0,0395	-0,9093	-0,9061	0,352

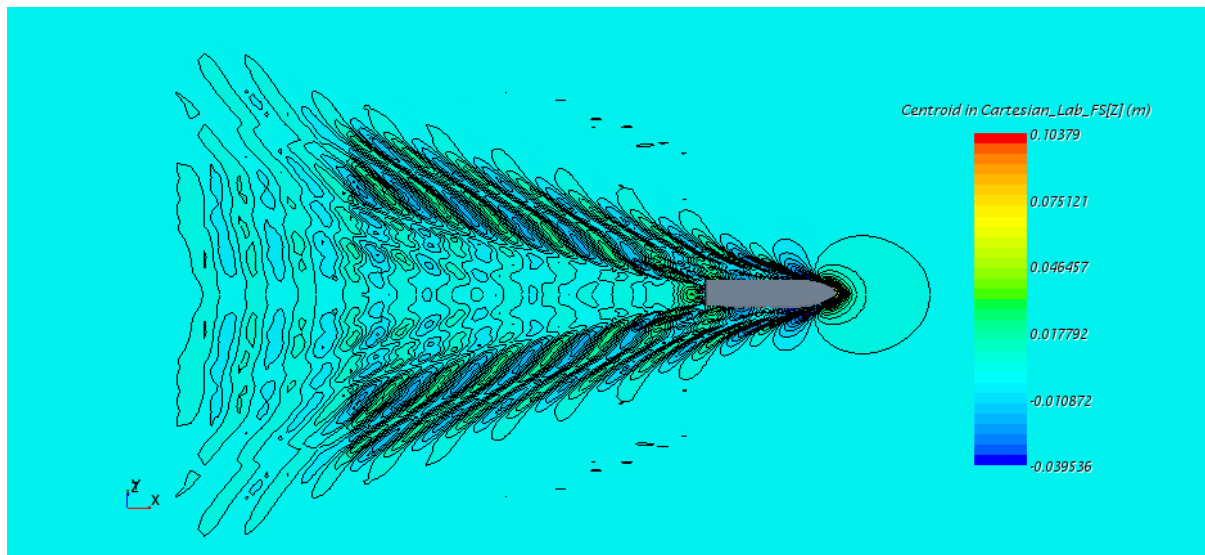


Figure 5-13 Model scale FS elevation

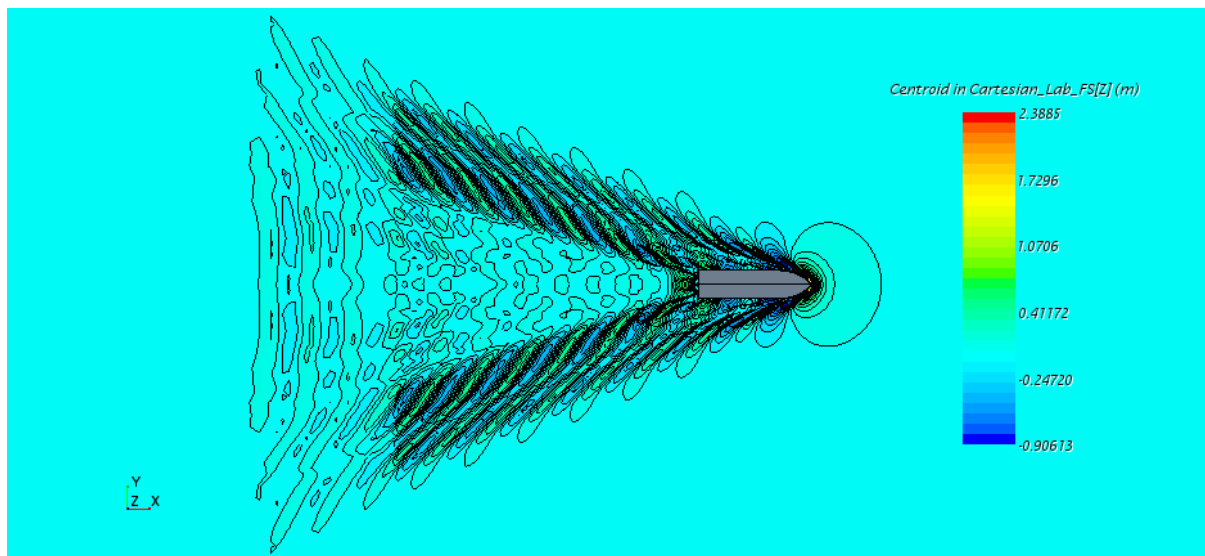


Figure 5-14 Full scale FS elevation

In next two figures results are given for wave profile at position y of maximum beam in water line area, i.e. $y=11\text{m}$ in full scale and $y=0,478\text{m}$ in model scale computations. Zero in plots (5-15 and 5-16) stands for global x axis, which is in the stern of vessel. Note that ship length in two cases is $L_{pp}=82,1\text{m}$ and $L_{pp_{\text{model}}}=3,57\text{m}$.

Plots looks exact same at the length of the models. There are some minor differences, but not by huge margin. On the other hand wave profile towards back from ship hull looks slightly

different. Amplitudes of wave profile looks a bit higher in model scale and less intense, i.e. there are less peaks than in full scale.

Other Froude number simulation results on a FS elevation and wave profile figures are given in appendix E.

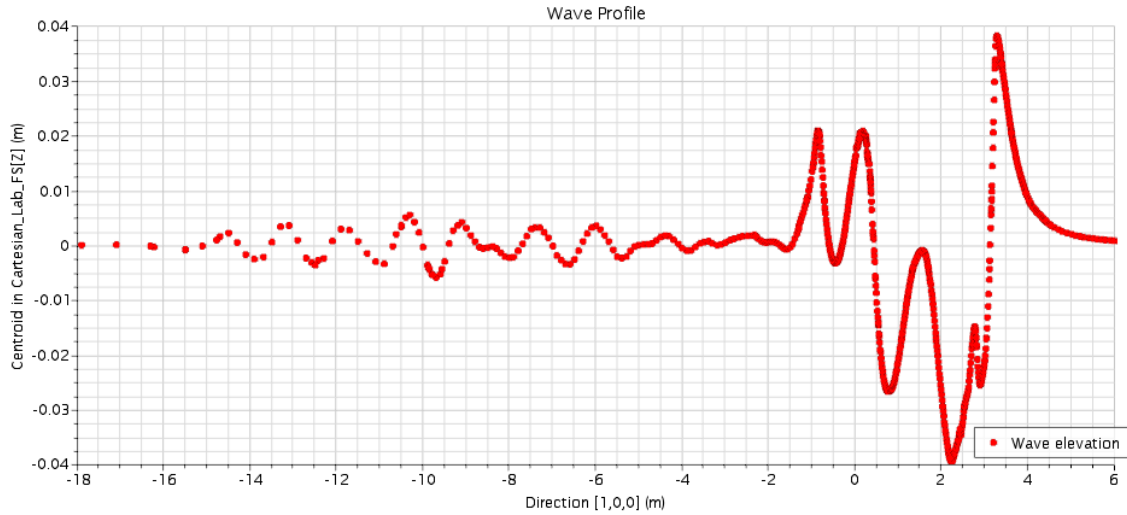


Figure 5-15 Model scale

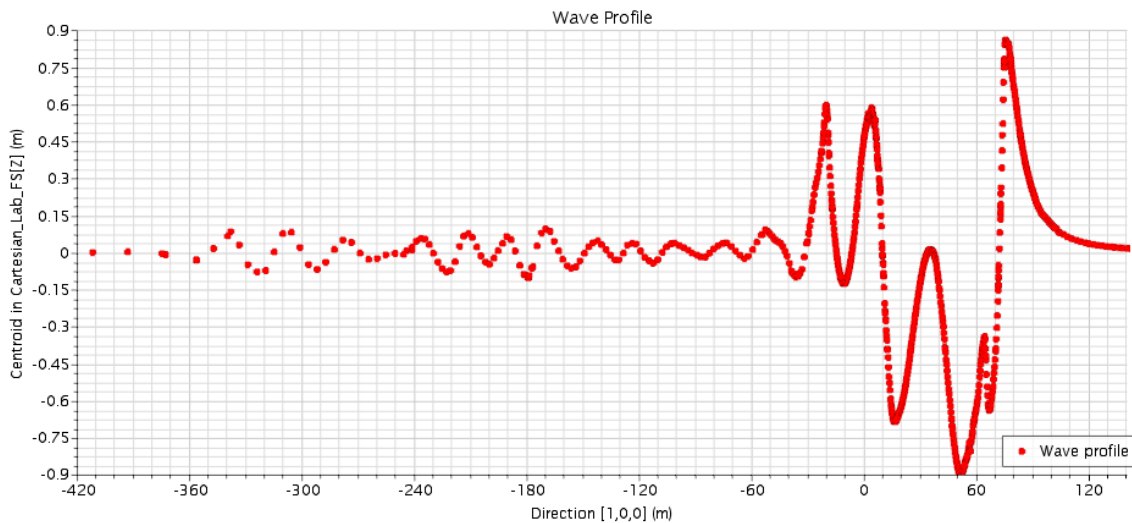


Figure 5-16 Full scale

5.6 Nominal wake

Section contains with the most important results of this Master Project. Here is given an example about nominal wake fraction on a propeller plane in a vessel's speeds equal to Froude number -0.2628 , which is vessel's service speed. All other relevant simulation results for wake fraction on propeller plane and averaged nominal wake distribution along propeller radius is given in appendixes G and H.

5.6.1 Nominal wake fraction on a propeller plane

Visualization of wake fraction on a propeller plane, requires addition field function which have to be defined by user in a STAR CCM+ simulation software. Functions in software looks like this:

$$\text{Wake fraction} = (V_{\text{ship}} - \{\text{Velocity}\})/V_{\text{ship}} \quad (5.3)$$

Where V_{ship} is vessel speed in m/s.

Beside wake fraction in visualization of results, also is given cross flow (arrows in Fig 5-16 and 5-17). The cross flow stands for the geometrical sum of the tangential and radial velocity components, i.e. $V_t/V + V_r/V$.

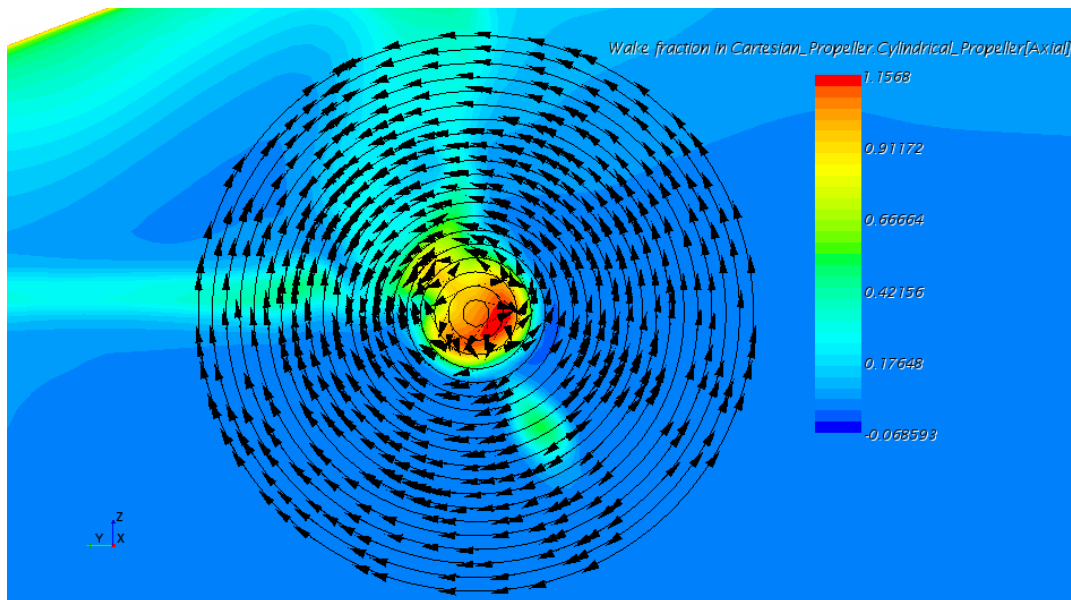


Figure 5-17 Nominal wake fraction. Model scale

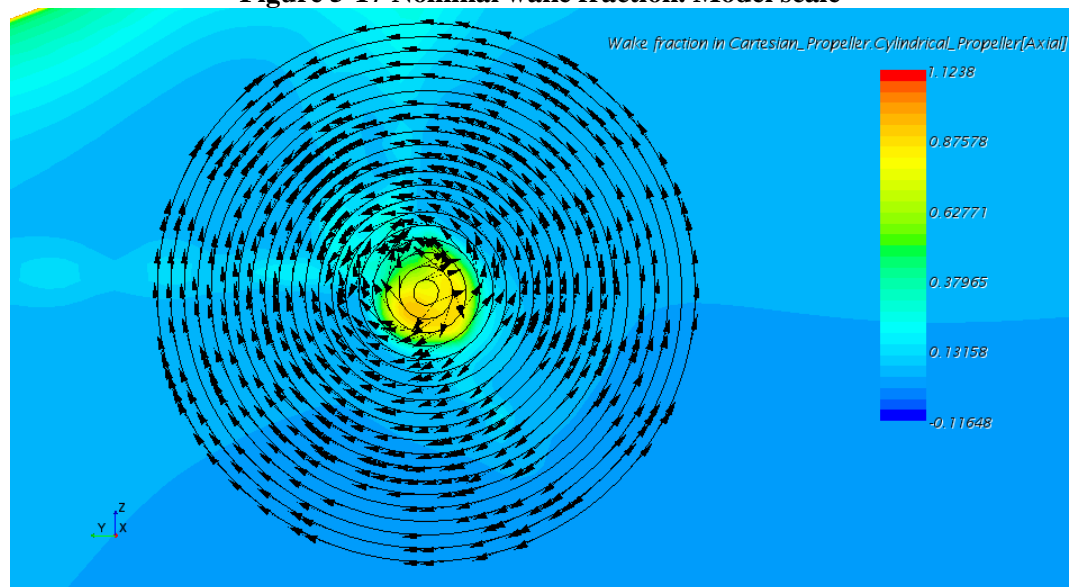


Figure 5-18 Nominal wake fraction. Full scale

Circular sections in figures above represents propeller various radius, in model scale each section have a step of 0.005m and in full scale – 0.115m, where propeller plane diameters are 0.1m and 2.3m in model and full scale respectively.

In model scale simulation wake fraction maximum and over all values looks a bit higher, but cross flow distribution looks the same. Brighter areas in each figures are presents of appendixes in stern of the vessel.

5.6.2 Averaged wake on propeller plane

For getting mean values of the wake fraction in each propeller plane section, information from STAR CCM+ was transferred to excel spread sheet, due to get better overview how wake is distributed. Example of $Fr=0.2628$ wake distribution plots from CFD software is given in figure below.

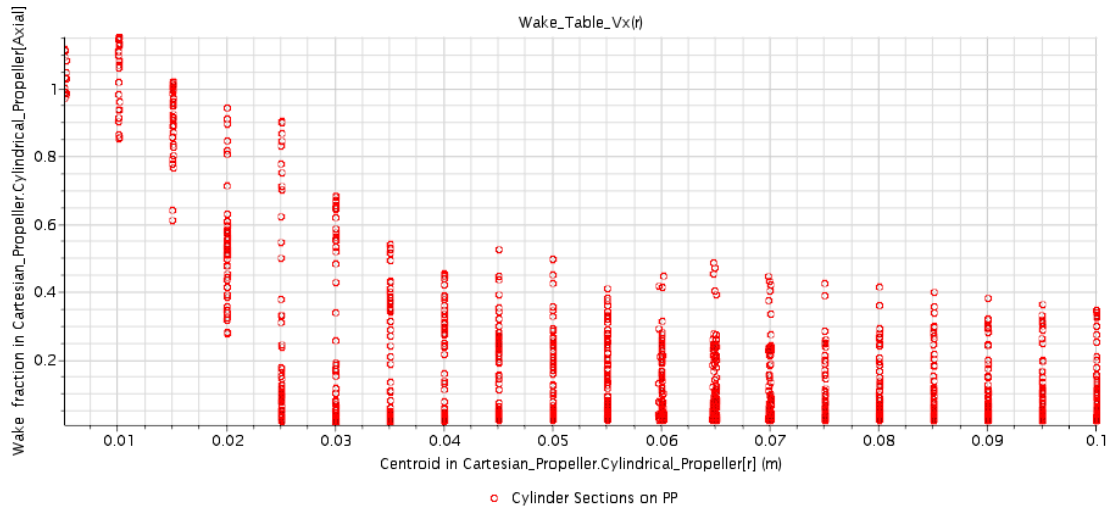


Figure 5-19 Wake distribution on model scale

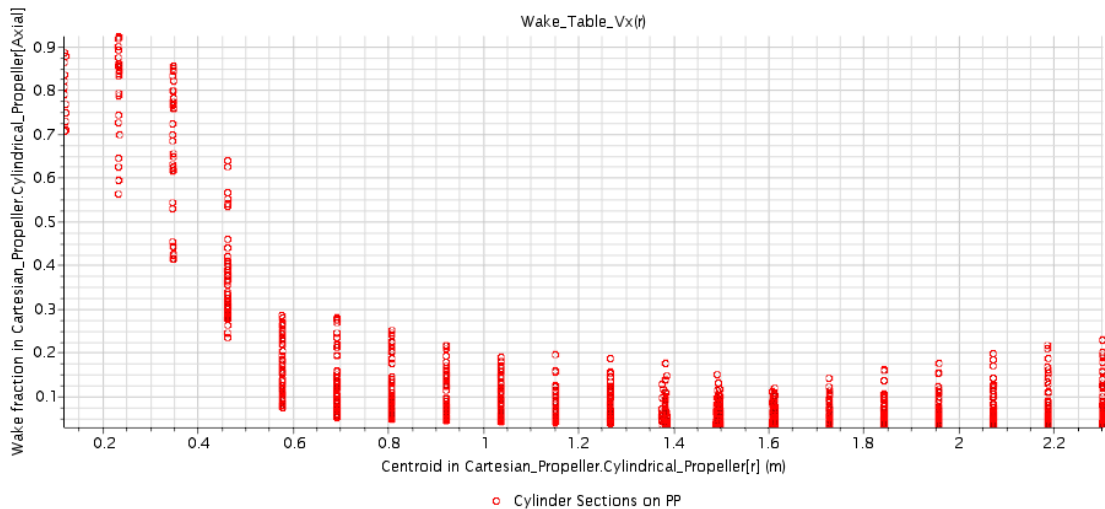


Figure 5-20 wake distribution in full scale

From results in figures 5-18 and 5-19 is hard to get values which could be more suitable for comparison between simulations. Hence table 5-10 shows averaged values on each propeller section.

Table 5-10 Averaged wake fraction distribution (Fr=0,2628)

Model scale		Full scale	
Radius	Wt	Radius	Wt
0,005	1,050	0,118	0,795
0,010	1,018	0,232	0,796
0,015	0,849	0,346	0,663
0,020	0,495	0,461	0,365
0,025	0,226	0,576	0,156
0,030	0,171	0,691	0,115
0,035	0,133	0,805	0,098
0,040	0,122	0,920	0,083
0,045	0,112	1,036	0,072
0,050	0,099	1,150	0,063
0,055	0,094	1,265	0,061
0,060	0,087	1,380	0,057
0,065	0,092	1,492	0,055
0,070	0,084	1,609	0,053
0,075	0,077	1,726	0,054
0,080	0,074	1,841	0,055
0,085	0,071	1,955	0,055
0,090	0,068	2,071	0,056
0,095	0,068	2,186	0,058
0,100	0,068	2,301	0,059
Wt_{average}= 0,253		Wt_{average}= 0,188	

Figure 5-21 shows axial wake fraction distribution along propeller radius according calculated values in table 5-10. In these plots dashed line represents **mean wake** value at all propeller plane. It should be noted that that nominal wake fraction is within the axial direction.

Distribution plots and table 5-10 indicates that mean wake fraction in model scale is higher than in full scale, but full scale simulation shows that wake seems to be more evenly distributed along propeller plane, especially from approx. $\frac{1}{2}$ R to the end of propeller tip.

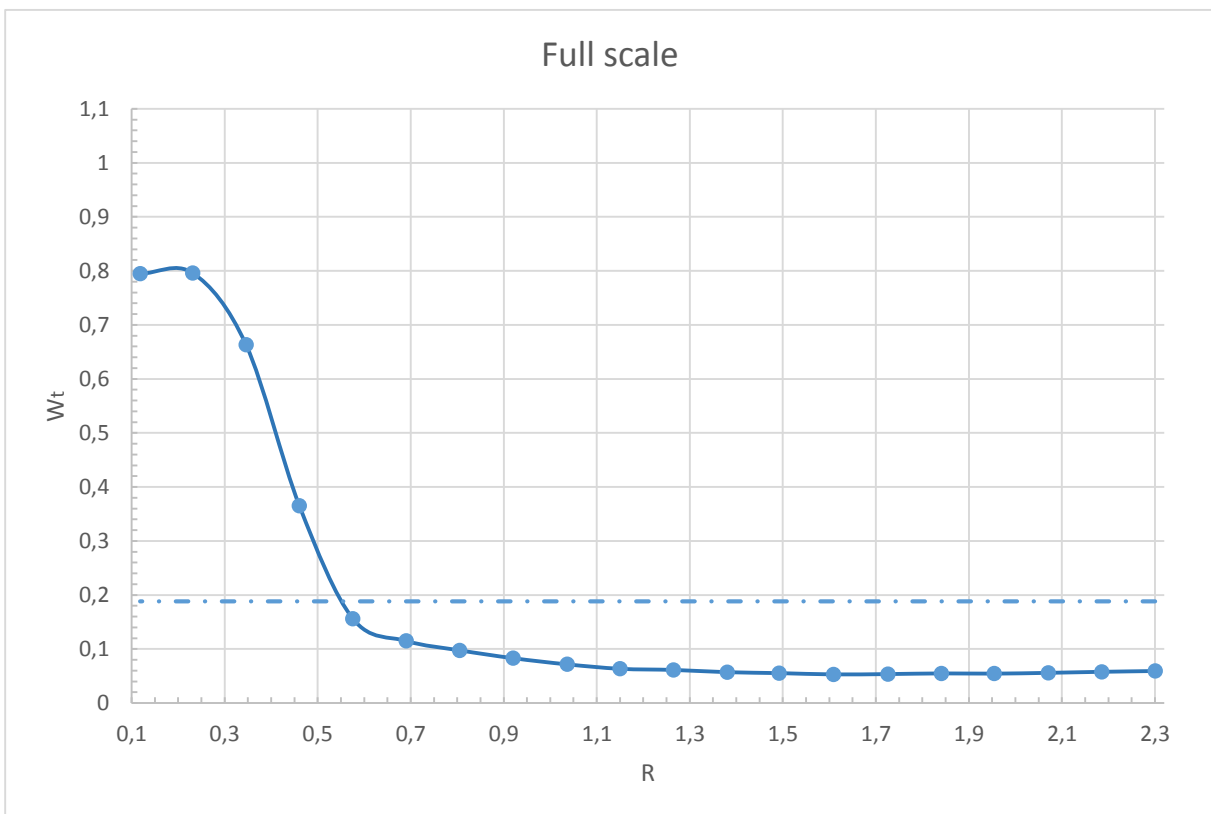
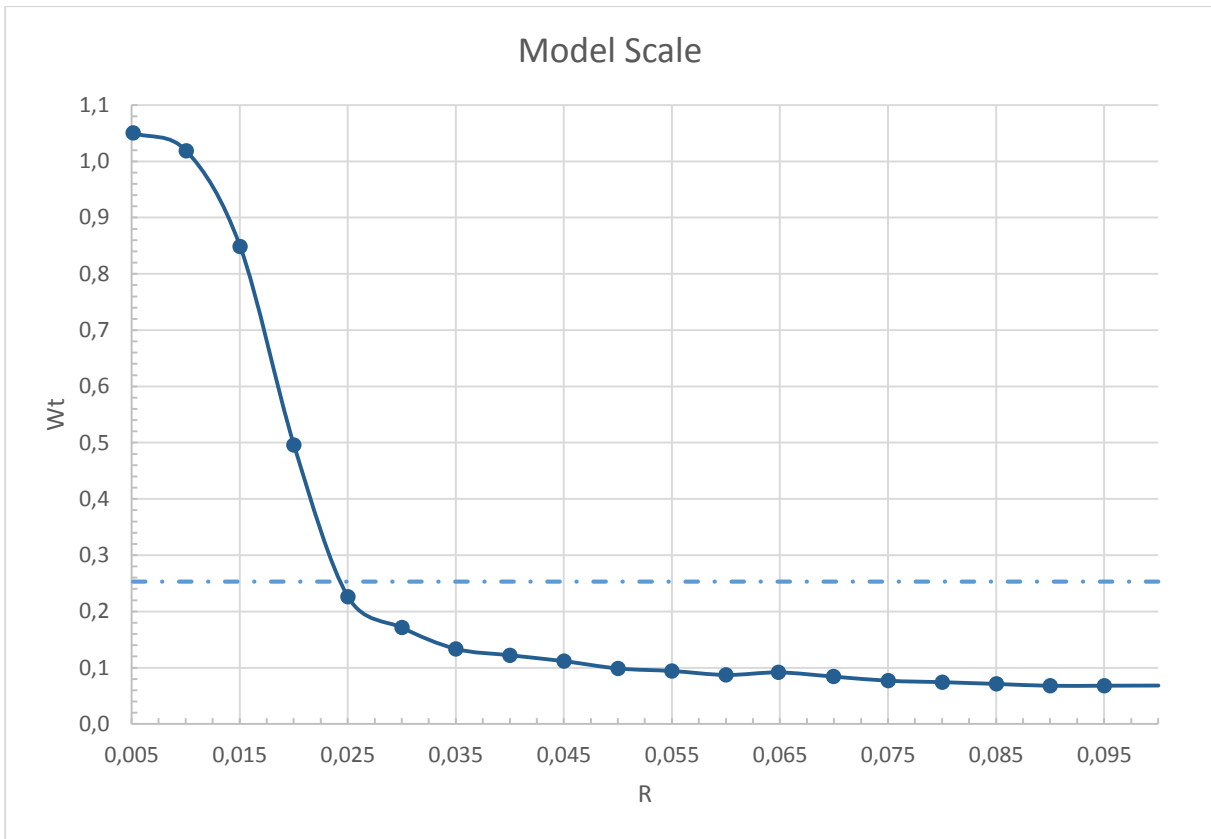
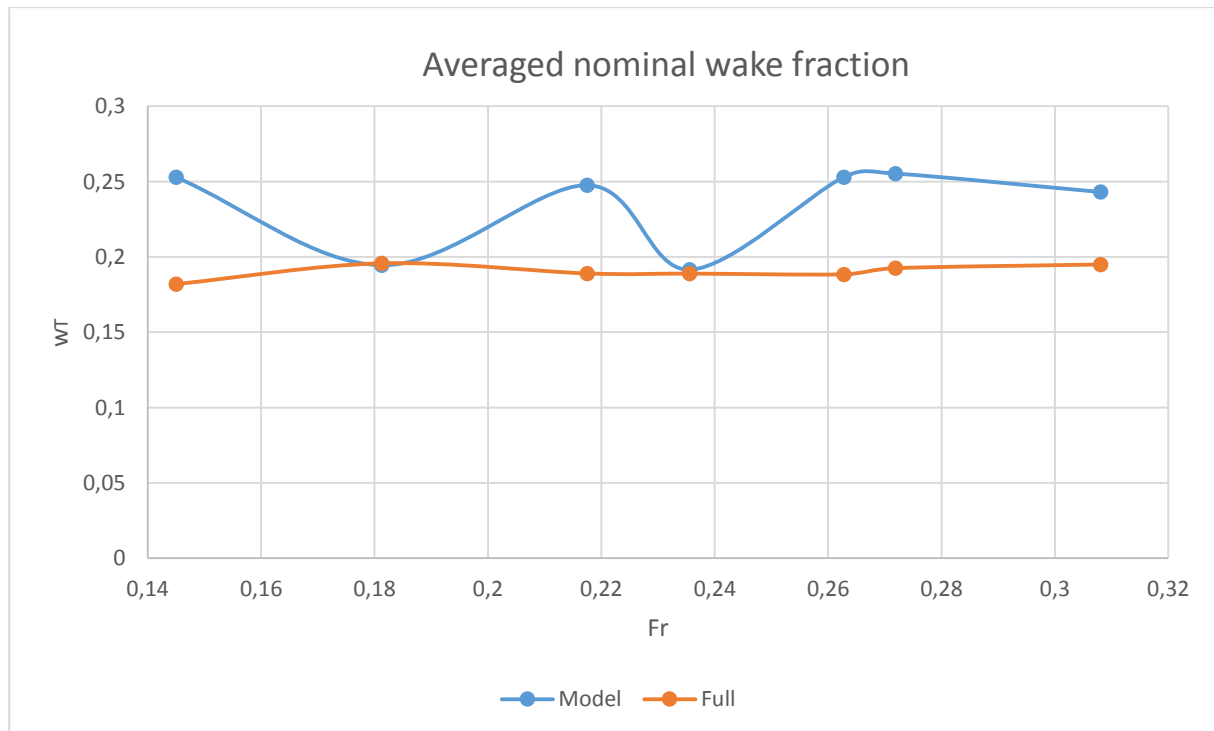


Figure 5-21 $Fr=0,2628$

Table 5-11 Mean nominal wake fraction values in model and full scale

Fr	Model	Full	Diference [%]
0,145	0,25284	0,18199	28,02149
0,1813	0,194486	0,195739	0,644422
0,2175	0,247579	0,189036	23,64608
0,2356	0,191535	0,188922	1,364009
0,2628	0,253004	0,188439	25,51957
0,2719	0,255258	0,192538	24,5713
0,3081	0,243055	0,194997	19,77248

Results shown in table 5-11 and figure below gives an overview how mean nominal wake fraction on propeller plane is distributing along Froude number which were used for simulations. In model scale wake fraction looks unstable and have significant two deflections in $Fr=0.1813$ and 0.2356 , where in full scale simulation curvature of this wake fraction is smoother. Except these two cases where are deflections in model scale calculations, wake fraction results in full scale indicates that values are more than 20% lower.

**Figure 5-22 Mean wake in model and full scale simulations**

6 DISCUSSION

6.1 *Applied settings*

6.1.1 Mesh

Domain mesh in this project were automated mesh generated automatically in STAR CCM+. This was set to be in contribution with geometry parts, but not with the region boundaries, due to that if there would be any changes in geometry (for example: increasing size, change location or scaling whole domain, etc.), mesh can easily be rebuilt by simply repeated automated mesh operation. Also if region settings are modified or deleted, one does not lose any mesh settings, and they can again be easily reproduced, by re-executing the same automated mesh operation. This leads to faster way to set up simulations in a different cases (for this project model and full scale).

Simulations on model scale were performed with example of mesh settings given by Marintek, but when it came to enlarge it to full scale there were used two different options:

- Direct scaled mesh, i.e. whole mesh is simply scaled to the desirable size by simply specifying scaling factor.
- Scaled whole domain with geometry parts, and then with increased base cell size according to scale factor, mesh is re-executing with automated mesh generating option.

First leads to the completely same number of cells in a simulation, where second option have a bit less, 20 thousand in precise. Because simulations ($Fr=0,2628$) with these two mesh types shown results which have almost no different in a C_p values (figure 6-1), computations on other Froude numbers were follow second meshing type, in order to reduce calculation time.

C_p values for evaluating results were chosen, because this shows that pressure coefficient is very sensitive to any changes of computation domain that includes boundaries, number of cells, their size, etc. Note that due to wrong reference area of wetted surface in simulation with direct scaled mesh (figure 6-1 a)), values in the plot must be multiplied by 2.

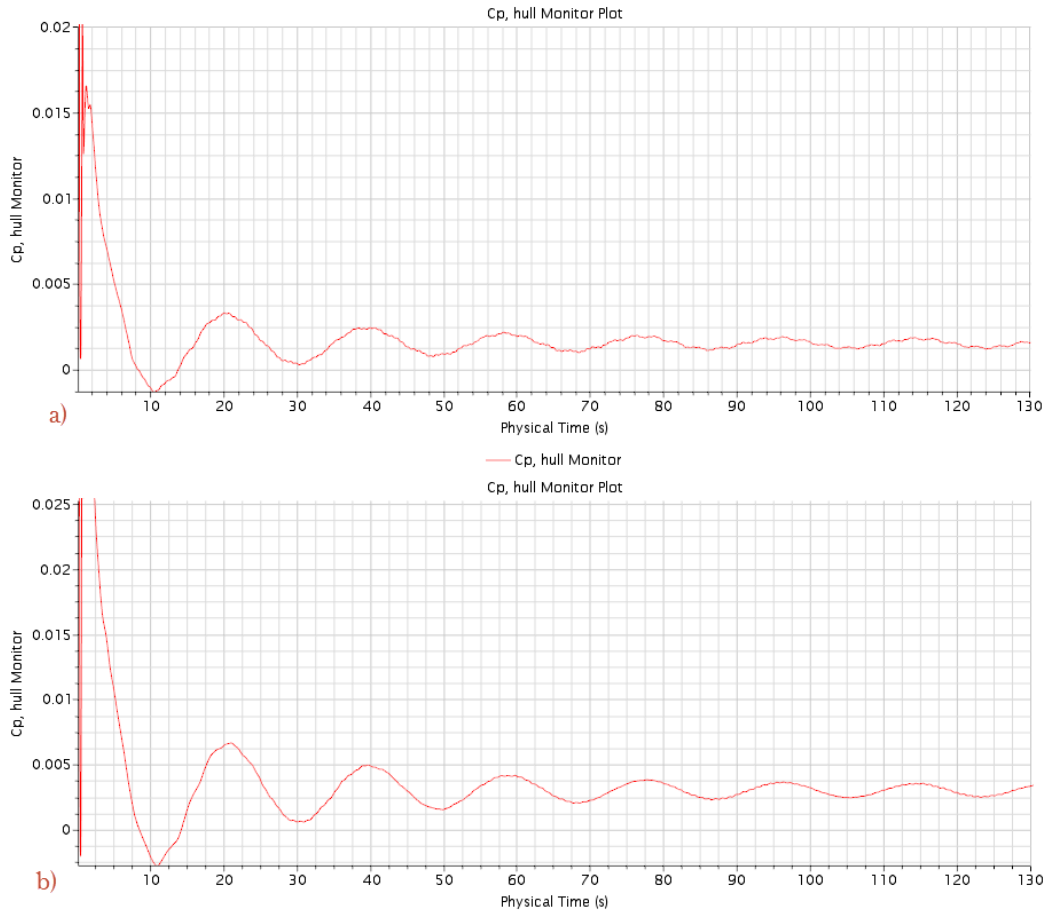


Figure 6-1 Cp force coefficients. a) Directly scaled mesh, b) Scaled geometry & domain

6.1.2 Turbulence model

Decision of what turbulence model should be used in all computations was made by performing simulations in model scale with $Fr=0,2628$. As it shown in table 6-1 force coefficient results from simulations with different turbulence models are basically the same, but $k-\epsilon$ model have poorer performance in a cases where is flow separation involved, and this Master Project contains with such a problem. According to [4] $k-\omega$ model is the most advanced of the two-equation isotropic turbulence models which are available in presents and this model is recommended for most application, hence for project simulations, both in full and model scale $k-\omega$ turbulence model was used.

Table 6-1 Force coefficients according to turbulence model

Turbulence model	Ct	Cp	Cf
	10-3		
k-ε	6,90	3,28	3,62
k-ω	7,04	3,42	3,62

6.1.3 Time step

Investigation of what time step should be in the simulations has been done different in both cases – full and model scale. Time step is very important in this project simulations, due to vortex shedding phenomena caused by central skeg and appendixes in the stern of ship. To choose appropriate time step values, CFL (courant number) was under investigation. Target for CFL is to get a range of 0-2 in most of domain, but in areas such as surface break-up, separation lines and sharp edges, courant number have local “jumps”. Analysis of time step influence for model and full scale simulations have been done on set ups with Froude number = 0.2628.

Model scale. Analysis of influence on time step in model scale was made with two values 0.025 and 0.05 seconds. As it was represented in chapter 5.3.1 force coefficient values were very close for each simulation with these different time steps. Although residuals with time step 0.025s shown that it was more stable along the calculations than in case with time step 0.05 seconds. Besides residuals and force coefficients case with smaller time step gave results of CFL numbers in desirable range, where simulation with time step=0.05s was twice bigger values, due to 4.2 equation.

Because results with smaller time step were almost to the limitations of CFL desirable range, any changes of time step values while keeping all other set up unchanged, this will cause bigger CFL. To reduce CFL with bigger time step it would be necessary to do changes in mesh settings, for example to reduce its size, but this would lead to increased overall time spend on computations, because of greater number of cells in computation domain. Taking everything into account, for model scale simulations most efficient and accurate solution is with **time step = 0.025 seconds.**

Full scale. Computations which were under investigation of time step influence to results in full scale have been made in such a manner: time step = 0.05s, time step = 0.15s and one simulation with mixing both time steps. First simulation with smaller time step value shown results for C_p values which were fluctuated massively compared to two other calculations. This due to convergence which was did not reached yet, even there have been made 500 seconds of simulated time. Also time spend on computation with this time step set up was approx. 150 hours (see table 5-4).

By increasing time step 3 times, computation time have been reduced also 3 times, but results for force coefficients were a bit bigger, where combination of these two time steps in one simulation gives close results as the calculations with time step = 0.05s. Besides that residual

values were decreased significantly, hence the force coefficient values became much less oscillating, i.e. amplitudes of fluctuations became much smaller (see figures 5-5 and 5-6). This combination of time steps option is in the middle between other two in terms of overall time consumption, because of that all other simulations have been performed under mixed time step method.

6.2 Scale effects of force coefficients

In Chapter 5.4 results shown that in model and full scale calculations force coefficients follow same curvature, but values are bit lower in full scale simulations. When it comes to total and shear force coefficients they actually have to be smaller, but pressure coefficient should be at least close values to each other simulation (i.e. model and full scale). Calculations give an overview that in full scale computations C_p values are lower with not significant different, but the percentage tells different story, where it is within a range of 6.4-17.4% reduced values in full scale simulations.

The different in these terms becomes quite big, and could cause a huge underpowered propulsion system if designer would rely on only full scale simulations. This would lead to inefficient vessel operation and huge economical loses. It is hard to say how accurate results are on the force coefficients without experimental data. During project there wasn't a possibility to get these empirical data from other sources for this particular vessel (STX-413).

Having in mind that model scale simulations have been performed with wrong wetted surface area, needed as a reference to force coefficient calculations that could be a main purpose why model scale simulations have a bit higher values. Now results on these computations are multiplied by 2 in order to get right values for force coefficients, but guestimate would if simulations would be ran again with right surface area, resulting plots would probably have bigger oscillations. By calculating those results averaged values, might be improved accuracy of them, which could lead to more similar resulting graphs on C_p coefficients between model and full scale.

Another reason why there are differences on C_p values could be that in model scale have been done much less iterations, resulting lower simulated physical time. This was done due to assumption that model scale simulations have been reached there convergence after approx. 80 seconds of simulated time. This assumption could be wrong and the best way would be redone some of the simulations in order to ensure is this the main cause of those inaccuracies.

Another important thing which could be a part of different pressure coefficient results is values of y^+ (see appendix B). In full scale simulations y^+ values are way over of desired range, i.e. $30 < y^+ < 300$. In regions of ship hull where force coefficients are calculated, actual values of y^+ in some of simulations reaches more than 6000. So in this case near-wall treatment might not work properly in full scale computations. To reduce values of y^+ could be achieved simply by reducing cell size on boundary layer and increasing of prism layers in that region. In project simulations Prism layer number is 5, which is absolute minimum stated in [4], so this could be considered to be increased.

6.3 Scale effects of nominal wake fields

Same as pressure force coefficient, averaged nominal wake values in simulated range of Froude numbers are lower in full scale simulations. As it shown figure 5.22 nominal wake in full scale looks steadier throughout simulations, where in model scale are fluctuations. It is probably another indication that model scale computations have not reached their convergence or there could be needed to change some settings in CFD software. Author of this project believes that the presents of oscillating nominal averaged wake values are due to poor convergence of model scale simulations.

In most of the simulated cases resulting wake values on propeller plane are lower in full scale, but graphs shown (fig 5-21 and appendix H) that in these simulations are much smother curves representing wake fraction throughout propeller radius than in those in model scale. Again that main cause could be of not enough iterations done on model scale computations. Even though if simulations would be calculated with much more time steps or iterations, it is hardly possible that resulting overall picture would be different. It is possible that model and full scale wake fraction values would be closer to each other, but with the current settings tendency would became similar – nominal wake fraction in full scale would be below model scale resulting wake curve. For getting better impression how scaling is effecting wake field its necessary to get empirical data from experiments and to continue simulations on model scale in order to get better convergence of the results.

Overall figures given in appendix G shows very similar image how the wake is distributed behind of the vessel, in this case on the plane located directly where actual propeller should be. Arrows representing of sum of tangential and radial velocity components have some minor differences, due to scaling and getting proper picture of this, but still there are ability to see very close similarities between full and model scale simulations. Many figures in appendix G

where it shown model scale resulting picture are a bit darker, this is because of STAR CCM+ visualization tools doesn't have many option to create scaling which be same in two different cases, and another reason that the actual wake fraction is a bit higher (in some cases lower) than in full scale. So by having 32 colour range in both types of simulations it is not possible to visualize results which would be more comparable, this could be done by exporting results in another software like AKPA developed by Marintek.

7 CONCLUSIONS

Domain size used in full and model scale computations is given in a table 7-1. After scaled whole domain and geometry parts from model to full scale, and changed base cell size according to scale factor – there have been 20 000 cells decrease in a computation domain.

Table 7-1 Summary of domain size

Scale	Number of cells in millions
<i>Model scale</i>	4.67
<i>Full scale</i>	4.65

During simulations in model and full scale, there was not made any changes with settings except time step was set to be different (see table 7-2). Model scale calculations have been done by using one time step value throughout all simulation, where in full scale simulations time step have been combined. First 5000 iterations was done with bigger time step and what was left with smaller values of time step. This method have been done in order to reduce computation time, and also as results had shown that there have been a significant improvement of residuals (see appendix A.).

Table 7-2 Summary of time step used

Simulation	Time step
Model scale	0.025
Full scale	0.15 & 0.05

Table 7-3 gives a results of computed force coefficients. It have to be noted that in model scale part of this table, values are multiplied by 2, because during simulations there have been made user mistake in defining wetted surface area of ship hull. Force coefficients in model scale

calculations were simulated according full ship hull, where actual domain was made only on half of vessel by introducing symmetry plane.

Table 7-3 Summary of force coefficient results

Fr number	Model Scale			Full scale		
	Ct	Cf	Cp	Ct	Cf	Cp
	10 ⁽⁻³⁾			10 ⁽⁻³⁾		
0,1450	7,395	4,083	3,312	4,845	2,093	2,752
0,1813	7,337	3,895	3,442	5,089	2,037	3,052
0,2175	7,069	3,763	3,306	4,753	1,974	2,779
0,2356	6,992	3,650	3,342	4,709	1,948	2,761
0,2628	7,088	3,622	3,466	4,937	1,917	3,020
0,2719	7,315	3,597	3,718	5,151	1,907	3,244
0,3081	9,050	3,714	5,336	6,969	1,975	4,994

In table above results are calculated on 7 different Froude numbers, figure 7-1 illustrates averaged wake fraction on the same simulations on Fr numbers in model and full scale. Results has been shown that full scale nominal averaged wake fraction on propeller plane is in most simulated cases lower than in model scale. Also same simulations have more stable wake distribution along propeller radius (see appendix G.), where model scale results shown that towards to propeller tip averaged wake distribution curve is a bit fluctuating, but not significantly. On another hand figure 7-1 shows quite big oscillations of averaged nominal wake along simulated cases compared to full scale simulations. This might be due to poor convergence of calculations done in model scale, where assumption have been made that in model scale results are already converged after 80 seconds of simulated time.

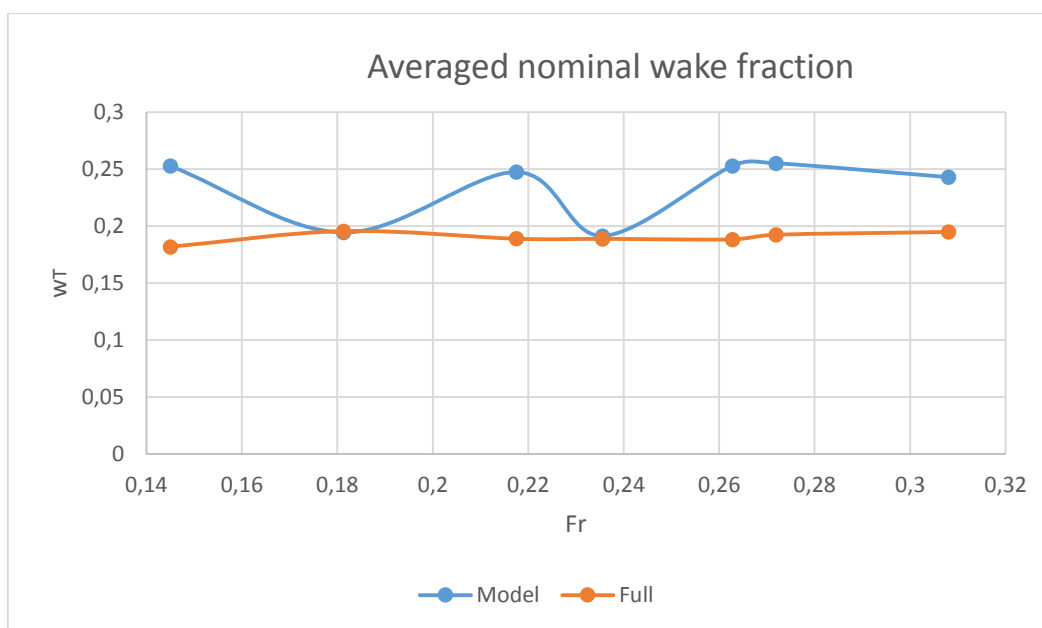


Figure 7-1 Averaged nominal wake fraction on a propeller plane

In general differences between pressure force coefficients and nominal wake fraction in model and full scale could be appeared because as it was mentioned of poor convergence in model scale simulations. Also there could be a minor impact of wrong given reference area of wetted surface, where force coefficients are calculated. If the calculations would be repeated, there probably would appear a bigger oscillations in results of force coefficients in model scale. Those then should be calculated as the mean values in the same manner as it was done in full scale computation results.

Even if the simulations would be redone in model scale with suggested methodology, it would be hard to compare and evaluate results, due to missing experimental data. During the project, there haven't been any possibility to get empirical data for vessel which is under investigation in this Master Thesis. This must be the most important information in order to do further analysis and evaluation of the simulated results.

Another important thing which have to be taken into account is same simulations, which should be done with ability for model to trim and sink. This could indicate more uncertainties which could lead in wrong settings for computation domain or in opposite that simulations are done correctly with proper set up. It was planned to do these kind of simulations where model will have sinkage and trim in the planning of this Master Thesis, but during spring there was not provide necessary information to proceed this calculations, i.e. point of gravity and inertia moments. But having in mind that those simulations had to be done with the resources which were provided, this would be impossible to finish simulations in time even necessary information would be provided.

After all, simulations has been shown that in full scale nominal wake has decreased values in comparison with model scale calculations. Results indicates that differences can reach more than 28% of averaged nominal wake on propeller plane. It is hard to say if the results are in line with reality without further investigation on this particular problem.

8 FURTHER WORK

As it was mentioned above results in this Master Thesis cannot be taken as a reference for expectations what could be in real life situations. Thus there have to be further investigation on this particular problem, i.e. scale effects of wake field behind twin screw vessel.

After experience achieved during this project, first thing would be to repeat or further calculate all cases in model scale simulations with proper reference values of wetted surface area and

performing much longer computation time, for example to 250 seconds or as it was done in full scale simulations to 500 seconds of simulated physical time. This could be done by trying to implement same strategy of time step as in full scale, i.e. combining bigger and smaller values, in order to reduce overall solution time, for example in the beginning perform simulations with time step=0.05s and after several thousand iterations change it to 0.025s.

Second thing which is necessary is to perform simulations in both model and full scale, where ship hull will have ability to sink and trim. This must be done with additional information data about vessel's gravity point and of course information about inertia moments of hull, which have to be included in a set up in CFD simulation software (STAR CCM+).

Another simulations could be done with domain which includes whole ship hull. This could give more accurate results, because in simulations which are done there have been noticed vortex shedding phenomena. So it is not particular right or accurate enough to have simulations with domain where calculations are done with half vessel and symmetry plane.

And finally the most important thing is to get experimental data to evaluate results which are calculated mathematically in CFD analysis tool. This have to be done in order to know is the simulation results are good enough to be taken in further investigation and developing of prediction model for wake field on a propeller plane.

REFERENCES

- [1] Molland, A., Turnock, S. and Hudson, D. (2011). *Ship resistance and propulsion: Practical Estimation of Propulsive Power*. New York: Cambridge University Press.
- [2] Ferziger, J. and Perić, M. (2002). *Computational methods for fluid dynamics*. Berlin: Springer.
- [3] Bertram, V. (2000). *Practical ship hydrodynamics*. Oxford: Butterworth-Heinemann.
- [4] Krasilnikov V. I. (2011). *First Introduction in to Computational Fluid Dynamics for Marine Applications: Lecture Notes*. 1st edition. Ålesund University College.
- [5] Ponkratov D. (2014). *Marine CFD for Engineering Applications: Lecture Presentation*. Ålesund University College.
- [6] WS Atkins Consultants And members of the NSC. *Best Practice Guidelines for Marine Applications of Computational Fluid Dynamics*. Imperial College of Science and Technology, Germanischer Lloyd, Astilleros Espanoles.
- [7] ITTC (2011). *Recommended Procedures and Guidelines: Experimental Wake Scaling Methods*. Available from: <http://itc.sname.org/> [Accessed: April 2015].
- [8] ITTC (2011). *Recommended Procedures and Guidelines: Resistance Test*. Available from: <http://itc.sname.org/> [Accessed: April 2015].
- [9] ITTC (2011). *Recommended Procedures and Guidelines: Practical Guidelines for Ship CFD Applications*. Available from: <http://itc.sname.org/> [Accessed: April 2015].
- [10] ITTC (2008). *Recommended Procedures and Guidelines: Propulsor Nominal Wake Measurement by LDV Model Scale Experiments*. Available from: <http://itc.sname.org/> [Accessed: April 2015].
- [11] ITTC (2008). *Recommended Procedures and Guidelines: Testing and Extrapolation Methods, General Guidelines for Uncertainty Analysis in Resistance Towing Tank Tests*. Available from: <http://itc.sname.org/> [Accessed: May 2015].
- [12] ITTC (2008). *Recommended Procedures and Guidelines: Uncertainty Analysis in CFD Verification and Validation Methodology and Procedures*. Available from: <http://itc.sname.org/> [Accessed: April 2015].
- [13] ITTC (1999). *Recommended Procedures and Guidelines: CFD, Resistance and Flow Uncertainty Analysis in CFD Examples for Resistance and Flow*. Available from: <http://itc.sname.org/> [Accessed: April 2015].

- [14] ITTC (1999). *Recommended Procedures and Guidelines: CFD, Resistance and Flow Benchmark Database for CFD Validation for Resistance and Propulsion*. Available from: <http://itc.sname.org/> [Accessed: April 2015].
- [15] [http://www.numeca-usa.com/fileadmin/Papers/2013 - On the Importance of Full-Scale CFD Simulations for Ships - COMPIT cortona.pdf](http://www.numeca-usa.com/fileadmin/Papers/2013_-_On_the_Importance_of_Full-Scale_CFD_Simulations_for_Ships_-_COMPIT_cortona.pdf) [Accessed: May 2015]
- [16] <http://www.cd-adapco.com> [Accessed: March 2015]
- [17] file:///C:/Program%20Files/CD-adapco/STAR-CCM+10.02.010/doc/en/online/index.html#page/STARCCMP%2FGUID-B8098081-75D7-4A30-B0EC-5C1691B8D304%3Den%3D.html%23wwconnect_header [Accessed: May 2015]

APPENDIX

Appendix contain most of the figures which are compared, i.e. model scale and full scale. In all those figures first comes results from model scale simulation and lower part from full scale calculations.

A. Residuals

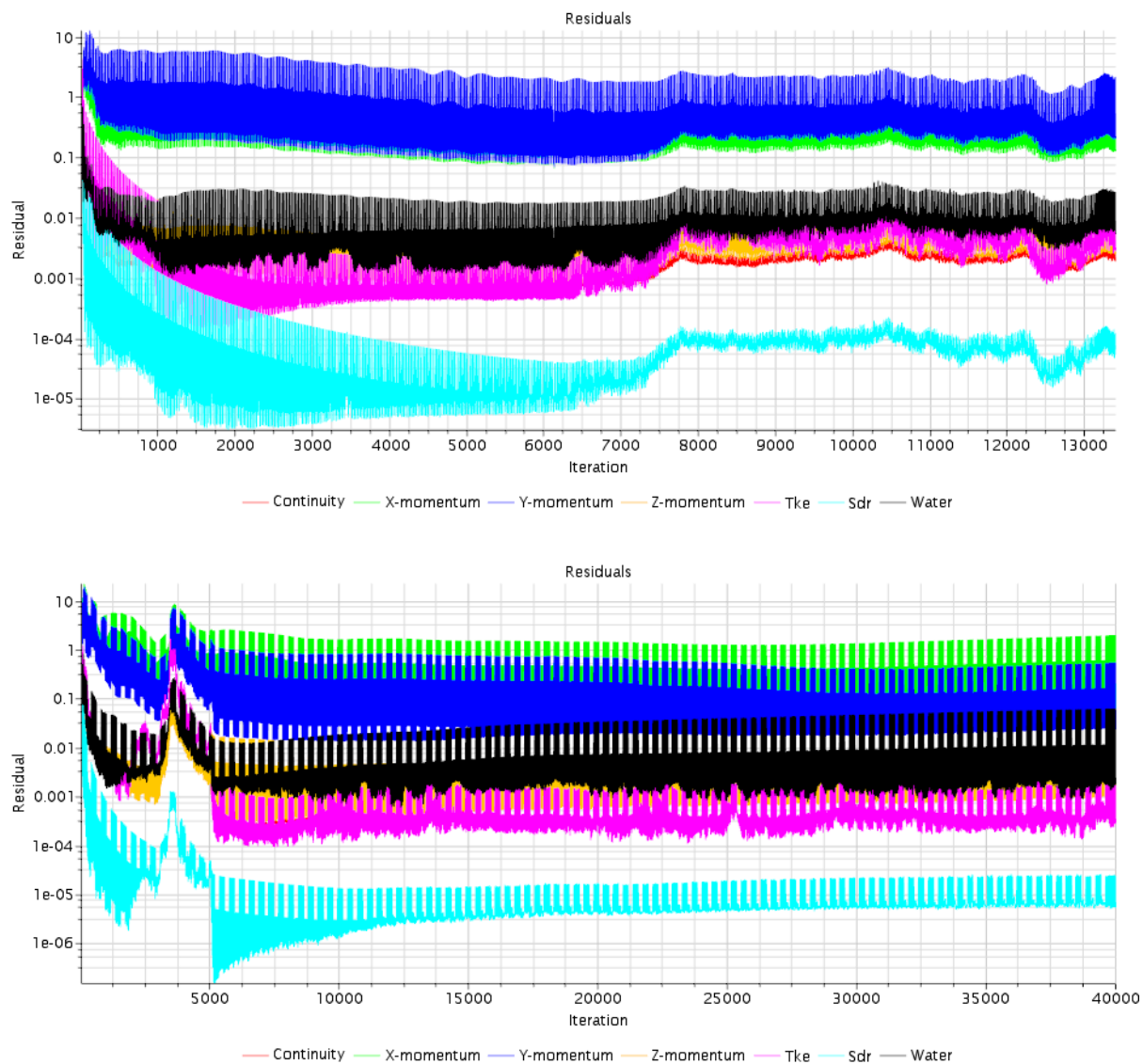


Fig. 1 $Fr=0,1450$

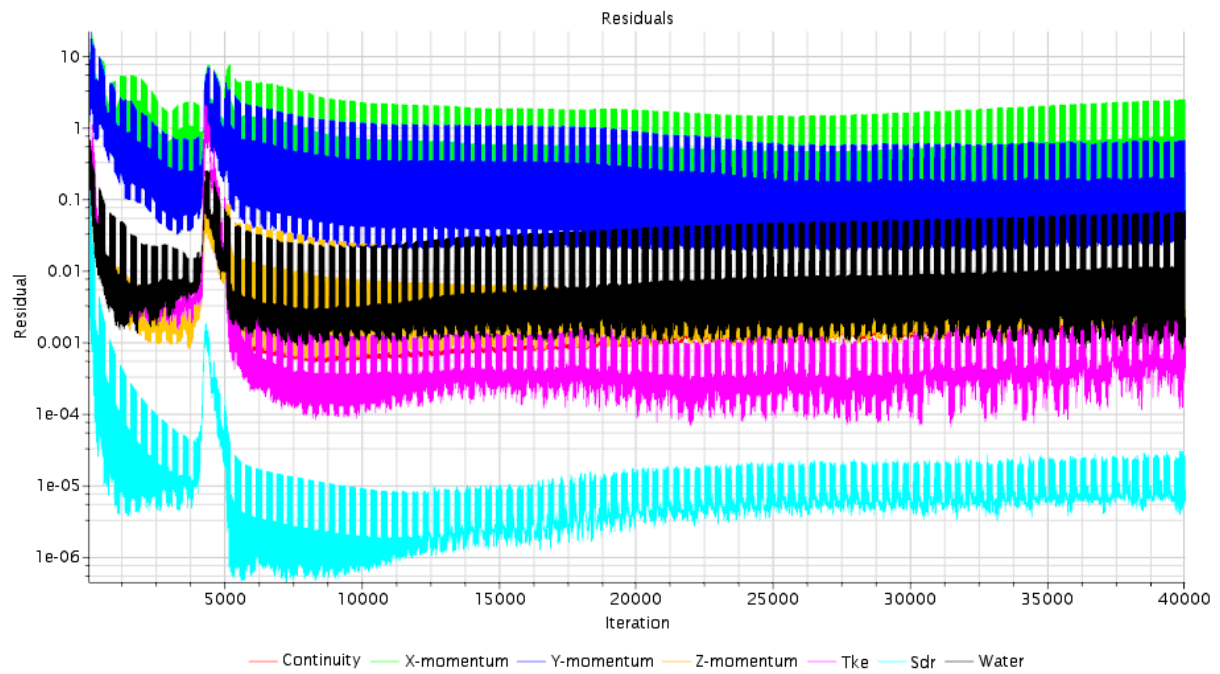
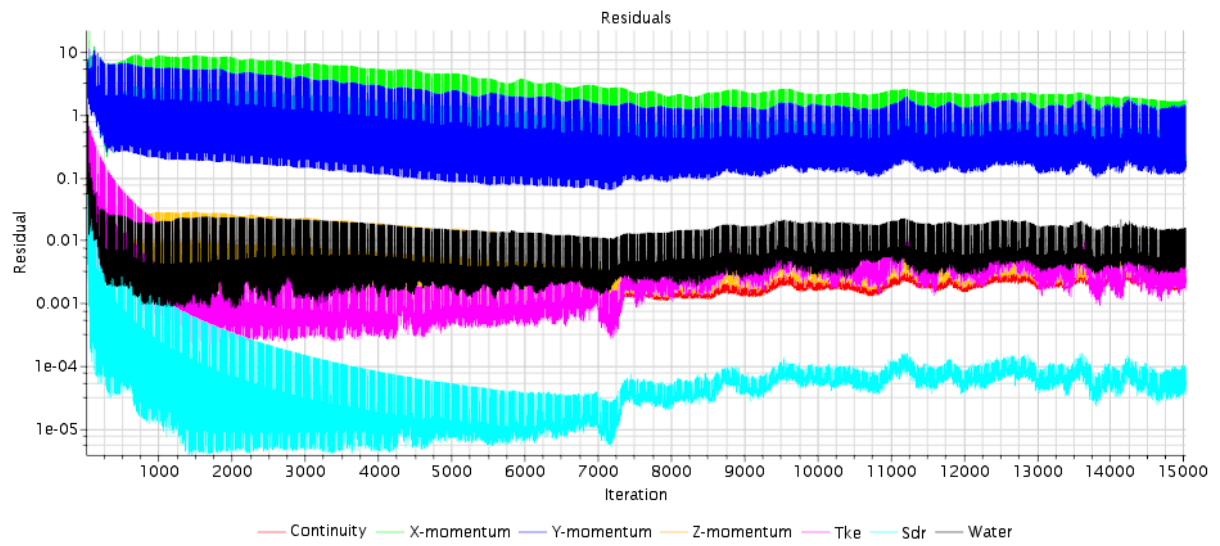
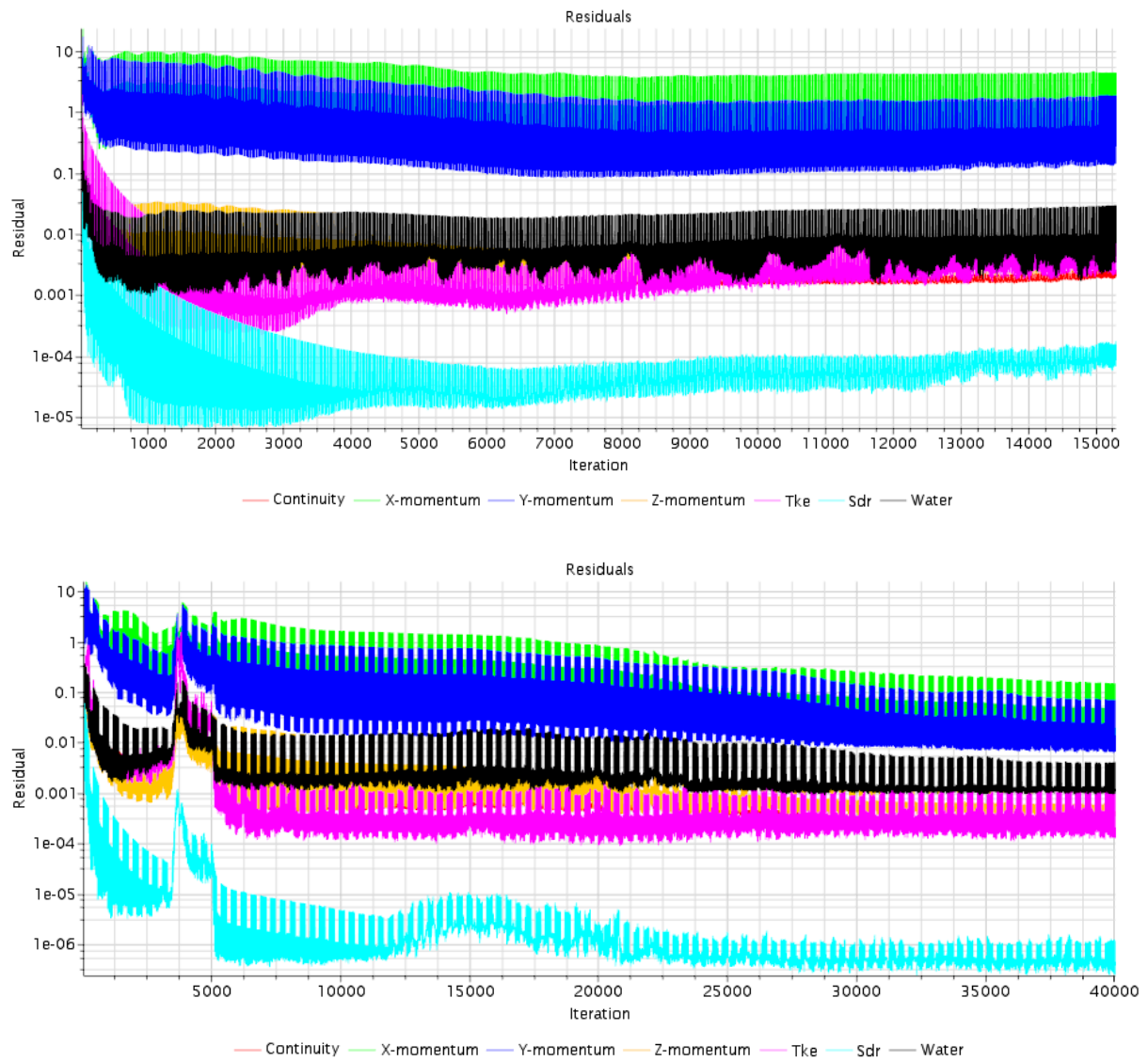


Fig. 2 Fr=0,1813

**Fig. 3** $Fr=0,2175$

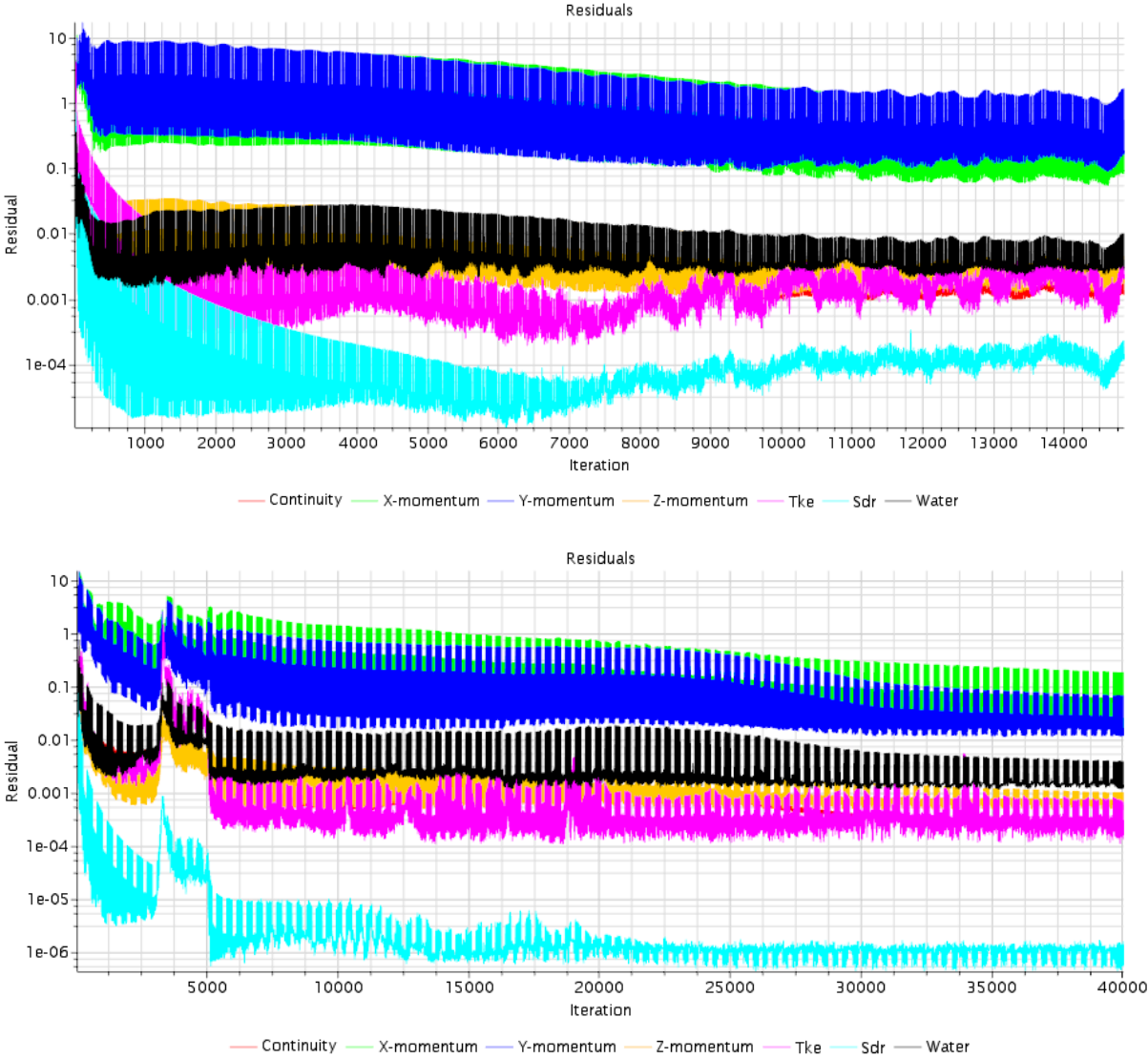


Fig. 4 Fr=0,2356

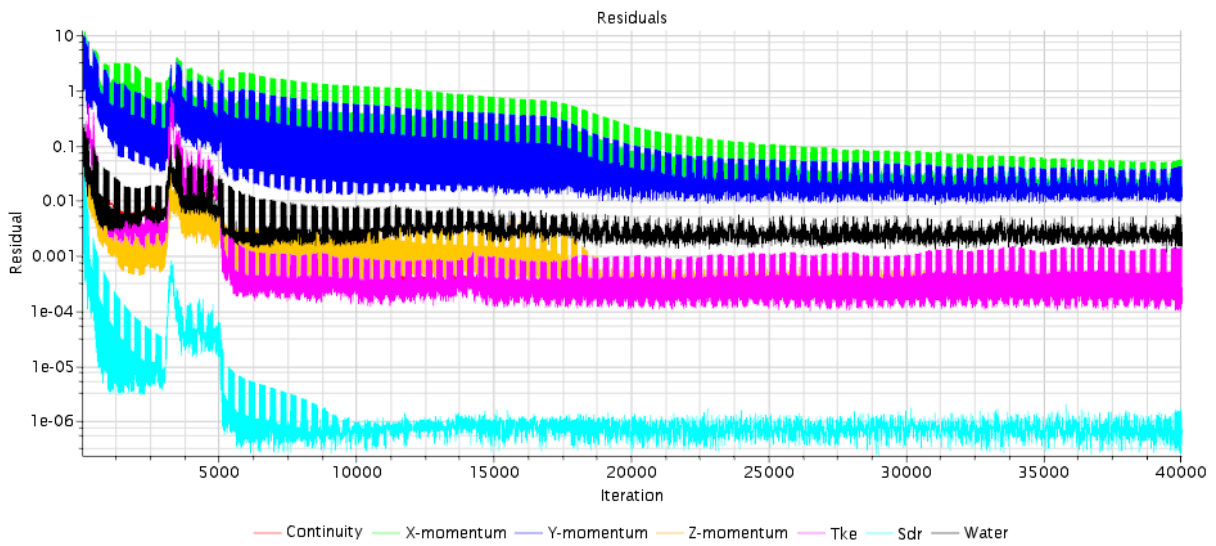
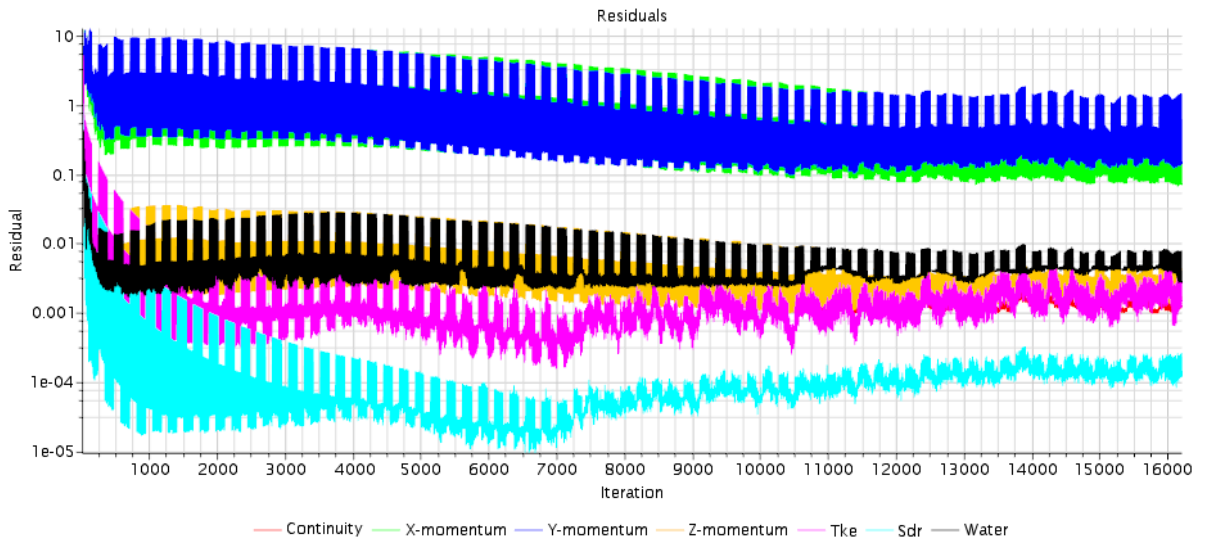


Fig. 5 Fr=0,2628

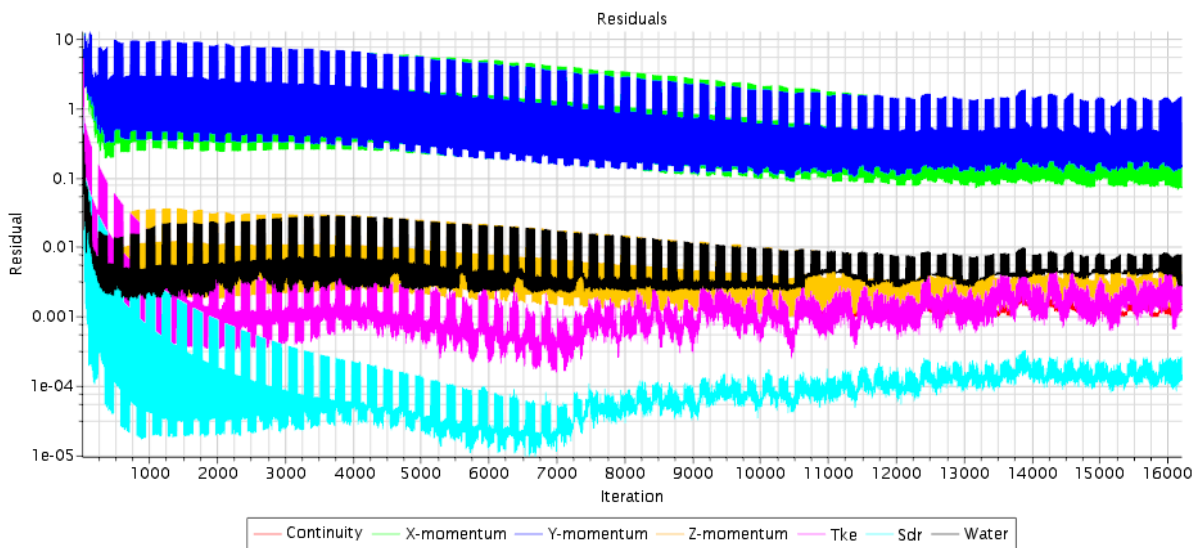


Fig. 6 Model scale_time step 0.025 (Fr=0,2628)

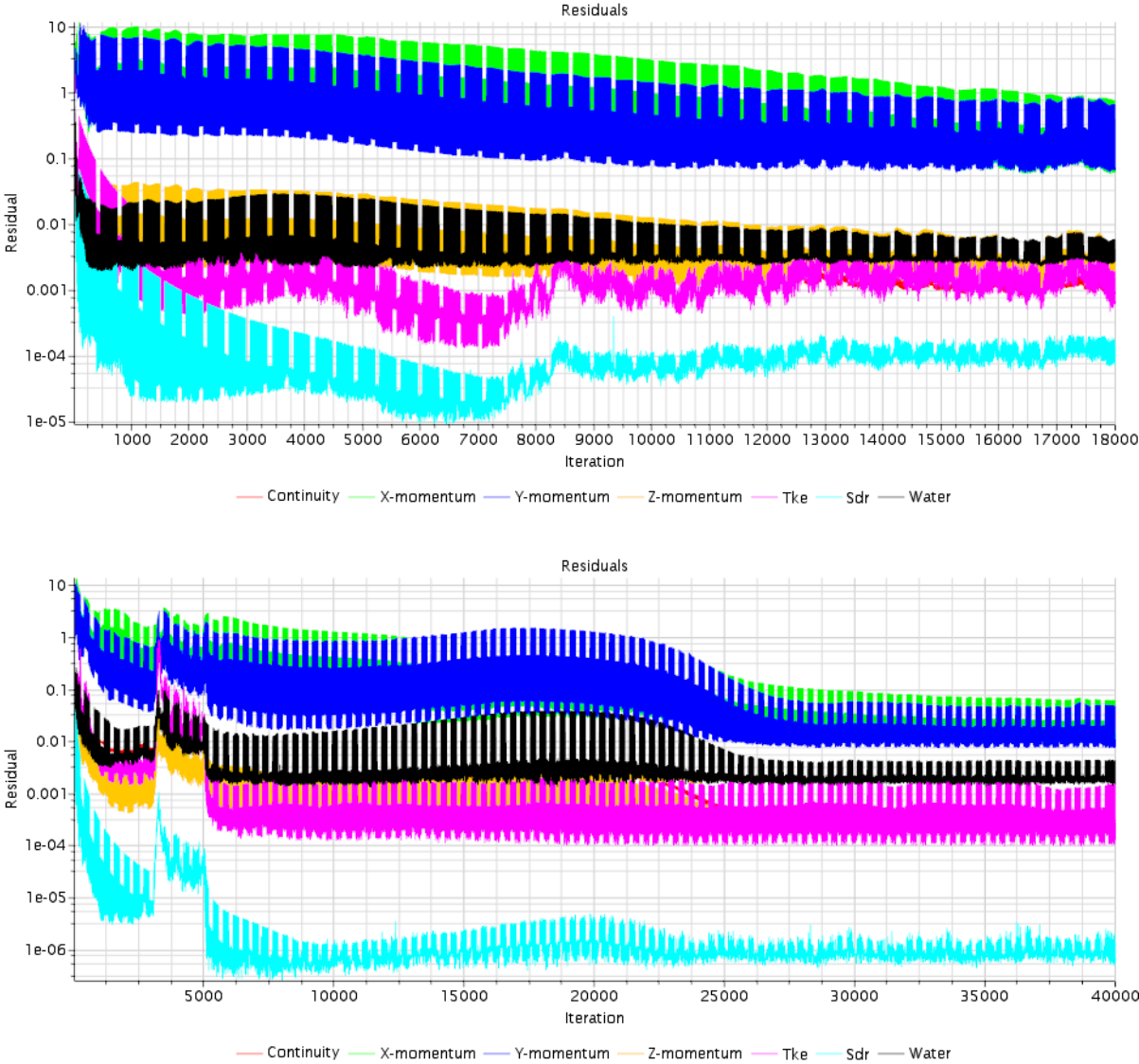


Fig. 7 $Fr=0,2719$

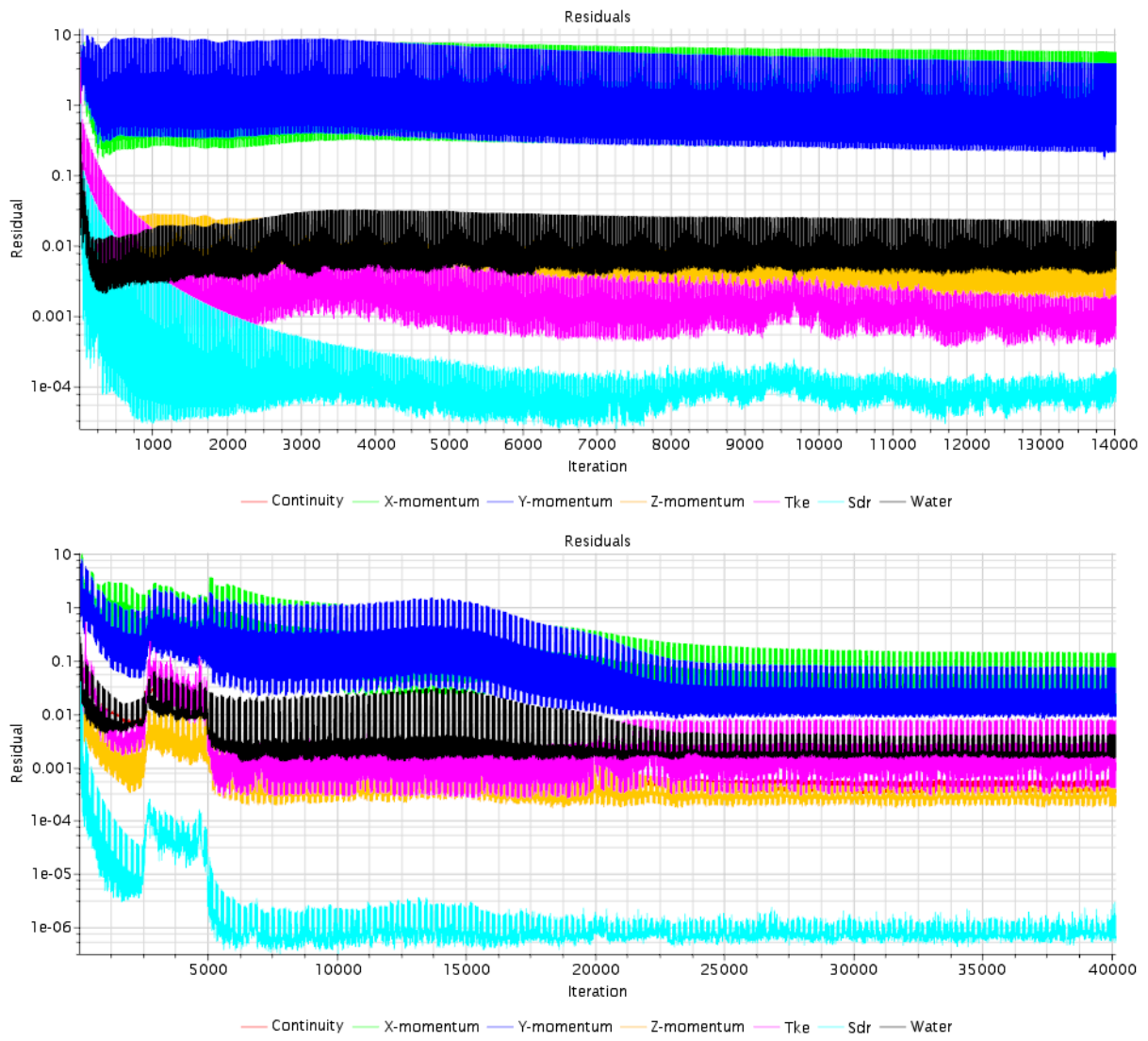


Fig. 8 Fr=0,3081

B. Y+

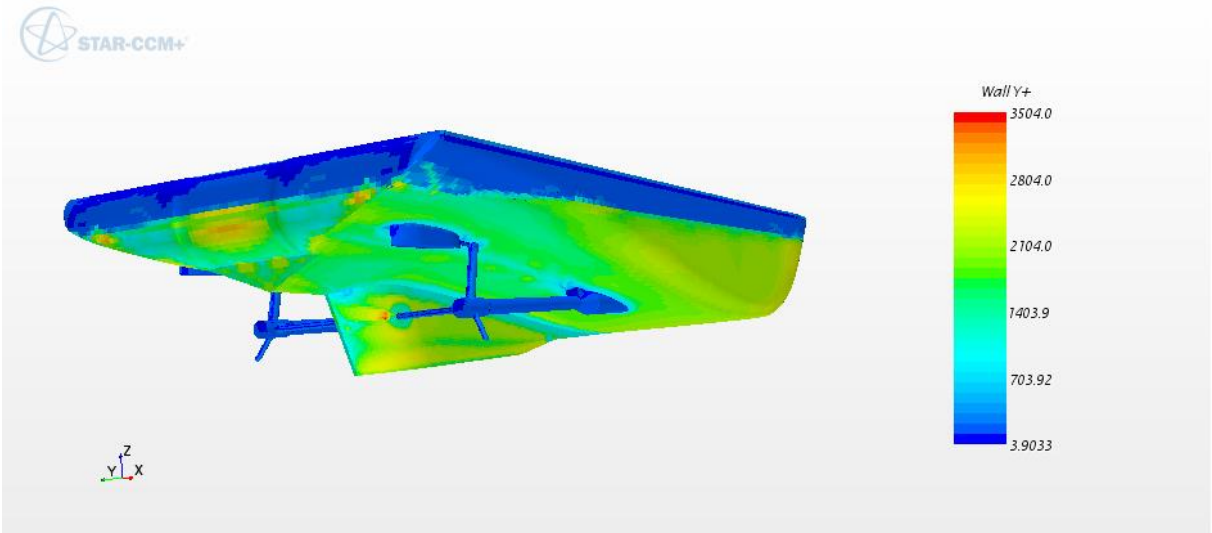
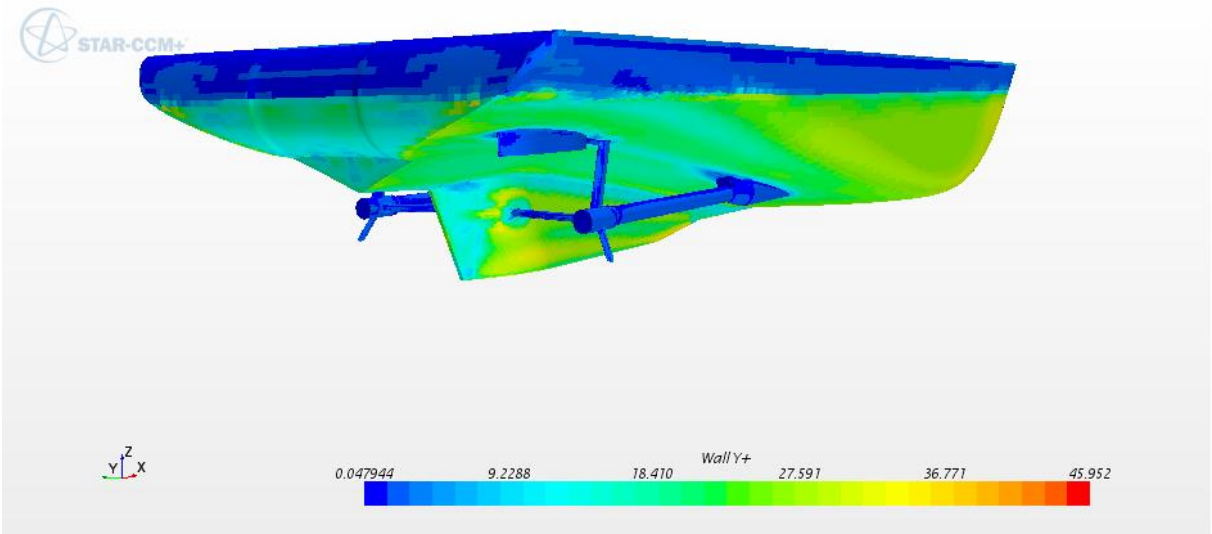


Fig. 9 Fr=0,1450

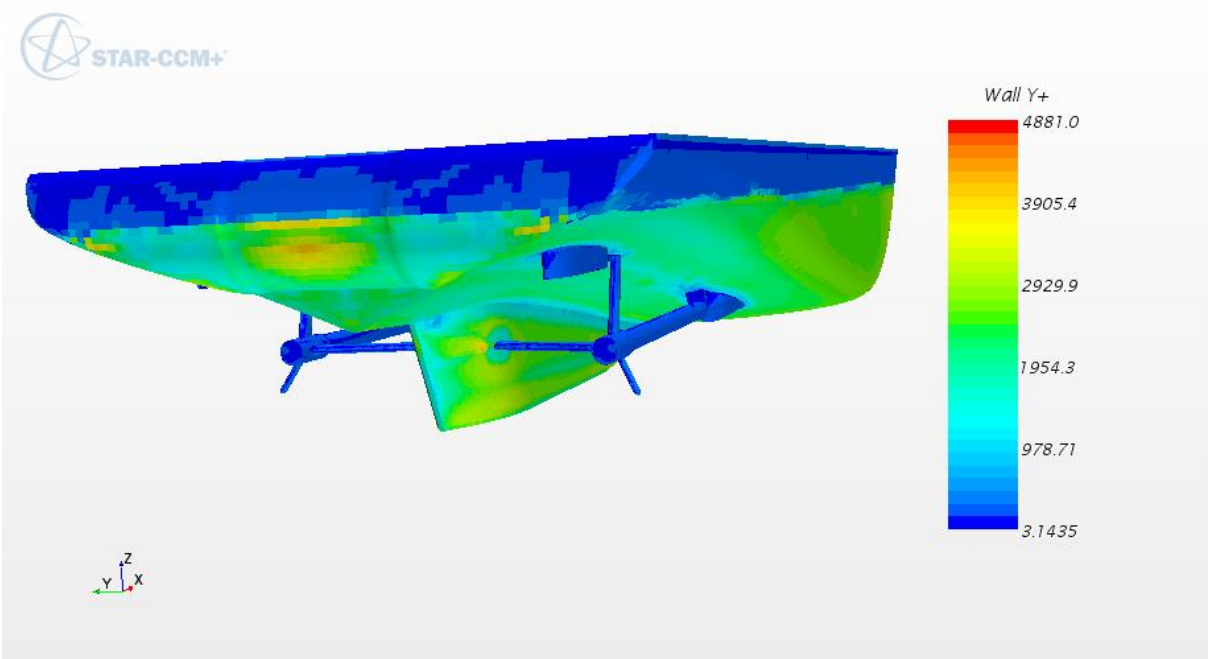
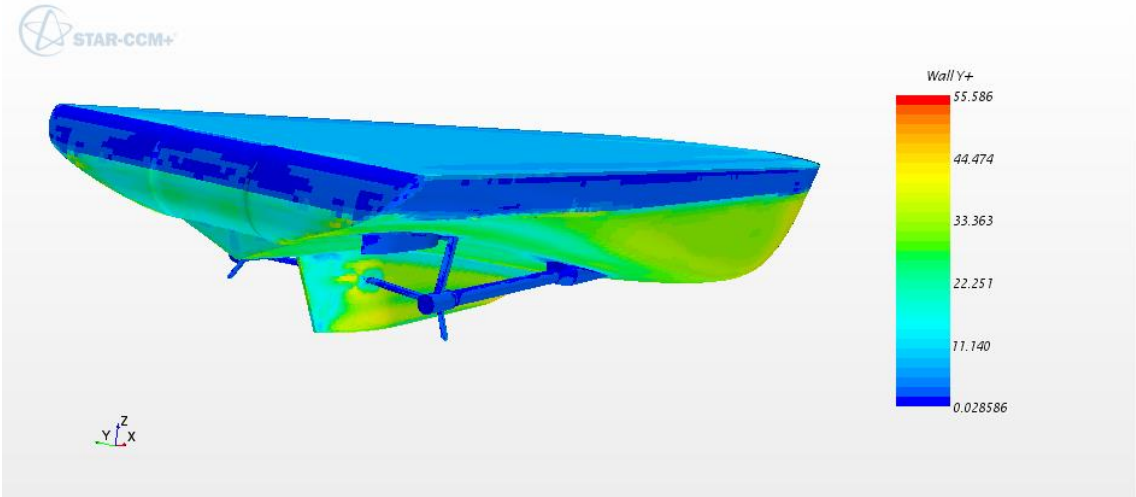


Fig. 10 Fr=0,1813

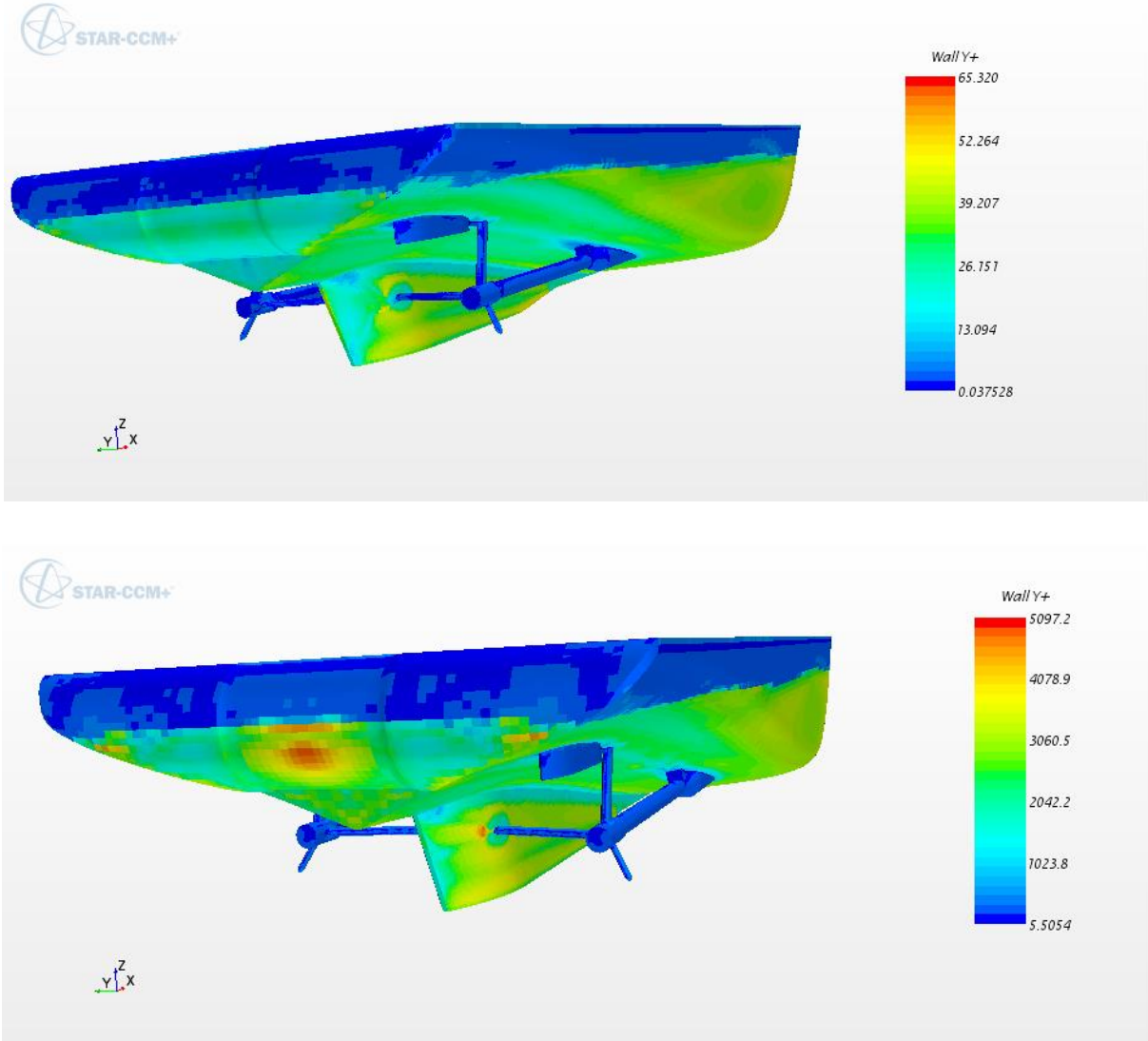


Fig. 11 $Fr=0,2175$

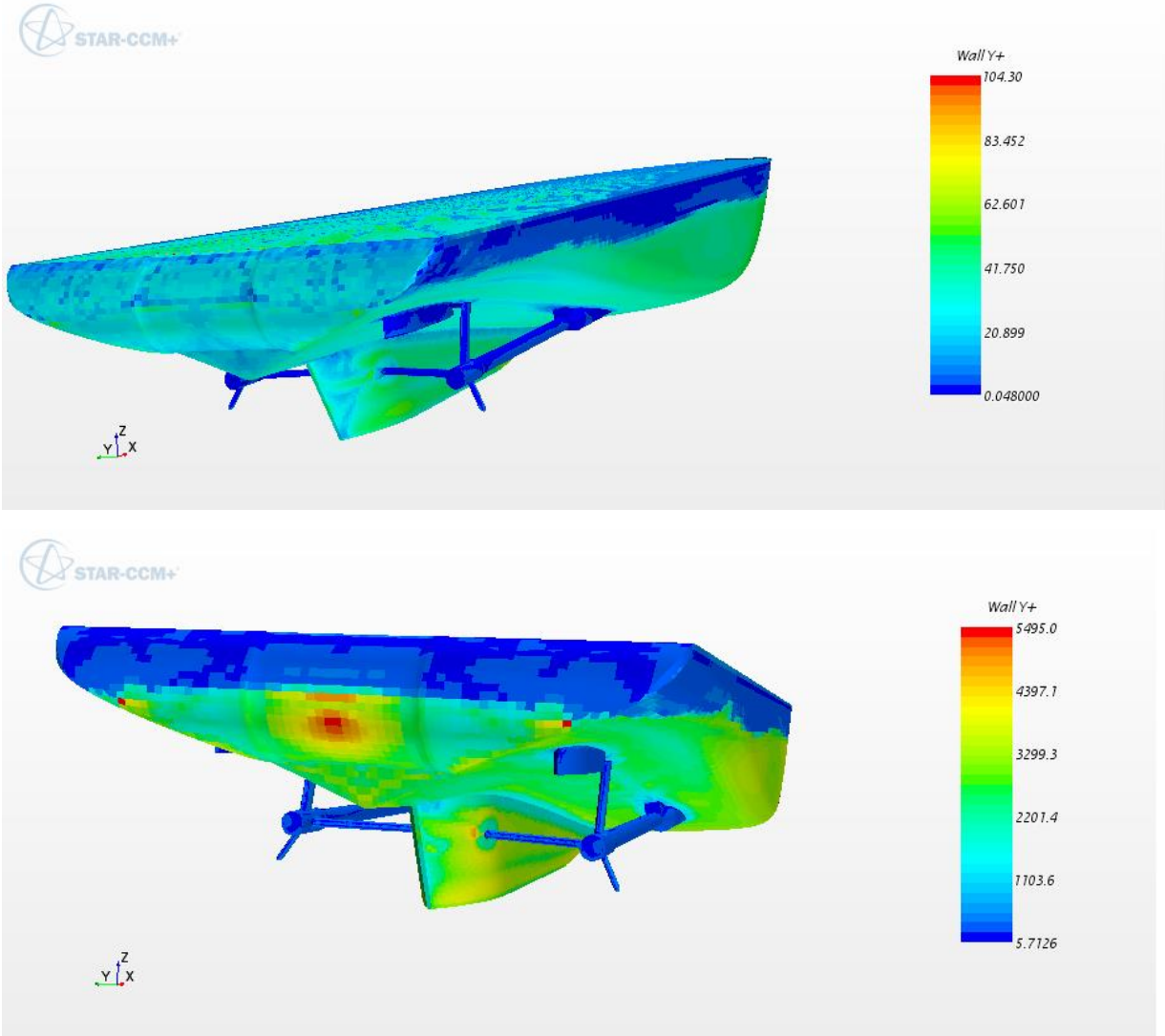


Fig. 12 $Fr=0,2356$

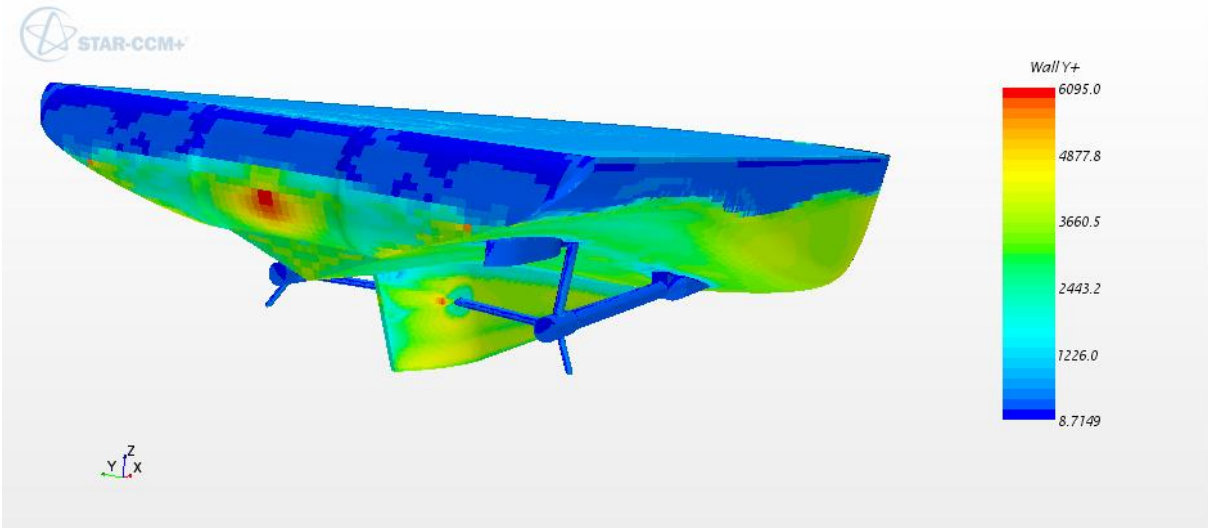
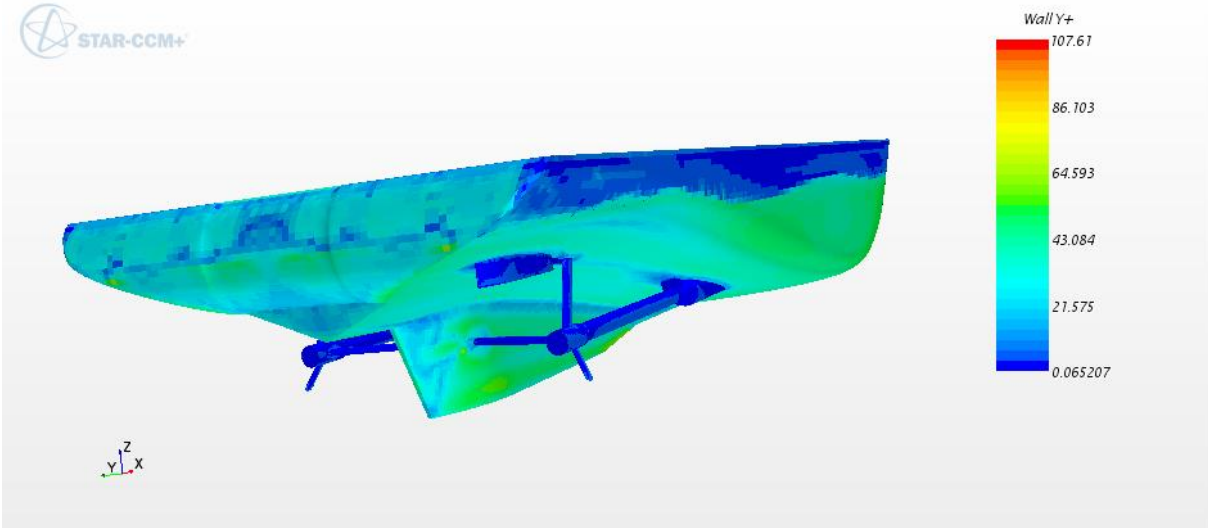


Fig. 13 Fr=0,2628

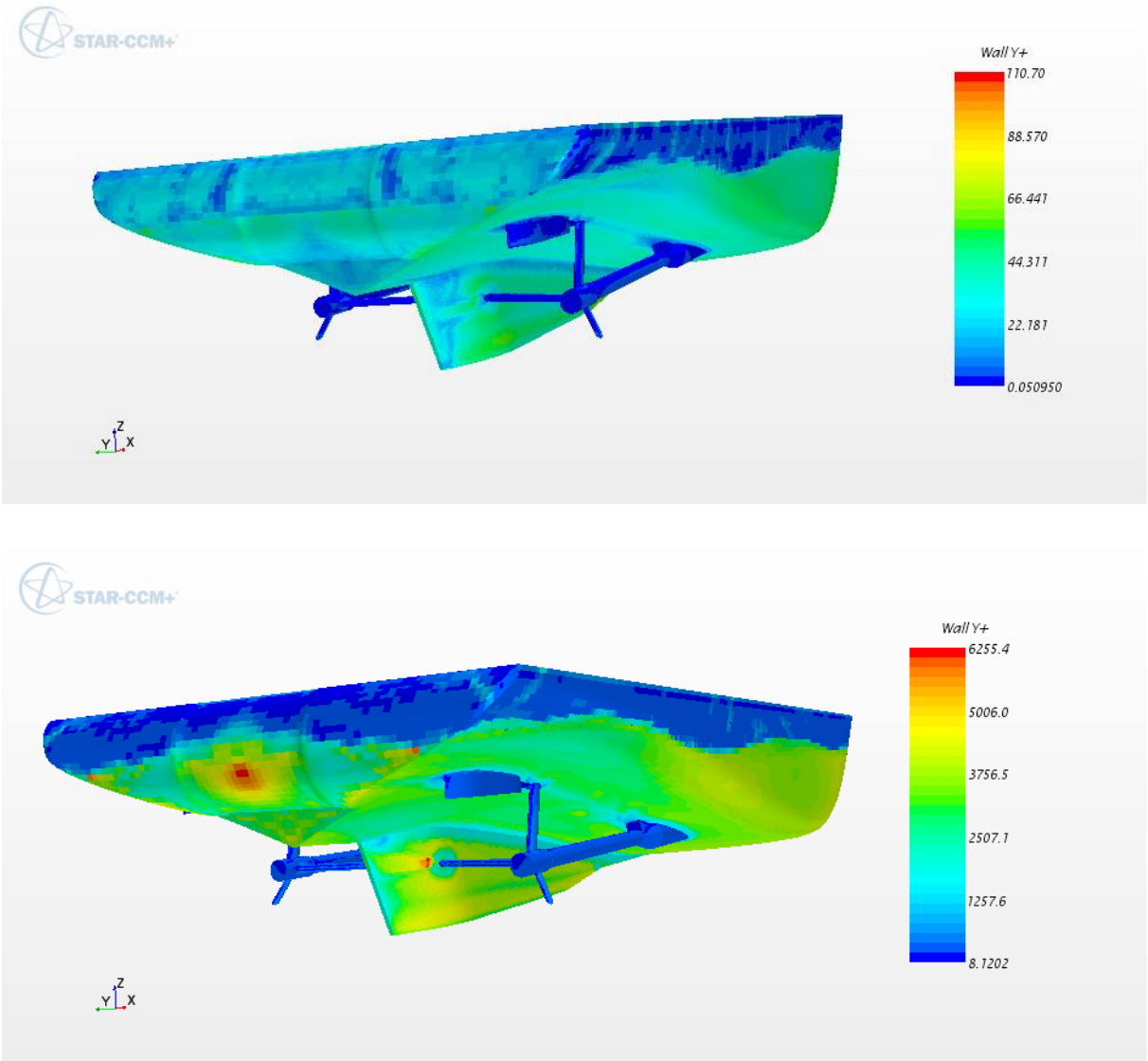


Fig. 14 $Fr=2719$

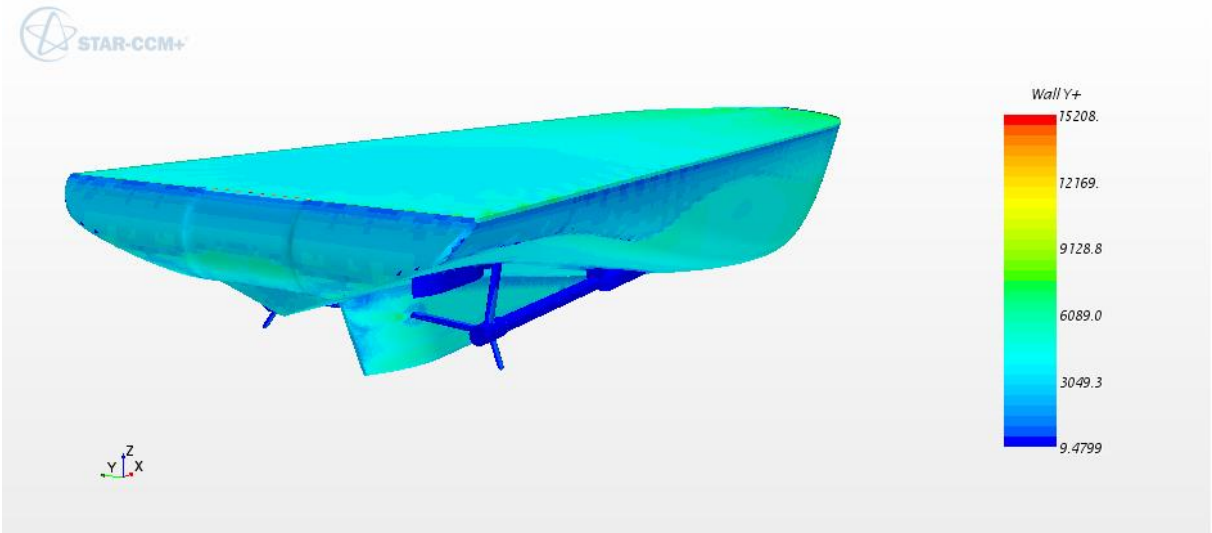
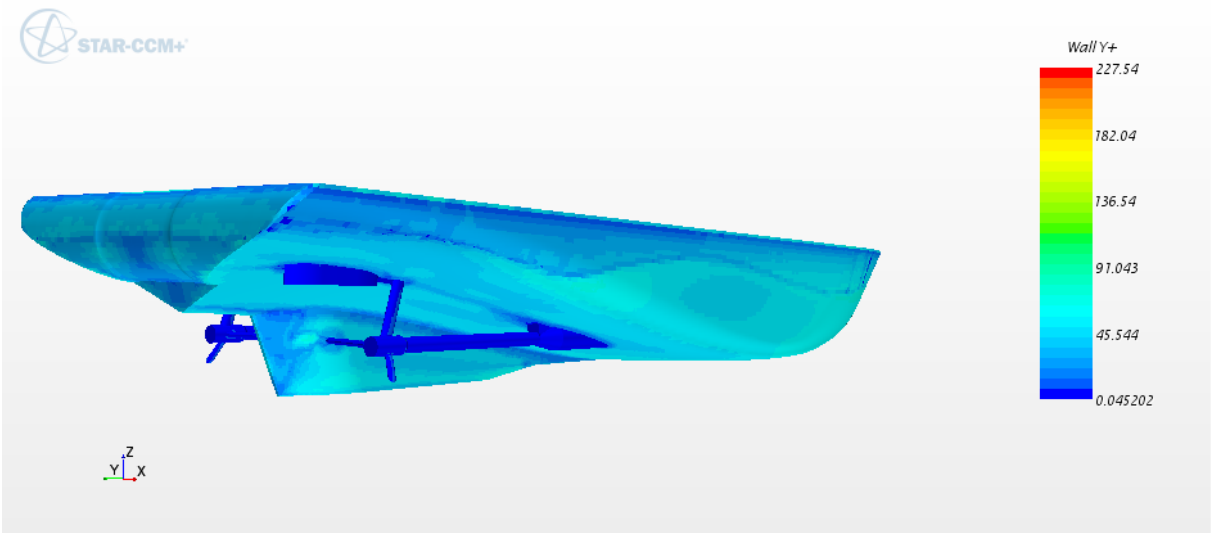


Fig. 15 Fr=0,3081

C. Courant number

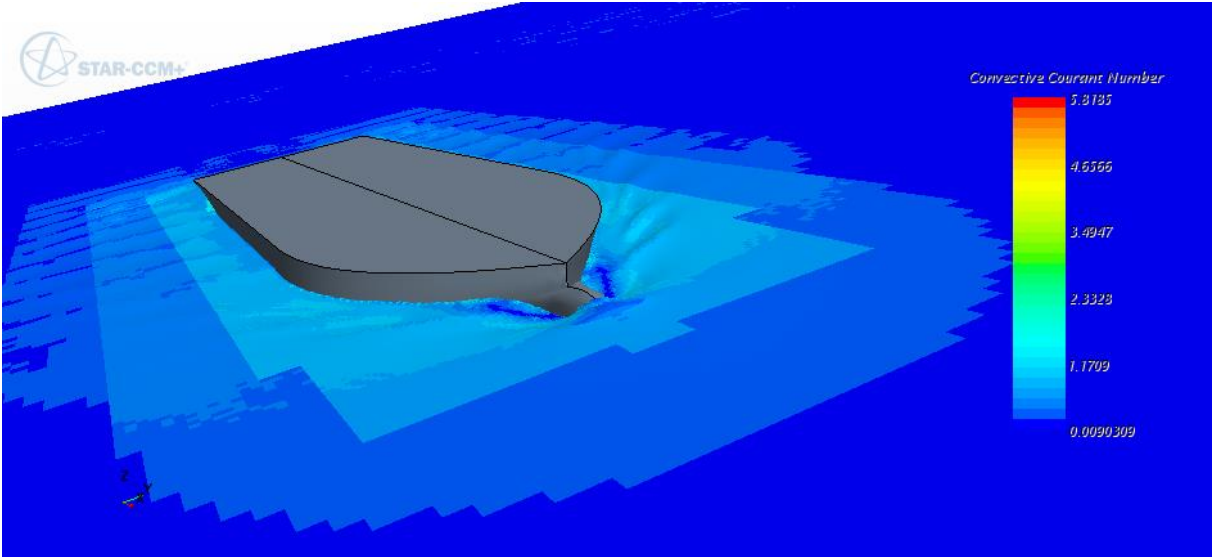
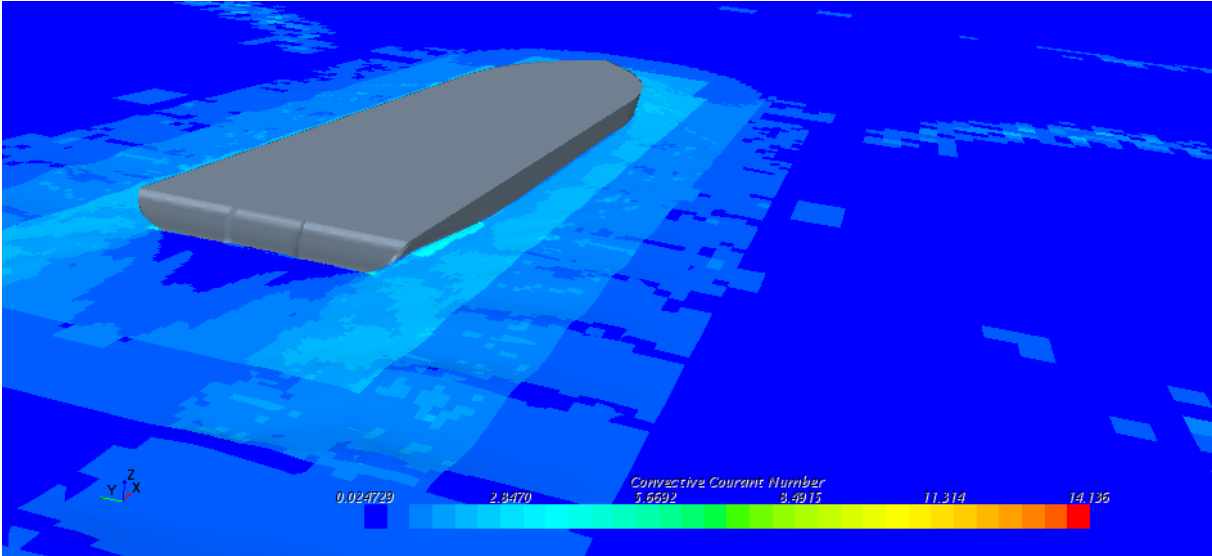


Fig. 16 Fr=0,1450

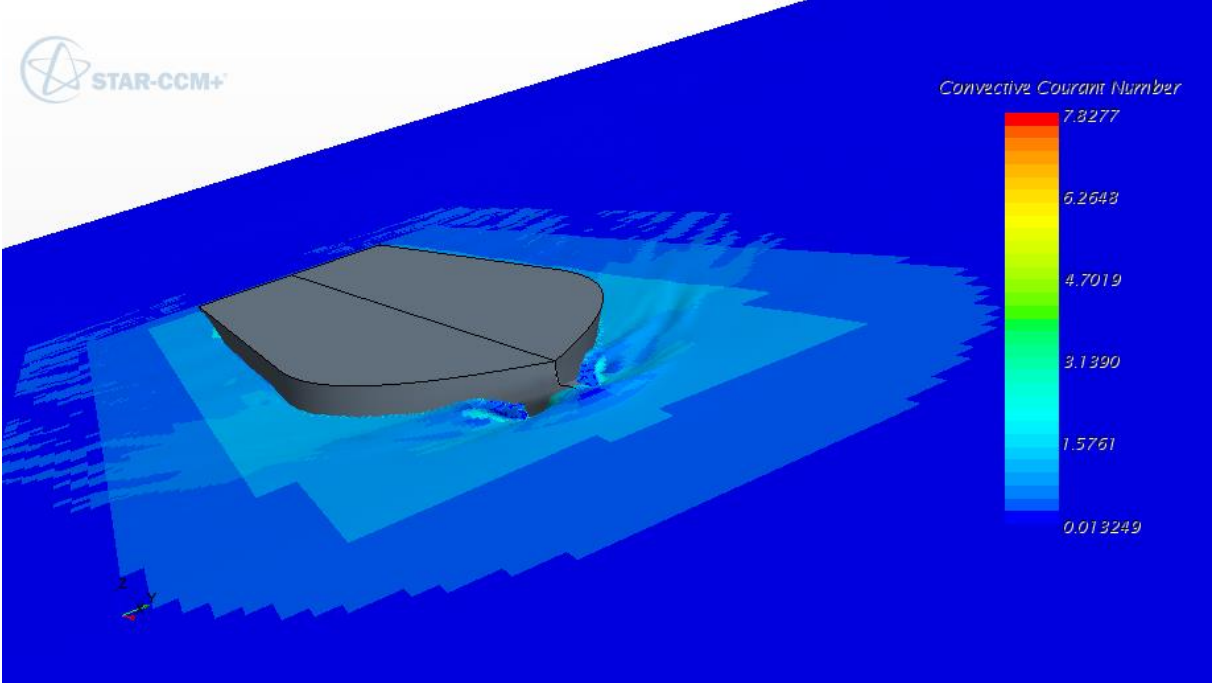
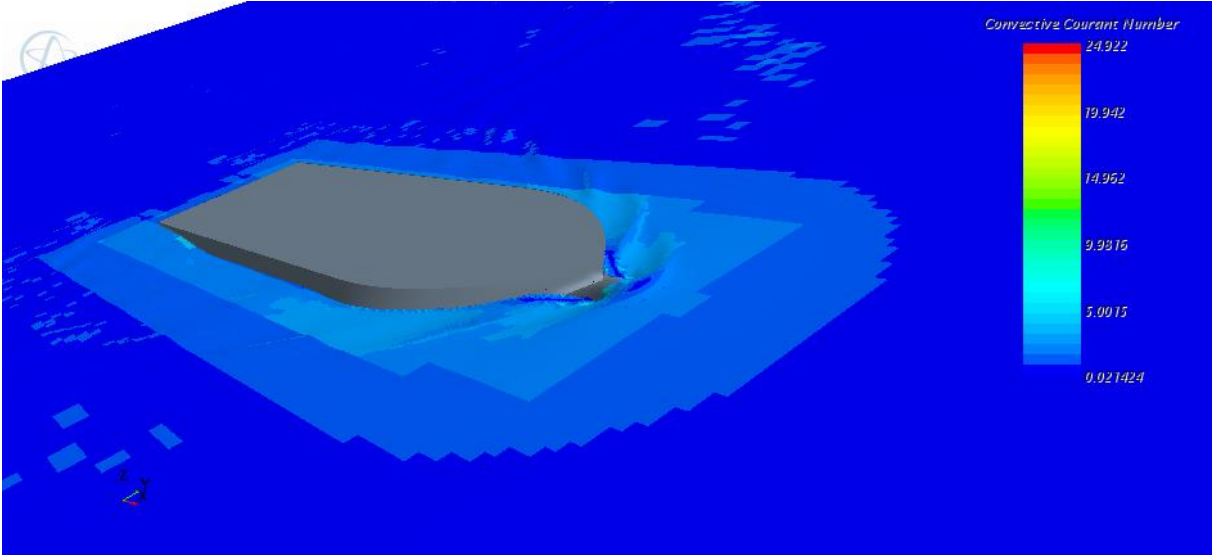


Fig. 17 Fr=0,1813

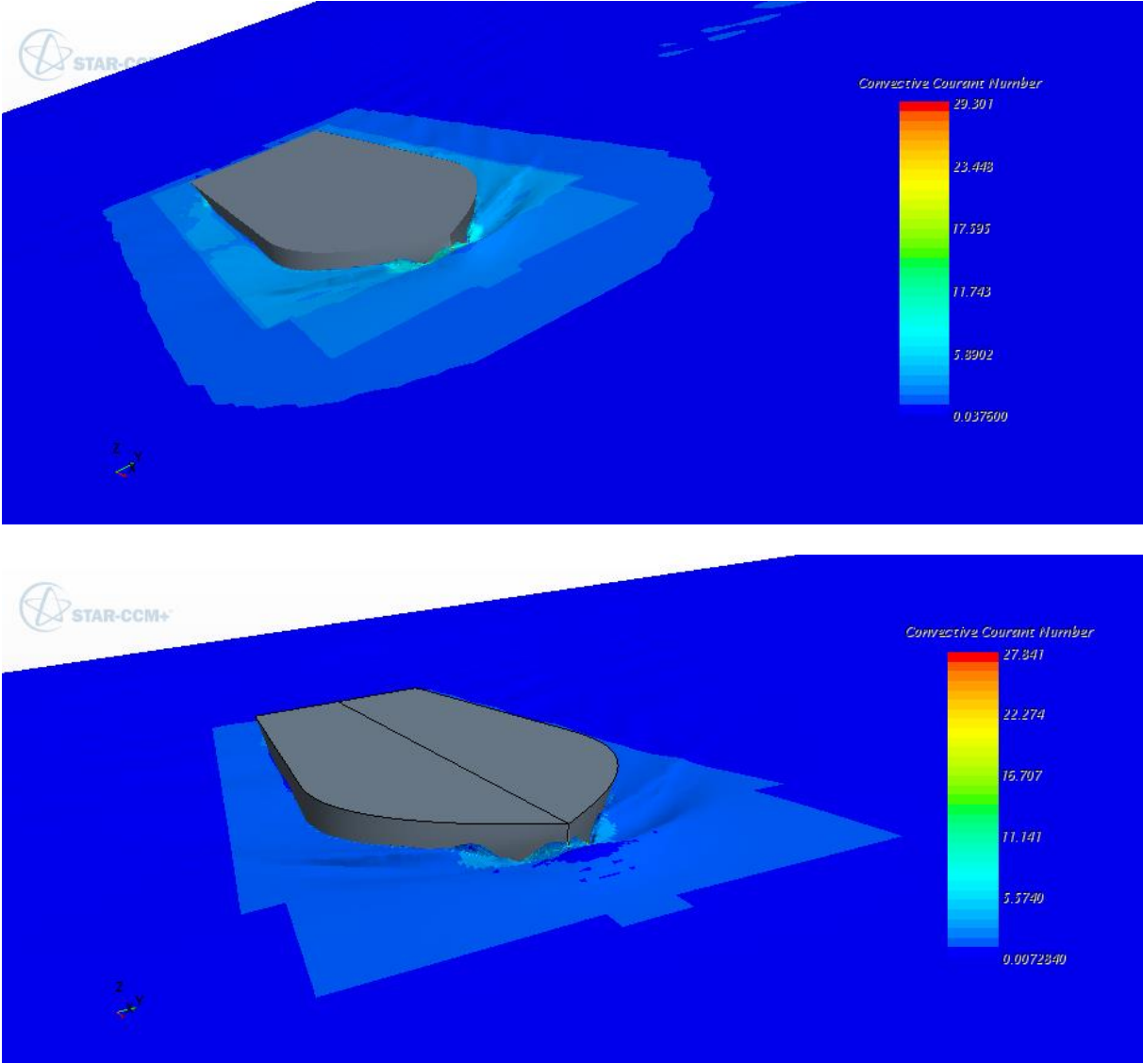


Fig. 18 Fr=0,2175

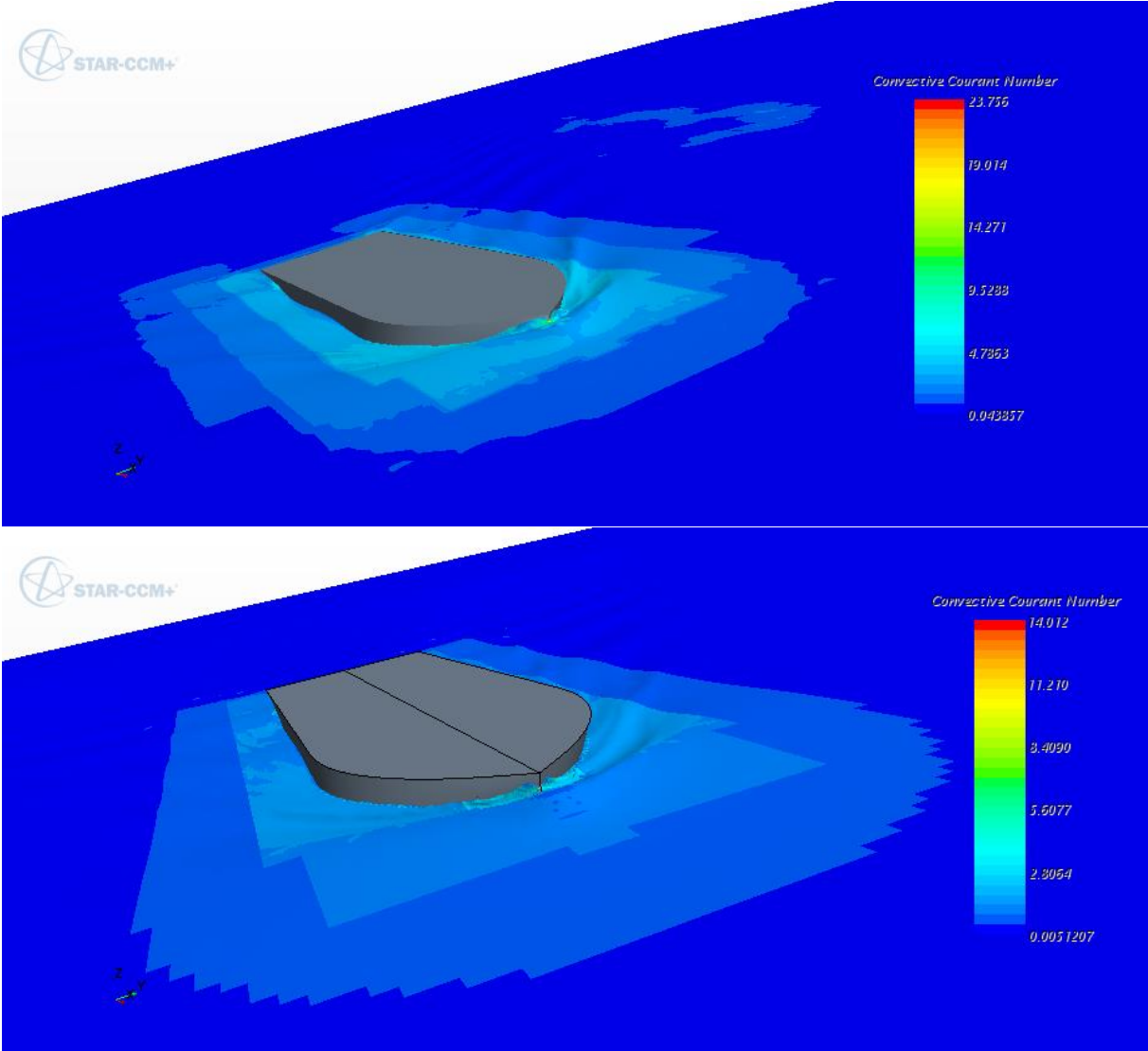


Fig. 19 Fr=0,2356

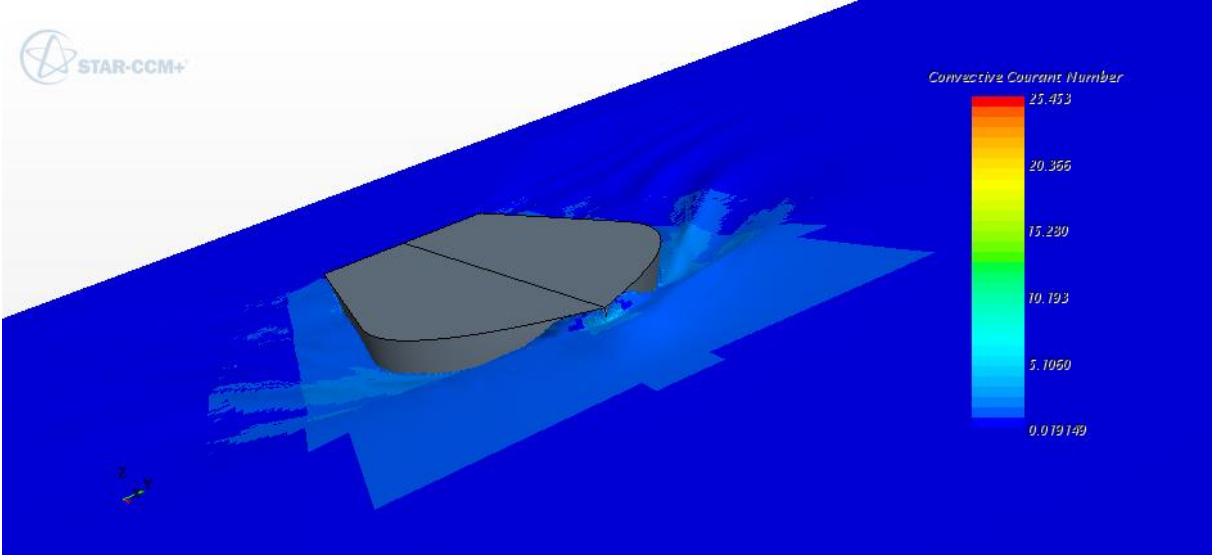
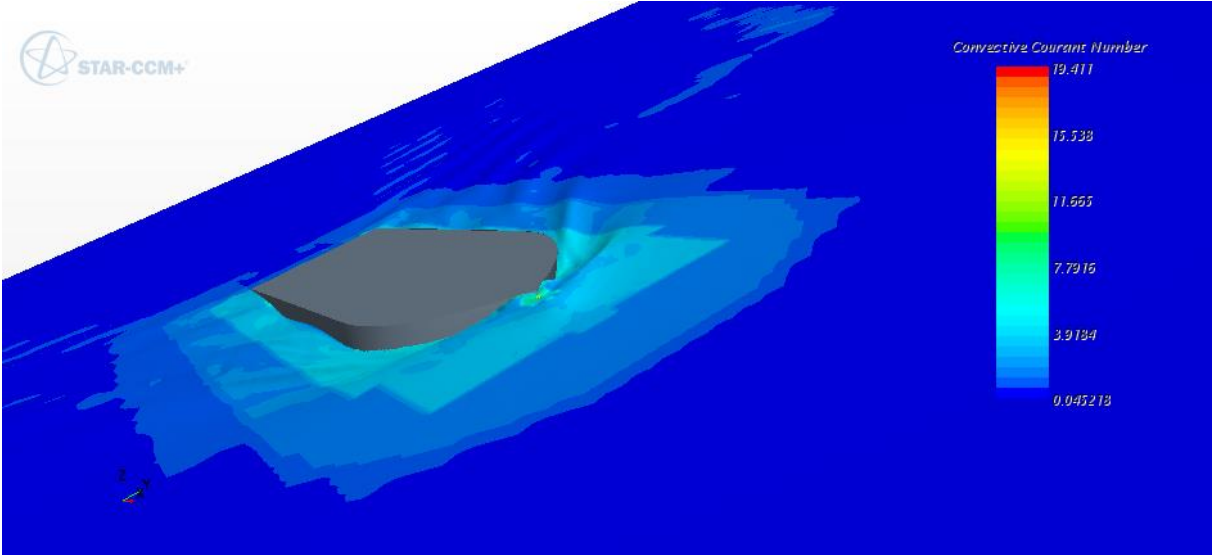


Fig. 20 Fr=0,2628

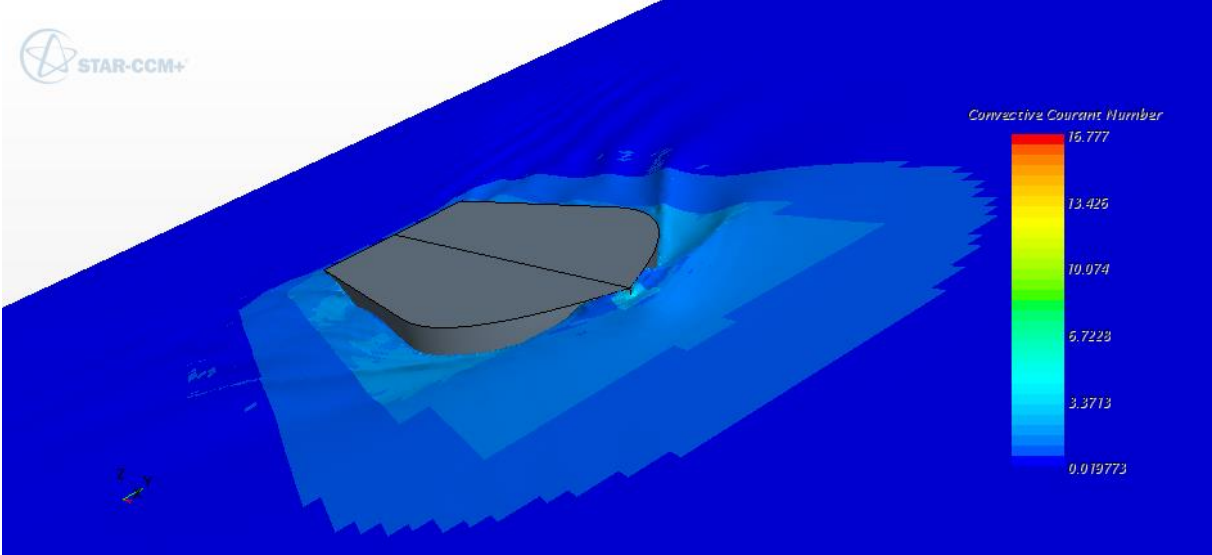
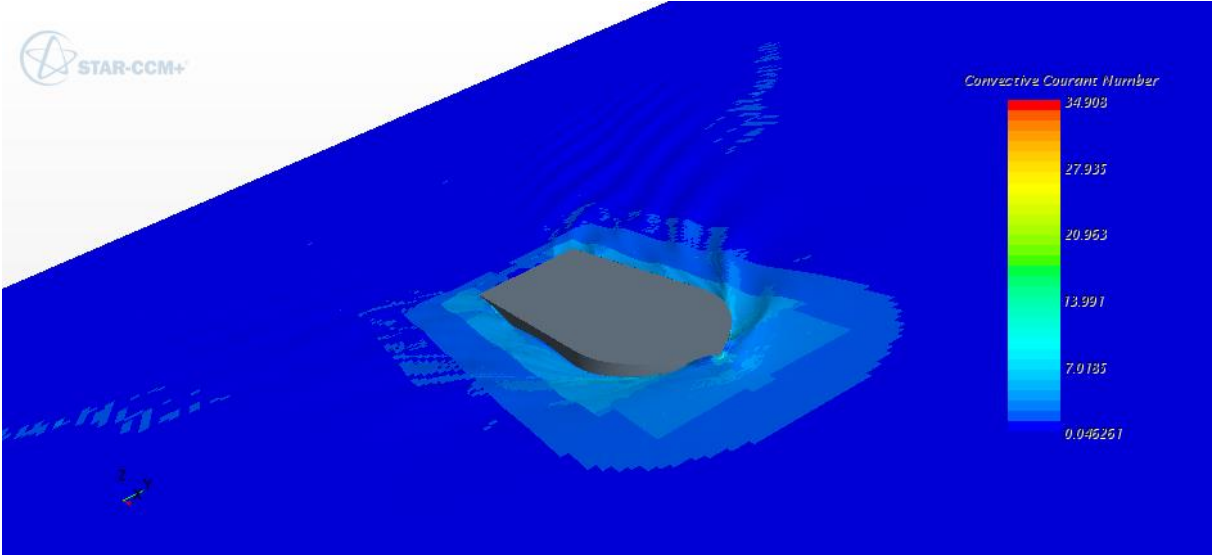


Fig. 21 $Fr=2719$

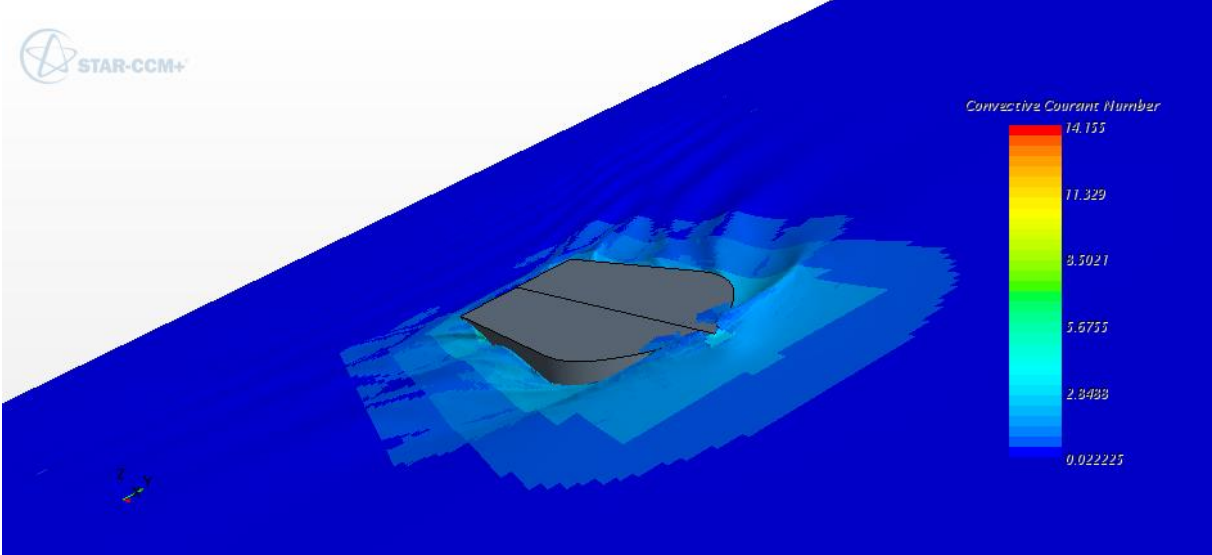
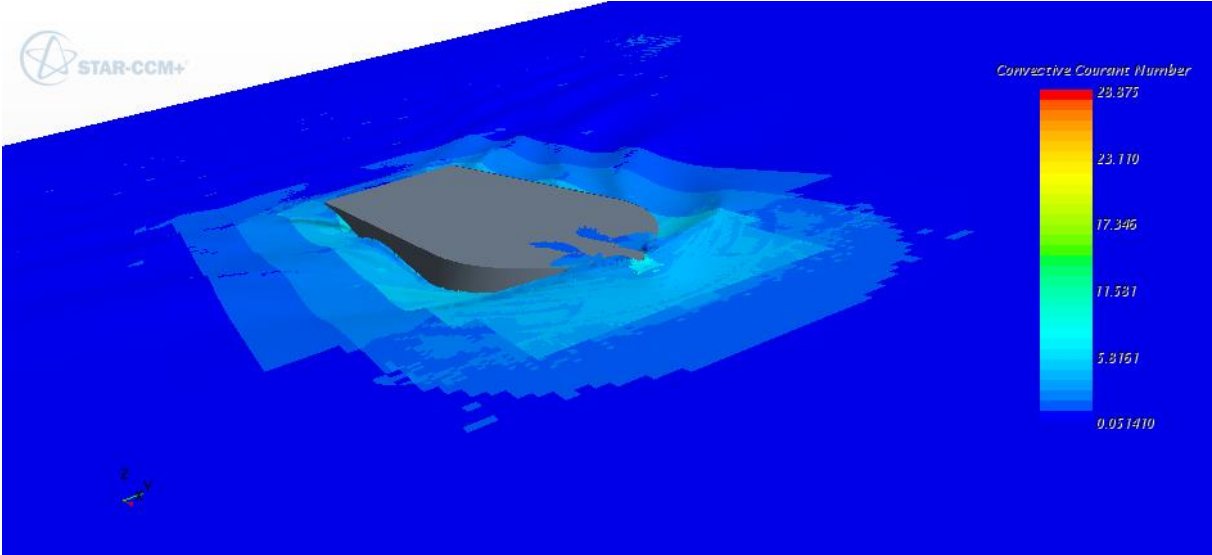
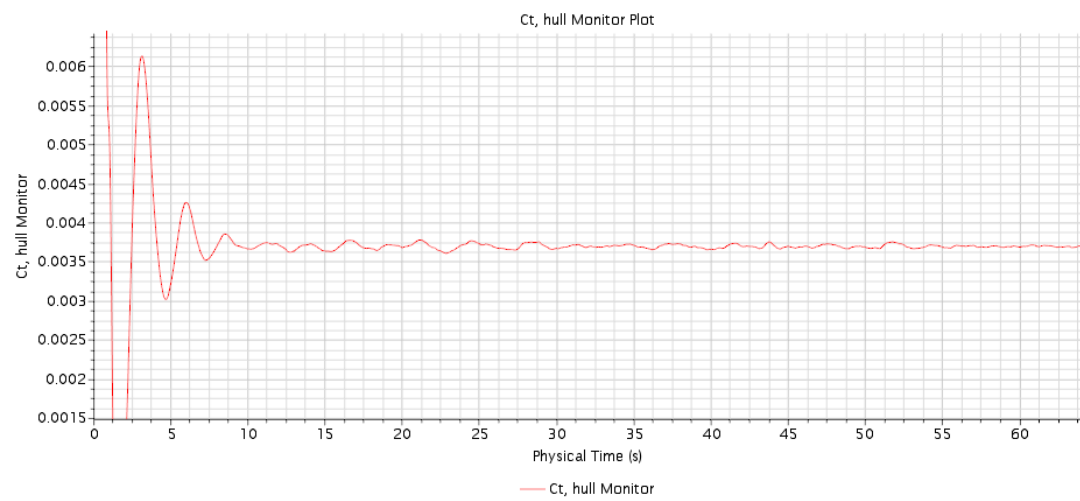
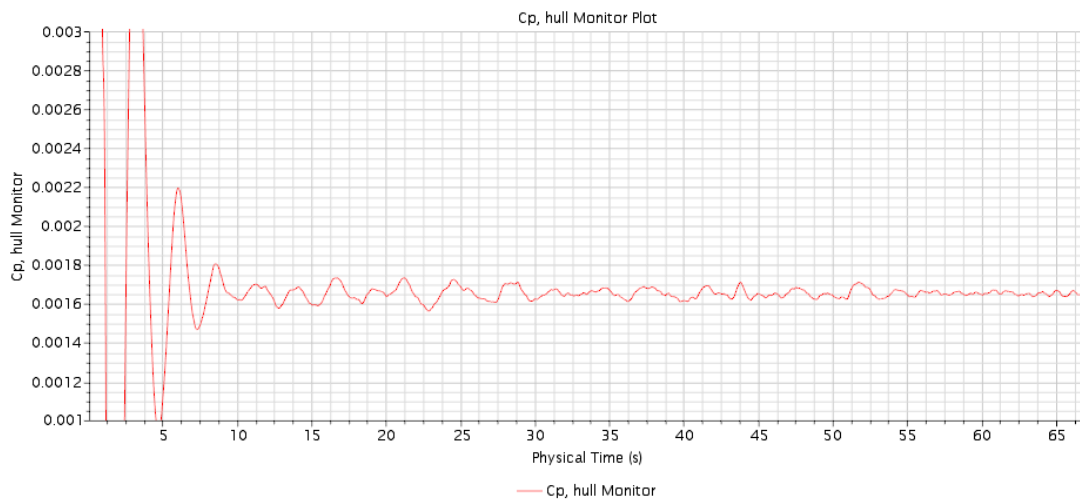
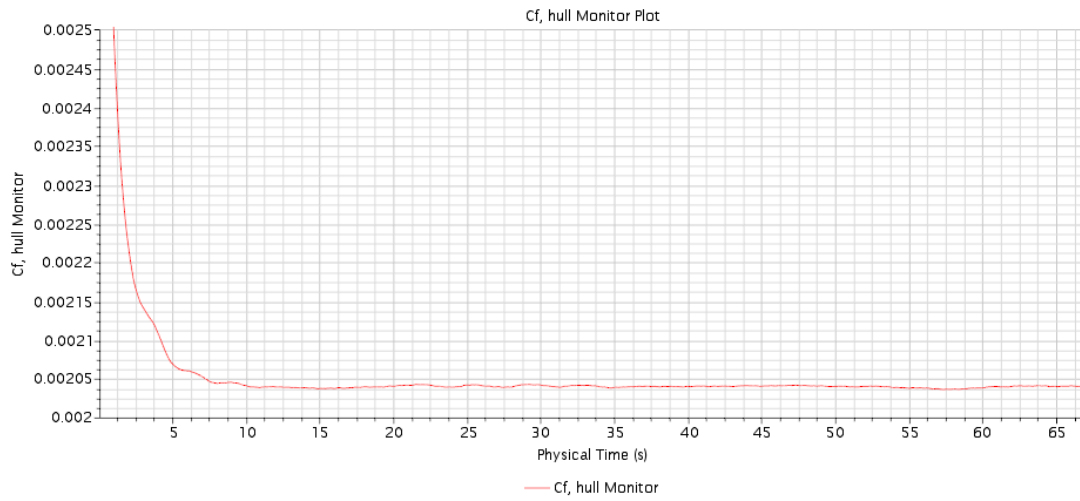


Fig. 22 Fr=0,3081

D. Force coefficients

Note that in this section model scale results (first 3 plots) on each simulated cases have to be multiply by 2.



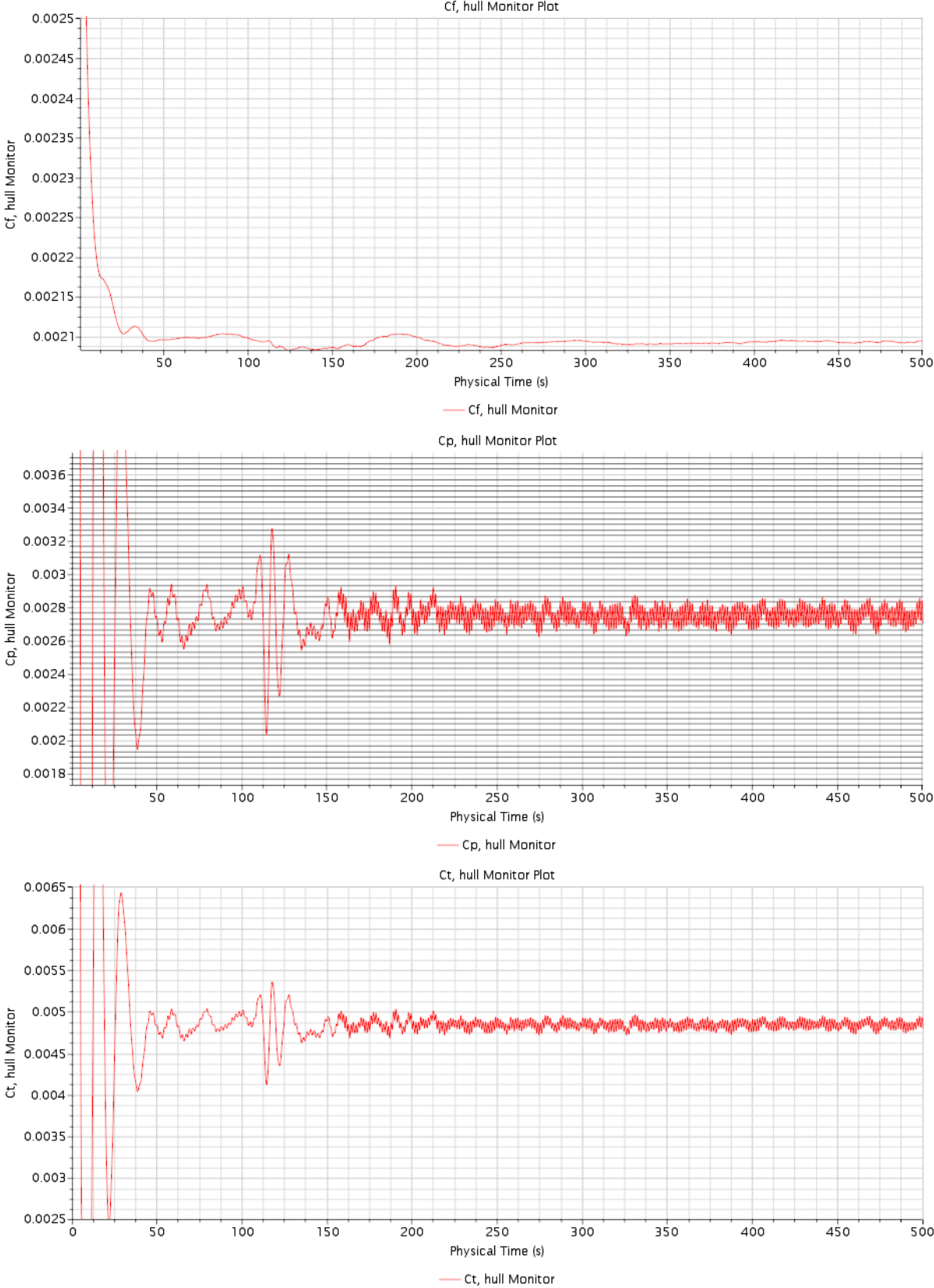
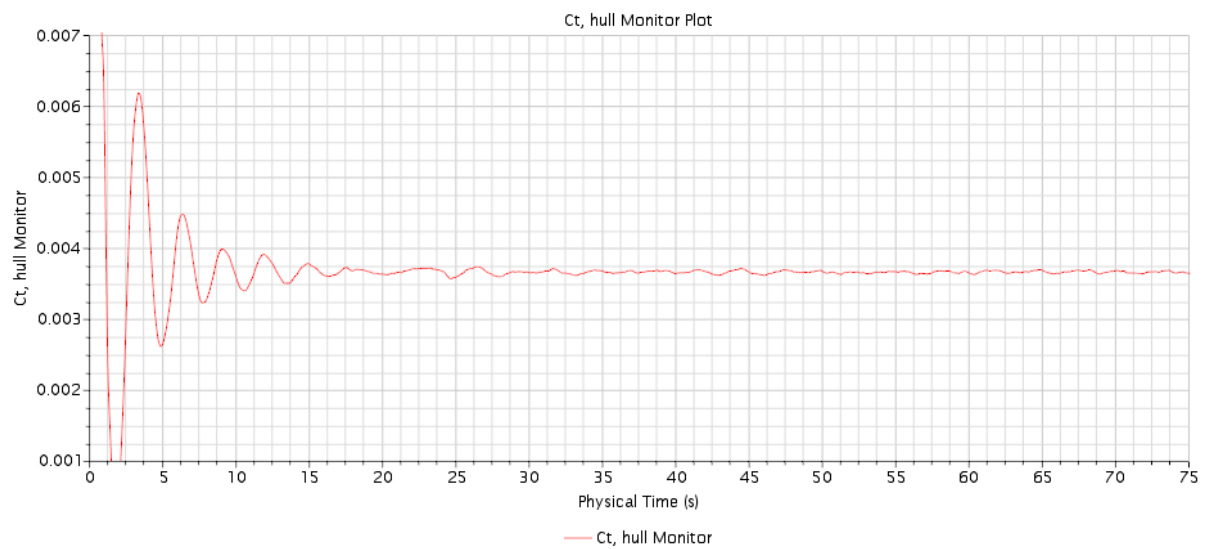
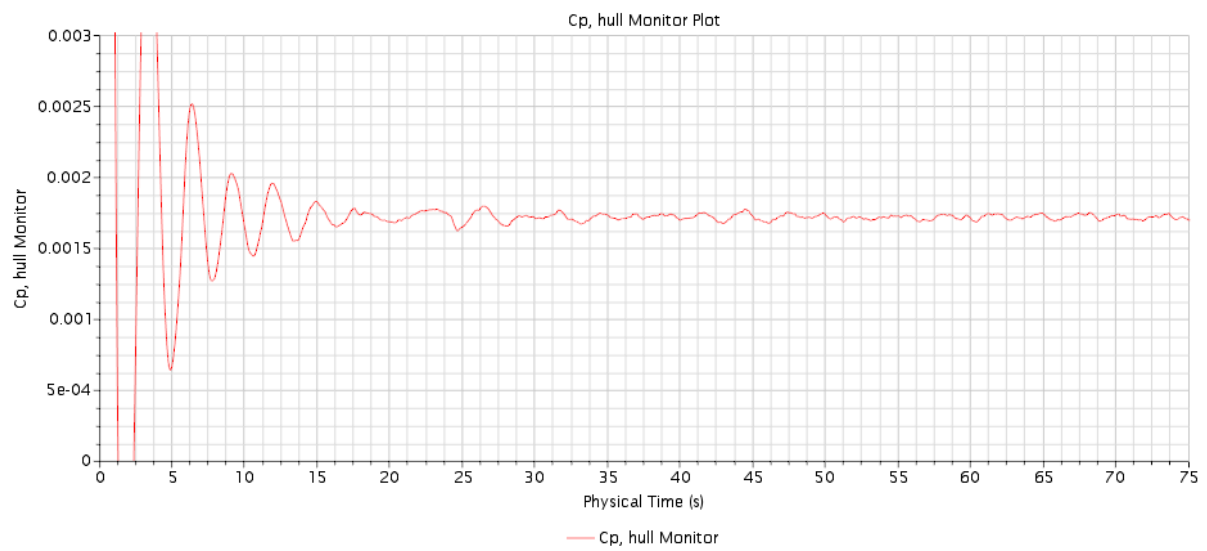
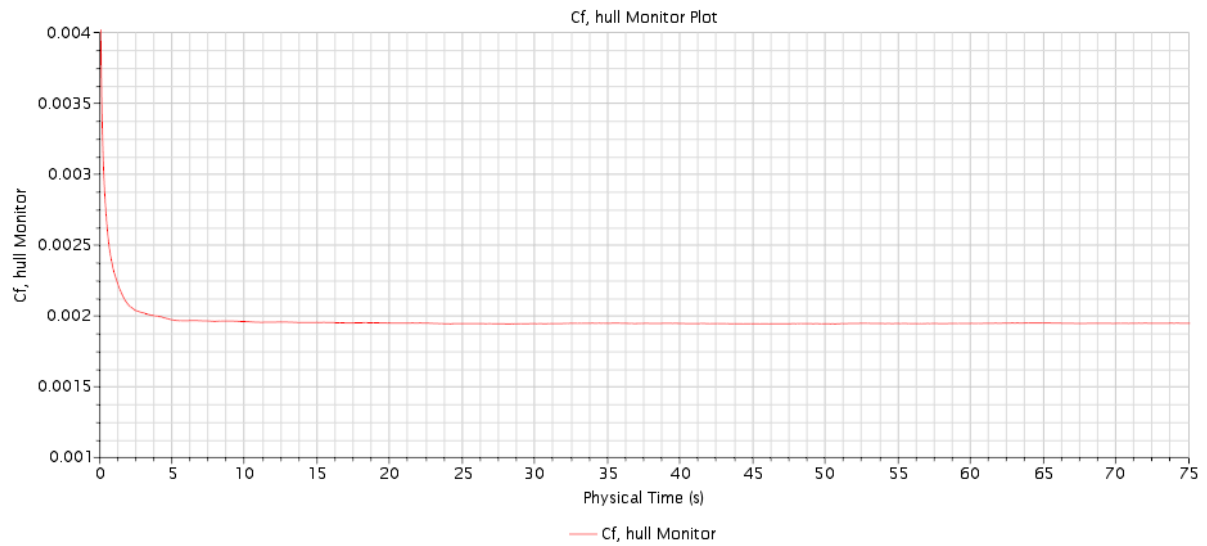
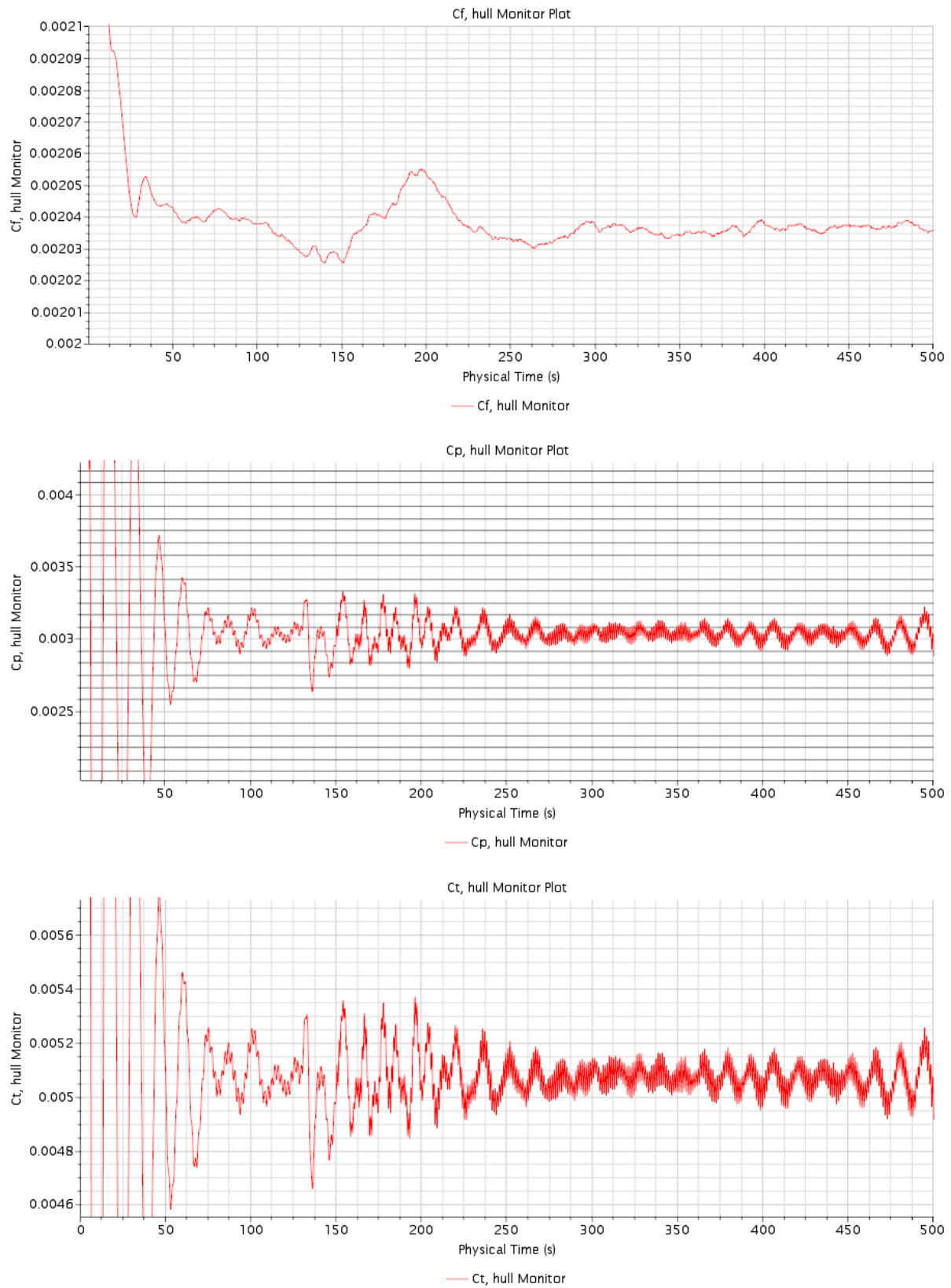
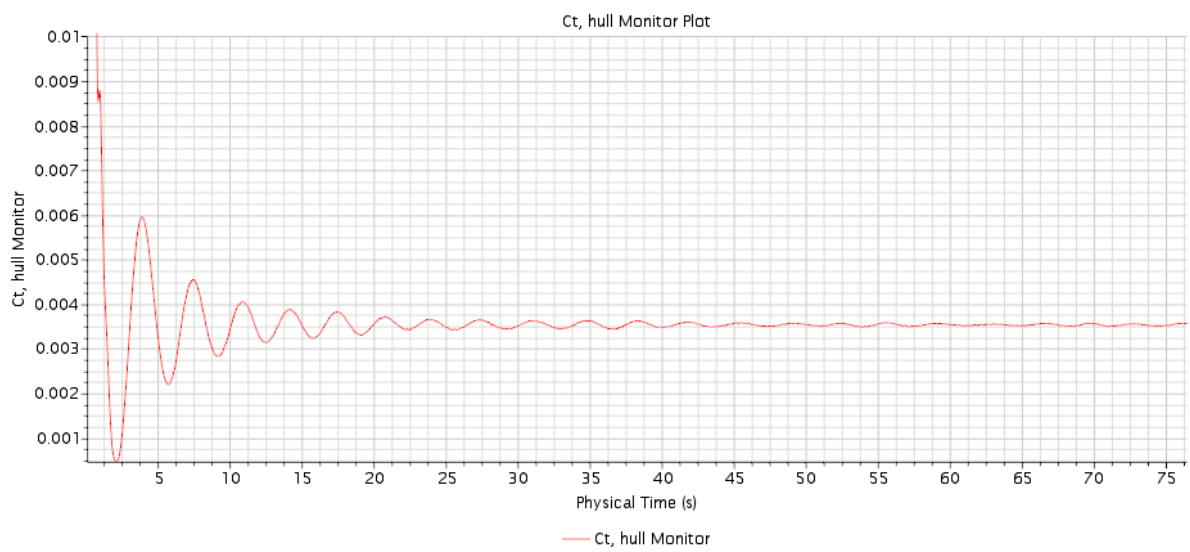
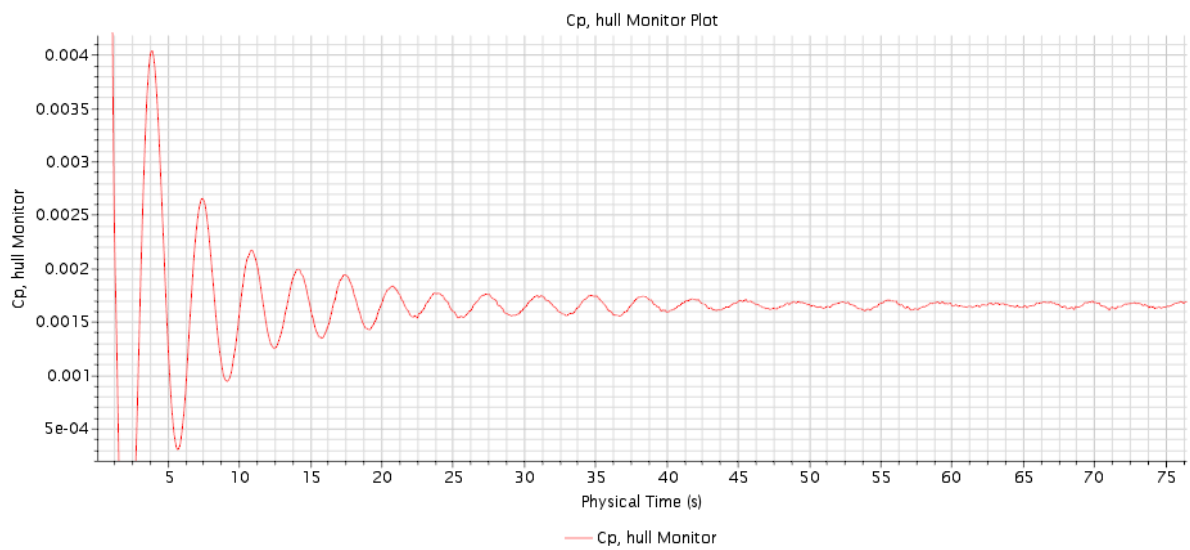
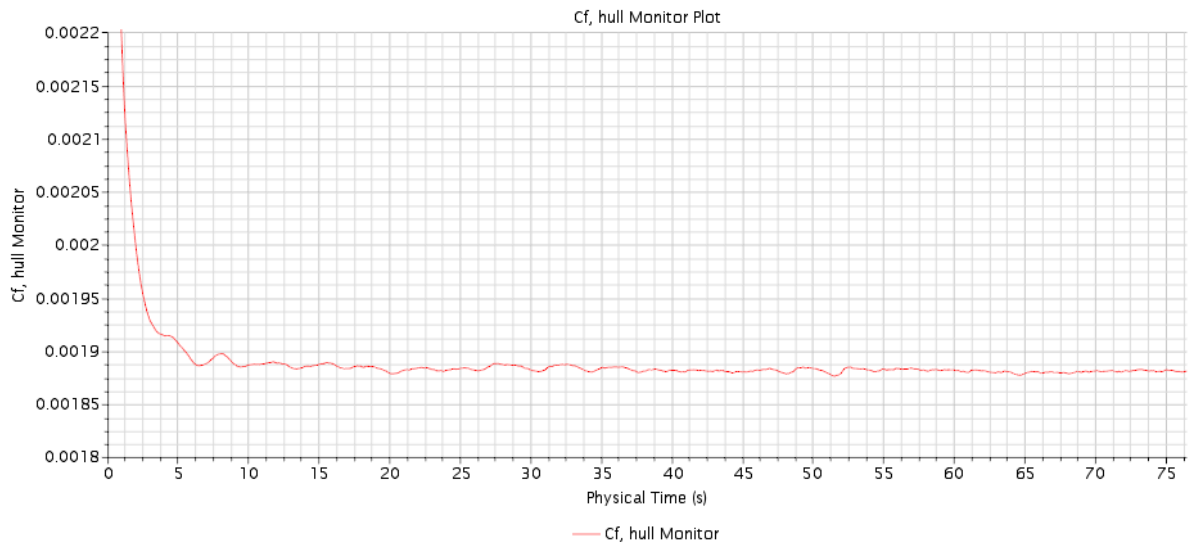


Fig. 23 Fr=0,1450



**Fig. 24** $Fr=0,1813$



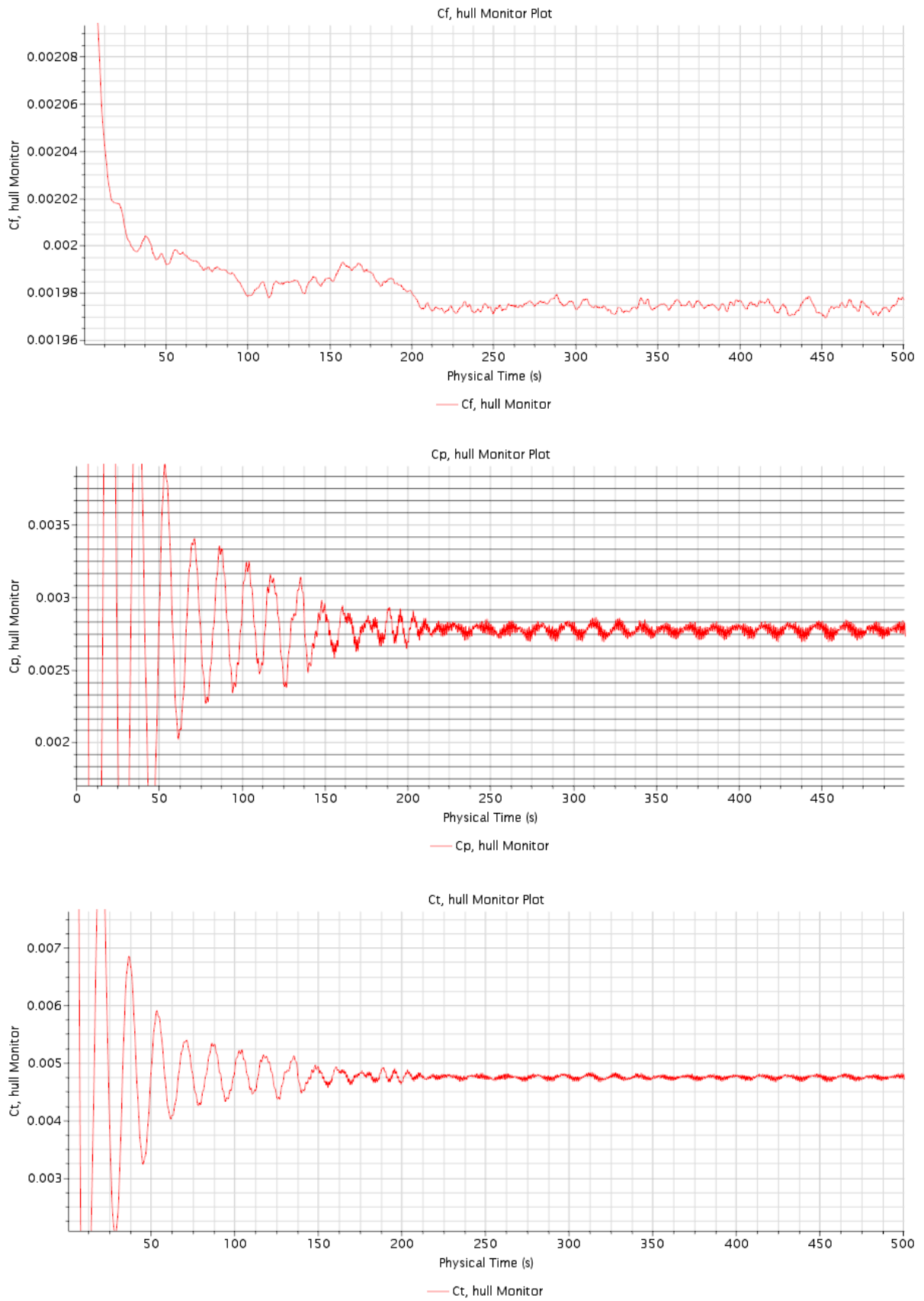
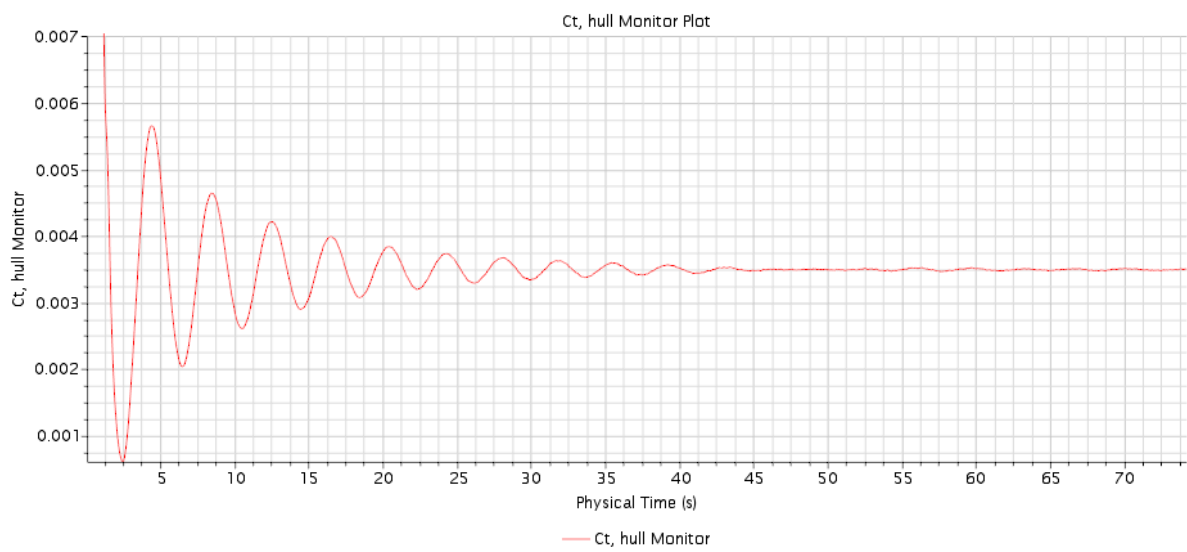
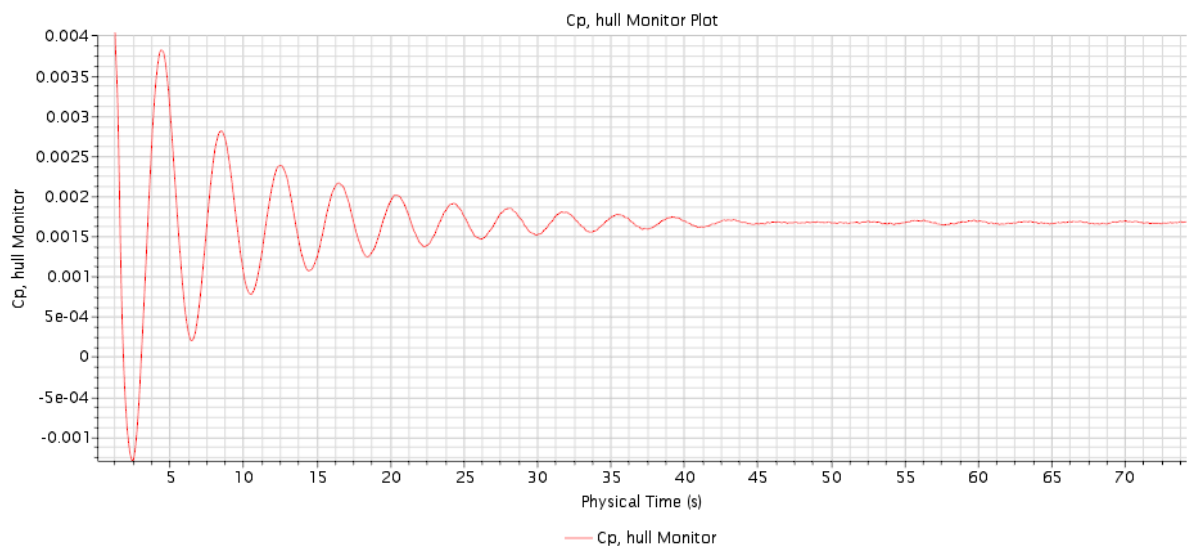
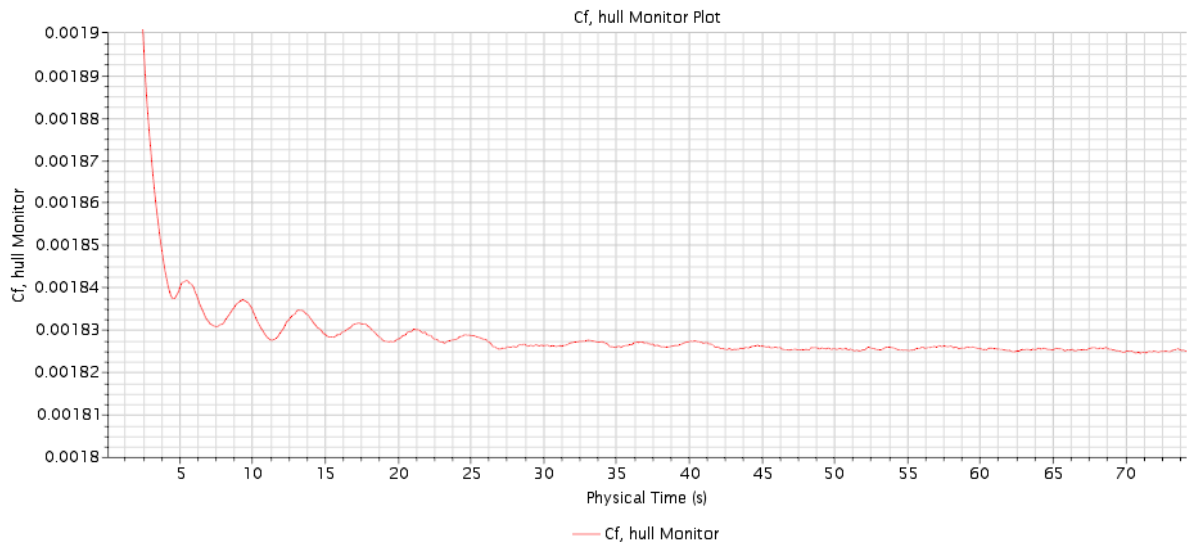


Fig. 25 Fr=0,2175



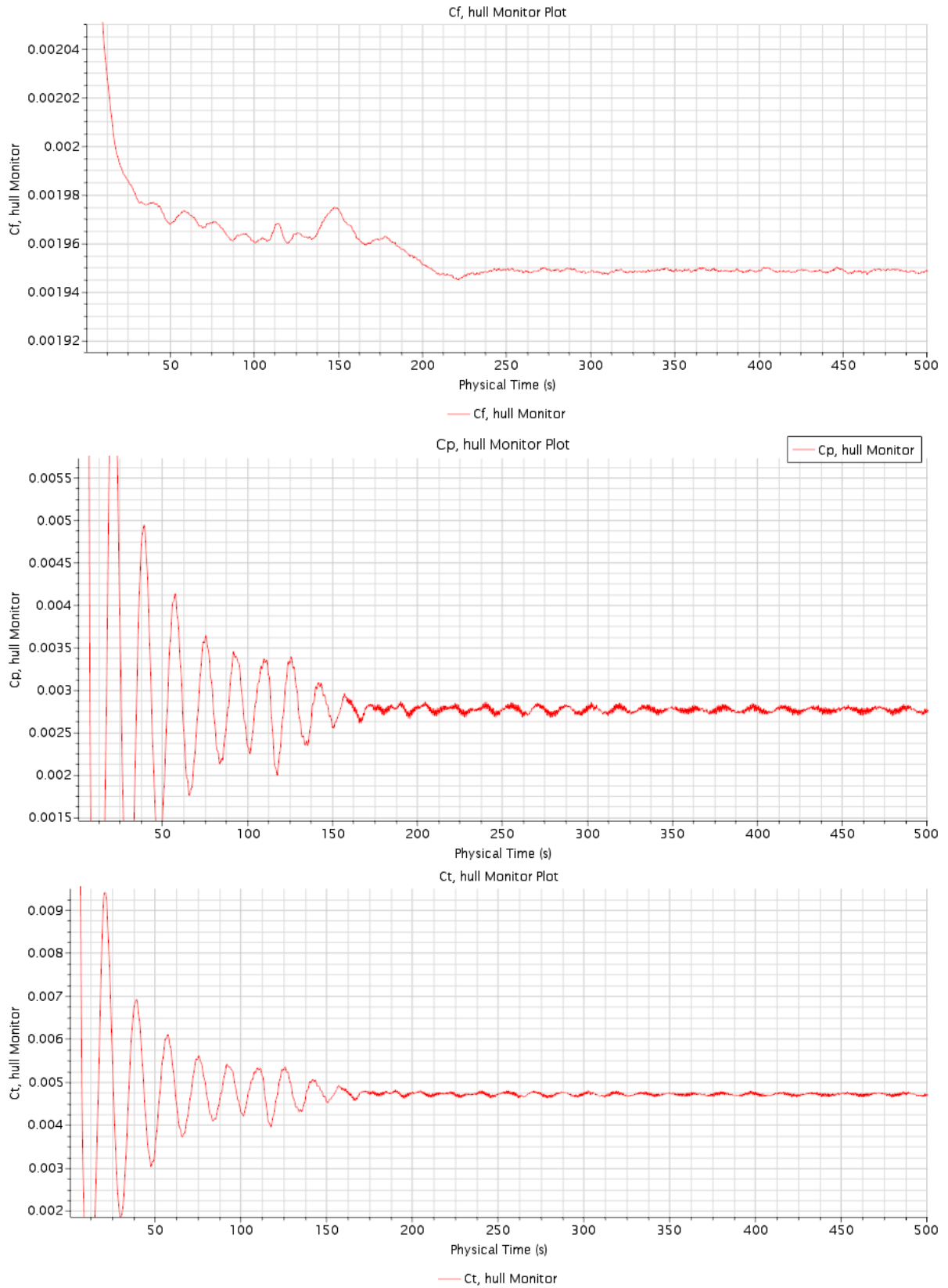
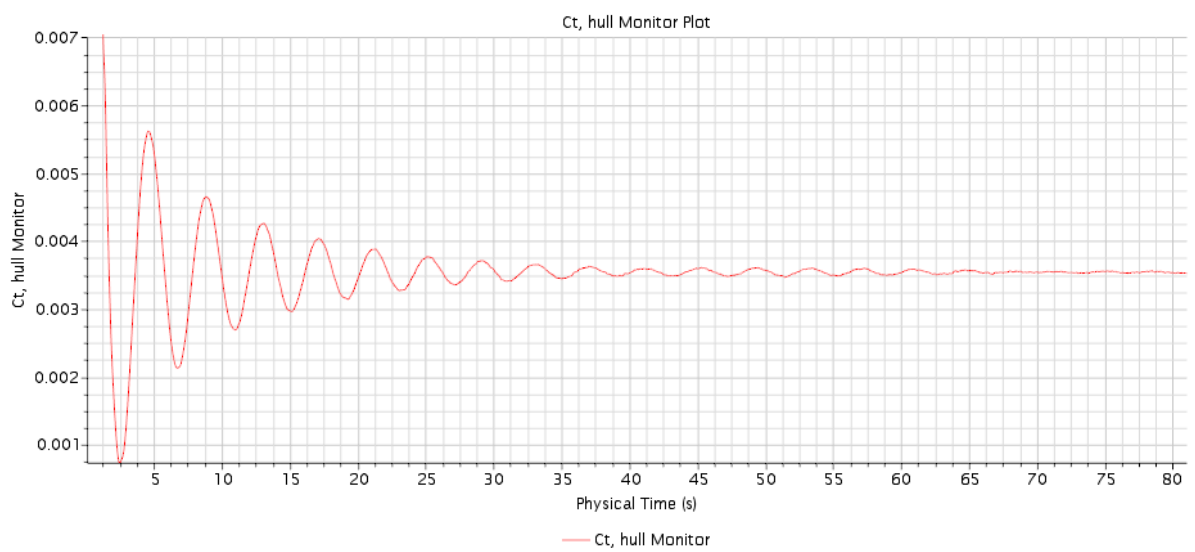
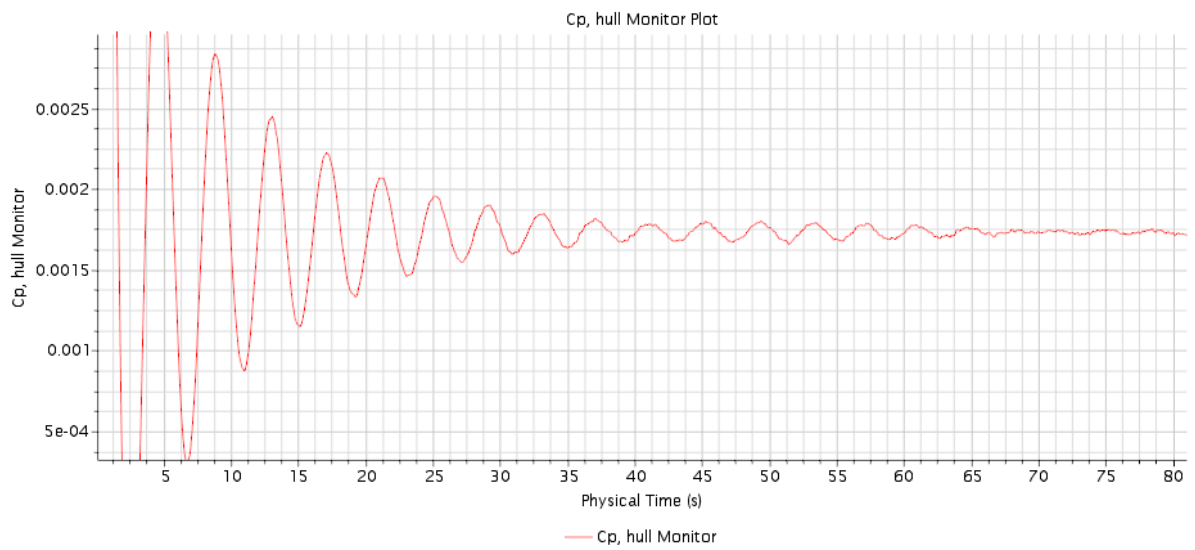
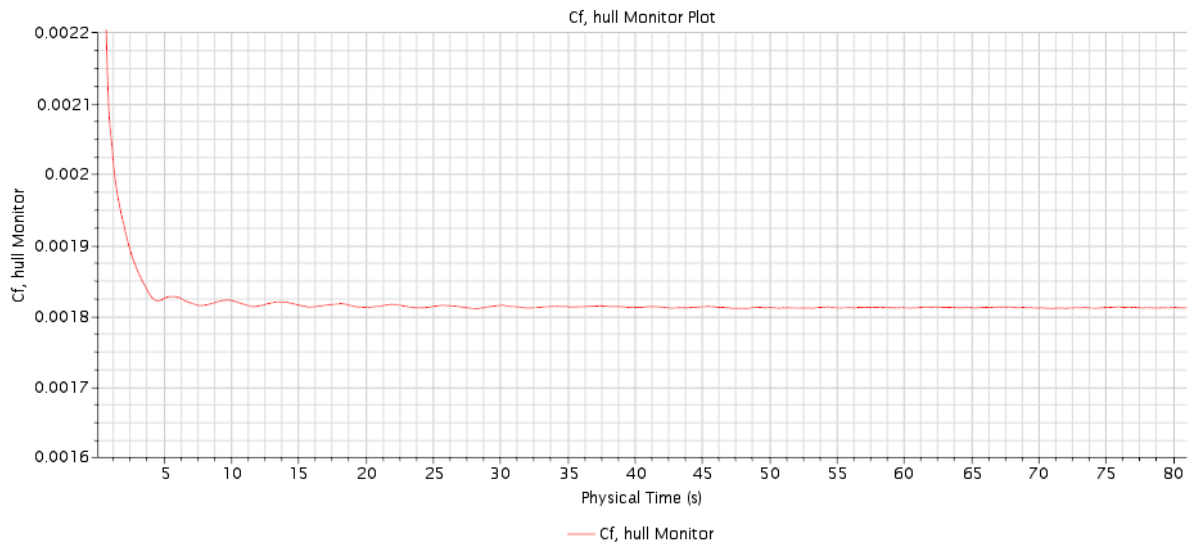
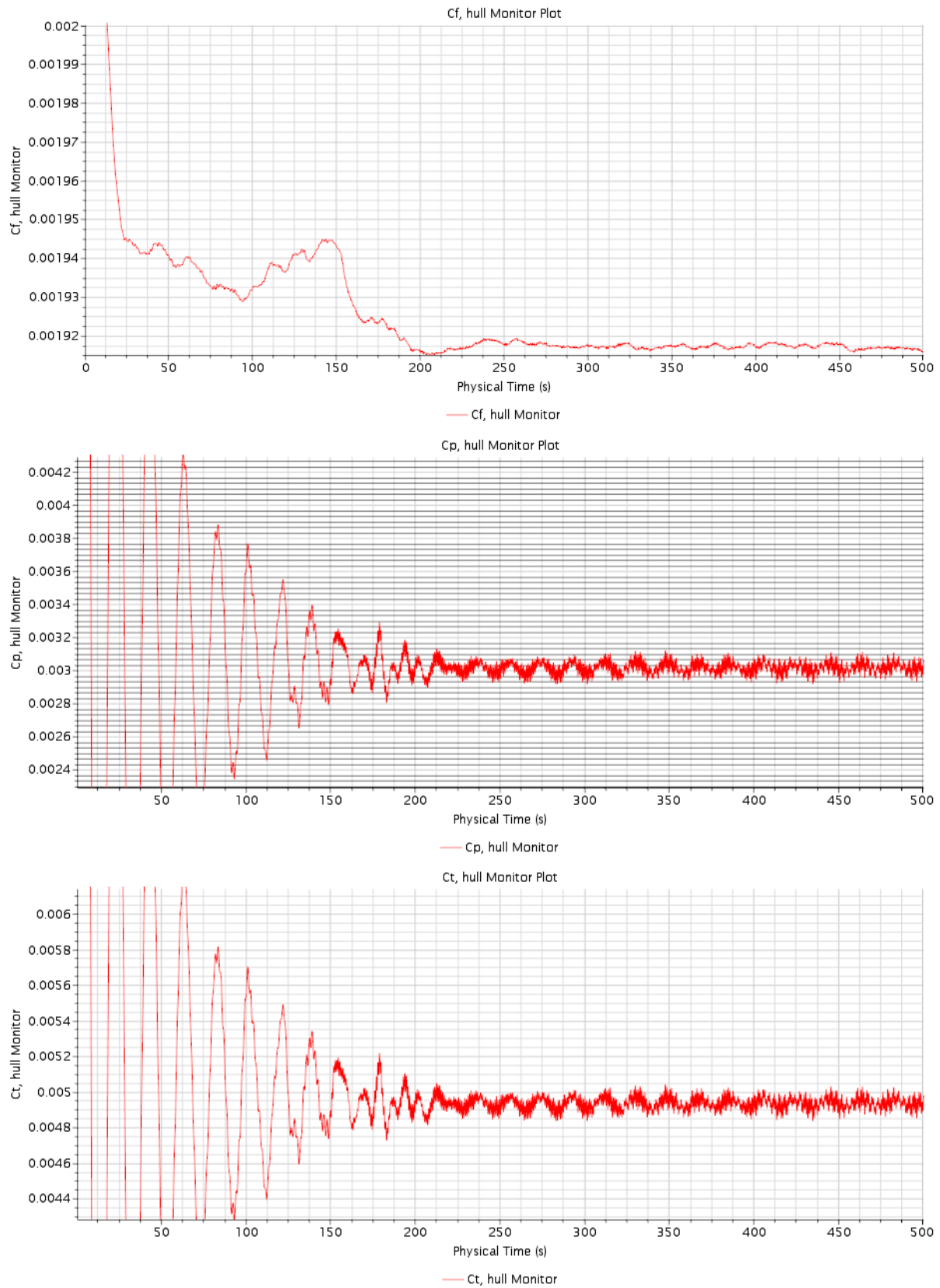
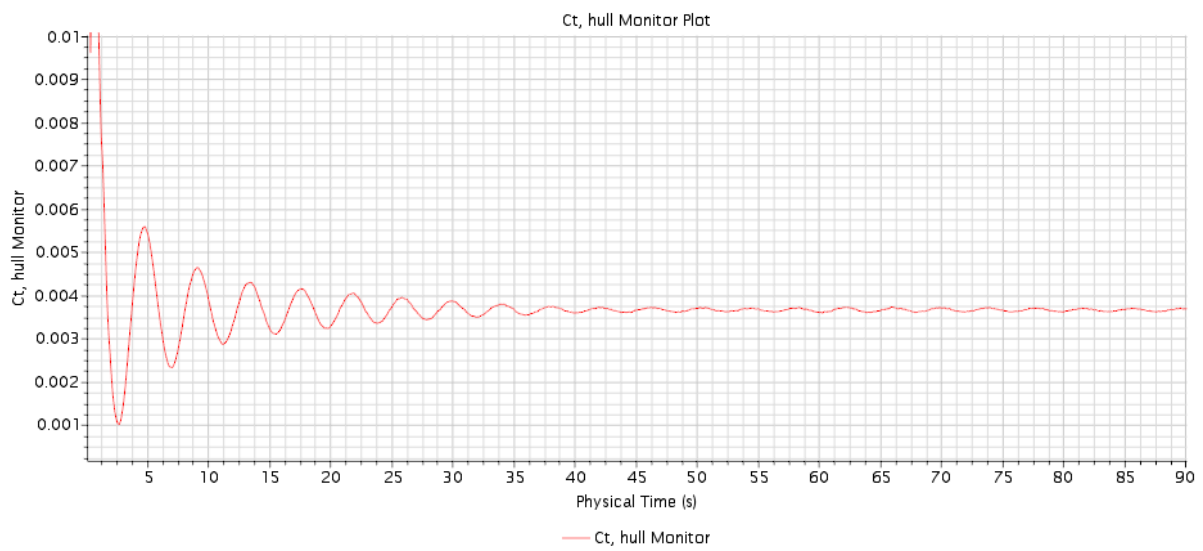
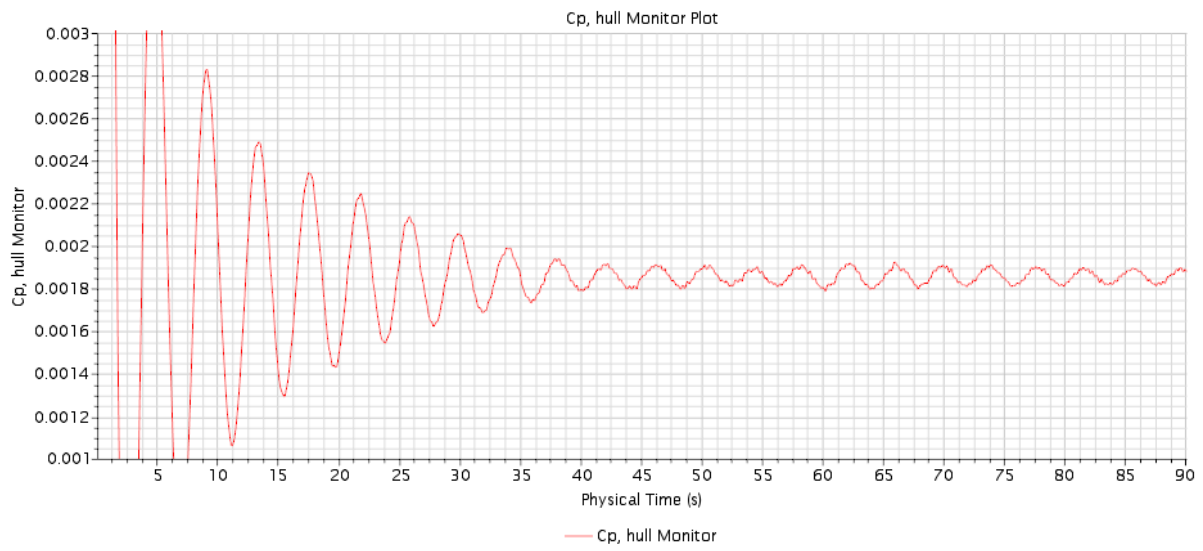
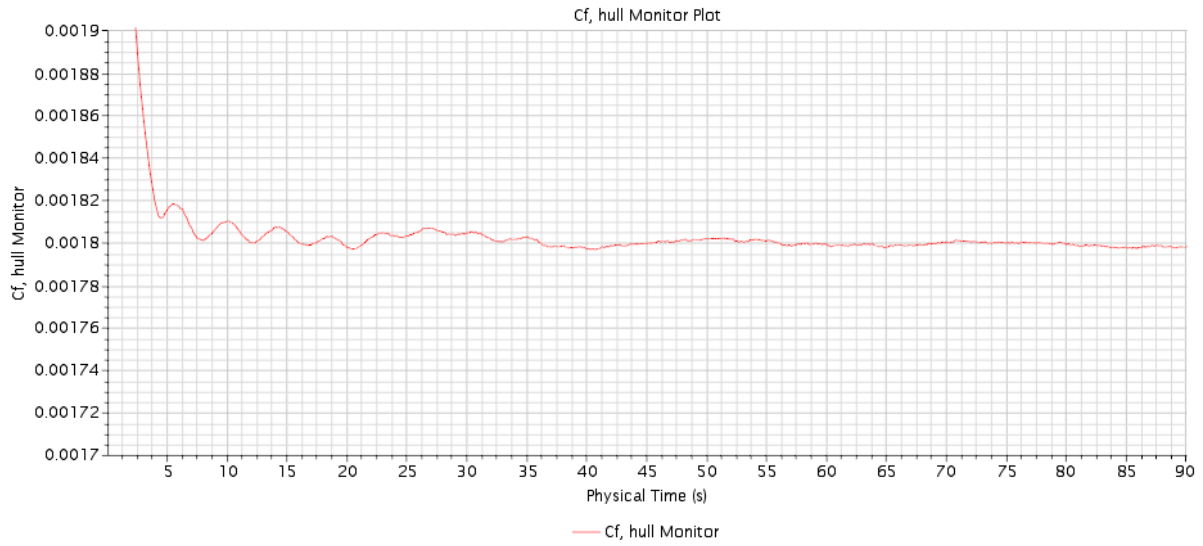


Fig. 26 Fr=0,2356



**Fig. 27** $Fr=0,2628$



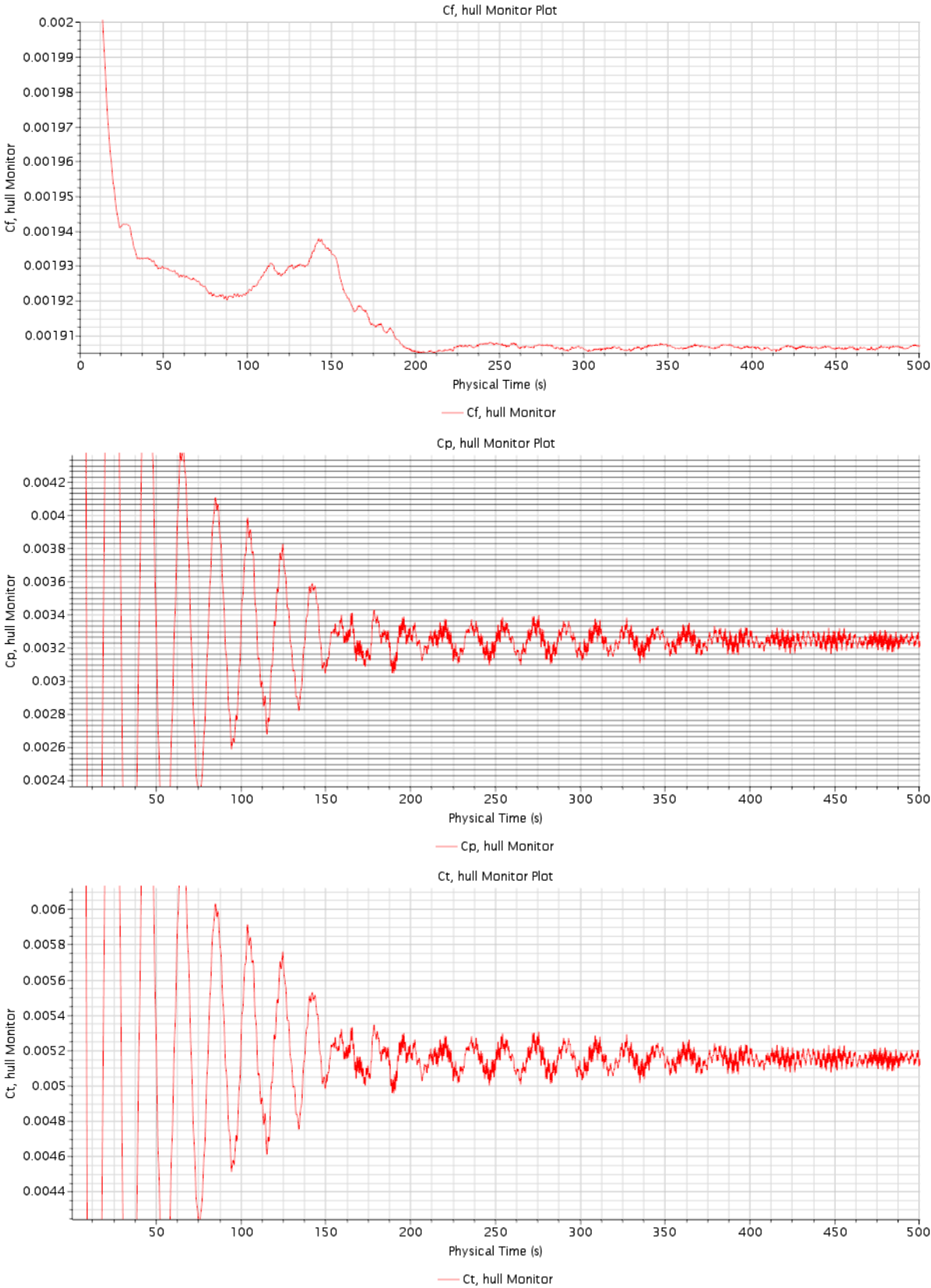
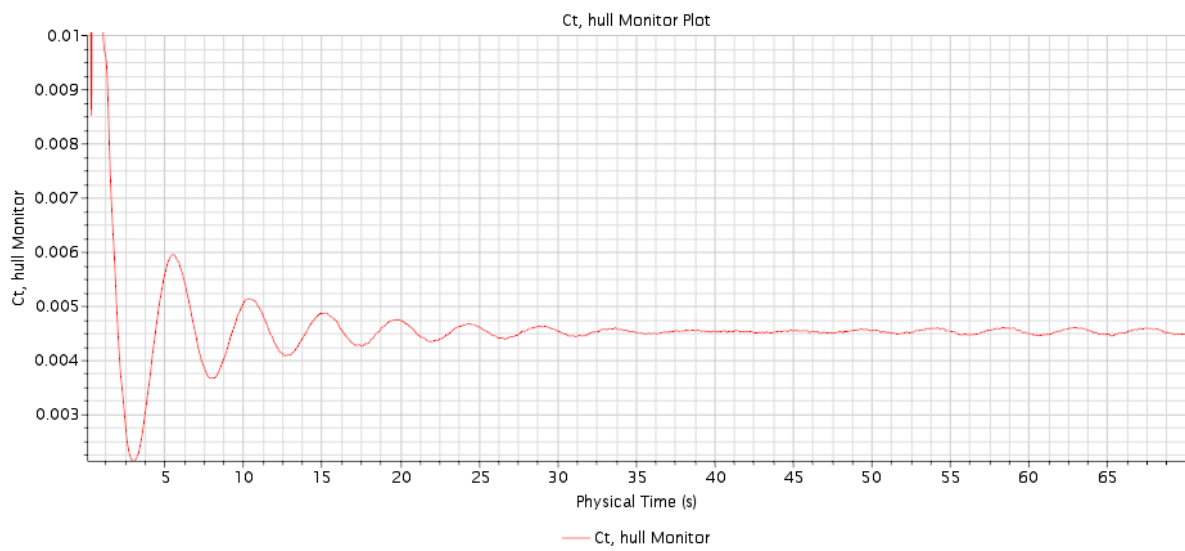
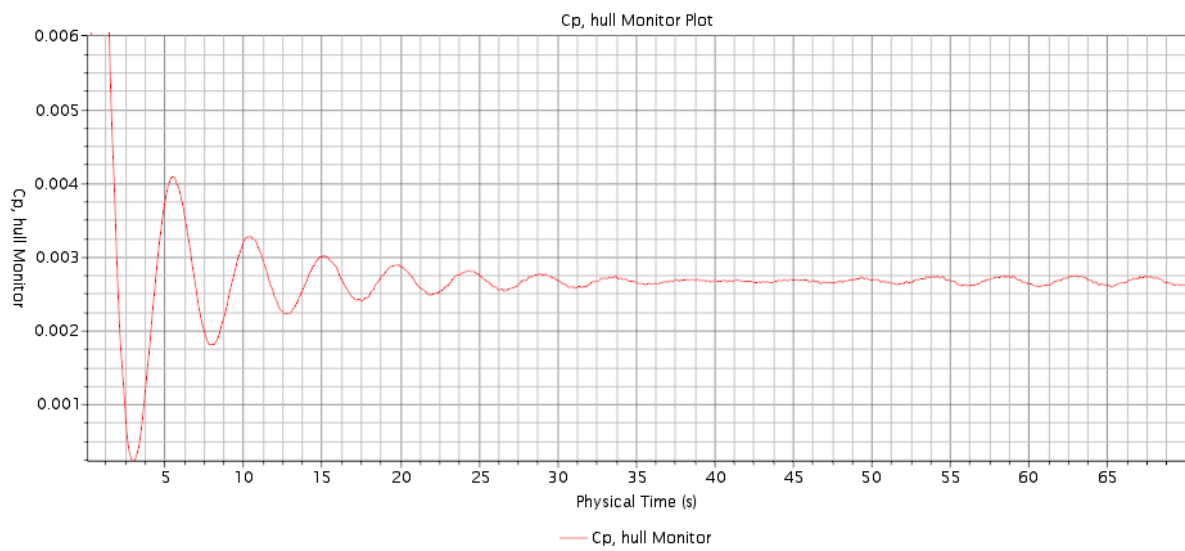
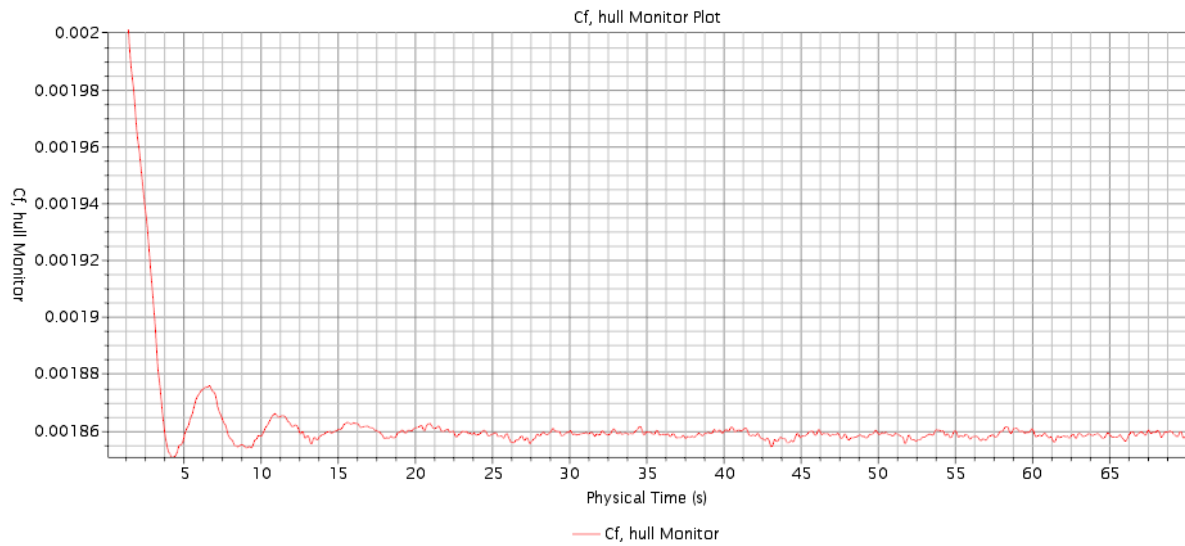
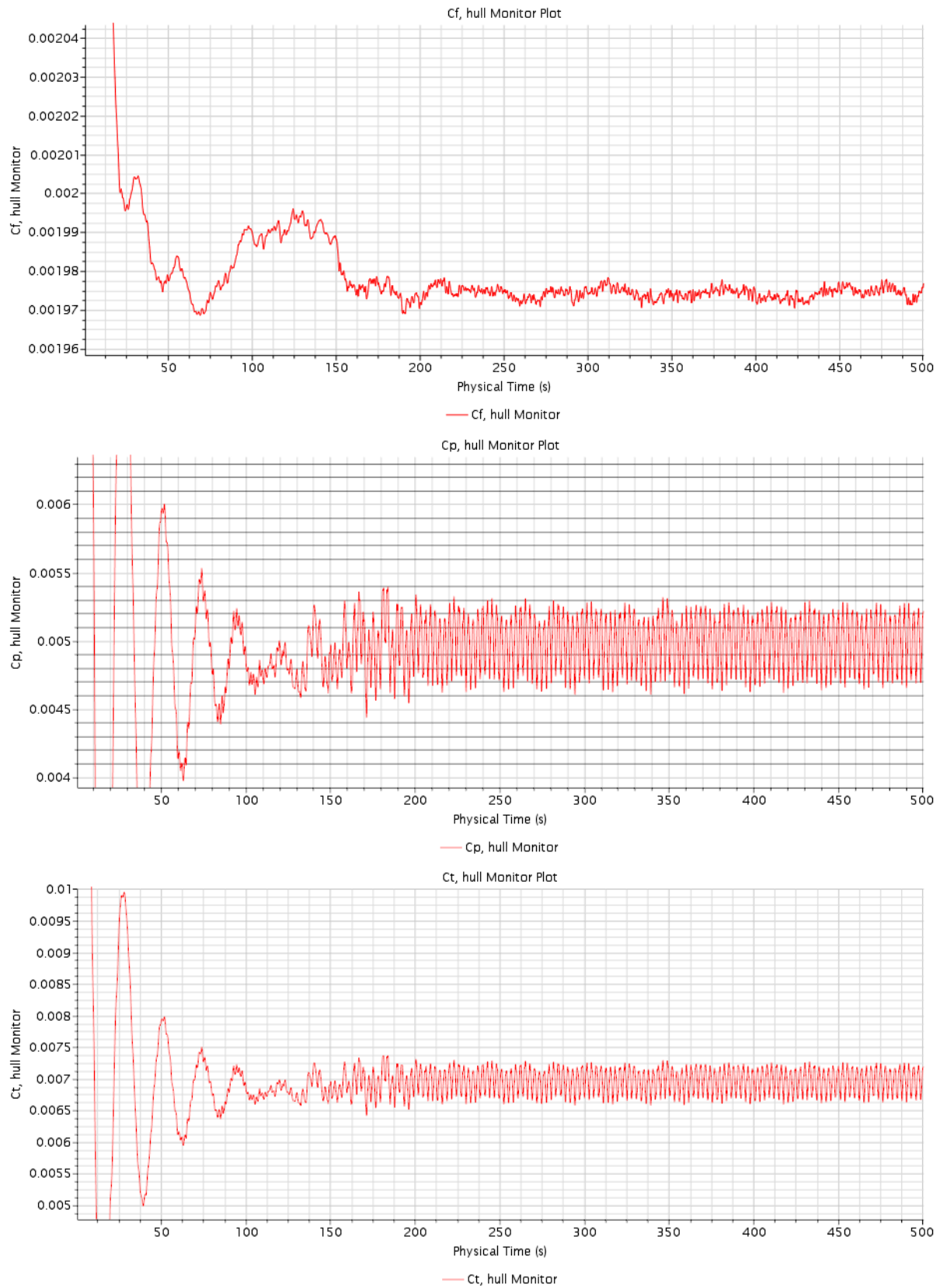


Fig. 28 Fr=2719



**Fig. 29 $Fr=0,3081$**

E. FS elevation

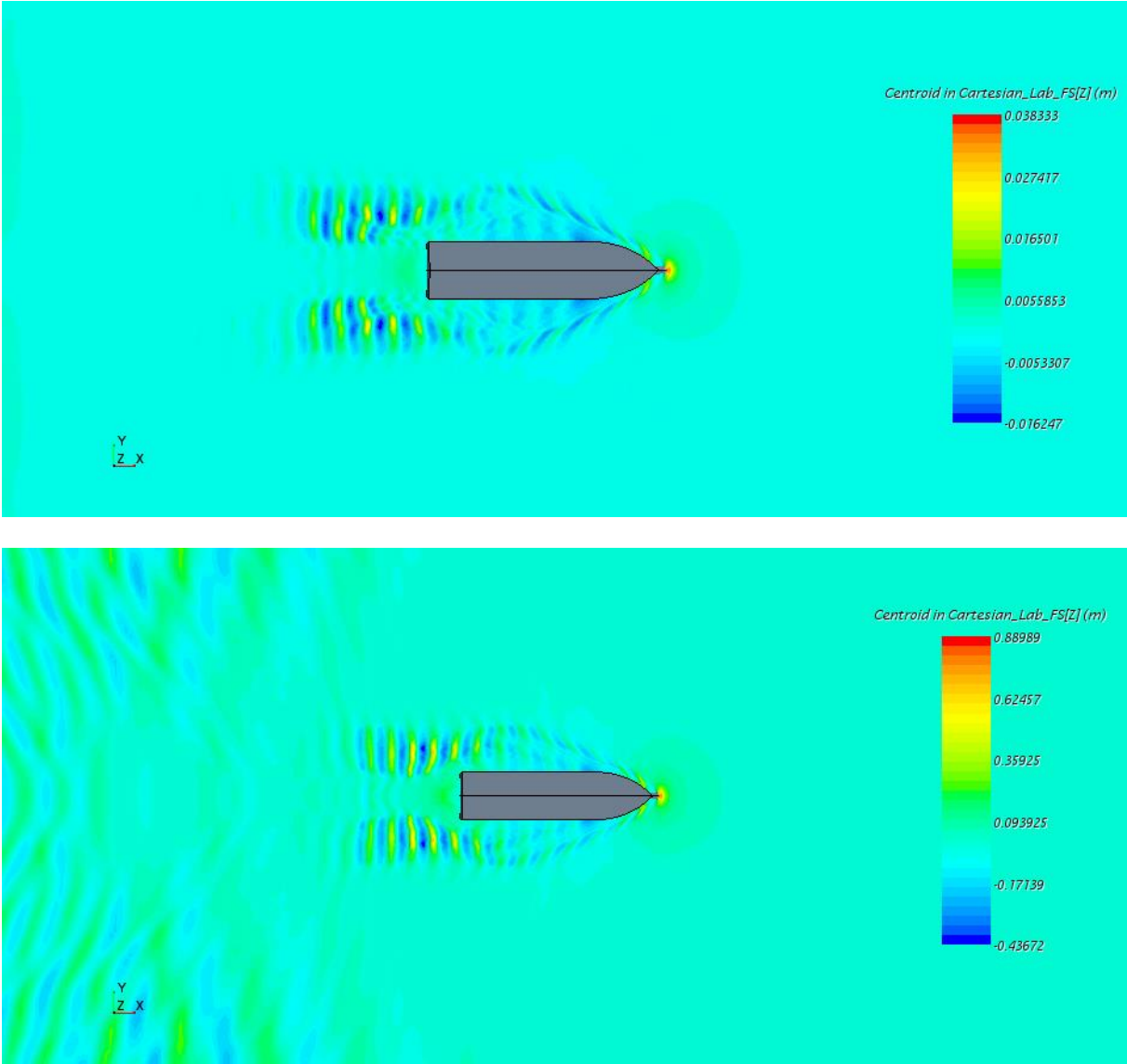


Fig. 30 Fr=0,1450

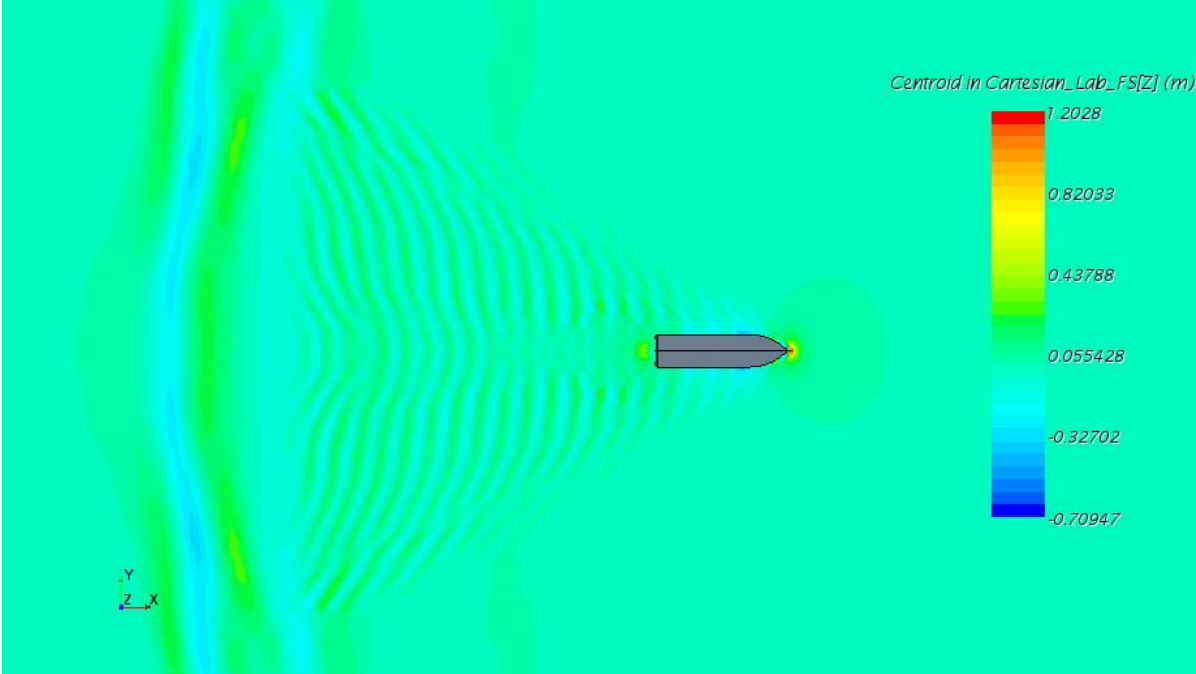
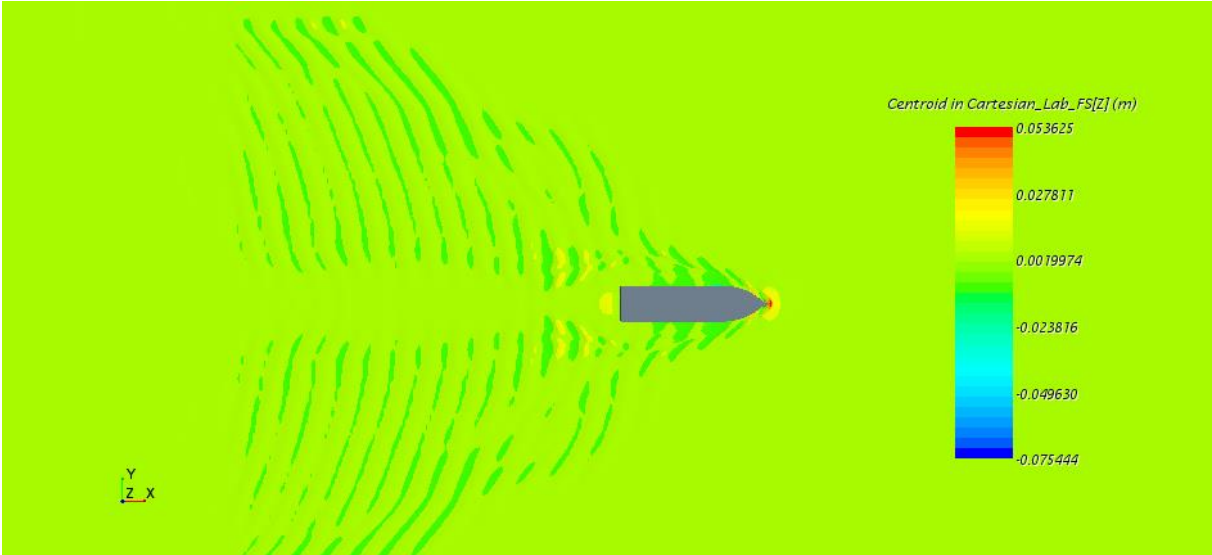


Fig. 31 Fr=0,1813

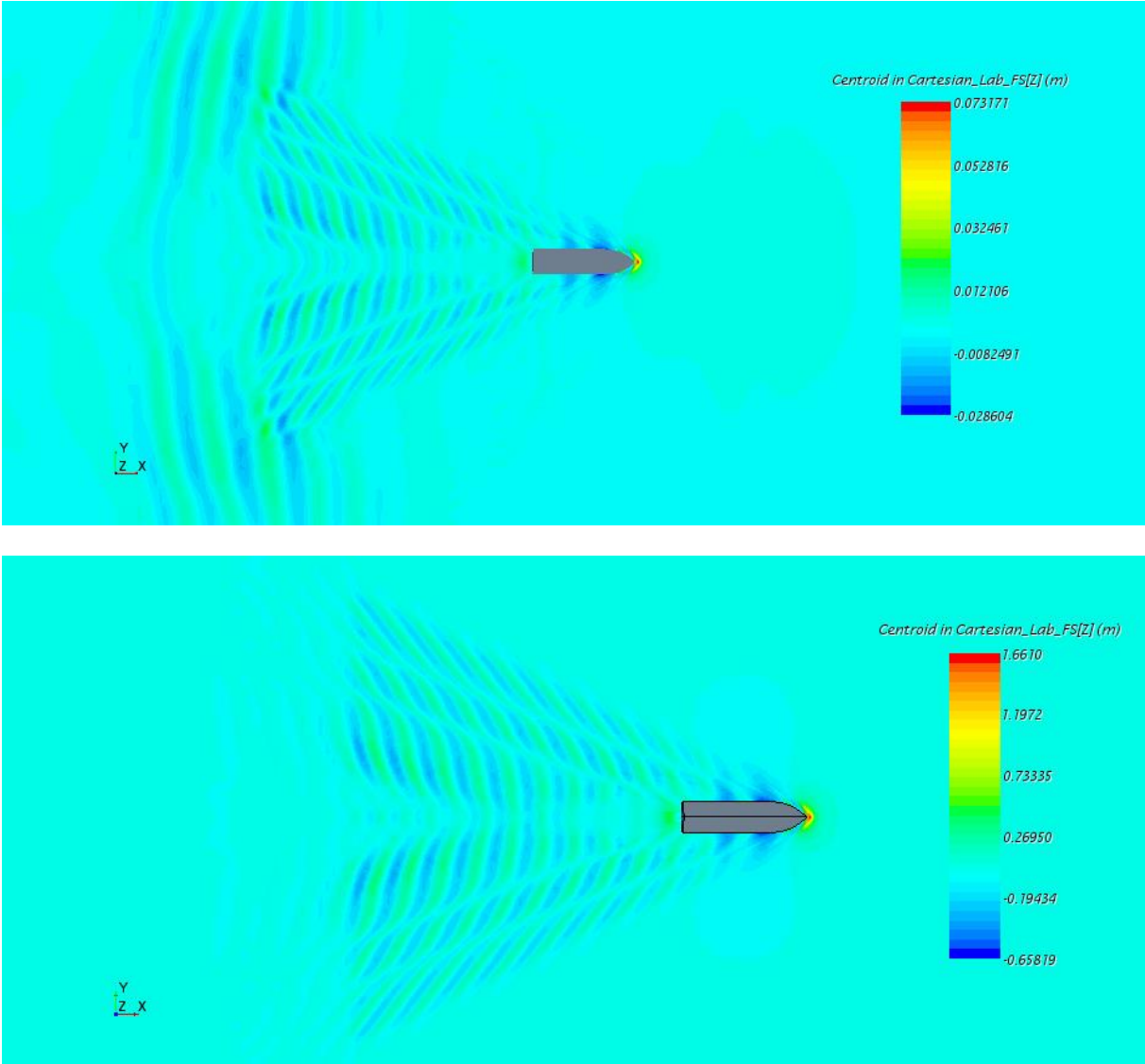


Fig. 32 Fr=0,2175

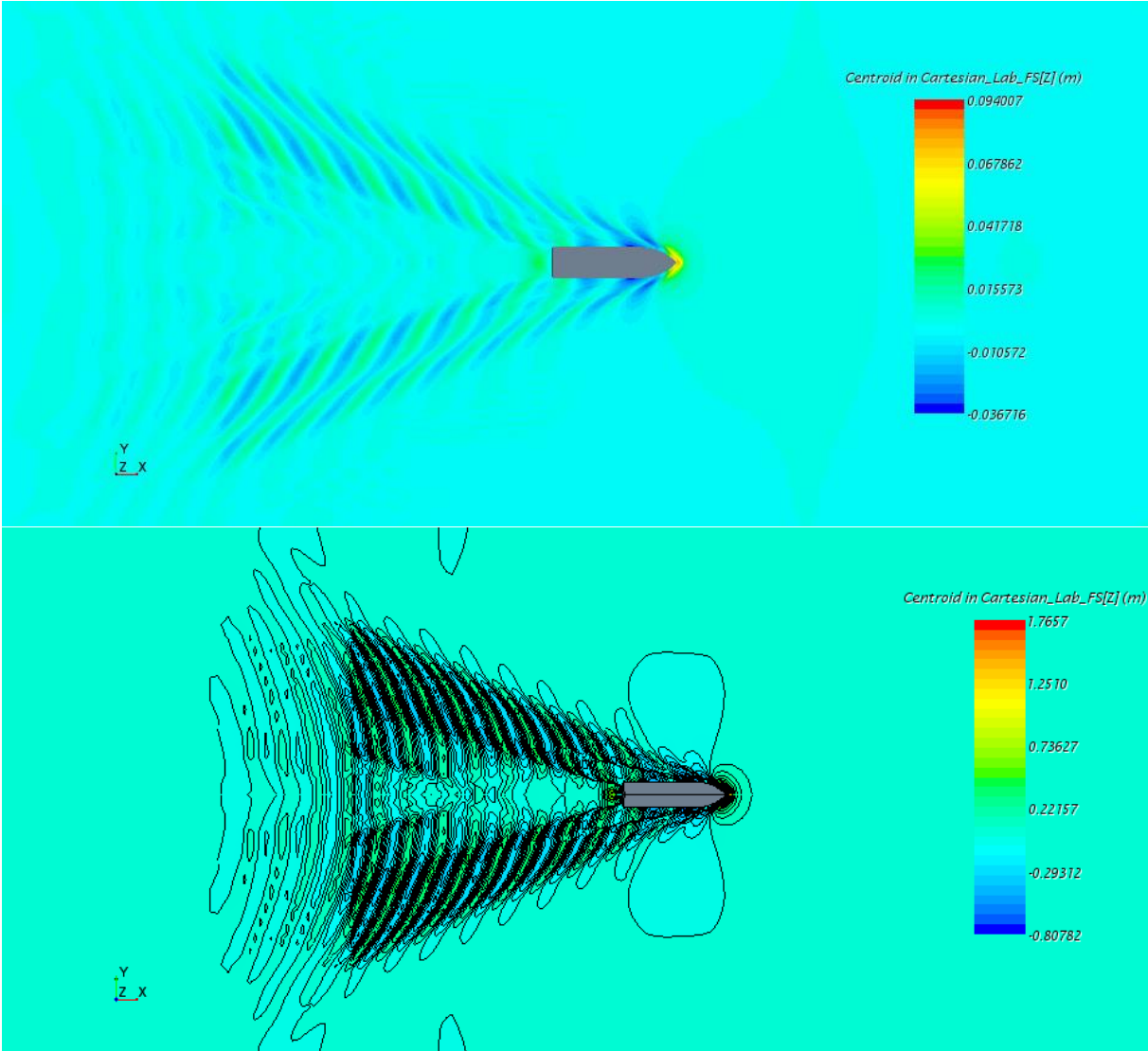


Fig. 33 $Fr=0,2356$

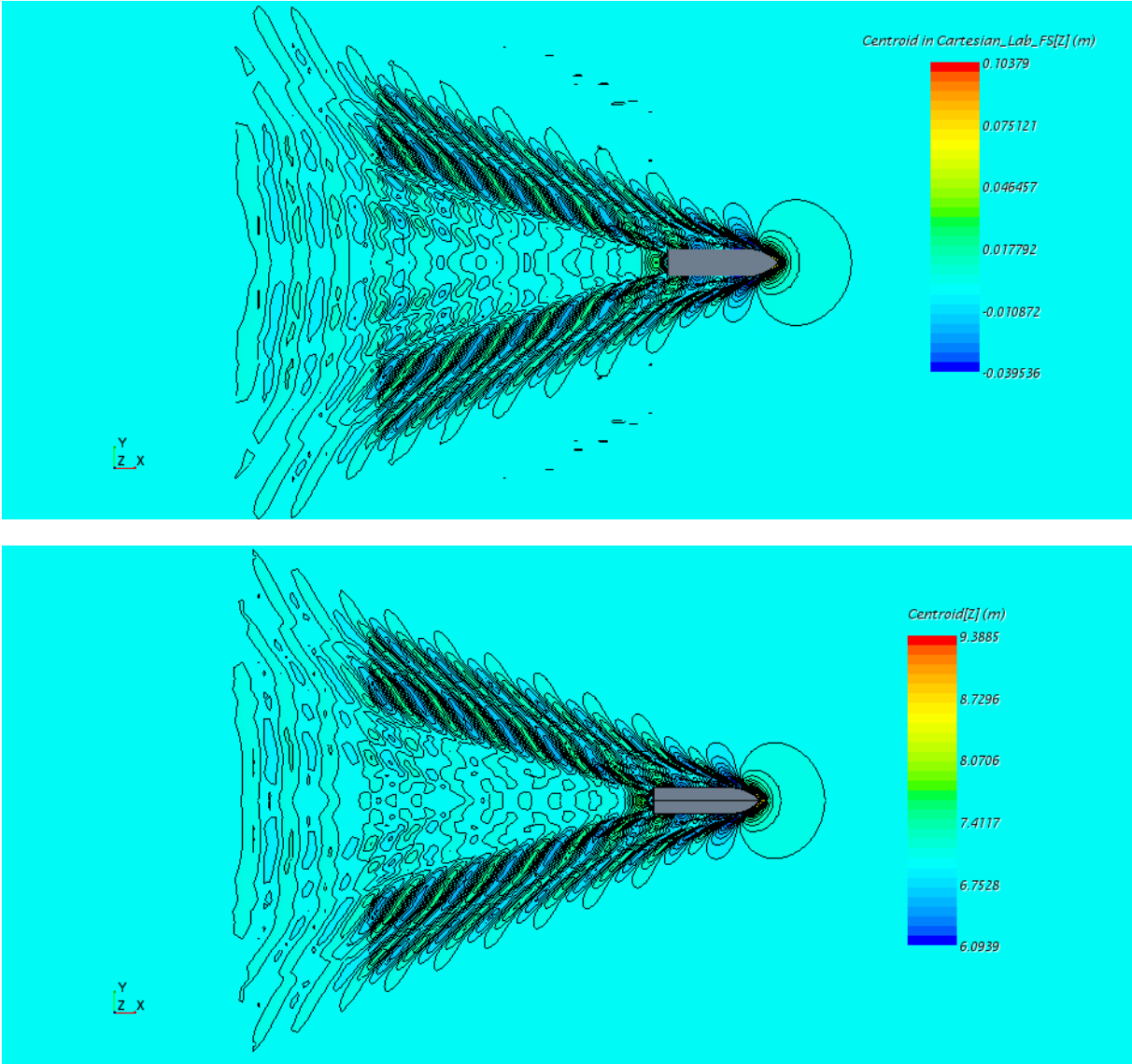


Figure 0-1 Fr=0,2628

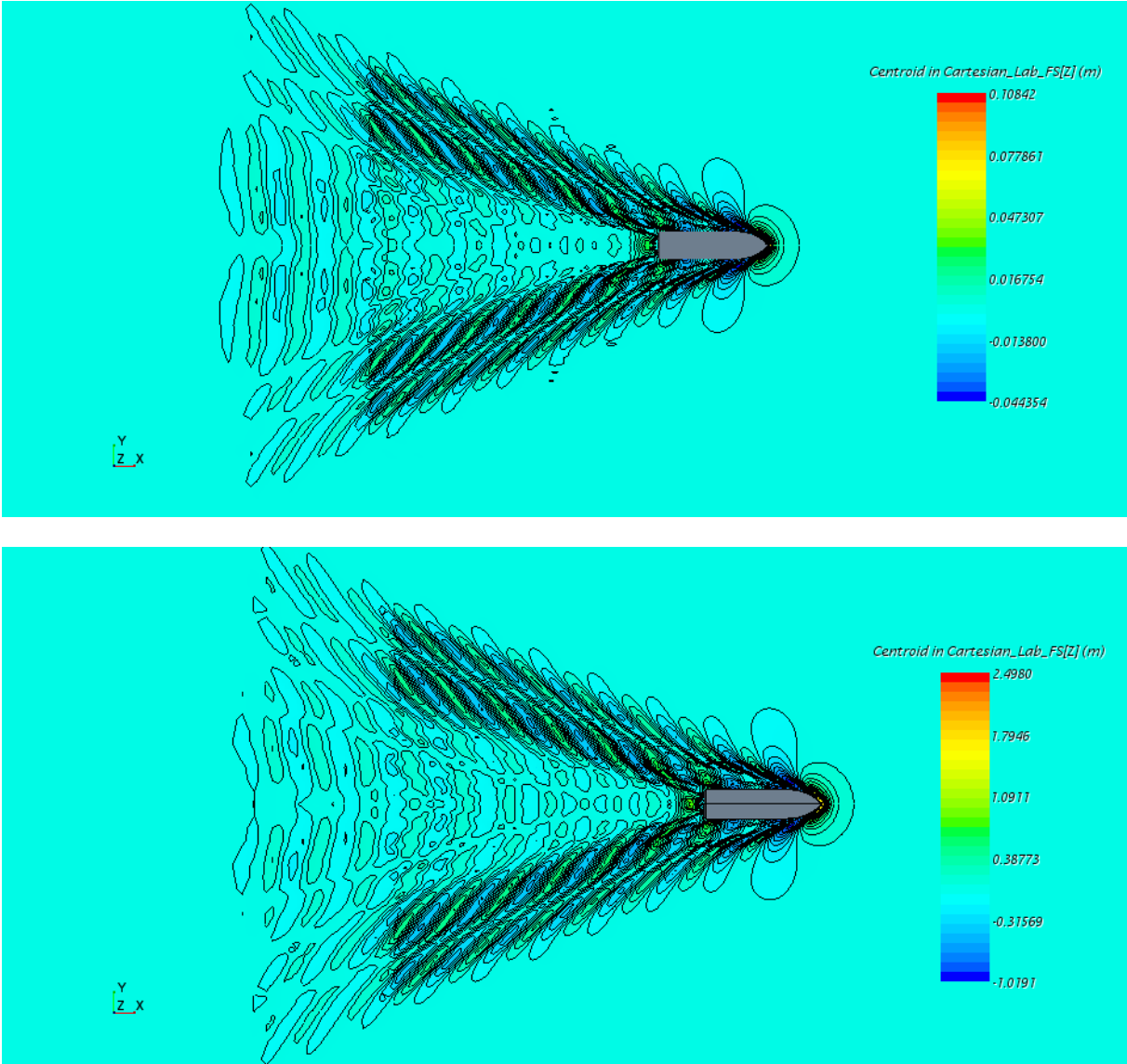


Fig. 34 Fr=2719

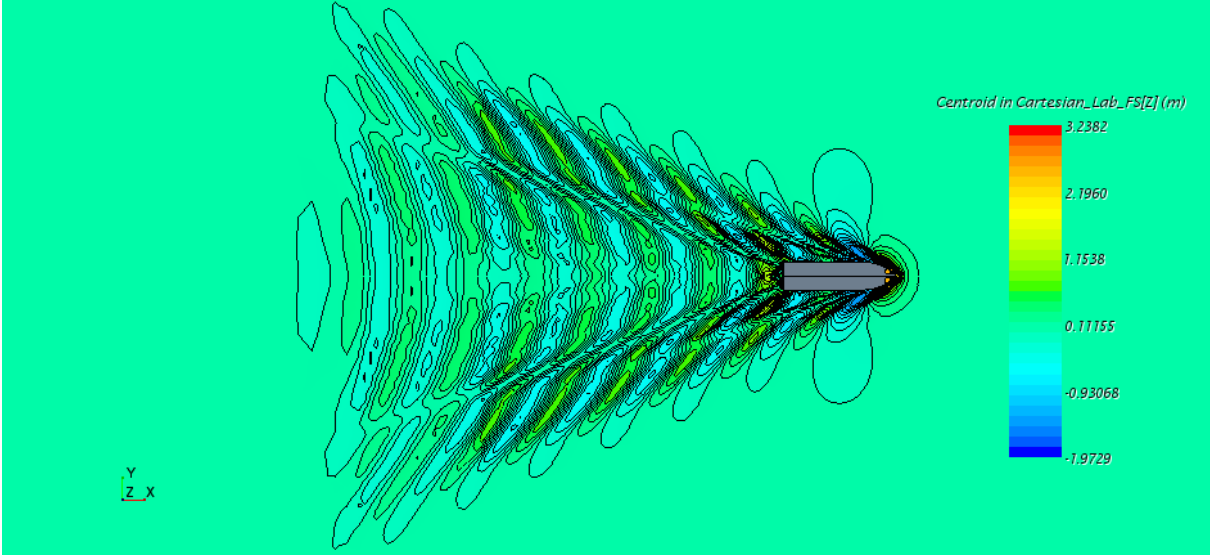
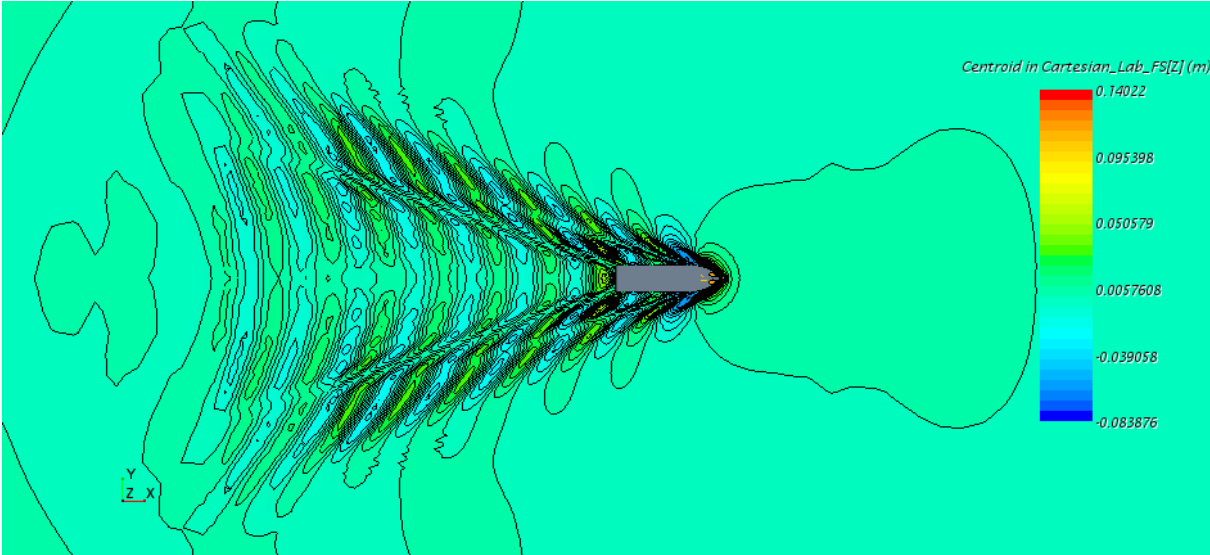


Fig. 35 Fr=0,3081

F. Wave profile

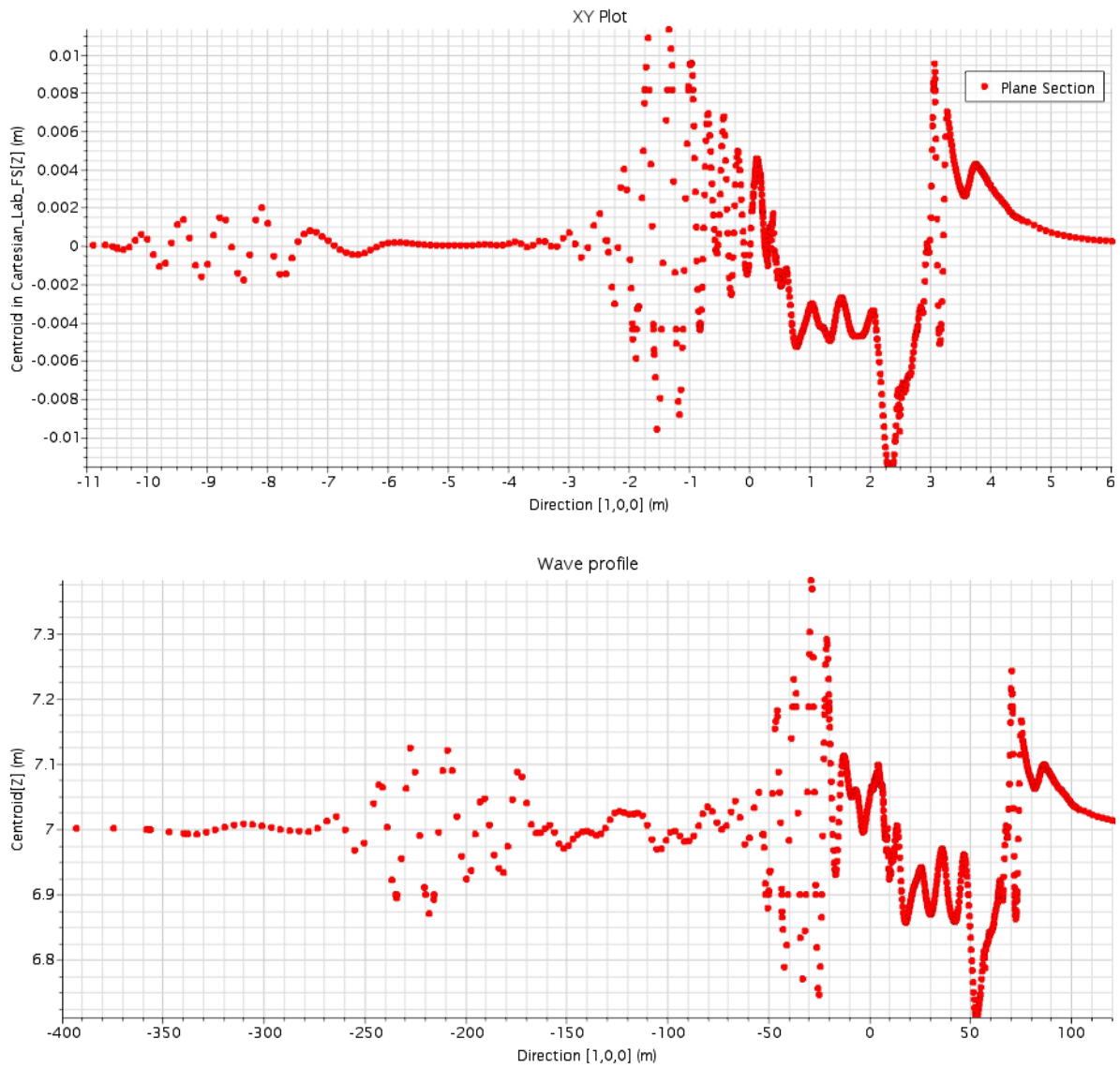


Fig. 36 $Fr=0,1450$

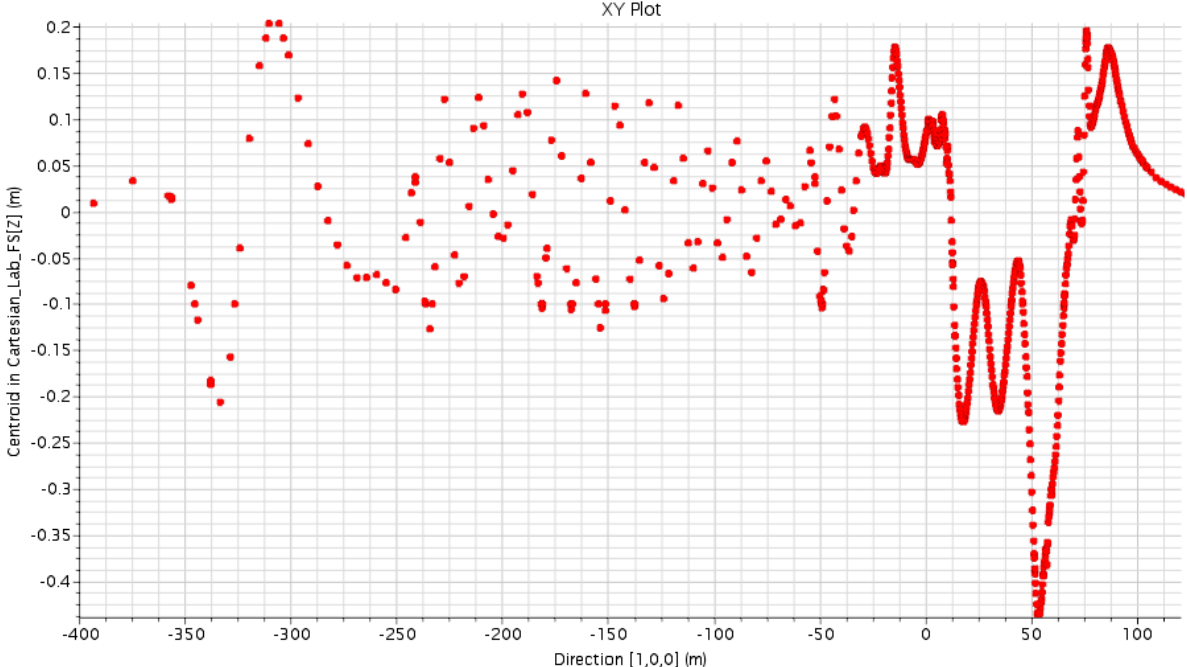
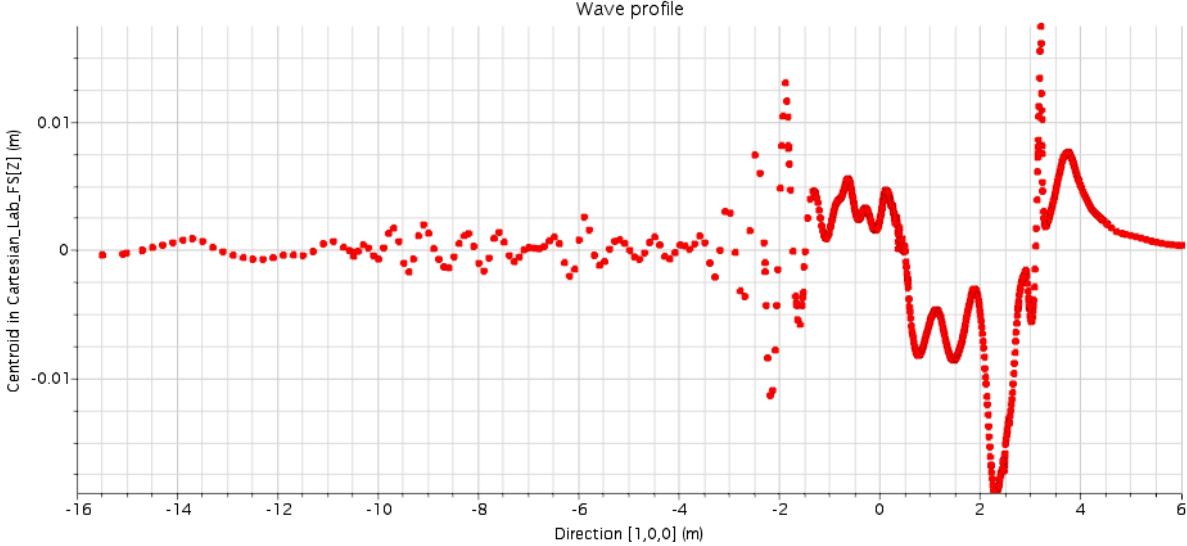


Fig. 37 Fr=0,1813

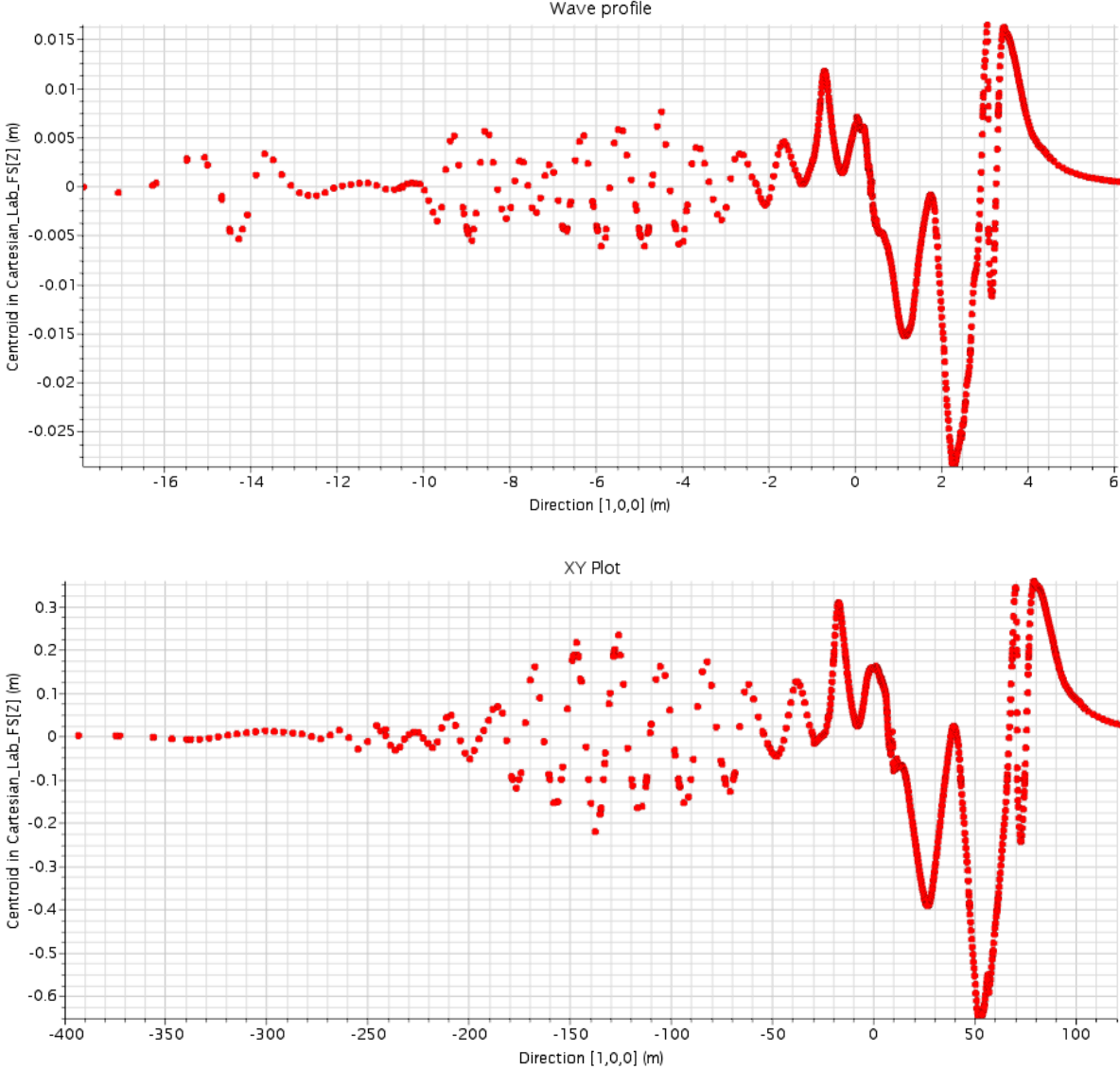


Fig. 38 Fr=0,2175

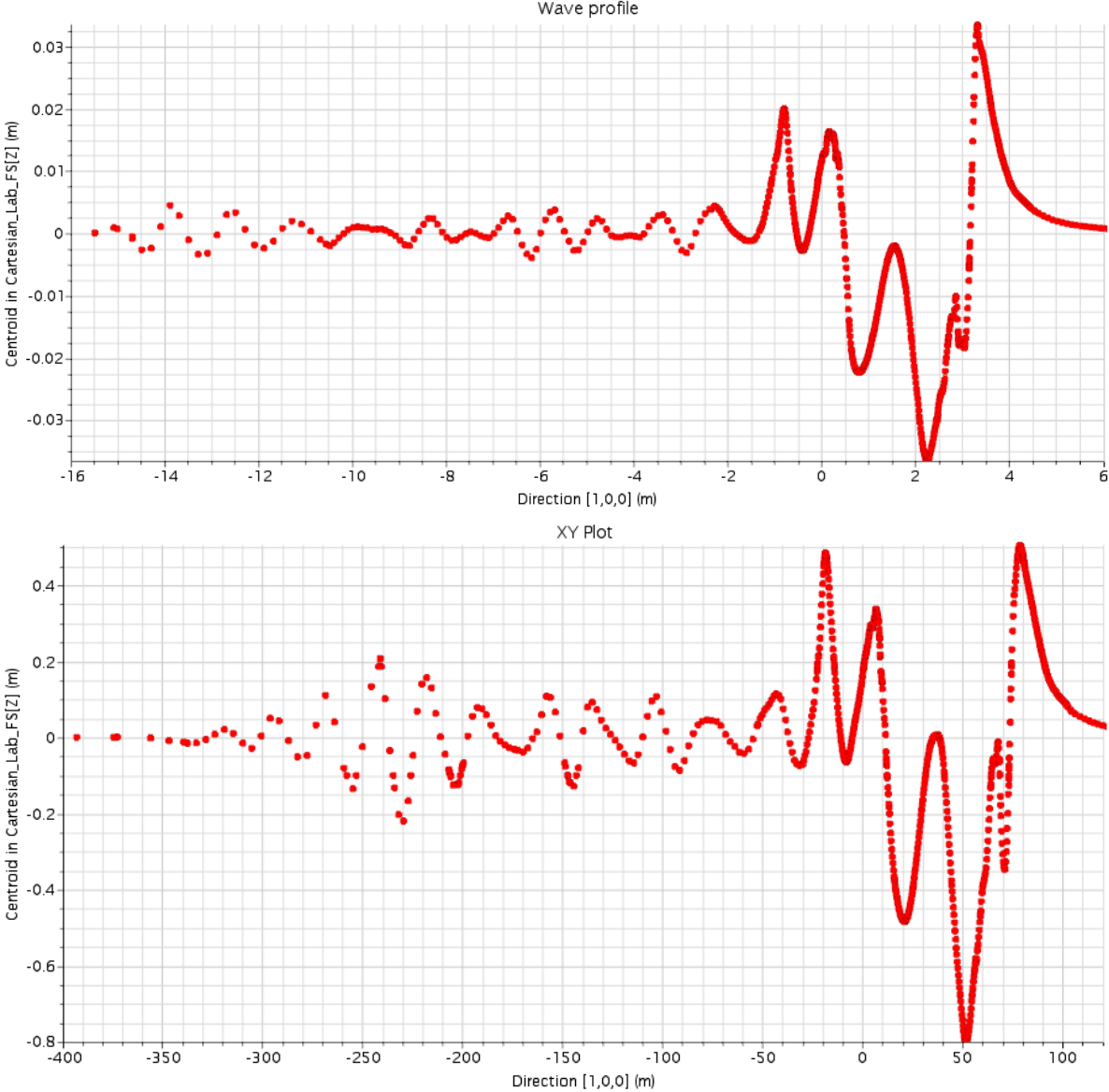


Fig. 39 Fr=0,2356

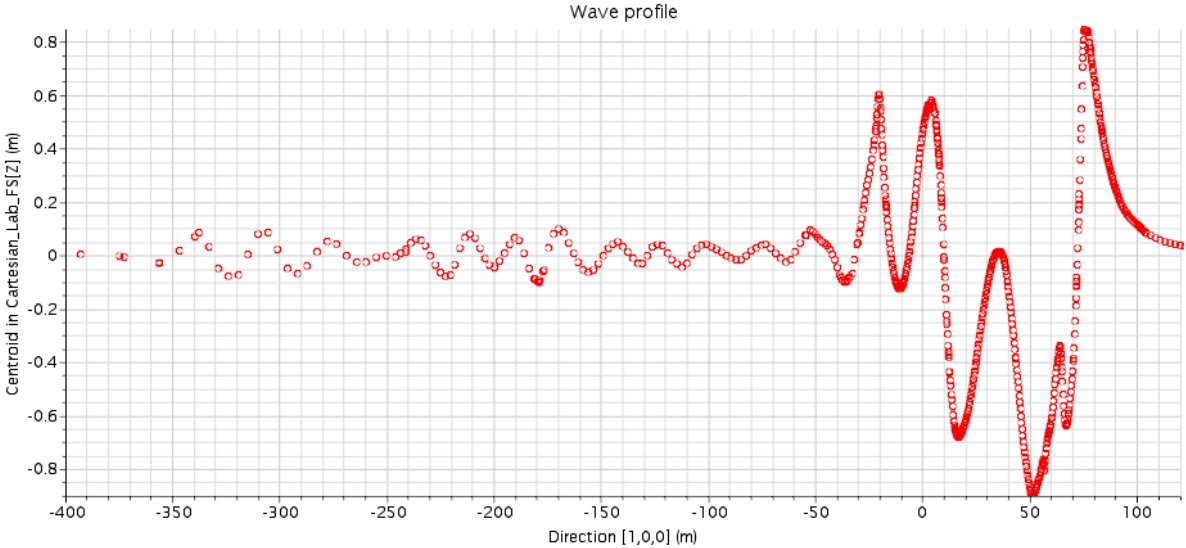
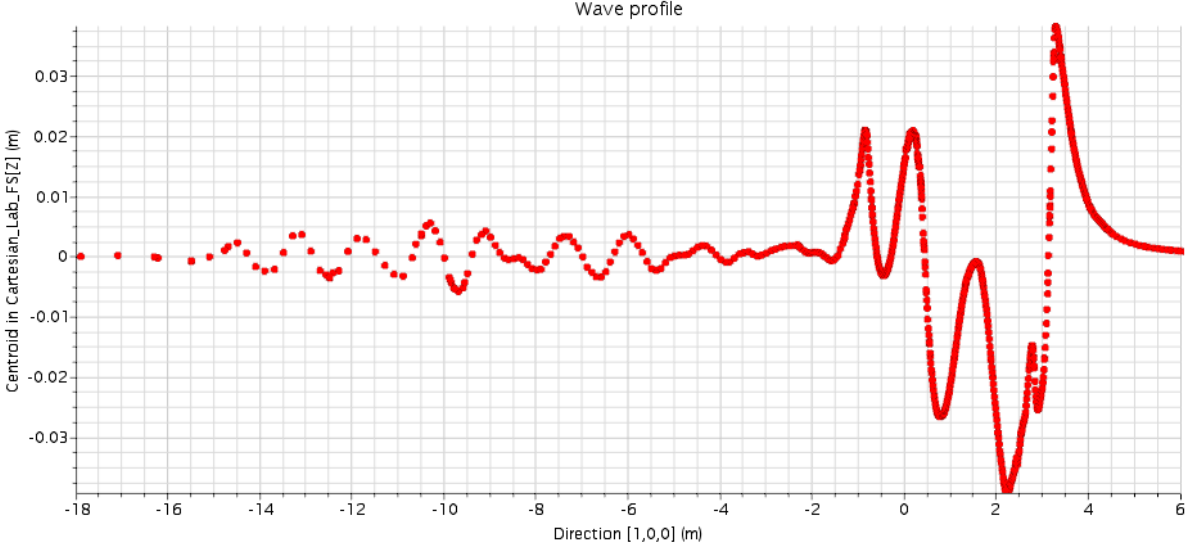


Fig. 40 Fr=0,2628

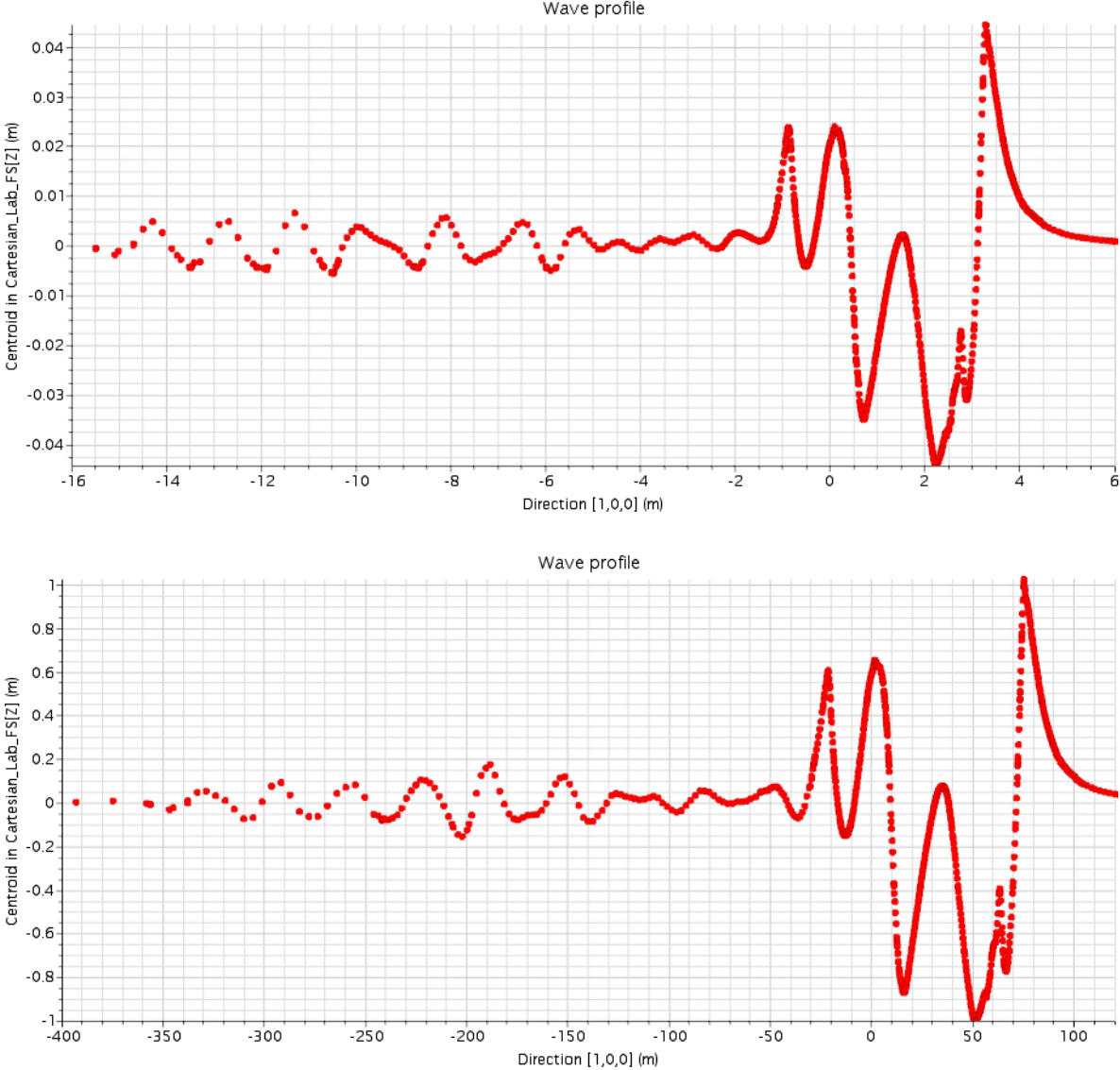


Fig. 41 Fr=2719

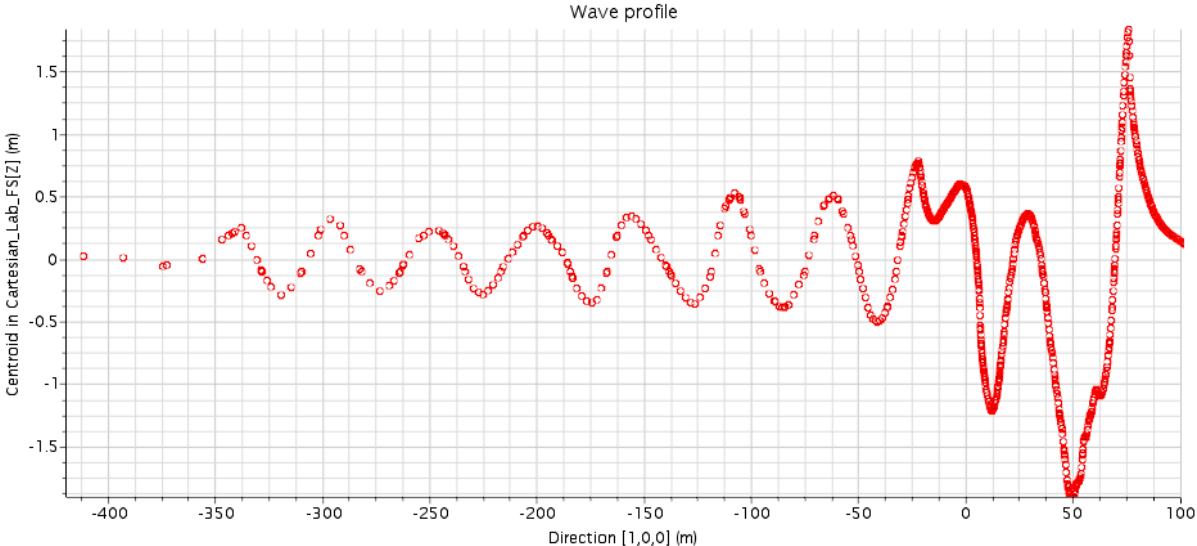
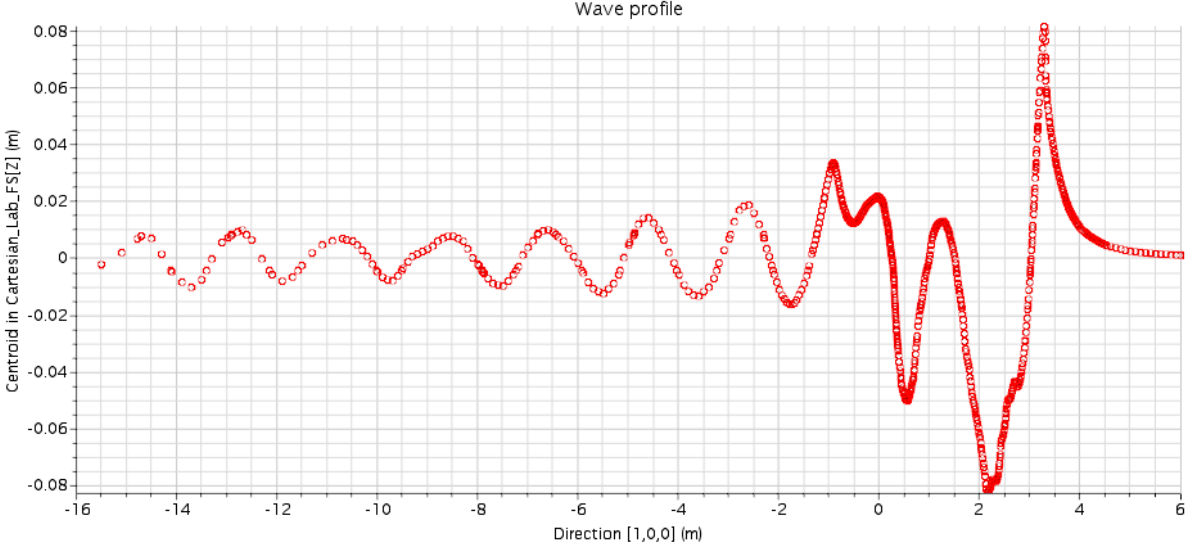


Fig. 42 Fr=0,3081

G. Wake fraction

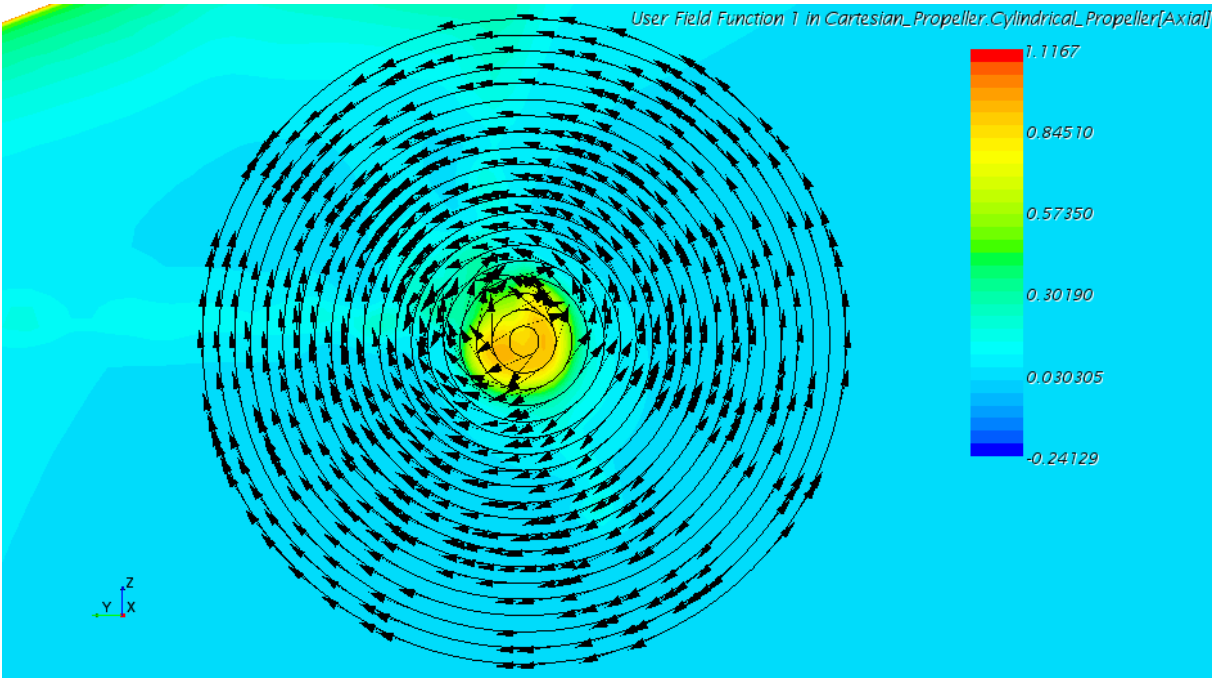
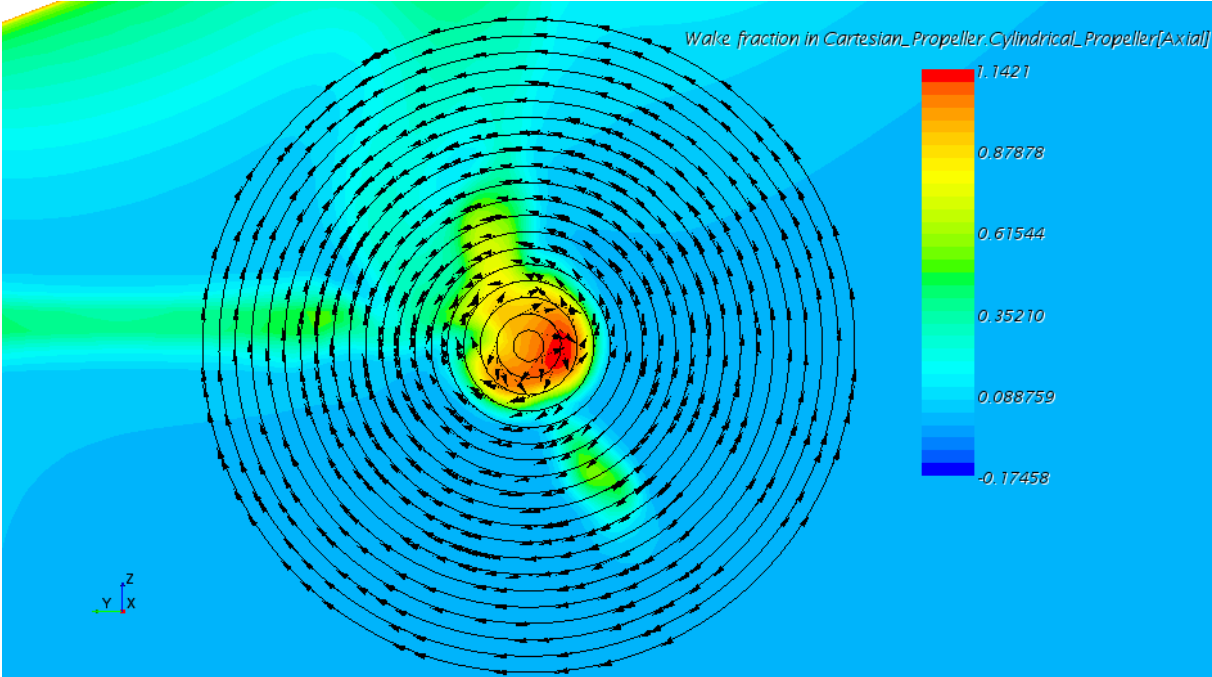


Fig. 43 Fr=0,1450

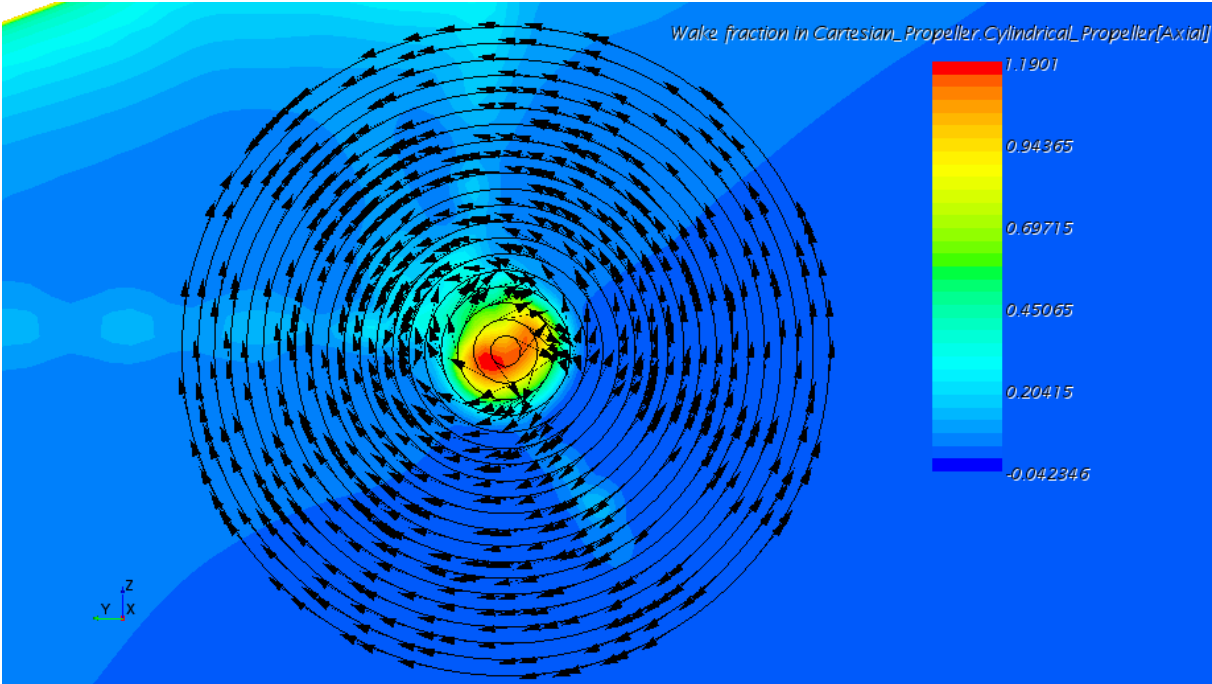
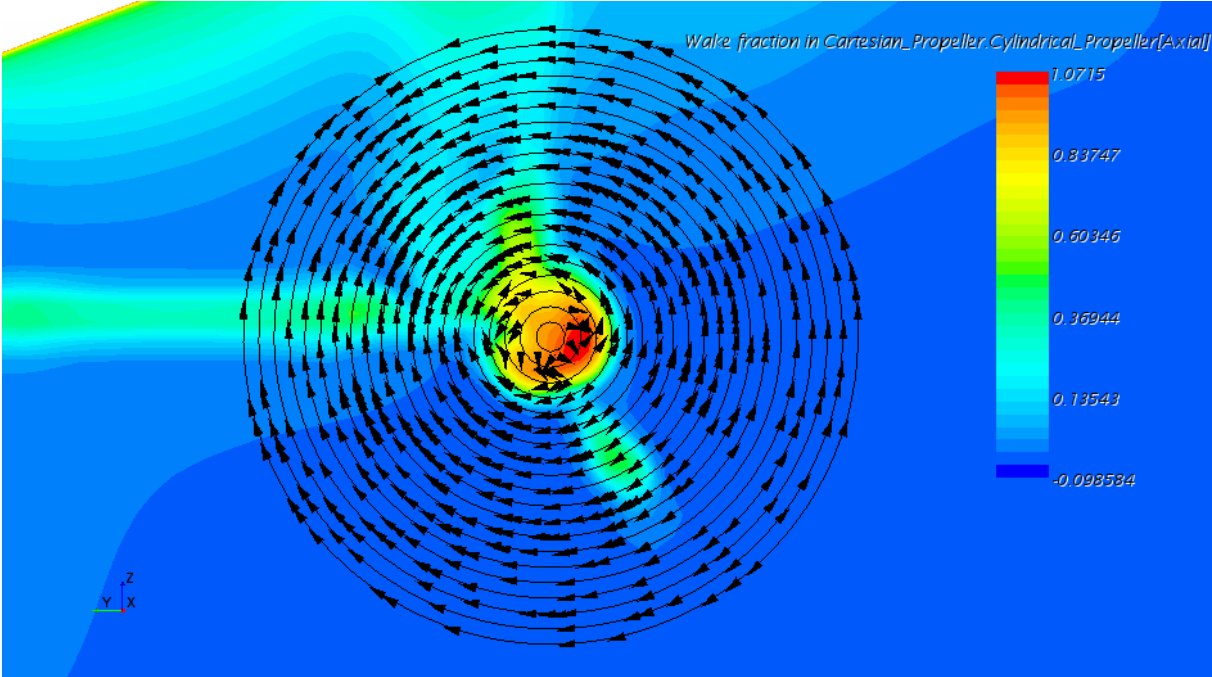


Fig. 44 Fr=0,1813

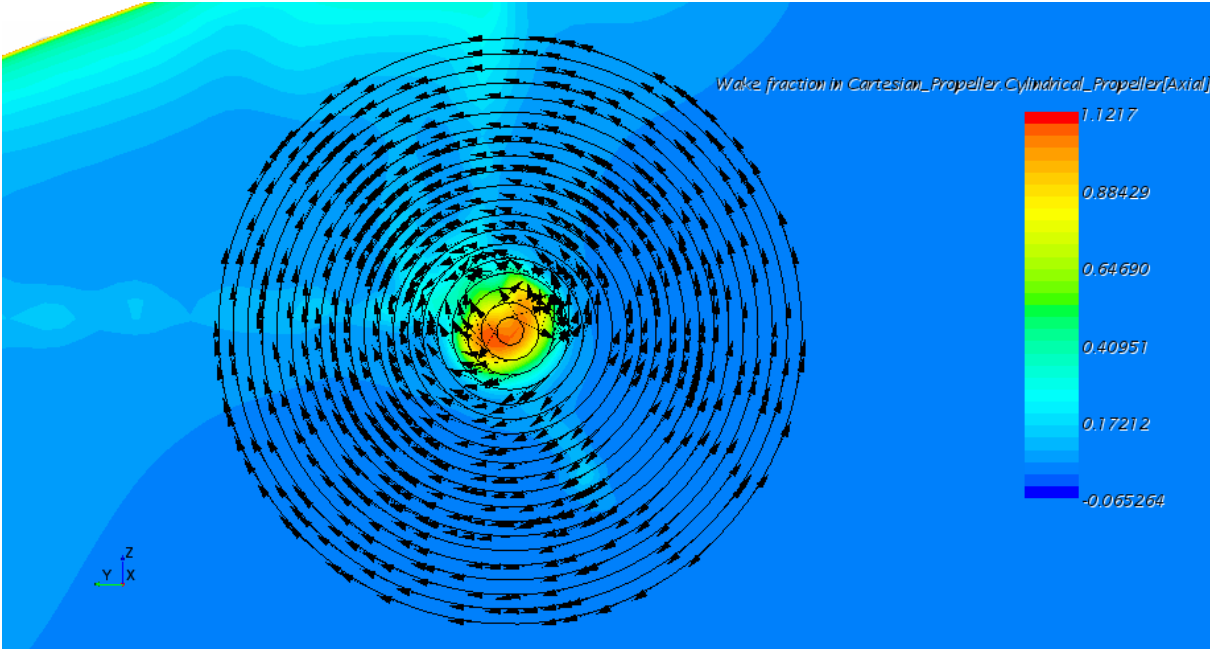
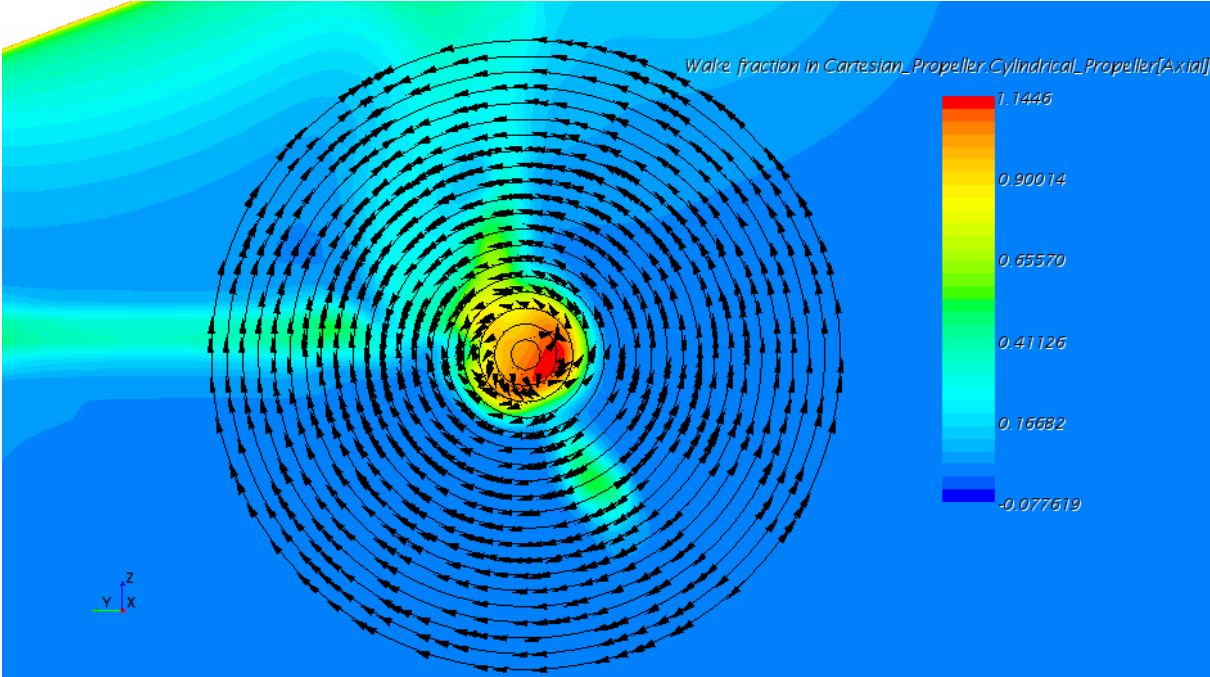


Fig. 45 Fr=0,2175

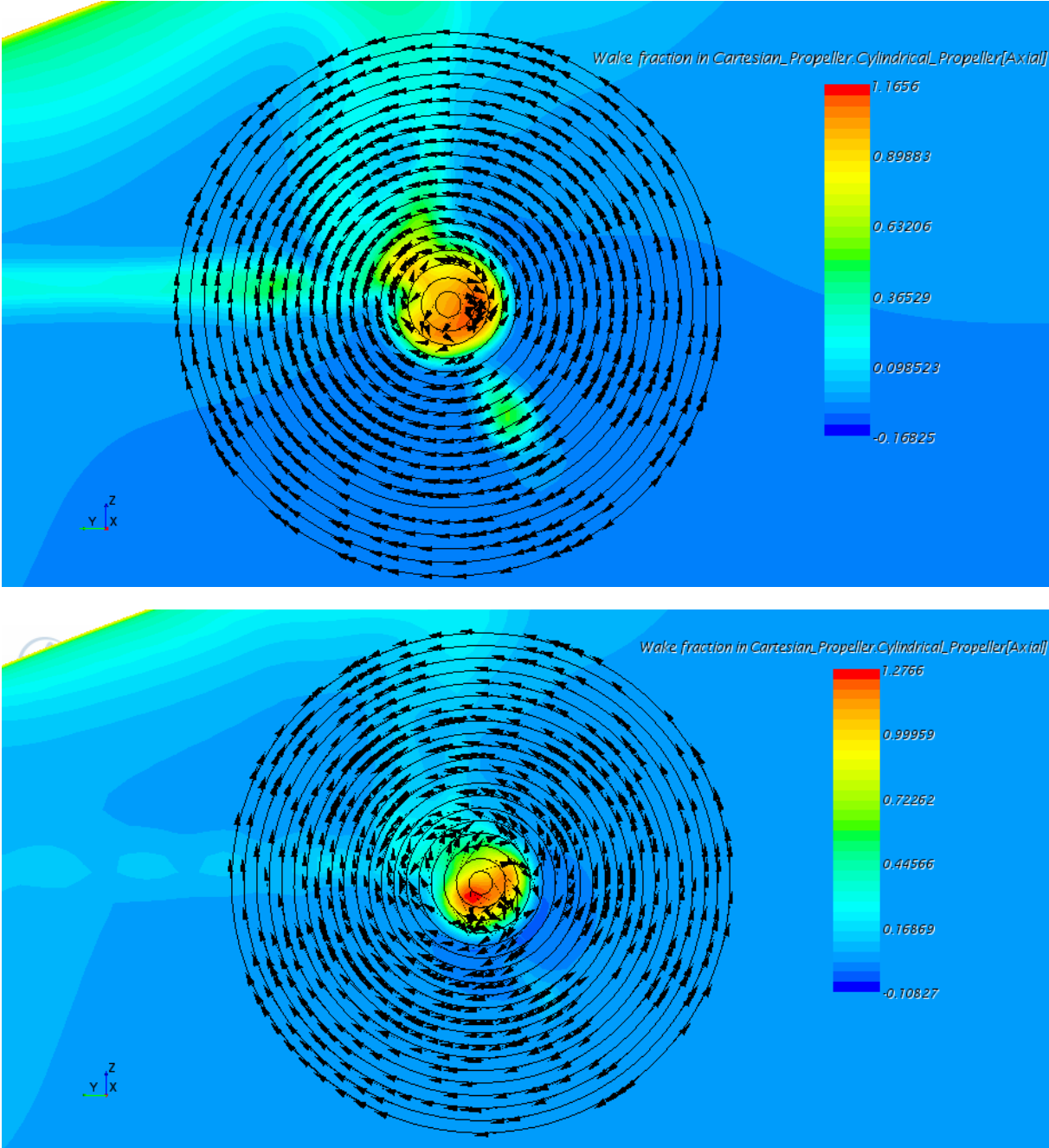


Fig. 46 Fr=0,2356

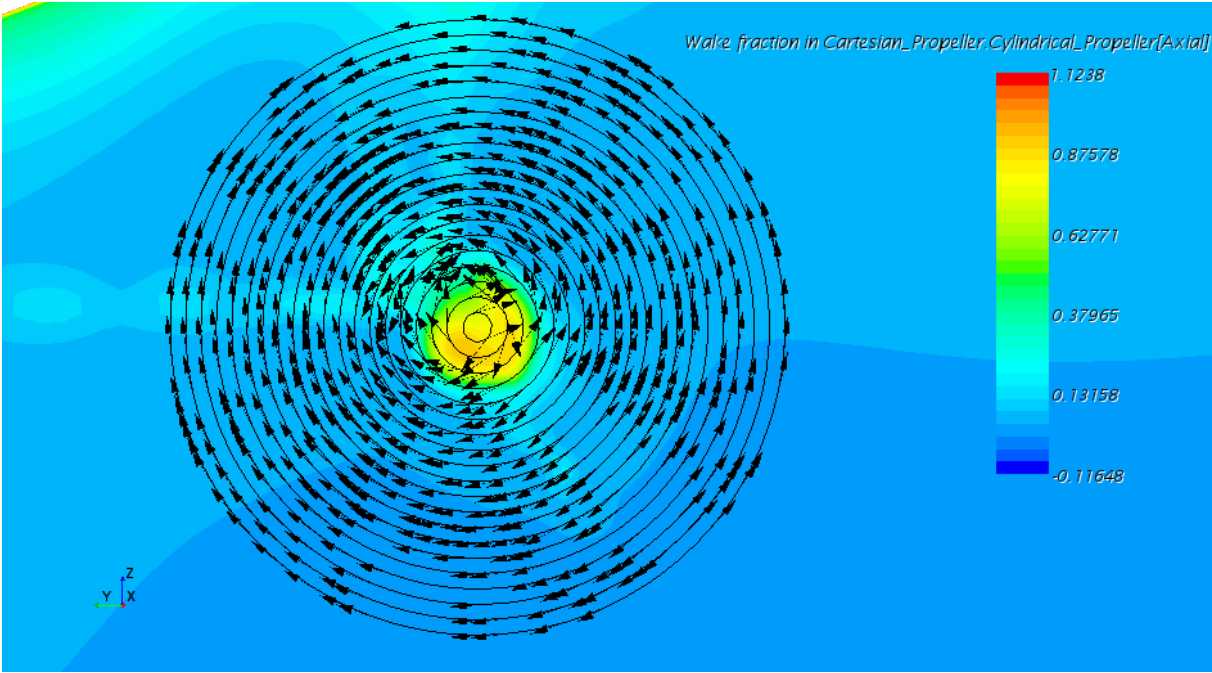
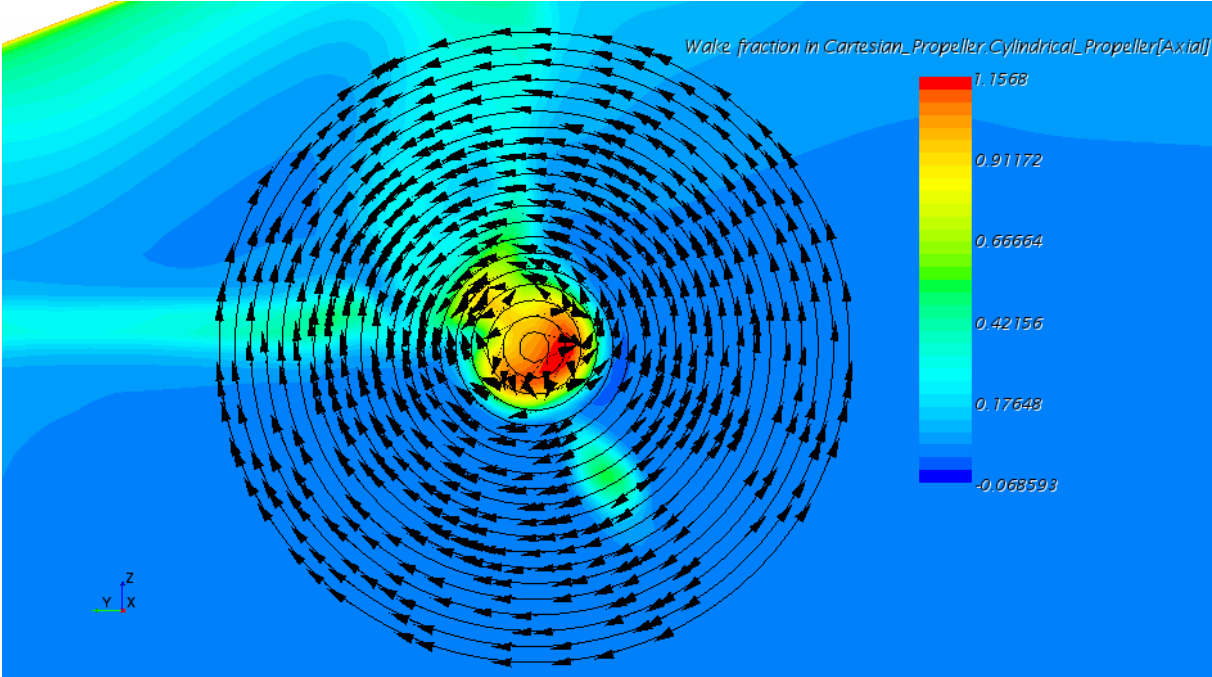


Fig. 47 $Fr=0,2628$

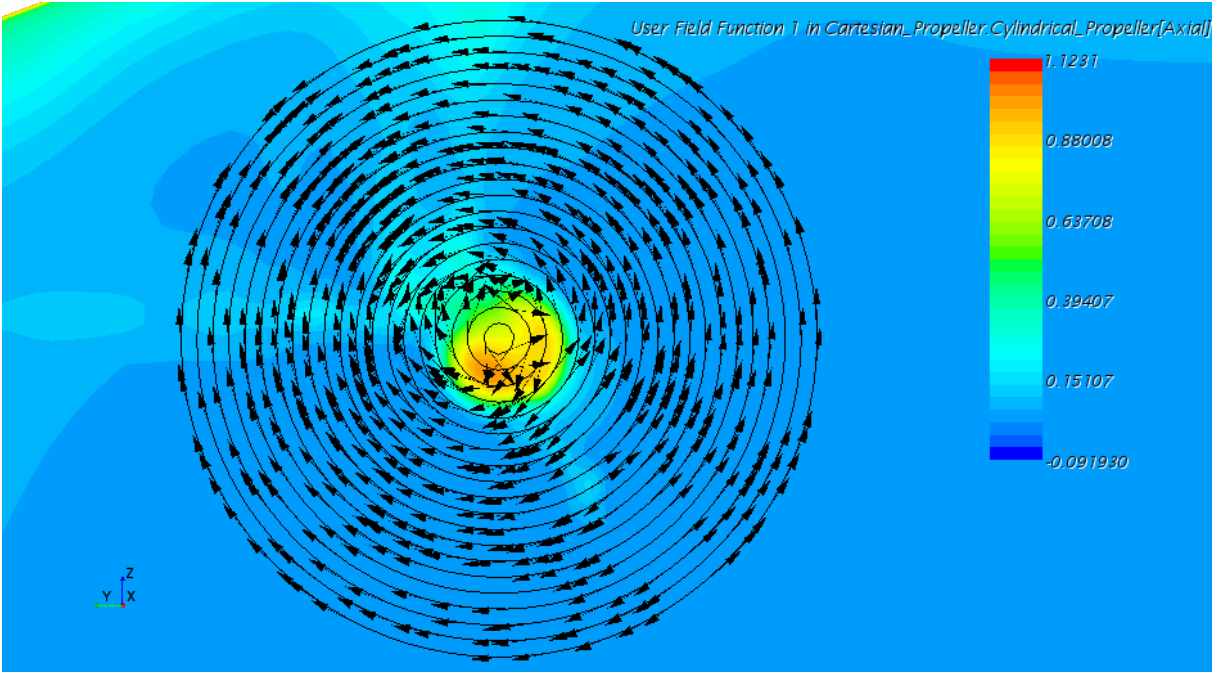
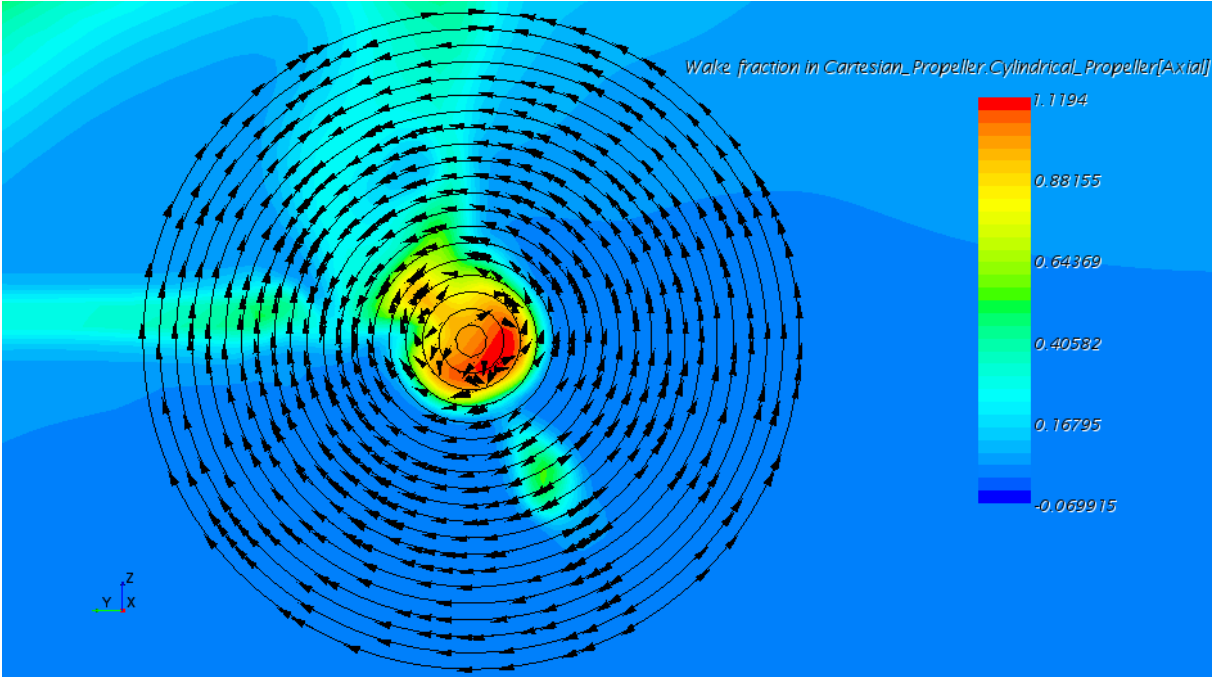


Fig. 48 Fr=0,2719

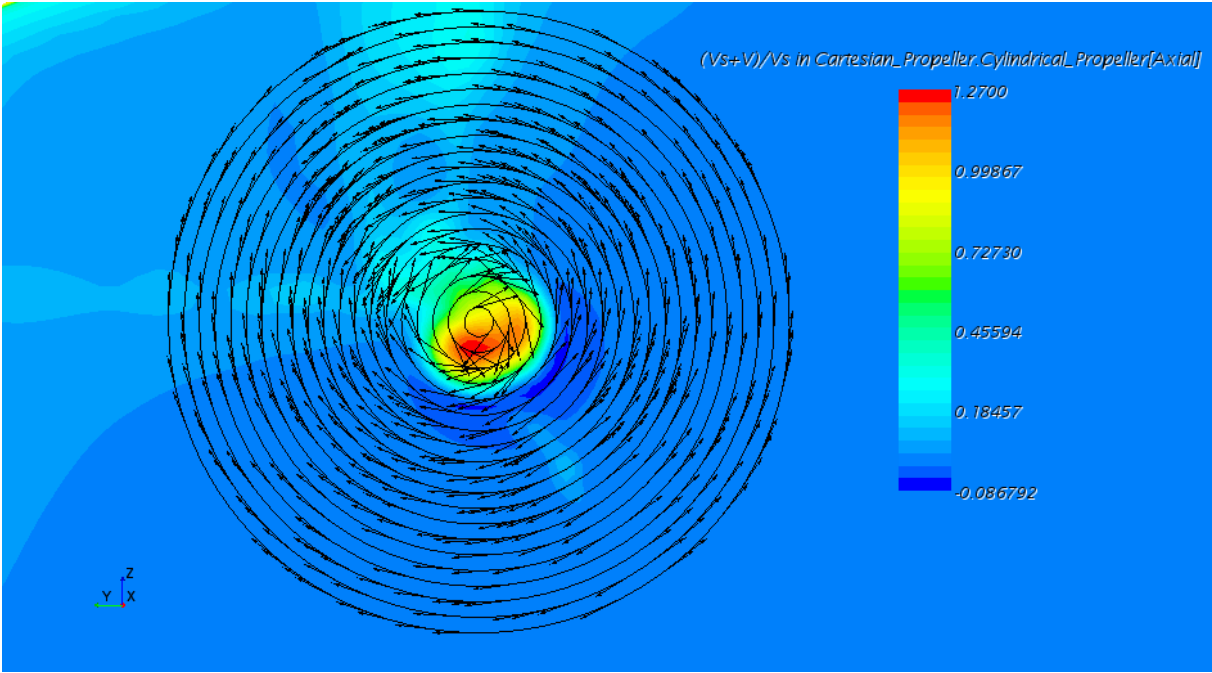
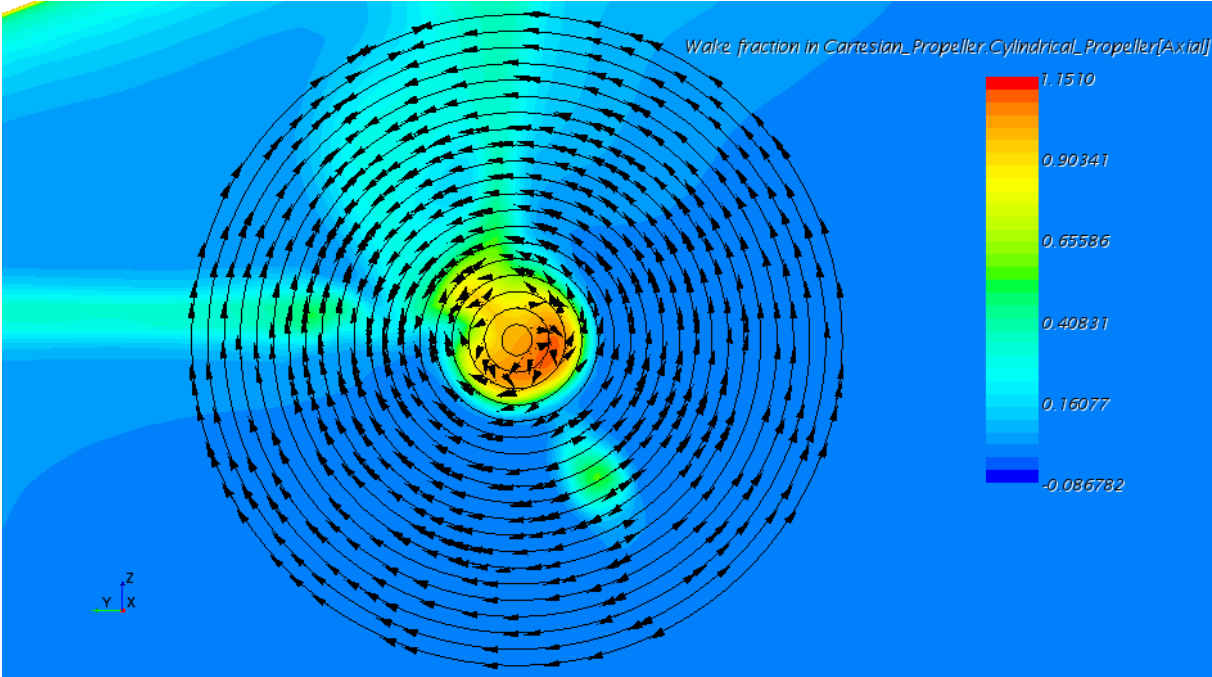


Fig. 49 Fr=0,3081

H. Mean wake fraction on propeller plane

Model scale													
Fr=0,1450		Fr=0,1813		Fr=0,2175		Fr=0,2356		Fr=0,2628		Fr=0,2719		Fr=0,3081	
Radius	Wt	Radius	Wt	Radius	Wt	Radius	Wt	Radius	Wt	Radius	Wt	Radius	Wt
0,100	0,069	0,100	0,015	0,100	0,065	0,100	-0,004	0,100	0,068	0,100	0,070	0,100	0,055
0,095	0,067	0,095	0,013	0,095	0,063	0,095	-0,005	0,095	0,068	0,095	0,071	0,095	0,058
0,090	0,066	0,090	0,011	0,090	0,061	0,090	-0,006	0,090	0,068	0,090	0,072	0,090	0,062
0,085	0,069	0,085	0,013	0,085	0,063	0,085	-0,003	0,085	0,071	0,085	0,076	0,085	0,068
0,080	0,072	0,080	0,015	0,080	0,066	0,080	0,001	0,080	0,074	0,080	0,081	0,080	0,075
0,075	0,074	0,075	0,016	0,075	0,068	0,075	0,002	0,075	0,077	0,075	0,082	0,075	0,077
0,070	0,082	0,070	0,025	0,070	0,076	0,070	0,011	0,070	0,084	0,070	0,087	0,070	0,082
0,065	0,087	0,065	0,031	0,065	0,076	0,065	0,016	0,065	0,092	0,065	0,087	0,065	0,092
0,060	0,083	0,060	0,028	0,060	0,081	0,060	0,012	0,060	0,087	0,060	0,087	0,060	0,085
0,055	0,092	0,055	0,037	0,055	0,089	0,055	0,019	0,055	0,094	0,055	0,092	0,055	0,093
0,050	0,107	0,050	0,050	0,050	0,100	0,050	0,032	0,050	0,099	0,050	0,098	0,050	0,096
0,045	0,130	0,045	0,069	0,045	0,117	0,045	0,048	0,045	0,112	0,045	0,113	0,045	0,100
0,040	0,143	0,040	0,080	0,040	0,119	0,040	0,057	0,040	0,122	0,040	0,118	0,040	0,103
0,035	0,149	0,035	0,085	0,035	0,124	0,035	0,065	0,035	0,133	0,035	0,127	0,035	0,111
0,030	0,164	0,030	0,103	0,030	0,171	0,030	0,081	0,030	0,171	0,030	0,185	0,030	0,145
0,025	0,223	0,025	0,169	0,025	0,198	0,025	0,192	0,025	0,226	0,025	0,210	0,025	0,224
0,020	0,511	0,020	0,453	0,020	0,527	0,020	0,486	0,020	0,495	0,020	0,557	0,020	0,537
0,015	0,847	0,015	0,787	0,015	0,873	0,015	0,824	0,015	0,849	0,015	0,910	0,015	0,839
0,010	0,991	0,010	0,930	0,010	1,011	0,010	0,980	0,010	1,018	0,010	1,002	0,010	0,966
0,005	1,029	0,005	0,960	0,005	1,002	0,005	1,024	0,005	1,050	0,005	0,979	0,005	0,992
W_{average}	0,253	W_{average}	0,194	W_{average}	0,248	W_{average}	0,192	W_{average}	0,253	W_{average}	0,255	W_{average}	0,243

Fig. 50 Summary of mean wake fraction in model scale

Full scale													
Fr=0,1450		Fr=0,1813		Fr=0,2175		Fr=0,2356		Fr=0,2628		Fr=0,2719		Fr=0,3081	
Radius	wt	Radius	wt	Radius	wt	Radius	wt	Radius	wt	Radius	wt	Radius	wt
2,301	0,054	2,301	0,052	2,301	0,053	2,301	0,055	2,301	0,059	2,301	0,061	2,301	0,046
2,186	0,051	2,186	0,050	2,186	0,051	2,186	0,053	2,186	0,058	2,186	0,060	2,186	0,046
2,071	0,049	2,071	0,048	2,071	0,049	2,071	0,051	2,071	0,056	2,071	0,058	2,071	0,045
1,955	0,047	1,955	0,047	1,955	0,047	1,955	0,050	1,955	0,055	1,955	0,056	1,955	0,044
1,841	0,048	1,841	0,049	1,841	0,048	1,841	0,051	1,841	0,055	1,841	0,056	1,841	0,046
1,726	0,047	1,726	0,047	1,726	0,047	1,726	0,050	1,726	0,054	1,726	0,054	1,726	0,044
1,609	0,046	1,609	0,046	1,609	0,047	1,609	0,050	1,609	0,053	1,609	0,054	1,609	0,041
1,492	0,048	1,492	0,047	1,492	0,050	1,492	0,052	1,492	0,055	1,492	0,056	1,492	0,042
1,380	0,050	1,380	0,047	1,380	0,050	1,380	0,052	1,380	0,057	1,380	0,057	1,380	0,040
1,265	0,054	1,265	0,051	1,265	0,053	1,265	0,055	1,265	0,061	1,265	0,059	1,265	0,040
1,150	0,058	1,150	0,053	1,150	0,054	1,150	0,056	1,150	0,063	1,150	0,059	1,150	0,037
1,036	0,067	1,036	0,060	1,036	0,061	1,036	0,060	1,036	0,072	1,036	0,066	1,036	0,040
0,920	0,075	0,920	0,065	0,920	0,071	0,920	0,066	0,920	0,083	0,920	0,077	0,920	0,046
0,805	0,089	0,805	0,074	0,805	0,083	0,805	0,071	0,805	0,098	0,805	0,090	0,805	0,054
0,691	0,111	0,691	0,086	0,691	0,097	0,691	0,075	0,691	0,115	0,691	0,103	0,691	0,053
0,576	0,150	0,576	0,110	0,576	0,129	0,576	0,100	0,576	0,156	0,576	0,169	0,576	0,101
0,461	0,307	0,461	0,294	0,461	0,293	0,461	0,338	0,461	0,365	0,461	0,445	0,461	0,420
0,346	0,599	0,346	0,648	0,346	0,605	0,346	0,724	0,346	0,663	0,346	0,704	0,346	0,785
0,232	0,828	0,232	0,961	0,232	0,879	0,232	0,999	0,232	0,796	0,232	0,791	0,232	0,957
0,118	0,862	0,118	1,079	0,118	1,011	0,118	1,077	0,118	0,795	0,118	0,776	0,118	0,974
Waverage	0,182	Waverage	0,196	Waverage	0,189	Waverage	0,204	Waverage	0,188	Waverage	0,193	Waverage	0,195

Fig. 51 Summary of mean wake fraction in full scale

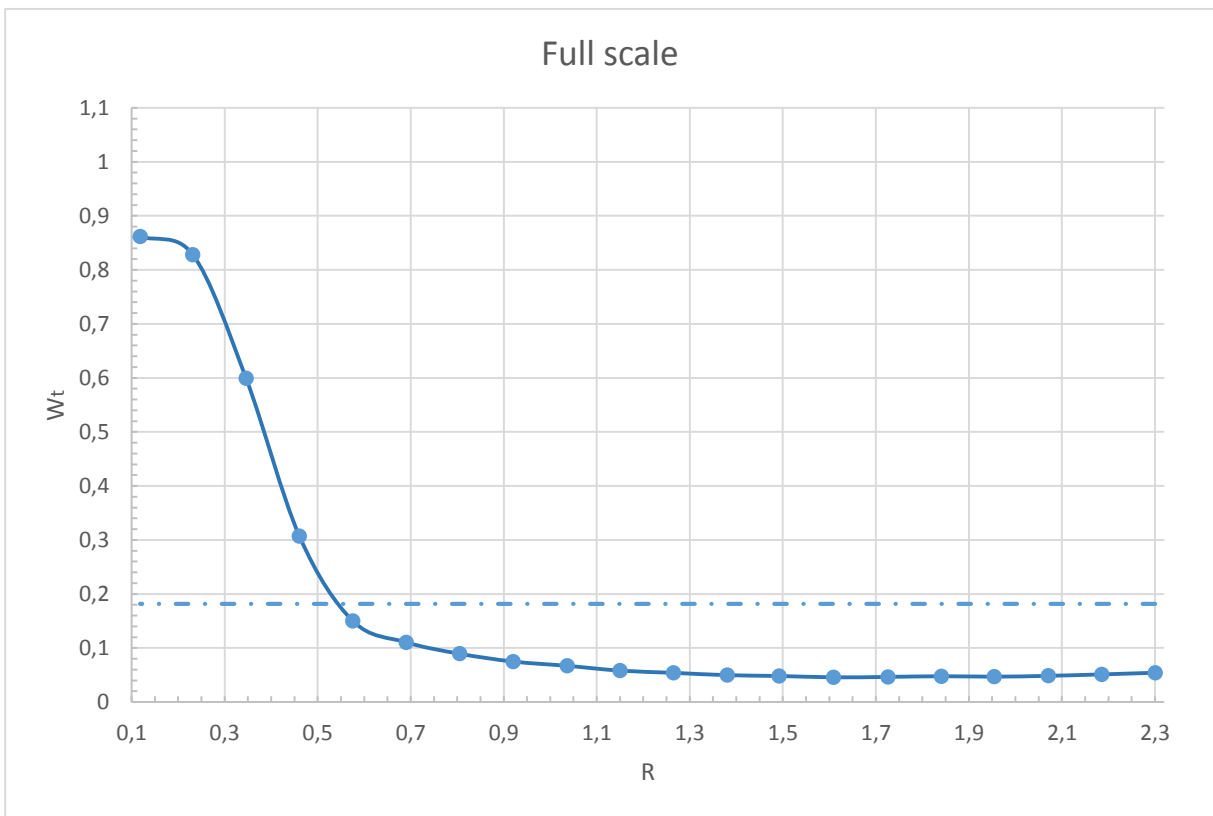
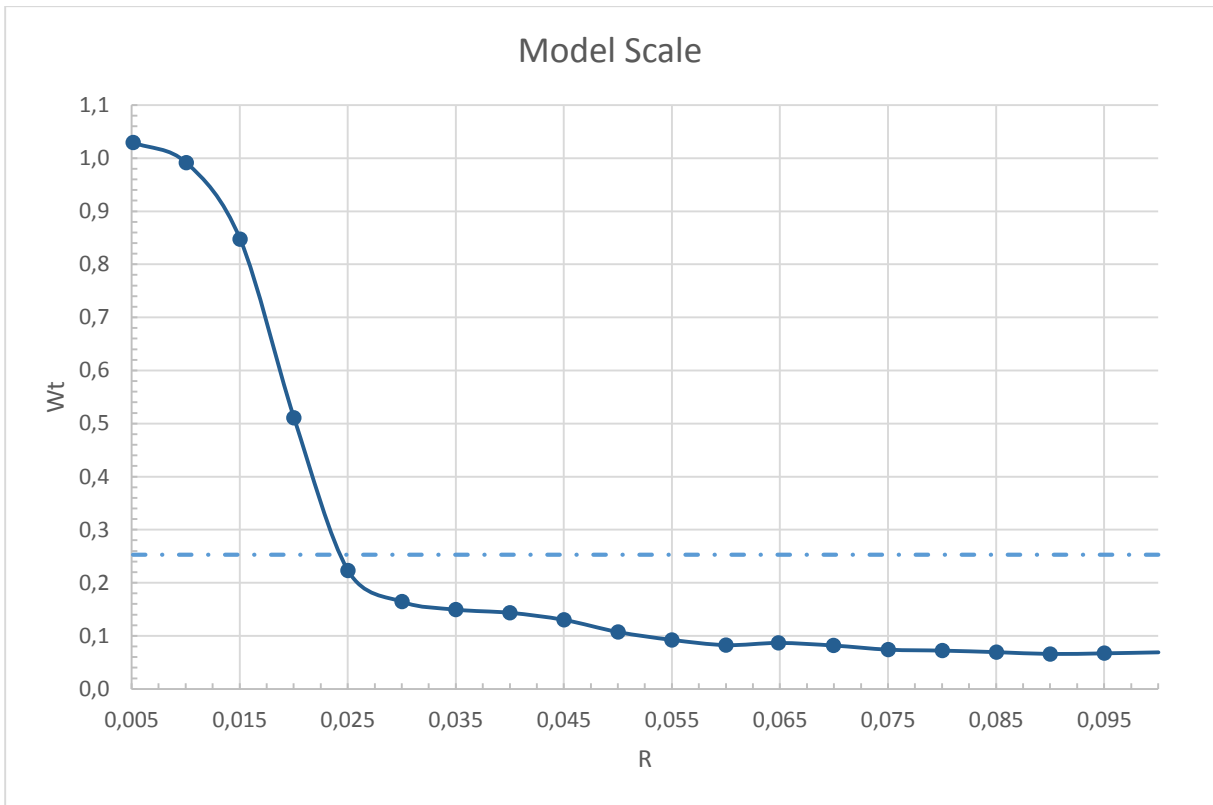


Fig. 52 $Fr=0,1450$

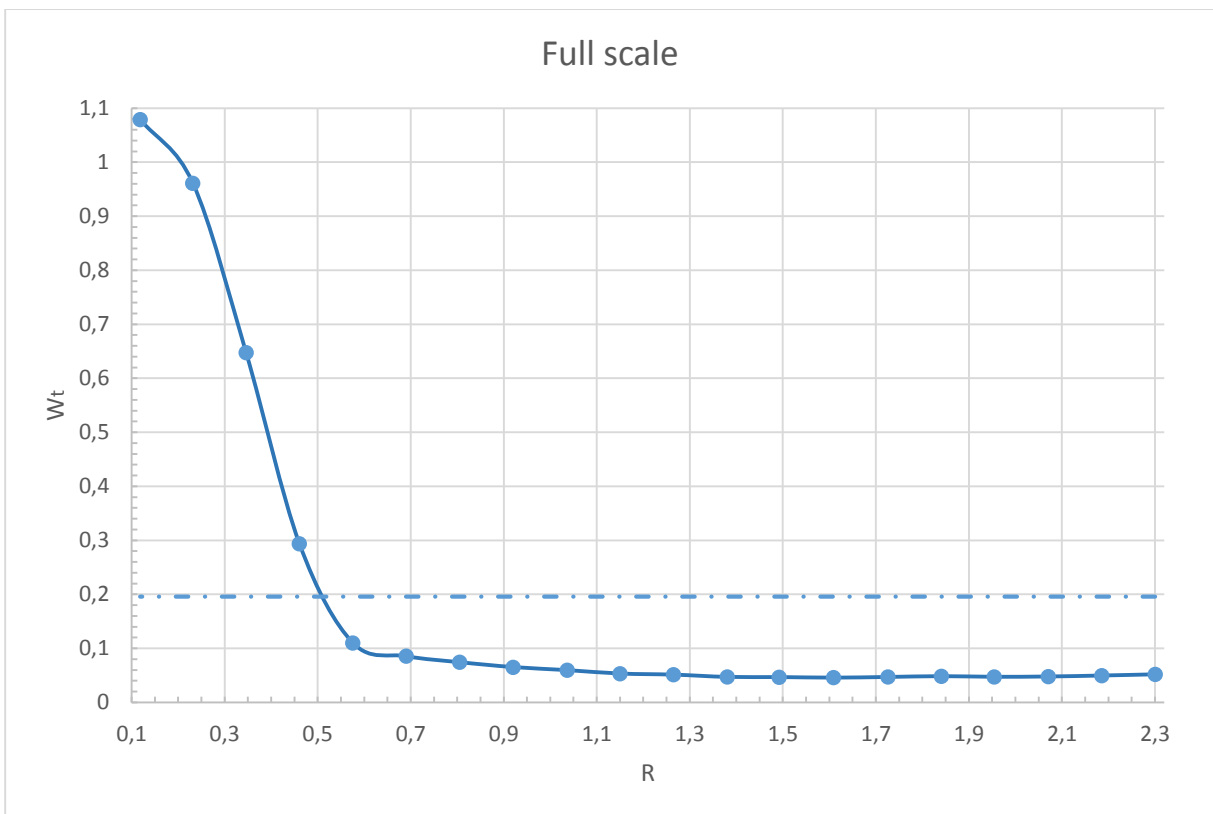
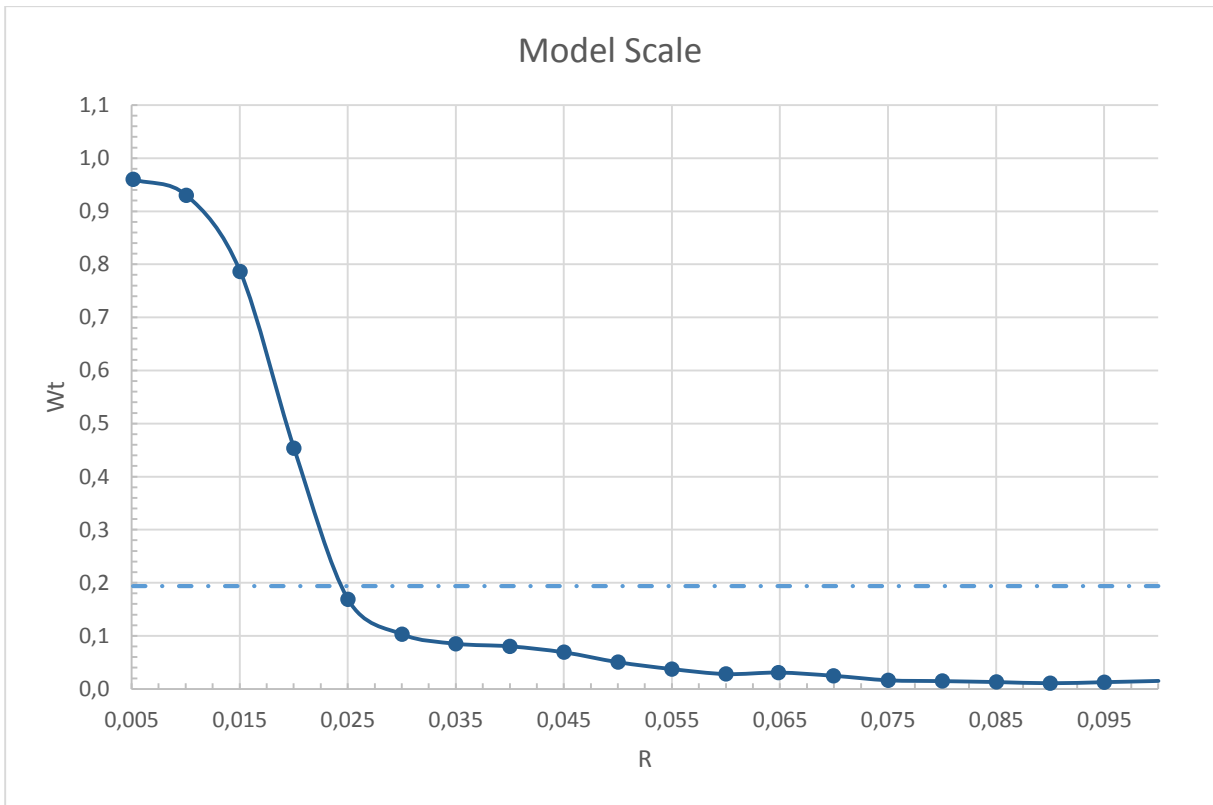


Fig. 53 Fr=0,1813

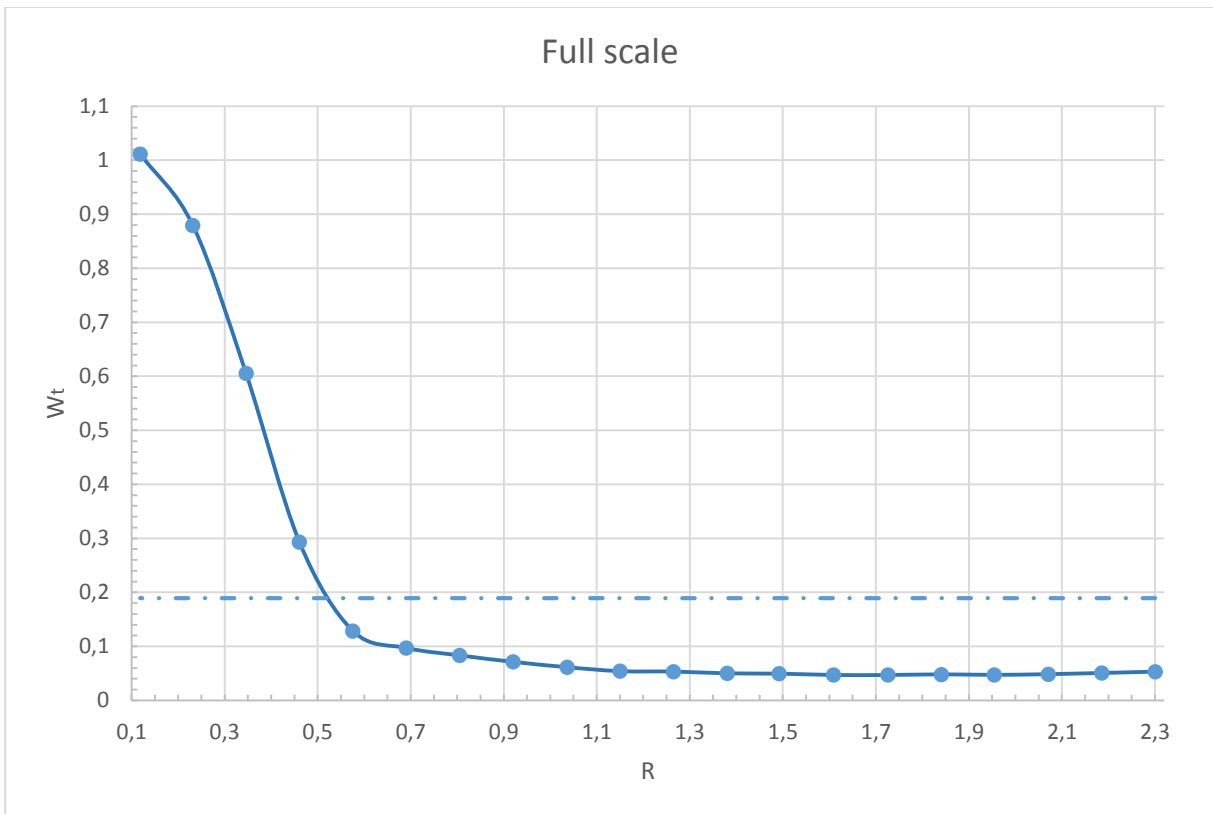
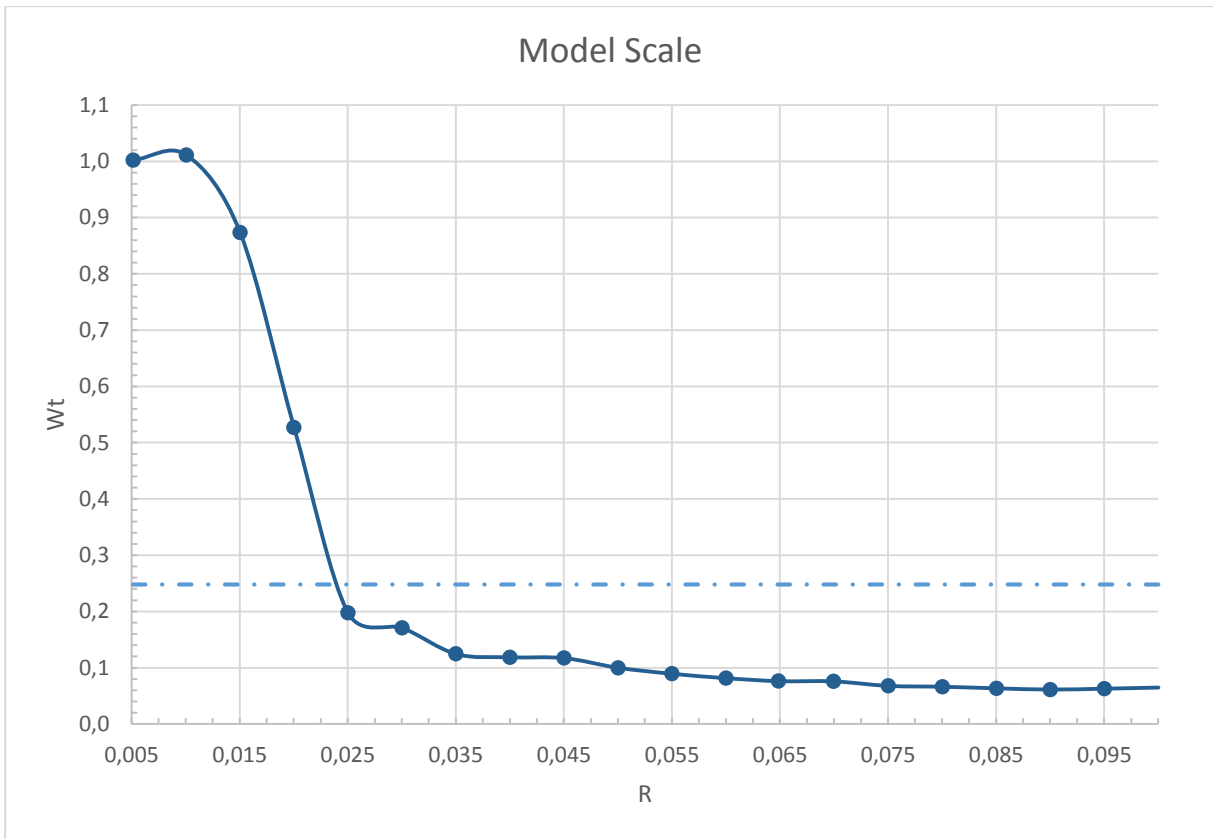


Fig. 54 Fr=0,2175

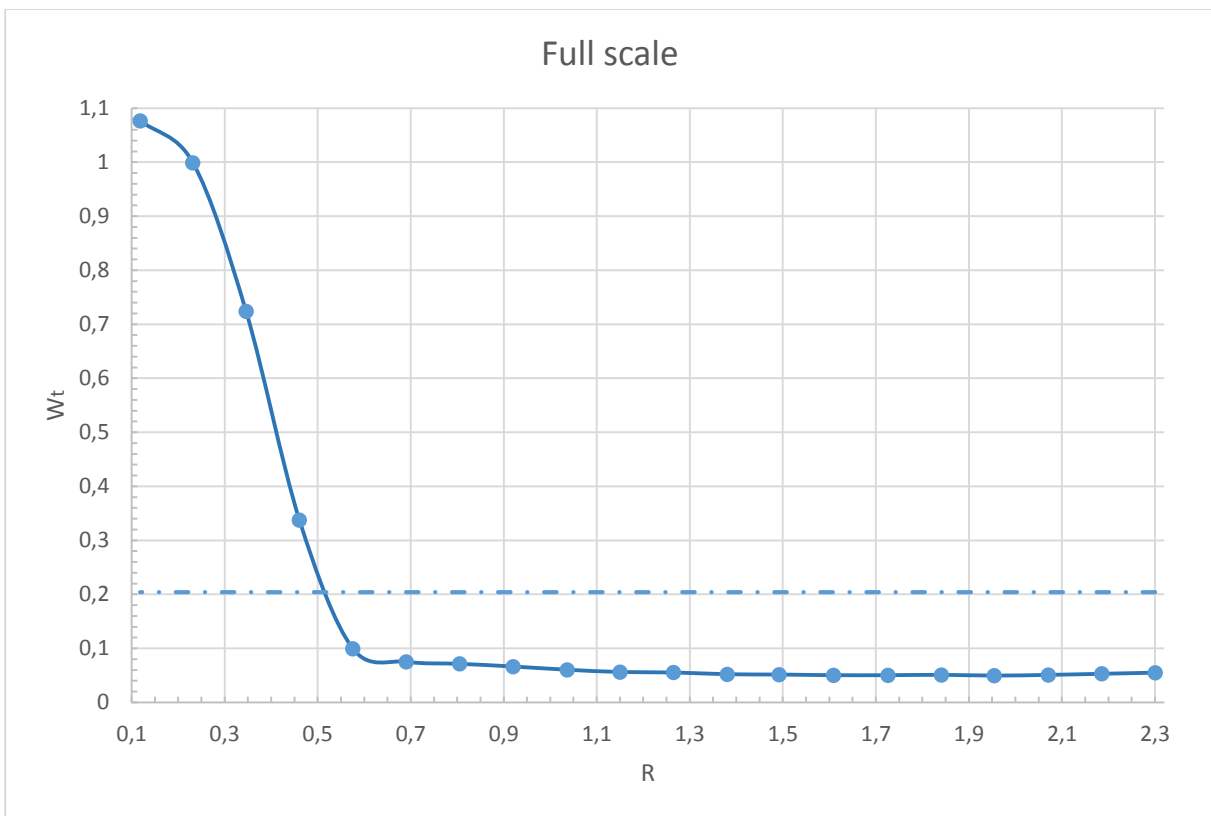
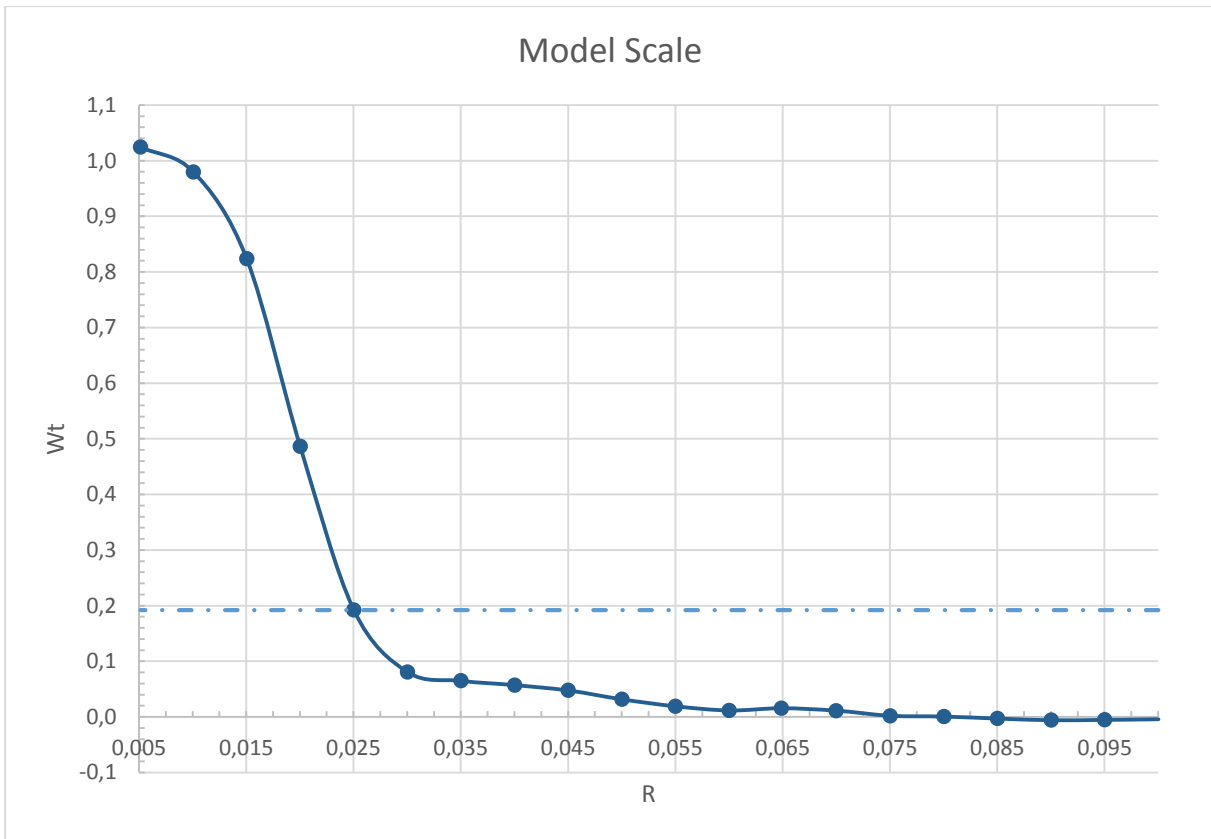


Fig. 55 Fr=0,2356

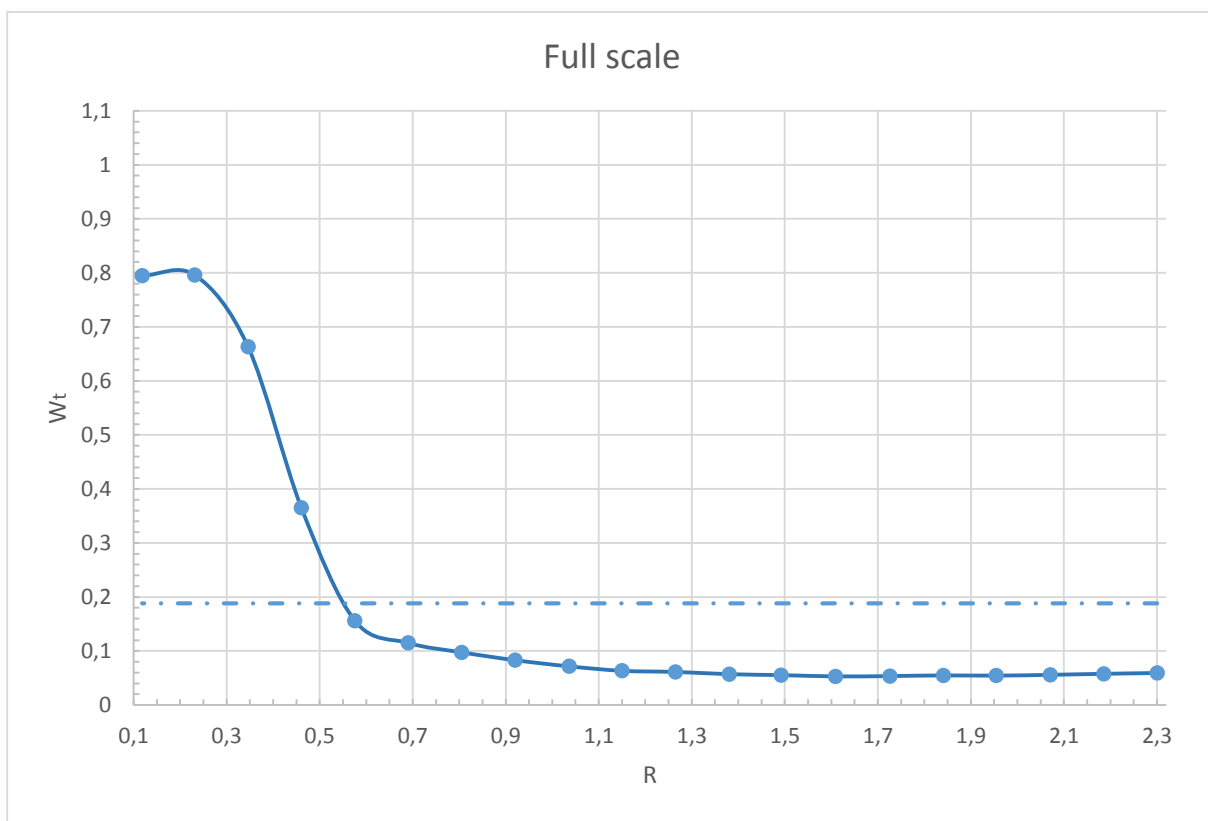
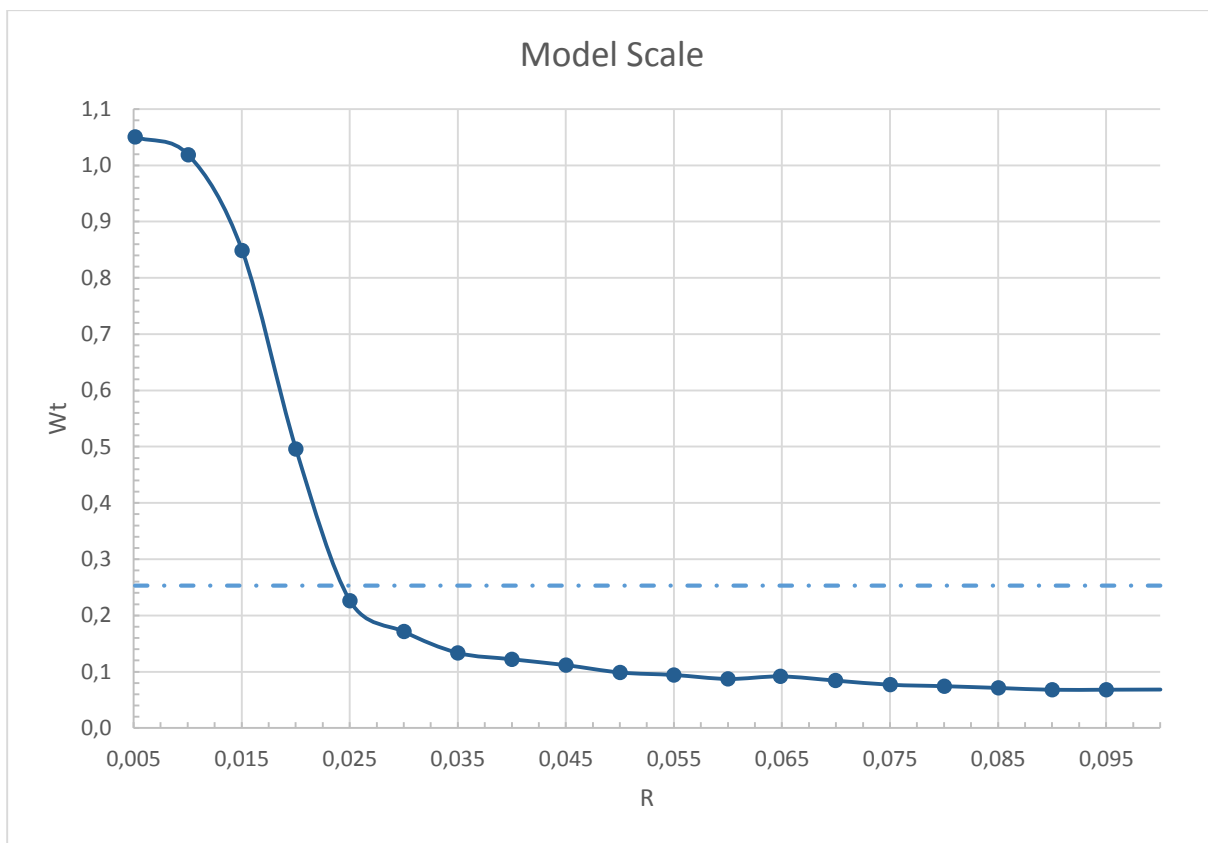


Fig. 56 Fr=0,2628

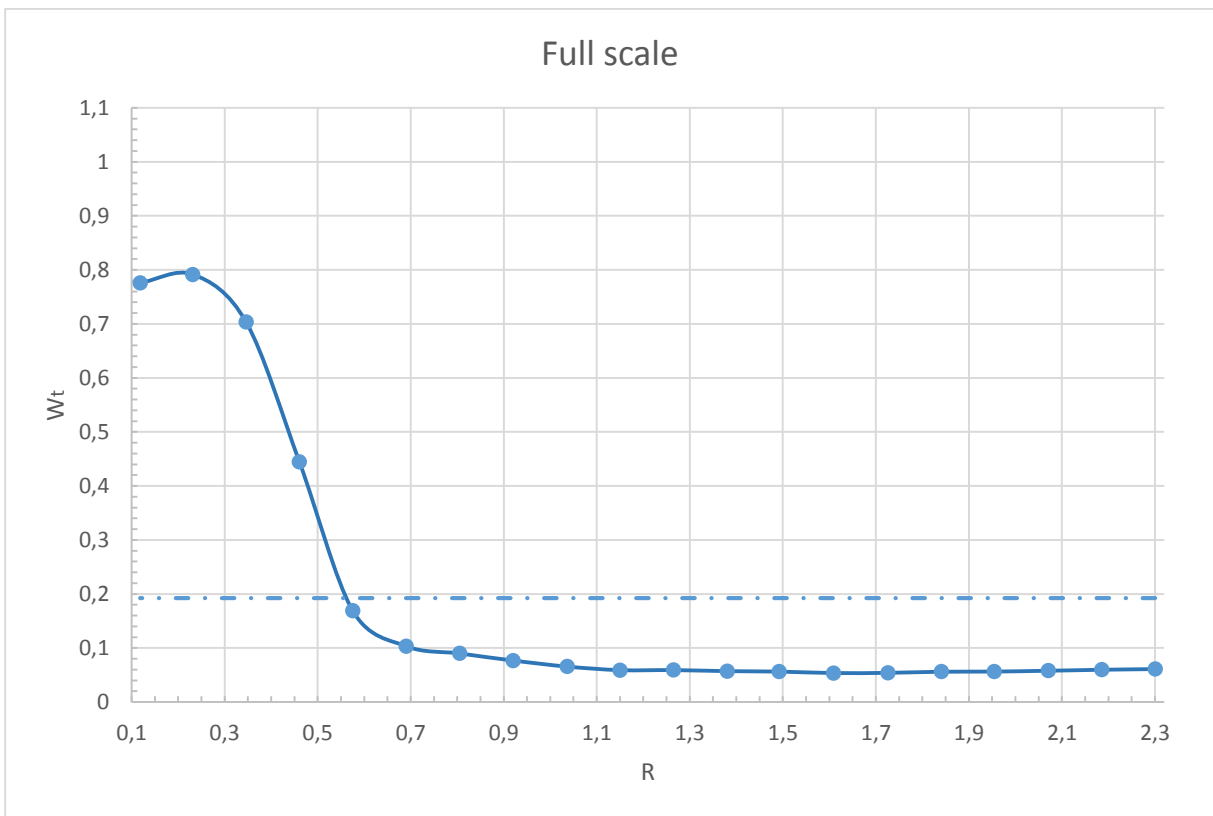
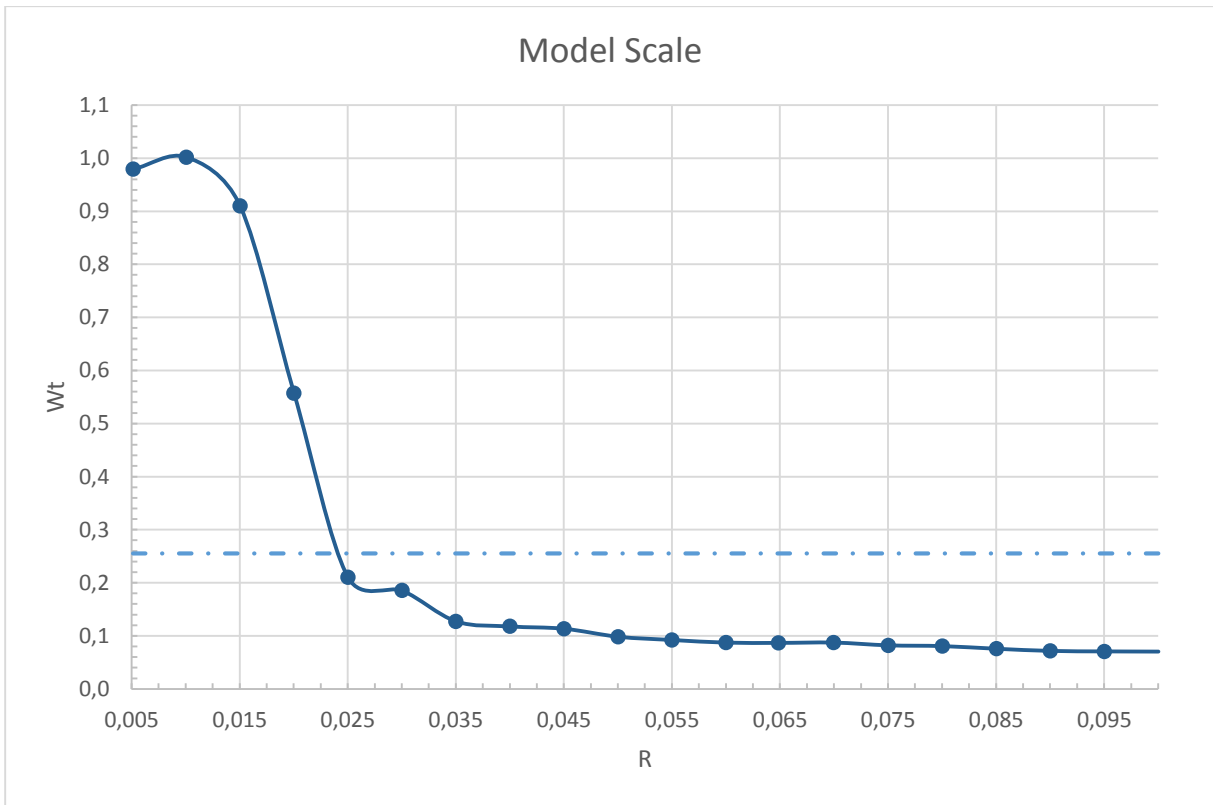


Fig. 57 $Fr=0,2719$

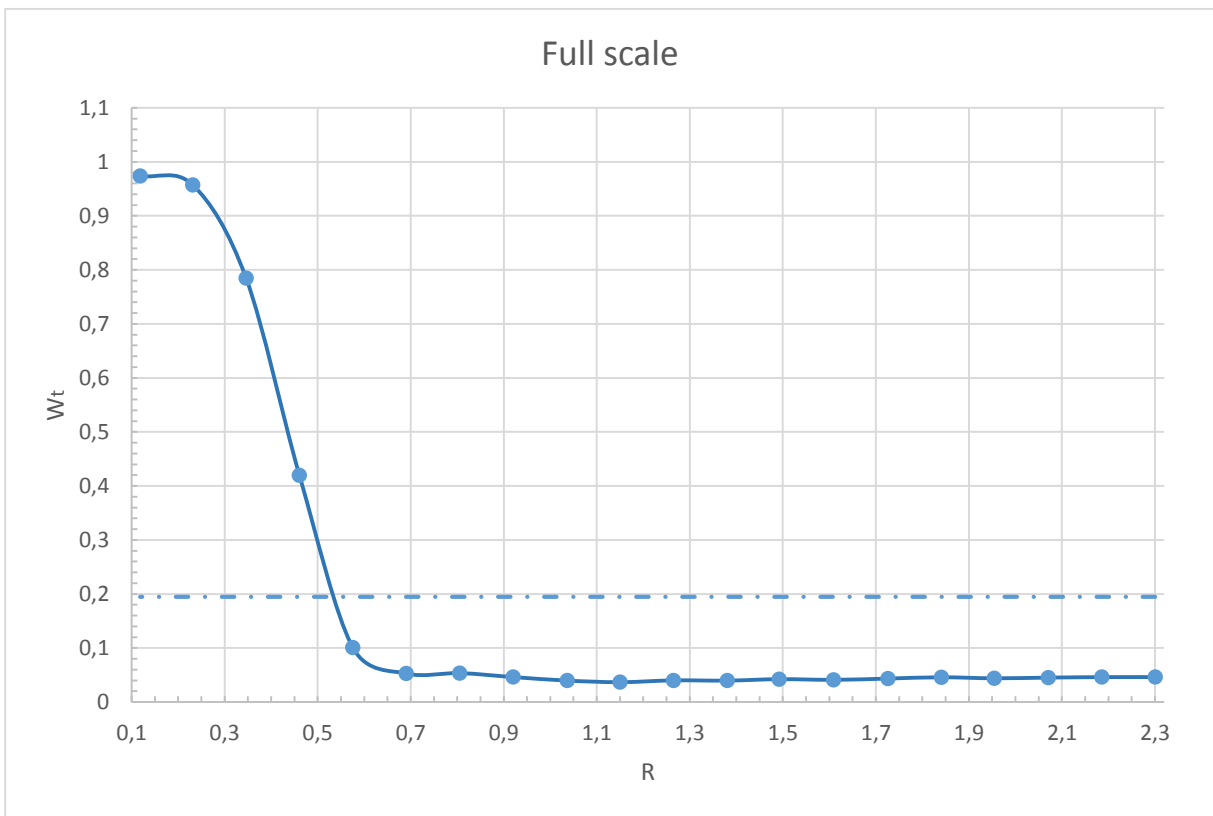
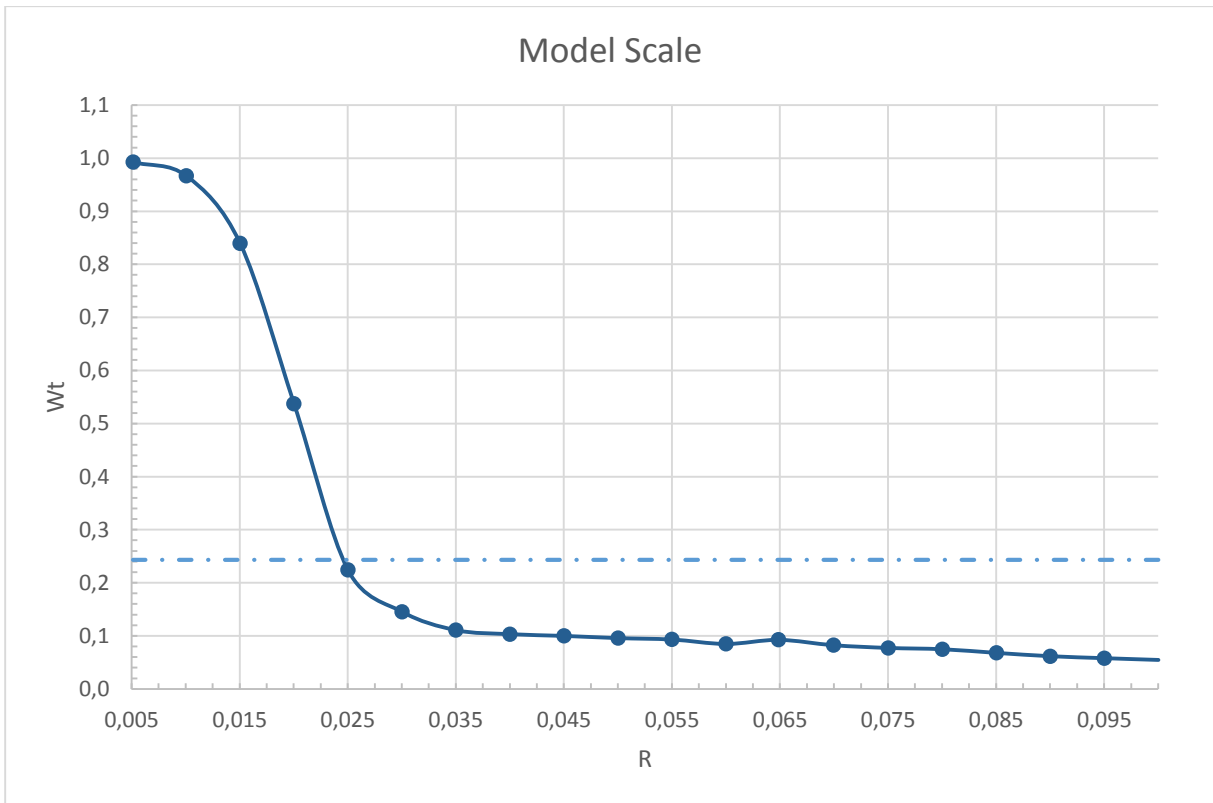


Fig. 58 $Fr=0,3081$

SCALE EFFECT PROPELLER CALCULATIONS - TWIN SCREW WAKE FIELD

Stud. Justas Kavaliauskas
Alesund University College

Abstract

This Master Thesis is all about scale effects which appears in results after performing model and full scale simulations of a twin screw vessel hull, which is anchor handler (STX-413). In this project main purpose is to perform towing tank tests where main considerations are done on results which contain resistance force coefficients and nominal wake fraction on a propeller plane. These are compared to each other in a range of Froude numbers. Simulations for model and full scale ship are done by software called STAR CCM+. Computations has been performed on a case where hull does not have ability to sink and trim. In general all set up for computations was given by Marintek as an example.

Because there is no experimental data to validate computational results, in thesis are done several different calculations to compare with: two different turbulence models are tried, calculations made with several different time steps to determine which is best for each case (model and full scale), and few simulations containing different domain size in number of cells. Main results shows that pressure force coefficients are lower in full scale up to 17% and wake fraction distribution follows the same: in full scale averaged values in propeller plane in certain Froude numbers are up to 28% lower than in model scale computations. Conclusions gives an indication that it needs to have further investigation regarding these scale effects on this particular vessel which is under investigation.

1. Introduction

To design propulsion system designer needs to take into account things like, what kind of resistance ship have, how big is hull efficiency, machinery systems, type of propulsor, etc. As it was already mentioned this project deals with scale effects of the wake field on a propeller plane. Presents of that effect is also import as all other things which have to be weighted before taking decision what system for propulsion should be used.

Scaling model to full scale it is crucial to know for designer, what will be real values. This can lead to more advance design solutions, when architects will have a good prediction model and understanding how values in a wake field would be changed when full size product will be under operations. By performing towing tank resistance tests in both model and full scale, with help of CFD tools, designer can investigate nominal wake on a propeller plane effected by scaling. This could help for naval architect to:

- Design better stern shapes in order to get more evenly distributed wake along the propeller, this would lead to for example less vibrations or even better overall propulsion system efficiency.
- Achieve same propeller characteristics with less performance from power plant.
- Decrease of exhaust emissions.

Purpose of this Master Thesis is to analyse presents of scale effects on nominal wake field behind twin screw

vessel. Thesis contains simulations of full and model scale ship hulls, to determine wake fields. This is done in case where vessel is in fixed position without sinkage and trim. Results in the project have been analysed and their differences been defined, which appeared due to scale effects made on simulations for model and full scale ship hulls.

2. Method

RANS

The RANS, i.e. Reynolds Averaging of Navier Stokes equations, approach is based on time averaging of general transport equations and representation of total flow characteristics (velocity and pressure) as a sum of averaged and fluctuating values.

RANS equations contain additional unknowns, which are cause of turbulent stresses. These stresses are often termed Reynolds stresses and they form, by analogy with viscous laminar stresses, a symmetric matrix which contains six additional unknowns:

$$\begin{bmatrix} -\overline{\rho u' u'} & -\overline{\rho u' v'} & -\overline{\rho u' w'} \\ -\overline{\rho v' u'} & -\overline{\rho v' v'} & -\overline{\rho v' w'} \\ -\overline{\rho w' u'} & -\overline{\rho w' v'} & -\overline{\rho w' w'} \end{bmatrix}$$

These six additional unknowns requires either six additional transport equations either empirical or semi-empirical turbulence model. In project there mainly have been used $k-\omega$ turbulence model.

The $k-\omega$ turbulence models is the same as $k-\epsilon$, when it comes for number of equation. Those two transport equations solves kinetic energy k and its specific dissipation rate ω . The specific dissipation rate, which is used instead of ϵ , is understood as the dissipation rate per unit turbulent kinetic energy and which is, thus, proportional to ϵ/k .

The $k-\omega$ models are more suitable to the simulations of flows involving re-circulation and separation. The standard $k-\omega$ model is known to predict reliable results for the free shear turbulent flows (jets, wakes, mixing layers). However, it reveals sensitivity to initial and boundary

conditions in the free stream region, especially for internal flows.

CFD analysis software

There are many CFD simulation tools such as Open FOAM, Flash, Gadget CFX, FLOW3D and many more, but during the master thesis all analysis regarding to CFD simulations will be done by using CD-ADAPCO product. Alesund University College has a licensed version of 10.02.010 version, which is in virtual desktop solution by University's system.

STAR-CCM+ is unrivalled in its ability to tackle problems involving multi-physics and complex geometries. STAR-CCM+ has an established reputation for producing high-quality results in a single code with minimum user effort.

Designed to fit easily within your existing engineering process, STAR-CCM+ helps you to entirely automate your simulation workflow and perform iterative design studies with minimal user interaction.

3. Case

Ship hull

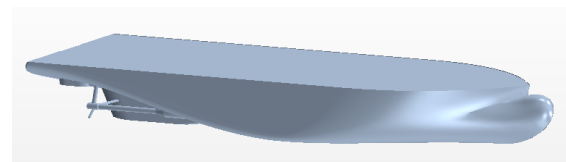


Fig. 1 Ship geometry STX413

The model geometry, which is under CFD simulation came from Marintek and it is anchor handler STX413 (fig. 4-1). This twin screw vessel with design water line 7m above base line in full scale and designed velocity is 14,5 knots. Model does not consist with structures, which are above main deck. Those are not necessary attributes for this project simulation, because here, hull resistance and nominal wake fraction investigations are done.

In table 1 below main particulars of vessel is given. Note that in table 4-1 values are for the whole vessel, but in order to reduce computational time in simulation only half of the vessel in domain is used, because ship is symmetrical, so values such as BWL, ∇ and wetted surface area

have to be reduced twice. This should be done in CFD software, where it demands those parameters.

Table 0-1 Main particulars

Parameter	Full scale	Model scale [1:23]
LPP (m)	82,1	3,570
BWL (m)	22	0,957
T (m)	7	0,304
∇ (m ³)	9192,8	0,756
SW (m ²)	2550	4,820
$\nabla/(LPP*BWL*T)$	0,7065	0,707

Meshing

All meshing operations are performed as Parts-Based Meshing, instead of Region-Based Meshing. The Parts-Based Meshing introduced in the recent versions of STAR-CCM+ has the advantage that it allows for a higher automation of the simulations setup when altering the input geometry. Unlike Region-Based Meshing, all meshing settings are contained in the Geometry group (Geometry -> Operations->Automated mesh), which means that they are attributed to the geometry parts, but not to the region boundaries. If one changes the geometry following the necessary name conventions, the mesh can easily be rebuilt by simply repeating the same automated mesh operation. If region settings are modified or deleted, one does not lose any mesh settings, and they can again be easily reproduced, by re-executing the same automated mesh operation.

In general mesh properties have been made to keep $y^+ > 30$. Also it should be noted that the y^+ have to be in a range from 30 to 300, this is necessary for accuracy of the results when there is used wall functions.

Table 2 gives a brief view what size of domain has been used in model and full scale simulations. The mesh in model scale was given as an example from Marintek, where in full scale simulation it had to be regenerated, and as a result there was 20 thousand less cells.

Table 0-2 Domain size

Scale	Number of cells in millions
Model scale	4.67
Full scale	4.65

Turbulence Model

In this project two turbulence models have been considered $k-\epsilon$ and $k-\omega$. Decision for which should be used is done on simulation in model scale $Fr=0.2628$, due to small simulation time. Model is simulated for approx. 82 seconds. Aspect which is evaluated is force coefficients: C_t , C_p and C_f . Table 3 shows simulated results of force coefficients. There isn't any difference between shear force coefficients, but pressure is slightly less in the $k-\epsilon$ turbulence model simulation, due to that also total force coefficient is also less than in $k-\omega$ model.

Because simulations with under predicted resistance is not desirable, in further simulations $k-\omega$ turbulence model will be used. Best practice of Marintek in wake prediction shows that is better to use $k-\omega$ model for these kind of simulations.

Table 0-3 Results of force coefficients

Turbulence model	C_t	C_p	C_f
	10-3		
$k-\epsilon$	3.45	1.64	1.81
$k-\omega$	3.52	1.71	1.81

Time step

Model scale. Analysis of influence on time step in model scale was made with two values 0.025 and 0.05 seconds. Force coefficient values were very close for each simulation with these different time steps. Although residuals with time step 0.025s shown that it was more stable along the calculations than in case with time step 0.05 seconds. Besides residuals and force coefficients case with smaller time step gave results of CFL numbers in desirable range, which is from 0 to 2, and in simulation with time step=0.05s CFL was twice bigger.

Full scale. Computations which were under investigation of time step influence to results in full scale have been made in

such a manner: time step = 0.05s, time step = 0.15s and one simulation with mixing both time steps. First simulation with smaller time step value shown results for Cp values which were fluctuated massively compared to two other calculations. This due to convergence which was did not reached yet, even there have been made 500 seconds of simulated time. Also time spend on computation with this time step set up was approx. 150 hours. By increasing time step 3 times, computation time have been reduced also 3 times, but results for force coefficients were a bit bigger, where combination of these two time steps in one simulation gives close results as the calculations with time step = 0.05s. Besides that residual values were decreased significantly, hence the force coefficient values became much less oscillating, i.e. amplitudes of fluctuations became much smaller. This combination of time steps option is in the middle between other two in terms of overall time consumption, because of that all other simulations have been performed under mixed time step method.

4. Results

Table 4 contains information in what Froude number simulations were done and velocity inputs during calculations in CFD software.

Table 0-4

Fr	Velocity		
	Full scale		Model scale
	[knots]	[m/s]	[m/s]
-			
0,145006	8	4,1152	0,858079
0,181257	10	5,144	1,072598
0,217508	12	6,1728	1,287118
0,235634	13	6,6872	1,394378
0,262823	14,5	7,4588	1,555267
0,271886	15	7,716	1,608897
0,308137	17	8,7448	1,823417

Force Coefficients

In table 5 are given computed resistance force coefficients. It should be noted that those numbers are based on mean values of last 20 seconds of simulated time. That

means it is calculated averaged of all computed results in this range. For validation of calculations most important was pressure force coefficients Cp. Expectations were that those values will be same or close to each other in both scale simulations.

Table 0-5 Summary of force coefficients

Fr	Model Scale			Full scale		
	Ct	Cf	Cp	Ct	Cf	Cp
	10 ⁻³			10 ⁻³		
0,145	7,39	4,08	3,31	4,85	2,09	2,75
0,181	7,34	3,90	3,44	5,09	2,04	3,05
0,218	7,07	3,76	3,31	4,75	1,97	2,78
0,236	6,99	3,65	3,34	4,71	1,95	2,76
0,263	7,09	3,62	3,47	4,94	1,92	3,02
0,272	7,31	3,60	3,72	5,15	1,91	3,24
0,308	9,05	3,71	5,34	6,97	1,98	4,99

Cp values shown in figure 2 are a bit lower in full scale than in model scale and these differences can reach up to 17.4%.

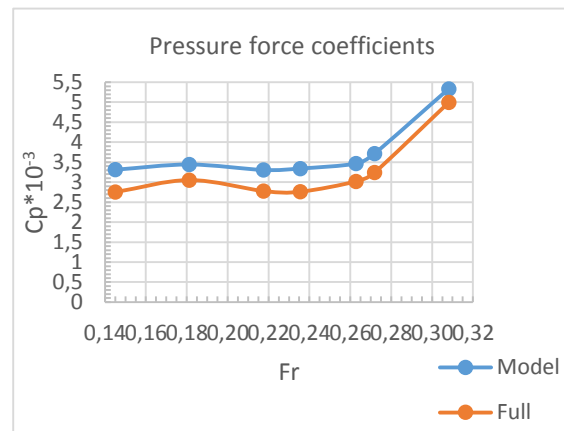


Fig. 2 Pressure force coefficients

Surface Elevation

This section contains results on how free surface is generated (fig 3 & 4) due to moving vessel in various speeds (given in a table 4). Free surface (FS) is set to be at the same level as design water line, which is 7m above the base line in full scale simulation and 0,304m in model scale.

Results indicates quite similar pattern in pretty much all calculations except in low Fr numbers there are strange behaviour of generated waves pattern.

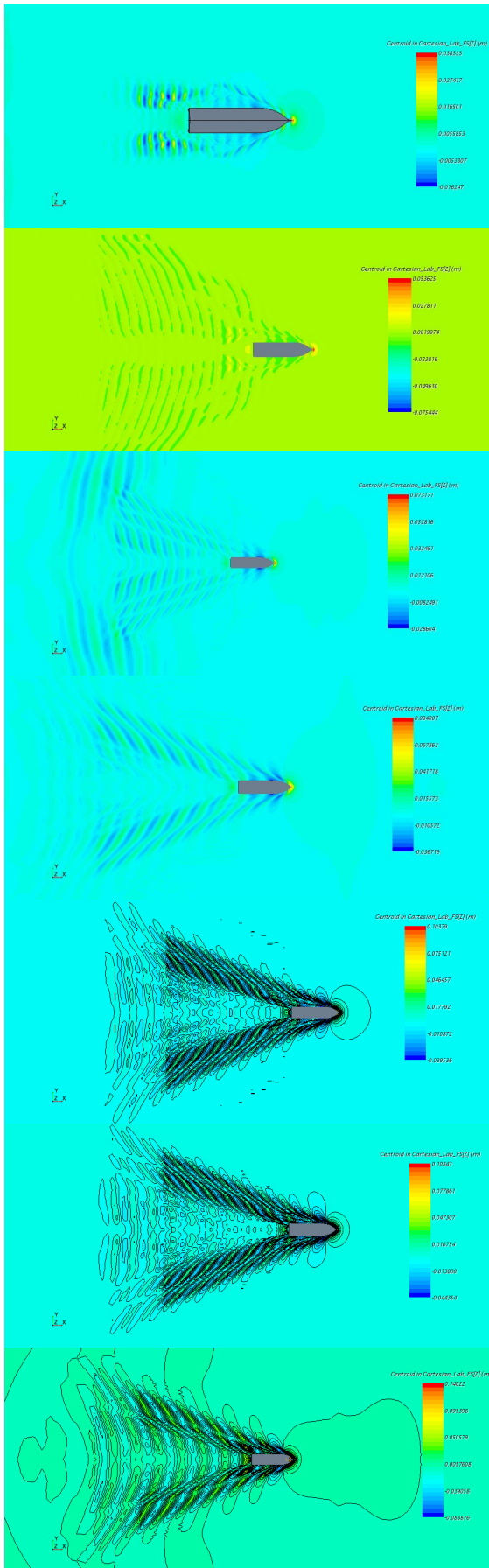


Fig. 3 Surface elevation in model scale

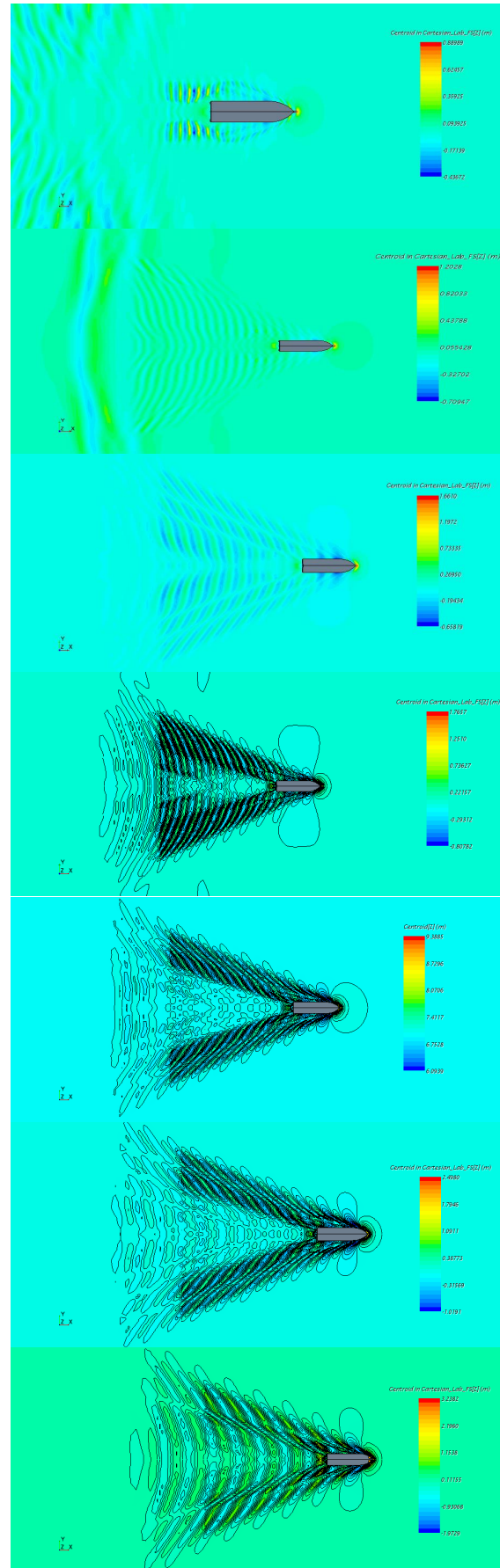


Fig. 4 Surface elevation in full scale

Nominal wake fraction

Visualization of wake fraction on a propeller plane, requires addition field function which have to be defined by user in a STAR CCM+ simulation software. Functions in software looks like this: Wake fraction = $(V_{ship} - \{\$Velocity\})/V_{ship}$ Where V_{ship} is vessel speed in m/s.

Beside wake fraction in visualization of results, also is given cross flow (arrows in Fig 3). The cross flow stands for the geometrical sum of the tangential and radial velocity components, i.e. $V_t/V + V_r/V$. Fig. 5 is an example from results with $Fr=0.2628$, where wake field in upper case represents model scale calculations, and lower – full scale.

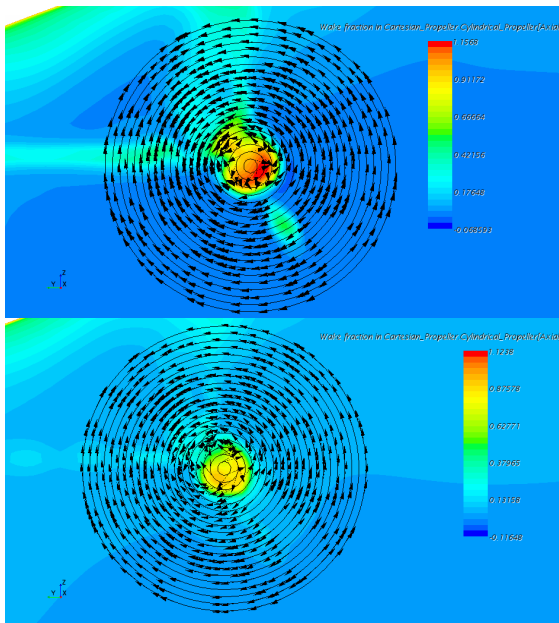


Fig. 5 Nominal wake fraction in model and full scale simulations (Fr=0.2628)

Figure 6 shows axial wake fraction distribution along propeller radius according calculated values in $Fr=0.2628$. In these plots dashed line represents **mean wake** value at all propeller plane. It should be noted that nominal wake fraction is within the axial direction. Distribution plots indicates that mean wake fraction in model scale is higher than in full scale, but full scale simulation shows that wake seems to be more evenly distributed along propeller plane, especially from approx. $\frac{1}{2} R$ to the end of propeller tip.

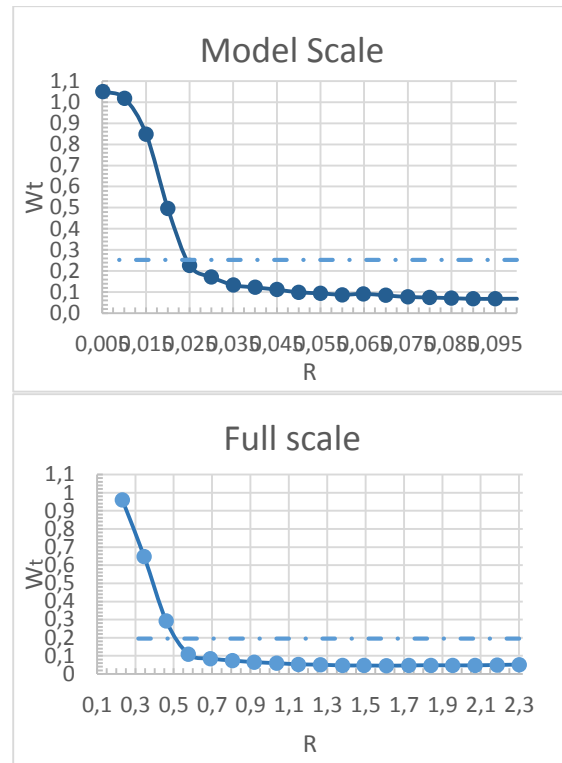


Fig. 6 Wake distribution (Fr=0.2628)

Table 6 Mean wake fraction in propeller plane

Fr	Model	Full	Diference [%]
0,145	0,25284	0,18199	28,02149
0,1813	0,194486	0,195739	0,644422
0,2175	0,247579	0,189036	23,64608
0,2356	0,191535	0,188922	1,364009
0,2628	0,253004	0,188439	25,51957
0,2719	0,255258	0,192538	24,5713
0,3081	0,243055	0,194997	19,77248

Results shown in table 6 and figure below gives an overview how mean nominal wake fraction on propeller plane is distributing along Froude number which were used for simulations. In model scale wake fraction looks unstable and have significant two deflections in $Fr=0.1813$ and 0.2356 , where in full scale simulation curvature of this wake fraction is smoother. Except these two cases where are deflections in model scale calculations, wake fraction results in full scale indicates that values are more than 20% lower in certain cases.

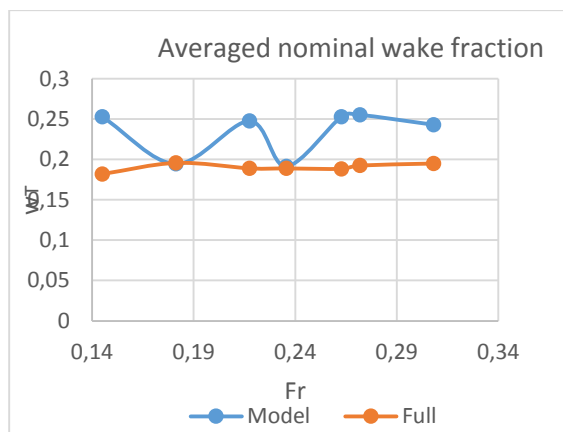


Fig. 6 Mean wake in model and full scale

5. Discussion

Force Coefficients

Calculations of force coefficients shown that in model and full scale simulations values follow same curvature, but results are bit lower in full scale simulations. When it comes to total and shear force coefficients they actually have to be smaller, but pressure coefficient should be at least close values to each other simulation (i.e. model and full scale). Calculations give an overview that in full scale computations C_p values are lower with not significant different, but the percentage tells different story, where it is within a range of 6.4-17.4% reduced values in full scale simulations.

The different in these terms becomes quite big, and could cause a huge underpowered propulsion system if designer would rely on only full scale simulations. This would lead to inefficient vessel operation and huge economical loses. It is hard to say how accurate results are on the force coefficients without experimental data. During project there wasn't a possibility to get these empirical data from other sources for this particular vessel (STX-413).

Having in mind that model scale simulations have been performed with wrong wetted surface area, needed as a reference to force coefficient calculations that could be a main purpose why model scale simulations have a bit higher values. Now results on these computations are multiplied by 2 in order to get right values for force coefficients, but guestimate would if simulations would be ran again with right surface area, resulting plots

would probably have bigger oscillations. By calculating those results averaged values, might be improved accuracy of them, which could lead to more similar resulting graphs on C_p coefficients between model and full scale.

Another reason why there are differences on C_p values could be that in model scale have been done much less iterations, resulting lower simulated physical time. This was done due to assumption that model scale simulations have been reached there convergence after approx. 80 seconds of simulated time. This assumption could be wrong and the best way would be redone some of the simulations in order to ensure is this the main cause of those inaccuracies.

Another important thing which could might be a part of different pressure coefficient results is values of y^+ (see appendix B). In full scale simulations y^+ values are way over of desired range, i.e. $30 < y^+ < 300$. In regions of ship hull where force coefficients are calculated, actual values of y^+ in some of simulations reaches more than 6000. So in this case near-wall treatment might not work properly in full scale computations. To reduce values of y^+ could be achieved simply by reducing cell size on boundary layer and increasing of prism layers in that region. In project simulations Prism layer number is 5, which is absolute minimum stated in [4], so this could be considered to be increased.

Nominal Wake

Same as pressure force coefficient, averaged nominal wake values in simulated range of Froude numbers are lower in full scale simulations. As it shown figure 6 nominal wake in full scale looks steadier throughout simulations, where in model scale are fluctuations. It is probably another indication that model scale computations have not reached their convergence or there could be needed to change some settings in CFD software. Author of this project believes that the presents of oscillating nominal averaged wake values are due to poor convergence of model scale simulations. For getting better impression how scaling is effecting wake field its necessary to get empirical data from experiments and to continue simulations on model scale in

order to get better convergence of the results.

Conclusions

In general differences between pressure force coefficients and nominal wake fraction in model and full scale could be appeared because as it was mentioned of poor convergence in model scale simulations. Also there could be a minor impact of wrong given reference area of wetted surface, where force coefficients are calculated. If the calculations would be repeated, there probably would appear a bigger oscillations in results of force coefficients in model scale. Those then should be calculated as the mean values in the same manner as it was done in full scale computation results.

Even if the simulations would be redone in model scale with suggested methodology, it would be hard to compare and evaluate results, due to missing experimental data. During the project, there haven't been any possibility to get empirical data for vessel which is under investigation in this Master Thesis. This must be the most important information in order to do further analysis and evaluation of the simulated results.

Another important thing which have to be taken into account is same simulations, which should be done with ability for model to trim and sink. This could indicate more uncertainties which could lead in wrong settings for computation domain or in opposite that simulations are done correctly with proper set up. It was planned to do these kind of simulations where model will have sinkage and trim in the planning of this Master Thesis, but during spring there was not provide necessary information to proceed this calculations, i.e. point of gravity and inertia moments. But having in mind that those simulations had to be done with the resources which were provided, this would be impossible to finish simulations in time even necessary information would be provided.

After all, simulations has been shown that in full scale nominal wake has decreased values in comparison with model scale calculations. Results indicates that differences can reach more than 28% of averaged nominal wake on propeller

plane. It is hard to say if the results are in line with reality without further investigation on this particular problem.

Further work

As it was mentioned above results in this Master Thesis cannot be taken as a reference for expectations what could be in real life situations. Thus there have to be further investigation on this particular problem, i.e. scale effects of wake field behind twin screw vessel.

After experience achieved during this project, first thing would be to repeat or further calculate all cases in model scale simulations with proper reference values of wetted surface area and performing much longer computation time, for example to 250 seconds or as it was done in full scale simulations to 500 seconds of simulated physical time. This could be done by trying to implement same strategy of time step as in full scale, i.e. combining bigger and smaller values, in order to reduce overall solution time, for example in the beginning perform simulations with time step=0.05s and after several thousand iterations change it to 0.025s.

Second thing which is necessary is to perform simulations in both model and full scale, where ship hull will have ability to sink and trim. This must be done with additional information data about vessel's gravity point and of course information about inertia moments of hull, which have to be included in a set up in CFD simulation software (STAR CCM+).

Another simulations could be done with domain which includes whole ship hull. This could give more accurate results, because in simulations which are done there have been noticed vortex shedding phenomena. So it is not particular right or accurate enough to have simulations with domain where calculations are done with half vessel and symmetry plane.

And finally the most important thing is to get experimental data to evaluate results which are calculated mathematically in CFD analysis tool. This have to be done in order to know is the simulation results are good enough to be taken in further investigation and developing of prediction model for wake field on a propeller plane.

References

- [1] Molland, A., Turnock, S. and Hudson, D. (2011). Ship resistance and propulsion: Practical Estimation of Propulsive Power. New York: Cambridge University Press.
- [2] Ferziger, J. and Perić, M. (2002). Computational methods for fluid dynamics. Berlin: Springer.
- [3] Bertram, V. (2000). Practical ship hydrodynamics. Oxford: Butterworth-Heinemann.
- [4] Krasilnikov V. I. (2011). First Introduction in to Computational Fluid Dynamics for Marine Applications: Lecture Notes. 1st edition. Ålesund University College.
- [5] Ponkratov D. (2014). Marine CFD for Engineering Applications: Lecture Presentation. Ålesund University College.
- [6] WS Atkins Consultants And members of the NSC. Best Practice Guidelines for Marine Applications of Computational Fluid Dynamics. Imperial College of Science and Technology, Germanischer Lloyd, Astilleros Espanoles.
- [7] ITTC (2011). Recommended Procedures and Guidelines: Experimental Wake Scaling Methods. Available from: <http://ittc.sname.org/> [Accessed: April 2015].
- [8] ITTC (2011). Recommended Procedures and Guidelines: Resistance Test. Available from: <http://ittc.sname.org/> [Accessed: April 2015].
- [9] ITTC (2011). Recommended Procedures and Guidelines: Practical Guidelines for Ship CFD Applications. Available from: <http://ittc.sname.org/> [Accessed: April 2015].
- [10] ITTC (2008). Recommended Procedures and Guidelines: Propulsor Nominal Wake Measurement by LDV Model Scale Experiments. Available from: <http://ittc.sname.org/> [Accessed: April 2015].
- [11] ITTC (2008). Recommended Procedures and Guidelines: Testing and Extrapolation Methods, General Guidelines for Uncertainty Analysis in Resistance Towing Tank Tests. Available from: <http://ittc.sname.org/> [Accessed: May 2015].
- [12] ITTC (2008). Recommended Procedures and Guidelines: Uncertainty Analysis in CFD Verification and Validation Methodology and Procedures. Available from: <http://ittc.sname.org/> [Accessed: April 2015].
- [13] ITTC (1999). Recommended Procedures and Guidelines: CFD, Resistance and Flow Uncertainty Analysis in CFD Examples for Resistance and Flow. Available from: <http://ittc.sname.org/> [Accessed: April 2015].
- [14] ITTC (1999). Recommended Procedures and Guidelines: CFD, Resistance and Flow Benchmark Database for CFD Validation for Resistance and Propulsion. Available from: <http://ittc.sname.org/> [Accessed: April 2015].
- [15] http://www.numeca-usa.com/fileadmin/Papers/2013_-_On_the_Importance_of_Full-Scale_CFD_Simulations_for_Ships_-_COMPIT_cortona.pdf [Accessed: May 2015]
- [16] <http://www.cd-adapco.com> [Accessed: March 2015]
- [17] file:///C:/Program%20Files/CD-adapco/STAR-CCM+10.02.010/doc/en/online/index.html#page/STARCCMP%2FGUID-B8098081-75D7-4A30-B0EC-5C1691B8D304%3Den%3D.html%23wconnect_header [Accessed: May 2015]